Agata Szade

Role of heme oxygenase-1 in squamous cell carcinoma: effects on carcinogenesis, tumor growth and mobilization of hematopoietic cells

Rola oksygenazy hemowej-1 w raku płaskonabłonkowym: wpływ na karcynogenezę, wzrost nowotworu oraz mobilizację komórek układu immunologicznego

PhD thesis prepared under supervision of prof. dr hab. Alicja Józkowicz
in the Department of Medical Biotechnology at Faculty of Biochemistry, Biophysics and Biotechnology of Jagiellonian University

Praca doktorska przygotowana pod kierunkiem prof. dr hab. Alicji Józkowicz
w Zakładzie Biotechnologii Medycznej na Wydziale Biochemii, Biofizyki
i Biotechnologii Uniwersytetu Jagiellońskiego

Kraków 2015

STRESZCZENIE

Raki płaskonabłonkowe (SCC, ang. *squamous cell carcinoma*) są zróżnicowaną grupą agresywnych nowotworów, o niewyjaśnionej do końca patogenezie. Niektóre obserwacje kliniczne sugerują, że na rozwój SCC może mieć wpływ aktywność oksygenazy hemowej-1 (HO-1). HO-1 katalizuje enzymatyczny rozkład hemu do jonów żelaza, tlenku węgla i biliwerdyny, która jest następnie redukowana do bilirubiny. Produkty reakcji rozkładu hemu posiadają właściwości antyapoptotyczne, antyproliferacyjne, przeciwutleniające, a także immunomodulujące, mogą więc wpływać na wzrost i przerzutowanie nowotworu.

Układ odpornościowy potrafi rozpoznać i zniszczyć stransformowaną komórkę nowotworową. Szacuje się, że codziennie w organizmie ludzkim wiele stransformowanych komórek jest eliminowanych w ten sposób. Jednakże ciągła presja immunologiczna powoduje selekcję komórek nowotworowych, które unikają eliminacji przez komórki układu odpornościowego. Przełamanie supresji immunologicznej, pozwoliłoby prawdopodobnie na ich skuteczną eliminację. Dlatego wiele uwagi poświęca się mechanizmom upośledzenia odpowiedzi antynowotworowej.

Badania wskazują, że HO-1 pełni istotną rolę w komórkach nowotworowych. HO-1 jest indukowana przez szereg czynników prozapalnych i ulega wysokiej ekspresji w wielu nowotworach. Uważa się, że HO-1, jako enzym cytoprotekcyjny, jest odpowiedzialna za ochronę komórek nowotworowych przed chemioterapią i terapią fotodynamiczną oraz ułatwia nabywanie oporności na niektóre leki przeciwnowotworowe. Pomimo znanej funkcji HO-1 w regulacji odpowiedzi immunologicznej dotychczas nie uwzględniano wysokiej ekspresji HO-1 w nowotworach, jako potencjalnego czynnika regulującego odpowiedź antynowotworową.

Celem pracy było zbadanie roli HO-1 w indukcji i progresji raka płaskonabłonkowego, w szczególności w regulacji migracji leukocytów do nowotworu.

W pierwszej części badań myszy o różnym poziomie ekspresji HO-1 (typu dzikiego, z niedoborem HO-1 oraz nadekspresją HO-1 w nabłonkach) były poddane chemicznej karcynogenezie jamy ustnej i przełyku. Nie odnotowano wpływu poziomu HO-1 na powstawanie zmian nowotworowych na języku. Zaobserwowano natomiast, że myszy z

niedoborem HO-1 (HO-1$^{-/-}$) były bardziej podatne na karcynogenne działanie 4NQO w przełyku niż myszy typu dzikiego oraz myszy z nadekspresją HO-1. Ponadto, tylko w grupie myszy HO-1$^{-/-}$ zaobserwowano wysoką śmiertelność spowodowaną ostrą toksycznością 4NQO w początkowym etapie trwania eksperymentu. W językach myszy poddanych działaniu 4NQO nastąpił wzrost ekspresji dysmutazy ponadtlenkowej 1 (Sod1) oraz keratyny 8, której ekspresja w nabłonku wielowarstwowym jest związana z nowotworzeniem. Jednocześnie obniżyła się ekspresja keratyny 4, charakterystycznej dla zróżnicowanych komórek nabłonka. W surowicy myszy poddanych działaniu 4NQO zaobserwowano wzrost stężenia IL-6 i eotaksyny. Niedobór HO-1 spowodował wzrost stężenia IL-7 oraz MCP-1 w surowicy zwierząt traktowanych karcynogenem, co może sugerować immunomodulujące działanie HO-1.

Następnie wszczepiono podskórnie myszom syngenicznym komórki linii raka płaskonabłonkowego o normalnym lub stabilnie podwyższonym poziomie HO-1. Wzrost guzów był monitorowany za pomocą pomiarów bioluminescencji. Po uśpieniu myszy, analizowano napływ leukocytów do guzów nowotworowych za pomocą cytometrii przepływowej. Komórki z nadekspresją HO-1 po podaniu do myszy syngenicznych tworzyły mniejsze guzy, ze zwiększoną infiltracją komórek układu odpornościowego (CD45^{+}), szczególnie linii mieloidalnej (CD11b^{+}): niektórymi populacjami makrofagów oraz mieloidalnych komórek supresorowych (MDSC). Nadekspresja HO-1 w guzie miała także wpływ na zmniejszoną infiltrację guzów komórkami o fenotypie limfocytów T regulatorowych (CD4^{+} CD25^{+}) oraz zmniejszony stosunek limfocytów CD4/CD8 w guzie oraz we krwi obwodowej.

Ekspresja HO-1 jest często podwyższona w tkance nowotworowej, ale jest także dodatkowo indukowana przez chemioterapię oraz radioterapię. Dlatego w kolejnym etapie badań, razem z podskórnym podaniem komórek nowotworowych, zastosowano farmakologiczną indukcję HO-1 za pomocą protoporfiryny kobaltu IX (CoPP). Wykazano, że podanie CoPP powoduje mobilizację komórek ze szpiku kostnego do krwi obwodowej, czemu towarzyszy wzrost stężenia G-CSF oraz IL-6 we krwi. Mobilizacja komórek krwi ze szpiku kostnego do krążenia obwodowego ma kluczowe znaczenie dla zapewnienia prawidłowego funkcjonowania układu odpornościowego. Proces ten jest ściśle regulowany zarówno podczas homeostazy hematologicznej, jak i w warunkach stresu, takich jak infekcje lub terapia lekami cytotoksycznymi. Mechanizmy regulujące

mobilizację komórek są złożone i pozostają nie w pełni poznane. Populacje leukocytów, zmobilizowanych przez podanie CoPP charakteryzowano bardziej szczegółowo przy użyciu cytometru przepływowego. Podanie CoPP spowodowało wzrost ilości granulocytów ($CD11b^+$ $Ly6C^-$ $Ly6G^+$) we krwi. Zaobserwowano także mobilizację hematopoetycznych komórek macierzystych/progenitorowych (KLS, $c\text{-}Kit^+$ Lin^- $Sca\text{-}1^+$). W porównaniu do rhG-CSF, CoPP mobilizuje granulocyty bardziej dojrzałe, o większej ziarnistości i wyższej ekspresji Ly6G oraz większą liczbę komórek KLS, regenerujących układ krwiotwórczy po przeszczepie. Wyniki naszych doświadczeń pokazują, że CoPP może być rozpatrywana jako potencjalny lek przeciwdziałający neutropenii lub środek służący do mobilizacji komórek macierzystych w celu ich izolacji i przeszczepienia. Podanie CoPP myszom pozbawionym genów kodujących HO-1 oraz czynnika transkrypcyjnego Nrf2 wywołało taki sam efekt mobilizacji komórek jak u myszy dzikich, co wskazuje na niezależne od HO-1 i Nrf2 działanie CoPP.

Podsumowując, zmieniona ekspresja HO-1 w raku płaskonabłonkowym może wpływać na powstawanie i wzrost nowotworu, ekspresję cytokin i czynników wzrostu oraz infiltrację guzów przez komórki układu odpornościowego. CoPP działając niezależnie od HO-1 powoduje mobilizację komórek hematopoetycznych ze szpiku kostnego do krwi.

ABSTRACT

Squamous cell carcinomas (SCC) are a diverse group of aggressive cancers of not yet clear pathogenesis. Some clinical observations suggest that the activity of heme oxygenase-1 (HO-1) can influence the development of SCC. HO-1 catalyses the enzymatic degradation of heme into ferrous ions, carbon monoxide and biliverdin, which is subsequently reduced to bilirubin. The products of heme degradation possess anti-apoptotic, anti-proliferative, anti-oxidant and immunomodulatory properties and may therefore affect the tumor growth and metastasis.

The immune system can recognize and destroy transformed cancer cells. It is estimated that every day many transformed cells are eliminated in this way in the human body. However, the constant pressure of immune system causes the selection of tumor cells which escape the elimination by immune cells. Overcoming immune suppression, may enable the efficient elimination of tumor cells. Therefore, much attention is paid to the dysregulation of mechanisms of anti-tumor response.

Studies show that HO-1 plays an important role in cancer cell biology. HO-1 is induced by a number of pro-inflammatory factors and is highly expressed in many tumors. It is believed that HO-1 as a cytoprotective enzyme, is responsible for protecting the tumor cells from the chemotherapy and photodynamic therapy and enables the resistance to some anti-cancer drugs. Despite the known function of HO-1 in the regulation of immune response, high expression of HO-1 in tumors was not considered as a potential control agent in anti-tumor response.

The aim of this work was to examine the role of HO-1 in the induction and progression of squamous cell carcinoma, particularly in the regulation of leukocyte migration into the tumor. In the first part of the study, mice with distinct levels of HO-1 expression (wild-type, HO-1 deficient and overexpressing of HO-1 in the epithelia) were subjected to chemical carcinogenesis of oral cavity and esophagus. There was no influence of the level of HO-1 on the formation of neoplastic lesions on the tongue. However, HO-1 deficient mice ($HO\text{-}1^{-/-}$) were more susceptible to carcinogenic effect of 4NQO in esophagus than wild-type mice and HO-1-overexpressing mice. Moreover, only in the group of $HO\text{-}1^{-/-}$ mice we observed a high mortality due to acute toxicity 4NQO at the initial stages of the experiment. We observed increased expression of superoxide

dismutase 1 (SOD1) in the tongues of mice treated with 4NQO. Tongues of mice treated with 4NQO had also higher expression of keratin 8, which presence in stratified squamous epithelium is associated with carcinogenesis and, at the same time, decreased expression of keratin 4, characteristic for differentiated epithelial cells. We observed increased concentration of IL-6 and eotaxin in the serum of mice treated with 4NQO. HO-1 deficiency resulted in an increased concentration of IL-7 and MCP-1 in serum of animals treated with the carcinogen, suggesting immunomodulatory effect of HO-1.

Next, we injected squamous cell carcinoma cell lines with normal or increased level of HO-1 subcutaneously into syngeneic mice. The growth of tumors was monitored by *in vivo* bioluminescence measurements. Following sacrifice, the tumors were excised and leukocyte infiltration was analyzed by flow cytometry. HO-1 overexpressing cells injected to syngeneic mice formed smaller tumors, which were more infiltrated with leukocytes ($CD45^+$), especially of myeloid lineage ($CD11b^+$): certain populations of macrophages and myeloid suppressor cells (MDSC). Overexpression of HO-1 in the tumor led to the reduced infiltration of tumor with the cells of regulatory T cell phenotype ($CD4^+$ $CD25^+$) and a decreased CD4/CD8 ratio of T lymphocytes in the tumor and in the peripheral blood.

HO-1 expression is often elevated in tumor tissue, but is also further induced by chemotherapy and radiotherapy. Therefore, along with a subcutaneous tumor cells injection, we induced HO-1 using cobalt protoporphyrin IX (CoPP). We show that administration of CoPP causes the mobilization of cells from bone marrow to peripheral blood, accompanied by increase in the concentration of G-CSF and IL-6 in the plasma. The mobilization of blood cells from the bone marrow into the peripheral circulation is essential for the proper functioning of the immune system. This process is highly regulated both during the homeostasis of hematologic system and in stress conditions, such as infection or use of cytotoxic drugs. The mechanisms regulating cell mobilization are complex and not yet fully understood. Leukocyte populations mobilized by administration of CoPP were characterized in more detail using flow cytometry. CoPP administration increased the number of granulocytes ($CD11b^+$ $Ly6C^-$ $Ly6G^+$) and hematopoietic stem/progenitor cells (HSC, c-kit^+ Lin^- $Sca\text{-}1^+$) in blood. As compared to rhG-CSF, CoPP mobilized more mature granulocytes (more granular and with higher expression of Ly6G) and higher number of HSC cells, which regenerated the

haemopoietic system when transplanted. The results of our experiments show that CoPP can be considered as a potential treatment of neutropenia or for mobilization of stem cells for their isolation and transplantation. Administration of CoPP to mice lacking genes encoding for HO-1 and transcription factor Nrf2 resulted in similar mobilization as in the wild type mice, indicating that effect of CoPP is independent of HO-1 and Nrf2.

In summary, the altered expression of HO-1 in squamous cell carcinoma may affect the formation and growth of tumor, the expression of cytokines and growth factors, and the infiltration of tumors by the immune cells. CoPP acting independently of HO-1 results in mobilization of hematopoietic cells from the bone marrow into the blood.

ACKNOWLEDGMENTS

Firstly, I would like to express my deepest gratitude to my supervisor prof. Alicja Józkowicz for her continuous support of my Ph.D study and related research, for her patience, trust and guidance. I would also like to express my sincere gratitude to prof. Józef Dulak for his support during my work in the Department of Medical Biotechnology.

I would like to thank Witold Nowak for his help whenever needed, Karolina Bukowska-Strakova for help with flow cytometry, Jacek Stępniewski for help with the vector construction, Maciej Cieśla for help with all protein analyses and CoPP work, Linh Nguyen Tuyet for histological analysis.

I would like to thank all the people who participated in the carcinogenesis experiment and helped with handling the large amount of samples: Halina Waś, Matusz Tomczyk, Lamia Ghezali, Paulina Marona and Magdalena Łośko.

I would like to acknowledge all animal facility members, especially Ewa Werner, Karolina Hajduk and Janusz Drebot for their help and support in performing animal experiments.

My deepest gratitude goes to all members of our department, for many years of work together, sharing protocols and advice, and creating a great atmosphere at work. I would like to especially thank Agnieszka Andrychowicz-Róg, for her indispensable help and advice.

I am very grateful to the members of other departments at the Faculty of Biochemistry, Biophysics and Biotechnology, especially Department of Cell Biochemistry and Department of Biophysics, for allowing me to use the equipment, borrowing reagents and may valuable advices.

I wish to acknowledge the help provided by dr Jacek Kijowski for help with bone marrow transplantations in mice, dr Lucie Muchova for measuring the HO-1 activity, prof. Claudine Kieda for providing endothelial cell lines and prof. Lukas Mach for providing SCC VII cell line.

I would like to thank my whole family, especially my parents and grandparents, for their support and to my sister and brother-in-law, for taking care of my daughter during the late night experiments.

Finally, I would like to thank my husband, Krzysztof Szade for help with experiments, endless discussions and encouragement. This work would be not possible without his support.

TABLE OF CONTENTS

1. ABBREVIATIONS

4NQO – 4-Nitroquinoline 1-oxide
AP-1 – Activator protein 1
ARE – Antioxidant response element
BM – Bone marrow
BMT – Bone marrow transplantation
BSCC - Buccal squamous cell carcinoma
Bv8 – *Bombina variegata* peptide 8
CoPP – Cobalt protoporphyrin IX
CORM – Carbon monoxide releasing molecule
COX-2 – Cyclooxygenase-2
DC – dendritic cell
DHR 123 – Dihydrorhodamine 123
DMSO – Dimethyl sulfoxide
EMT – Epithelial to mesenchymal transition
EP – Erythroid progenitors
FAP – fibroblast activation protein α
FBS – Fetal bovine serum
FH – Fumarate hydratase
fMLP – N-formylmethionyl-leucyl-phenylalanine
GFP – Green fluorescent protein
GMP – Granulocyte-macrophage progenitor
H&E – Hematoxylin and eosin
HMOX1 – Heme oxygenase-1 gene
HNSCC – Head and neck squamous cell carcinoma
HO – Heme oxygenase
HPC – Hematopoietic progenitor
HPV – Human Papilloma Virus
HRE – Hypoxia-responsive element
HRPCa – Hormone refractory prostate cancer
HSC – Hematopoietic stem cell
HSPC – Hematopoietic stem and progenitor cell
ICAM-1 – Intercellular Adhesion Molecule 1
iNOS – Inducible nitric oxide synthase
Jak – Janus kinase
KLS – c-Kit+Lin-Sca-1+ cell
KLS^- – c-Kit+Lin-Sca-1- cell
Krt – Keratin
LPS – Lipopolysaccharide
Luc – Luciferase
MDSC – Myeloid-derived suppressor cell
MEP – Megakaryocyte-erythroid progenitor
MFI – Mean fluorescence intensity
MHC II – Major histocompatibility complex class II
MMP – Matrix metalloproteinase
MPP – Multipotent progenitor
Mps – Metalloporphyrins
NFκB – Nuclear factor kappa-light-chain-enhancer of activated B cells
NK – Natural killer cells
NKT – Natural killer T cells
Nrf2 – Nuclear factor erythroid 2-related facotr-2
OSCC - Oral squamous cell carcinoma
PAC – Proangiogenic cell
PB – Peripheral blood
PBMC – Peripheral blood mononuclear cell
PBS – Phosphate buffered saline
PCNA – Proliferating cell nuclear antigen
PCR – Polymerase chain reaction
pDC – Plasmacytoid dendritic cell
PI – Propidium iodide
PMA – Phorbol 12-myristate 13-acetate

R123 – Rhodamine 123
RFU – Relative fluorescence units
ROS – Reactive oxygen species
RT – Room temperature
RV – Retroviral vector
SCF – Stem cell factor
SDF-1α - stromal cell-derived factor-1α
SLE – Systemic lupus erythematosus
SnPP – Tin protoporphyrin IX
SOD – Superoxide dismutase
STAT – Signal Transducer and Activator of Transcription
Teff – Effector T cell
TEM – Tie-2-expressing monocyte/macrophage
TLR – Toll-like receptor
TG – Transgenic
TIL – Tumor infiltrating lymphocyte
TKI – Tyrosine kinase inhibitor
Treg – Regulatory T cell
WT – Wild type
ZnPP – Zinc protoporphyrin IX

Complete blood count
GRA – Granulocytes
HCT – Hematocrit
HGB – Hemoglobin
LYM – Lymphocytes
MON – Monocytes
PLT – Platelets
RBC – Erythocytes (red blood cells)
WBC – Leukocytes (white blood cells)

Cytokines and growth factors
EGF – Epidermal growth factor
G-CSF – Granulocyte colony-stimulating factor
GM-CSF – Granulocyte-macrophage colony-stimulating factor
IFN – Interferon
IL – Interleukin
IP-10 – Interferon gamma-induced protein 10 (CXCL10)
KC – Keratinocyte-derived chemokine (CXCL1)
LIF – Leukemia inhibitory factor
LIX – LPS-induced CXC chemokine (CXCL5)
MCP-1 – Monocyte chemoattractant protein-1
M-CSF – Macrophage colony-stimulating factor
MIG – Monokine induced by gamma interferon (CXCL9)
MIP - Macrophage Inflammatory Protein
RANTES – Regulated on Activation, Normal T-cell Expressed and Secreted (CCL5)
TNFα – Tumor necrosis factor-α
VEGF – Vascular endothelial cell growth factor

2. INTRODUCTION

Fragments of introduction were published in following articles: A. Szade, A. Grochot-Przęczek, U. Florczyk, A. Józkowicz, J. Dulak: Cellular and molecular mechanisms of inflammation-induced angiogenesis, IUBMB Life 2015 Mar;67(3):145-59 and A. Szade, J. Dulak, A. Józkowicz: Rola oksygenazy hemowej-1 w patogenezie nieswoistych zapaleń jelit (The role of heme oxygenase-1 in the inflammatory bowel diseases). Przegląd gastroenterologiczny 2009, 4 (6): 283-287.

2.1. Characteristic of squamous epithelium

Epithelium lines cavities and organs of the body. It is built by tightly connected cells that reside on basal membrane with minimal amount of intracellular spaces. The epithelium contains no blood vessels, therefore nourishment and removal of wastes have to be exchanged by diffusion through the basal membrane [1].

The simple epithelium contains only a single layer of cells, while if more cell layers are present it is referred to as the stratified epithelium. Depending on their morphology the epithelial cells are categorized into three main classes: cuboidal, columnar and squamous [1, 2].

Simple squamous epithelium is found in the linings of heart and alveoli of the lungs. The stratified squamous epithelium is typical for oral cavity, esophagus, vagina and anal canal [1]. These are tissues that are continuously exposed to mechanical shedding, but are kept within wet microenvironment due to secretion of the glands [1].

Special kind of the stratified epithelium is found in the skin, which is composed of two main sublayers: dermis and epidermis. Dermis is made of connective tissue, with many collagen and elastic fibers filled with extrafibrillar matrix [2]. Epidermis of the skin is the most external zone and is built of keratinized stratified squamous epithelium [2].

The different layers of stratified epithelium play various biological functions. The basal layer is attached to basal membrane and consist dividing precursor cells. The cells that detach from basal membrane and move into spinous layer or intermediate layer (in keratinized and non-keratinized epithelia, respectively) lose their proliferative character and start to differentiate [1–3]. The most outer granular layer or superficial is

made of finally differentiated cells, that loose the nuclei and produce specific lipids and proteins [3, 4]. In the skin keratins and lipids together with dead anucleated corneocytes form the stratum corneum - the waterproof, most protective layer that is continuously sloughed into the environment [1–3] (Fig. 1).

While the localization of dividing cells in basal layer and movement of their progeny toward upper layers, that is linked with differentiation, is characteristic for all stratified squamous epithelia, the keratinization is observed only in skin [1]. The keratinization observed in stratified squamous epithelium in other localizations is an indication of pathological conditions [1, 5].

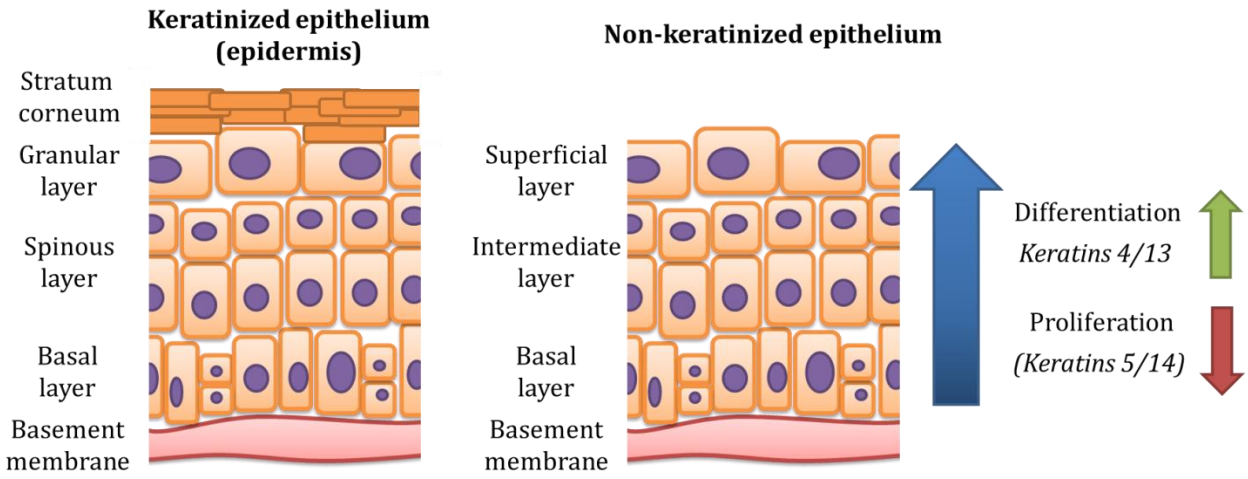

Fig. 1. Stratified epithelium differentiation scheme.

2.1.1. Selected types of squamous cell carcinoma

Squamous cell carcinomas (SCC) are derived from squamous epithelium [6]. SCC may occur in all organs where squamous epithelium exists [6]. Therefore, the SCC is a heterogeneous group of tumors that, depending on their localization, may significantly differ in progression, prognosis and treatment responsiveness [6].

SCC is the second most common type of skin cancer (after basal cell carcinoma) [7]. Although the sun exposure is the well-recognized risk factor and its avoidance can reduce the chance of SCC, the number of the cutaneous SCC is still rising [7]. While the incidence rate is rising, the SCC mortality rate over the years is decreasing and estimated to be 0.7% [7].

Nevertheless, other squamous cell carcinomas have worse prognosis. The head and neck squamous cell carcinoma (HNSCC), that involves cancers localized in mouth, nasal cavity and throat, is the sixth most common cancer in the world [8] and the mean 5-year survival does not exceed 50% [9]. Furthermore, there has been no improvement in treatment of HNSCC in last decades [10]. The HNSCC occurs mainly in elderly people (< 60 years), however during last years more cases are recorded among younger population [11].

Squamous cell carcinoma contains also a significant fraction of esophageal cancers [12]. This cancer is often diagnosed in advanced stage and 5 year survival is only around 15% [12]. The esophageal SCC (ESCC) occurs more frequently in central and south-eastern Asia, with over half of cases diagnosed in China [13]. Other region were ESCC is more frequent is Sub-Saharan Africa [13, 14].

It is well documented that SCC is linked with many environmental factors and life style. Apart from influence of UV-exposure on cutaneous SCC, the alcohol consumption and tobacco chewing significantly contribute to increased risk of HNSCC and ESCC [15, 16]. The areca chewing habit is taught to be one of the most important causes of HNSCC and ESCC in Asia [17]. SCC was also shown to be associated with human papilloma virus (HPV). HPV-positive tumors possess more mutations than HPV-negative ones, however better respond to the chemotherapy [18, 19]. Other risk factors are chemical compounds such as polycyclic aromatic hydrocarbons or asbestos [11]. It was also evidenced that patients who receive systemic immunosuppression drugs (e.g. transplant receivers) have increased risk of SCC [11].

The treatment of SCC is based on surgical excision. Often the therapy includes many combined strategies such as radiotherapy, chemotherapy or photodynamic therapy. Although the knowledge about biological mechanisms of SCC etiology is increasing, only few novel biological therapies for SSC are tested. These include cetuximab [20–22] and trastuzumab [23] monoclonal antibodies as well as small tyrosine kinases inhibitors (TKI) gefitinib [24–26], erlotinib [27, 28] or lapatinib [29] that target EGFR (epidermal growth factor receptor) pathway. TKIs targeting other pathways: sunitinib [30] and cediranib [31] are also under clinical investigation.

Concluding, there is a great interest to develop new targeted strategies to treat SCC. However, to make it possible, the better understanding of biological and cellular mechanism underlying the SCC development is needed.

2.1.2. Cellular mechanism of squamous cell carcinoma

Most of epithelial tissues are characterized by high turn-over rate [32]. The cells from outer epithelial layers are constantly shed off to the environment and have to be replaced by new cells. It is estimated that the mean turn-over of skin epidermis in humans is 40-56 days [33] (8-10 days in mice [34]). The homeostasis of this process is maintained by epithelial stem cells. Stem cells can divide asymmetrically: one of the progeny cells is differentiating and move toward outer layers, while the second one remains undifferentiated stem cell and thus self-renews stem cell pool throughout the lifetime [32].

Nevertheless, continuous self-renewal predisposes stem cells to accumulate mutations [35]. Accumulation of several mutations is required condition for malignant transformation [36]. Therefore, it was proposed that these are cancer stem cells that are responsible for uncontrolled expansion of tumor cells [35].

The existence of cancer stem cells in human HNSCC was confirmed by Prince and colleagues [37]. They identified minor population of tumor cells that expressed CD44 marker and showed properties of stem cells: reproduced tumor heterogeneity and could be serially passaged in vivo [37]. These results indicate that cancer stem cells should be the main target of novel target therapies.

2.2. Heme oxygenase-1

Heme oxygenase is an enzyme which degrades heme [38]. The products of the reaction catalyzed by heme oxygenase are: carbon monoxide (CO), ferrous ion and biliverdin, which is subsequently converted to bilirubin by biliverdin reductase [39]. Catalytic heme degradation requires electron donor, that is NADPH provided by P450 cytochrome reductase and oxygen (reviewed in [40], (Fig. 2)).

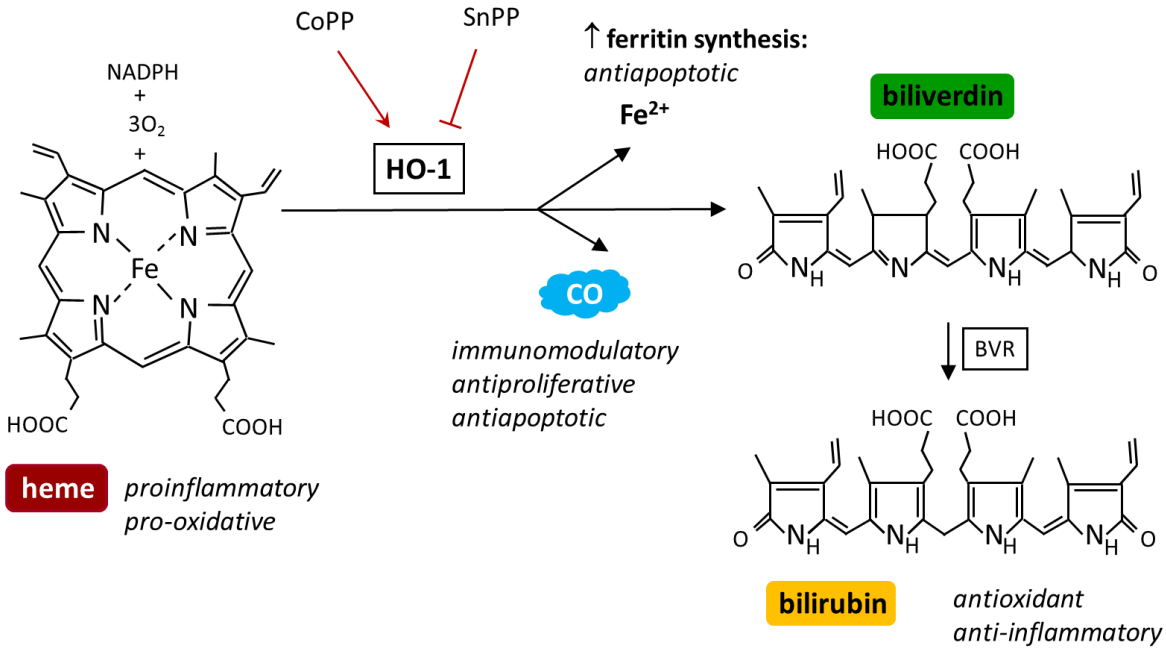

Fig. 2. Catalytic reaction of HO-1. Heme is degraded into CO, Fe2+ and biliverdin. The reaction requires molecular oxygen and NADPH. Water-soluble biliverdin is further reduced to insoluble bilirubin by biliverdin reductase.

Although heme oxygenase was discovered in the late 60's of last century, it attracted broad interest in a wider group of scientists twenty years later, when two isoforms where distinguished: constitutive HO-2 and inducible HO-1 [41, 42]. HO-1 and HO-2 are encoded by two different genes, in humans known as *HMOX1* and *HMOX2*, located on chromosomes 22 and 16, respectively [40]. In humans, there are differences in the level of induction of HO-1 in response to stress factors, which are caused by *HMOX1* promoter polymorphisms [43]. So far, in the literature, there are three described cases of HO-1 deficiency in humans. All affected children died due to pathological changes in various organs [44, 45].

Noteworthy, generation of genetically modified mice that lack the expression of HO-1 (HO-1$^{-/-}$) accelerated clarifying the complex role of this enzyme [46]. HO-1$^{-/-}$ are affected by chronic proinflammatory state and dysregulated iron homeostasis [46].

The induction of HO-1 expression is often described in the context of NF-E2-related factor 2 (Nrf-2) activity and referred to as HO-1/Nrf2 pathway. Nrf2 is a key transcription factor involved in cell response to oxidative and electrophilic stress. Under normal conditions, Nrf2 is bound by its repressor Keap1 (Kelch-like ECH-associated

protein 1), ubiquitinated and degraded in proteasome (reviewed in [47]). Pro-oxidative conditions cause Keap1 structure changes through cysteine thiol group modification, leading to Nrf2 stabilization and translocation to the nucleus. Then Nrf2 can bind to ARE (antioxidant response element) sequences in its target genes, that includes *Hmox1*, but also other genes such as glutamate-cysteine ligase (*Gclc*), thioredoxin reductase 1 (*Txnrd1*) and NAD(P)H-quinoneoxidoreductase 1 (*NQO1*) [48] (Fig. 3).

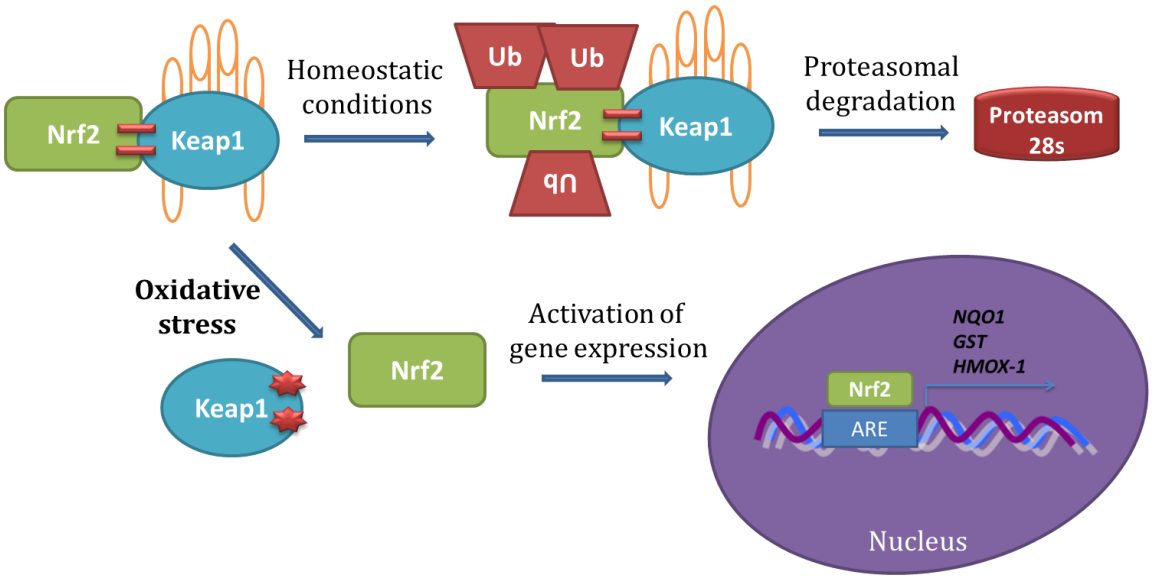

Fig. 3. Simplified scheme of gene expression activation by Nrf2.

2.2.1. Canonical and non-canonical role of HO-1

For a long time it was believed that the only positive effect of heme oxygenase reaction is the degradation of free heme, which is detrimental to cells in high concentrations - it contributes to oxidative stress and inflammation, increasing the permeability of endothelium and the expression of adhesion molecules, such as ICAM-1 (ang. intercellular adhesion molecule 1) and P-selectin [49]. Heme degradation products were considered to be unnecessary and even harmful. Indeed, the presence of Fe^{2+} can cause tissue damage by generating reactive oxygen species (ROS) [49, 50]. In newborns unconjugated bilirubin can damage neurons after crossing the blood-brain barrier [49]. Finally, carbon monoxide is considered mainly as a toxic gas, which binds irreversibly to

hemoglobin and leads to death in a short time when present in elevated concentrations in the air [40].

However, the detection of anti-inflammatory and anti-oxidant properties of products of catalytic heme degradation opened a new research field. This new direction aims to understand role of HO-1 not only in acute heme overload but also in several other processes important to sustain tissue homeostasis.

Oppositely to initial concepts, it was evidenced that increased expression of HO-1 and release of Fe^{2+} ions induce a corresponding increase of the ferritin expression which, in addition to binding iron ions, has cytoprotective [40] and anti-apoptotic effects [51]. Bilirubin at low concentrations has anti-inflammatory and anti-oxidative properties – it scavenges reactive oxygen and nitrogen species [40], inhibits the interaction of neutrophils with endothelium and reduces activation of cytotoxic T cells [52].

The most intensively studied product of heme degradation seems to be carbon monoxide (CO). Like nitric oxide, CO proved to be an important intercellular signaling molecule. CO increases the concentration of cGMP (cyclic guanosine 3',5'-monophosphate), and thus works as an anti-coagulant [53]. CO reduces the production of proinflammatory cytokines – IL (interleukin)-1, IL-6, TNFα (tumor necrosis factor α) and MIP-1α (macrophage inflammatory protein α) and the expression of adhesion molecules, and simultaneously increases the production of anti-inflammatory IL-10. In some cell types CO has antiproliferative activity [40] but it can increase the proliferation of endothelial cells [51]. CO affects the transmission of signals from certain TLRs (Toll-like receptors), which are very important in the initiation of immune responses against pathogens [54].

A lot of studies on the beneficial effects of CO in the body involves the use of compounds which release carbon monoxide (CORM, carbon monoxide releasing molecule). The positive results of experiments with the use of CORM give hope for their future use in therapy [55].

Discovery of these profound molecular effects mediated by products of HO-1-catalyzed reaction triggered the research on role of HO-1 in angiogenic and inflammatory processes.

2.2.2. HO-1 as regulator of angiogenesis

Angiogenesis is the process of new blood vessel formation. This process is often driven by inflammatory reaction, however new blood vessels could develop from preexisting ones also during steady-state conditions (reviewed in [56]). These processes are referred to as inflammatory and non-inflammatory angiogenesis. A number of studies demonstrated a significance of HO-1 in both of them [57].

First, HO-1 plays an important role in the wound healing – a complex process in which both inflammation and inflammation-induced angiogenesis are necessary to repair the tissue. Wound closure and vascularization are impaired in HO-1 deficient mice, whereas HO-1 overexpression in the skin improves neovascularization and wound healing [58].

Second, increasing HO-1 expression can provide a therapeutic benefit in the ischemic injury. Our group has shown that administration of plasmid with HO-1 cDNA under control of HRE (hypoxia responsive element) diminishes production of proinflammatory cytokines such as KC (keratinocyte-derived chemokine) or IL-6 and decreases apoptosis in ischemic skeletal muscles [59]. Inhibition of inflammation in hypoxic muscle was associated with improved neovascularization [59]. The similar proangiogenic effect of HO-1 was shown also in a model of hind limb ischemia in rats [60] and myocardial infarction in mice [61] or rats [62].

However, the involvement of HO-1 in the angiogenesis is not only connected with regulation of inflammatory response. HO-1 is implicated in signaling of two critical proangiogenic factors: vascular endothelial cell growth factor (VEGF) [63] and stromal cell-derived factor-1α (SDF-1α) [64]. HO-1 expression is upregulated both by VEGF and SDF-1α and mediates their proangiogenic activity. Additionally, HO-1 activity itself can increase levels of VEGF [65].

The studies on involvement of HO-1 in angiogenesis could not overlook the potential role of Nrf2 transcription factor which is responsible for the induction of HO-1 expression. Indeed, an inflammatory response has been proposed as a mechanism of ischemia-induced revascularization in several *in vivo* models using Nrf2-knockout mice. Recently, the proangiogenic role of Nrf2 was also demonstrated (as reviewed in [66]). For example, Wei *et al.* showed that Nrf2 acts in endothelium to regulate tip cell

formation and vascular branching [67]. On the other hand, our group reported involvement of Nrf2 in proangiogenic activities of endothelial cells and bone-marrow-derived proangiogenic cells (PAC) [68]. Lack of Nrf2 leads to decreased angiogenic potential of PAC and impairs their mobilization after hind limb ischemia [68]. However, the work by Ichihara *et al.* and further by our group both demonstrated that an ablation of the Nrf2 promotes ischemia-induced neovascularization likely due to enhanced inflammatory response [69].

Although Nrf2 induces strongly the HO-1 expression, it has to be underlined that proangiogenic activity of HO-1, at least to some extent, is independent of Nrf2. This was suggested by experiments in which HO-1 level was upregulated both in $Nrf2^{+/+}$ and in $Nrf2^{-/-}$ muscles after ischemia [68].

2.2.3. HO-1 as regulator of innate and adaptive immunity

As indicated above, HO-1 activity affects the levels of many inflammatory mediators, what understandably leads to modulation of numerous processes, e.g. angiogenesis. But the current knowledge on HO-1 extends a view that it only influences the levels of inflammatory factors, and points to a more complex role of HO-1 in mounting both the innate and adoptive immune response at cellular level [70].

Participation of HO-1 in the regulation of innate immunity was mainly investigated in the context of monocyte/macrophage lineage function. These studies were triggered by initial observations that $HO\text{-}1^{-/-}$ mice have elevated levels of MCP-1 (monocyte chemoattractant protein-1) – the proinflammatory factor regulating the response of monocytes and macrophages (reviewed in [71]). Further studies confirmed that lack of HO-1 causes the over-activated, proinflammatory phenotype of macrophages (reviewed in [70]). Otterbain et al. described the molecular mechanism that underlies this phenomenon. They showed that CO produced by HO-1 stimulates production of IL-10 by macrophages [72]. While IL-10 possesses potent anti-inflammatory properties, its decreased levels may explain the proinflammatory phenotype of macrophages in HO-1-deficiency. Moreover, not only the HO-1 activity stimulates the IL-10 production, but also IL-10 upregulates HO-1 expression [73]. This indicates the presence of positive

feedback mechanism and emphasizes the importance of HO-1 in anti-inflammatory function of IL-10.

The role of HO-1 in monocyte/macrophage lineage is not limited to regulation of function of mature macrophages. Recent study evidenced that HO-1 is involved in maturation of the myeloid cells from hematopoietic stem and progenitor cells. The specific deletion of HO-1 in myeloid lineage (Lyz-Cre:Hmox1$^{fl/fl}$) partially blocks differentiation of myeloid progenitors toward macrophages [74]. It was shown that CO, produced by HO-1, stimulates the differentiation of myeloid progenitors to macrophages, increases CD14 on their surface and enhances sensitivity toward M-CSF (macrophage colony-stimulating factor) stimulation [74].

The importance of HO-1 already in early differentiation steps of myeloid development was further confirmed by its role in myeloid derived suppressor cells (MDSC) – a population representing the immature myeloid cells circulating in the peripheral blood [75]. HO-1 was crucial for the immunosuppressive function of MDSC population also in IL-10-dependent manner [76].

HO-1 deficiency in macrophages has important consequence for maintenance of organism homeostasis as well as for resolution of pathological conditions. The latter was evidenced in a model of experimental autoimmune encephalomyelitis (EAE). The Lyz-Cre:Hmox1$^{fl/fl}$ mice developed more severe symptoms of EAE, what was correlated with exacerbated autoimmune T-cell response against myelin [77].

The connection of altered HO-1 expression in monocyte/macrophage lineage and autoimmune diseases are also supported by clinical observations. The CD14^{+} monocytes from patients with autoimmunological systemic lupus erythematosus (SLE) have decreased HO-1 expression both at mRNA and protein level [78].

The role of HO-1 in innate immunity is not limited solely to monocyte/macrophage lineage. Studies performed by our group showed that lack of HO-1 disturbs also granulocyte numbers. HO-1$^{-/-}$ mice have more granulocytes in peripheral blood, what is connected with disordered maturation of granulocytes in the bone marrow. Myelocytes, which are one of the steps in maturation of granulocytes in bone marrow, proliferate faster in HO-1$^{-/-}$ mice. Consistently, HO-1$^{-/-}$ myelocytes have higher expression of

C/EBPβ transcription factor, which drives the granulocyte differentiation (Bukowska-Strakova et al., in preparation).

Apart from important function in regulation of innate immunity, HO-1 is also implicated in regulation of adaptive immune response. First, the HO-1 affects the maturation of dendritic cells (DC). HO-1 induction reduced the antigen presentation by DC and inhibited their pro-inflammatory function [79]. On the other hand, HO-1 expression in DC conserves IL-10 expression that is connected with anti-inflammatory DC phenotype [80]. The mechanism of anti-inflammatory role of HO-1 in DC was linked with CO-dependent reduction of TLR signaling [81].

As expected, the inhibition of DC maturation by HO-1 leads to reduced T-cell toxicity. This was shown in a model of transgenic mice that have autoreactive $CD8^+$ T cells against insulin [81]. Such $CD8^+$ T-cells induce diabetes after adoptive transfer only when previously immunized with DC. However, when the DC were overexpressing HO-1, the $CD8^+$ cells lost ability to induce diabetes [81]. This confirms crucial role of HO-1 in DC in regulation of the adaptive immunity.

Finally, HO-1 was proposed to regulate the function of suppressive T regulatory cells (Tregs). It was shown that $CD4^+$ $CD25^+$ Tregs have constant expression of HO-1 [82]. The pharmacological inhibition of HO-1 in Tregs diminished their suppressive function [83]. Nevertheless, the next studies raised doubts about HO-1 role in Tregs, as the Tregs isolated from HO-$1^{-/-}$ mice showed normal suppressive function [84]. It was proposed, that it is HO-1 expression in DC that is required for Treg function, rather than intrinsic HO-1 in Tregs [85].

2.2.4. Nuclear form of HO-1

Majority of the effects ascribed to HO-1 are thought to be mediated by its enzymatic products. However, in 2002 the possibility of non-enzymatic function of HO-1 was underlined. The HO-1 mutant protein (H25A), that cannot bind heme and catalyze its degradation, was shown to protect cells against oxidative stress even better than the enzymatically active form [86].

The possible explanation of the non-enzymatic function of HO-1 came with discovery that HO-1 can localize in the nucleus [87]. It turned out that cytoplasmic HO-1 that is bound to the endoplasmic reticulum may be cut near the C-terminus and then is translocated into nucleus [87]. Furthermore, nuclear HO-1 may regulate binding of NFκB and SP-1 transcription factors as well as bind to the proteins involved in DNA repair [87]. Such activity of nuclear HO-1 might explain the observed non-enzymatic function.

Although the role of HO-1 in the nucleus seems to be independent of catalytic heme degradation, it cannot be excluded that HO-1 in nucleus sustains its enzymatic capabilities. Such possibility is suggested as the truncated form of HO-1 still possesses enzymatic activity [88]. But the question remains if HO-1 in the nucleus possesses an electron donor required to catalyze heme degradation. The electron donor for HO-1 reaction in cytoplasm is cytochrome P450 reductase [88]. However, cytochrome P450 reductase is absent in the nucleus. Thus the possible enzymatic activity of HO-1 in nucleus would be possible if the other electron donors can be used by nuclear HO-1.

2.2.5. HO-1 and tumor development

Increasing knowledge about importance of HO-1 in maintaining tissue homeostasis triggered questions about potential role in tumor development and its implication in tumor therapy. The first evidence indicating that HO-1 may be interesting in the context of tumor development was based on high HO-1 expression in many types of tumors (reviewed in [89]). In some cases, the HO-1 expression was induced by oncogenes such us viral G protein-coupled receptor (vGPCR) [90] or BCR/ABL fusion kinase [91]. HO-1 expression in tumor further increased after chemotherapy [92], radiotherapy [93] or photodynamic therapy [94], what might have important implications for tumor treatment outcome.

Research on immune response against tumors in patients revealed that HO-1 may be one of the crucial tumor antigens that is recognized by immune cells [95]. However, the recognition of the HO-1 in cancer cells did not result in elimination of the tumor, but governed the suppression of anti-tumor immunity [95]. While the accumulation of suppressive Tregs in tumor microenvironment that abrogates the anti-tumor response is well evidenced, the group of Andersen and colleagues isolated a novel population of

$CD8^+$ Tregs from cancer patient, that have higher suppressive capabilities than classical $CD4^+$ fraction of Tregs [95]. Interestingly, suppressive $CD8^+$ Tregs specifically recognized HO-1 in patients with three different types of tumors: melanoma, renal cell carcinoma and breast cancer [95]. There were no such cells in healthy controls. This study indicates that high HO-1 expression identified different types of tumor cells, what is crucial for regulation of immune response against tumors.

Although HO-1 was recognized as an important part of tumor biology, further research showed that the role of HO-1 in tumor development is highly complex (reviewed in [96]). First, HO-1 may have different role at different stages of tumor development, e.g. in initial carcinogenesis and subsequent tumor progression. Second, the role of HO-1 in different types of tumors may be contradictory. Finally, the nuclear localization of HO-1 in tumors, as well as the HO-1 expression in tumor microenvironment, also have to be considered.

2.2.6. HO-1 implications in carcinogenesis

The tumor transformation is a multistep process that initially requires accumulation of several mutations [36]. It is well accepted that chronic inflammation triggers DNA damage and additionally provides proliferative signaling environment, what all together results in accelerated tumor transformation [36]. Given that HO-1 is induced by many stress factors and exerts anti-inflammatory function, one may expect that HO-1 protects against malignant transformation.

One evidence confirming this supposition came from observations of areca chewers. Areca is a carcinogen that causes oxidative stress and genotoxicity what results in high incidence of oral squamous cell carcinoma (OSCC) among people chewing areca [97]. The risk of most common type of OSCC caused by areca, buccal squamous cell carcinoma (BSCC), is higher among subjects having more (GT) repeats in HO-1 promoter what is linked with lower HO-1 expression, while shorter (GT) repeat allele, that is linked with higher HO-1 expression, may protect from BSCC [97].

Several other studies also evidenced the association of the long (GT) repeats in proximal HO-1 promoter and higher risk in lung adenocarcinoma, gastric adenocarcinoma, breast

cancer and malignant mesothelioma (reviewed in [98]). However, few other analyses stated the opposite relation in case of melanoma, gastric and pancreatic cancer (reviewed in [98]).

Nevertheless, even if the correlation studies linked the lower HO-1 expression with higher risk of different tumors, the prospective studies are needed to confirm that the observed associations have a causative relation. Our group used a model of HO-$1^{-/-}$ mice and a chemical carcinogen inducing SCC to verify this hypothesis [99]. The carcinogen-induced lesions were detected earlier in HO-$1^{-/-}$ mice than in HO-$1^{-/+}$ and HO-$1^{+/+}$ mice. The number of lesions in HO-$1^{-/-}$ mice was higher and connected with higher mortality [99]. However, despite the faster tumor appearance in HO-1 deficient animals, the tumors in HO-$1^{-/-}$ mice resembled benign papillomas, while tumors in HO-$1^{+/+}$ mice where more dysplastic and invasive carcinomas [99]. This observation suggests that the HO-1 may be protective against tumor transformation, but may facilitate the growth of already established tumors.

2.2.7. HO-1 in tumor progression

Several experiments aimed to determine the function of high HO-1 expression in established tumor cell lines. Given the known cytoprotective function of HO-1, the primary question was if HO-1 governs tumor cell survival and resistance to apoptosis. Indeed, genetic silencing of HO-1 in hormone refractive prostate cancer cell lines reduced their viability [100]. Furthermore, HO-1 silencing decreased viability of chronic myeloid leukemia cells and sensitized acute myeloid leukemia cells to TNF-induced cell death [101]. Decreased HO-1 expression was also linked with higher apoptosis rate in lung cancer cell line [102].

Consistently, HO-1 induction by heme in thyroid cell carcinoma increased resistance to apoptosis by p38 MAPK- and ERK-mediated mechanism [103] and protected chronic myeloid leukemia from BCR/ABL inhibitor-induced apoptosis [91]. Elevated HO-1 expression governed insensitivity to apoptotic stimuli of gastric cancer cell lines, independently of the mutation among p53 gene [104]. Pharmacological induction of HO-1 by CoPP decreased apoptosis of colon carcinoma cell line in serum deprivation conditions by biliverdin/bilirubin connected mechanism [105]. Similarly, our group

showed that melanoma cell lines overexpressing HO-1 displayed higher resistance to H_2O_2-triggered oxidative stress and cell death [106].

Apart from resisting the cell death, hallmarks of cancer comprise also sustained, increased proliferation rate [36]. While the studies consistently suggested that HO-1 protects tumor cells from cell death, its role in proliferation is not clear. The lessons from non-transformed tissues showing that HO-1 can oppositely regulate different types of cells have also implications in tumor biology. Overexpression of HO-1 accelerated proliferation of melanoma cells and silencing HO-1 by pharmacological or genetic means resulted in decreased proliferation in case of pancreatic cancer, prostate carcinoma, hepatocellular carcinoma, neoplastic mast cells and urothelial cancer cells (reviewed in [89]). However, silencing HO-1 had also opposite effects, suggesting anti-proliferative properties of HO-1 in lung adenocarcinoma cell line [107], breast cancer [108] and prostate cancer cells [109]. This was further showed in non-small cell lung carcinoma model, where overexpression of HO-1 blocked cell proliferation [110]. Altogether, altering HO-1 expression in tumor cells suggested its role in protection from cell death, while HO-1 function in regulation of proliferation is less consistent and depends on type of tumor.

Finally, *in vivo* experiments verified how HO-1 affects the tumor growth. Most of the studies showed that HO-1 facilitates tumor growth, as demonstrated in case of hepatoma [111], sarcoma [90], lung cancer [112], melanoma [106] and some of the prostate cancer cell lines ([100], reviewed in [89]).

However, there are also few experiments evidencing anti-tumoral effect of HO-1. Non-small cell lung carcinoma cell line NCI-H292, overexpressing HO-1, formed smaller heterotopic tumors than the control cell line [110]. This was linked with upregulation of tumor suppressive microRNAs and downregulation of microRNAs facilitating the tumor growth, with the microRNA-378 being the most downregulated and at least partly responsible for the HO-1 antitumor effect [110].

The controversy exists also on how HO-1 influences the growth of prostate cancer cells. While it was shown that silencing HO-1 reduced *in vivo* tumor growth of hormone refractory prostate cancer cells (HRPCa) [100], other study evidenced that overexpression of HO-1 in androgen resistant PC3 blocked tumor growth *in vivo* [109].

To fully understand the complex role of HO-1 in tumor progression and potentially translate this knowledge to clinical applications one may need to understand the mechanism underlying the contradictory results. The explanation of HO-1-dependent inhibition of NCI-H292 tumor growth may be connected with the regulation of tumor angiogenesis. Although HO-1 is recognized as proangiogenic factor (described in subchapter "HO-1 as regulator of angiogenesis"), the overexpression of HO-1 in NCI-H292 resulted in downregulation of proangiogenic microRNAs: miR-17-92, miR-210 and miR-378, and upregulation of antiangiogenic miR-424 [110]. Secondly, HO-1 overexpression reduces the inflammatory status of the tumors, what may lead to diminished inflammation-driven tumor angiogenesis [110]. Altogether, this leads to less pronounced vascularization and oxygenation in HO-1 overexpressing NCI-H292 tumors. Nevertheless, it is important to underline that antiangiogenic effect of HO-1 seems to be unique for NCI-H292, as in other tumor models: melanoma, hepatocellular carcinoma, breast cancer and glioma HO-1 serves as proangiogenic factor (reviewed in [89]).

The inconsistent data on role of HO-1 in prostate cancer may be better understood in the context of different subcellular localization of HO-1. Węgiel and colleagues evidenced that nuclear localization of HO-1 in prostate cancer cells is correlated with worse survival prognosis of patients [113]. Moreover, the prostate cancer cells, including the PC3 cell line, also showed high nuclear localization of HO-1, what was linked with diminished enzymatic heme degradation capability [113]. Pretreatment of PC3 cells with carbon monoxide, the enzymatic product of HO-1, blocked tumor growth and additionally sensitized them to doxorubicin, by mechanism dependent on metabolic exhaustion of mitochondria [113]. This observation indicates that nuclear and cytoplasmic HO-1 might have opposite roles in tumor development: nuclear form may facilitate the tumor growth, while the cytoplasmic may reduce tumor growth by altering the cell metabolism.

Indeed, there are observations confirming pro-tumoral effects of nuclear HO-1. Hsu et al. showed that cytoplasmic HO-1, cut by signal peptide peptidase and then translocated to nucleus, facilitated growth of A549 lung cancer and DU145 prostate cancer cell lines [114]. Other reports also evidenced the correlation of nuclear HO-1 localization and progression of prostate cancer [115], lung cancer [116] and HNSCC [117].

2.2.8. HO-1 implication in resistance to treatment and cancer stem cells

HO-1 confers cytoprotection and apotosis resistance to cancer cells (described in "HO-1 in tumor progression" section). Given that HO-1 expression is induced by anti-cancer treatments: chemotherapy, radiotherapy and phototherapy, it was postulated that HO-1 may be one of the factors responsible for insensitivity to anti-cancer therapies.

The *in vitro* results confirmed this hypothesis. Inhibition of HO-1 allowed to overcome resistance of several different cancer cell lines to radiotherapy, chemotherapy and photodynamic therapy (reviewed in [89]). Not only HO-1 may protect cancer cells from classical therapies, but also may be implicated in resistance to novel tyrosine kinase inhibitors. It was shown that nuclear HO-1 is responsible for resistance to imatinib in chronic myeloid leukemia cells [118].

The *in vivo* experiments on pancreatic cancer also showed that inhibition of HO-1 potentiates the anti-tumoral efficacy of taxol [100]. Finally, the anti-tumoral effect of HO-1 inhibition may be exceptionally effective in cancer cells harboring specific mutations. This was shown in case of fumarate hydratase (FH), which is characteristic for the renal cell cancer [119]. The FH is an enzyme involved in tricarboxylic acid cycle (TCA) and its mutation blocks this crucial energetic process with simultaneous reprograming metabolism of the cancer cells [119]. It turned out that inhibition of HO-1 in cells with FH mutation is lethal [119]. This means that cancer therapy based on HO-1 inhibitors may be exceptionally effective in FH-deficient cancers.

These promising results were consistent with clinical observations of nasopharyngeal carcinoma patients. The patients with low HO-1 expression responded to the radiotherapy, in contrast to almost 60% of patients with high HO-1 expressing tumors who were insensitive to the therapy [93].

Data supporting role of HO-1 in facilitating tumor progression and resistance to treatment trigger the attempts to design HO-1 inhibitors as potential anti-cancer drugs. Initially, the efforts were focused on metalloporphyrins that inhibit enzymatic activity of HO-1, such us zinc and tin protoporphyrin (ZnPP and SnPP, respectively), including their pegylated and polymer-encapsulated forms (reviewed in [96]). However, their lack of specificity and upregulation of HO-1 mRNA moved the research toward imidazole-based

inhibitors (e.g. OB-24), but still the potential inhibitors are not ready to enter the clinical phase [96].

While exploring the possibility of HO-1 as potential drug target, one should consider the new discoveries in cancer biology indicating that the treatment resistance of cancers is connected with cancer stem cells [120]. The concept of cancer stem cells implies that there is a minor fraction of cancer cells, that show features typical for tissue stem cells: ability to self-renewal and production of differentiated progeny [120]. It is postulated that these cancer stem cells are the most resistant to treatment. Thus, even if the present therapies kill vast majority of tumor cells, still few surviving cancer cells with stem cell properties drive tumor relapse. Given that HO-1 confers the treatment resistance, it is justified to postulate that it is HO-1 function in cancer stem cells that is crucial for insensitivity for cancer therapy.

First evidence confirming this hypothesis was presented by Herrmann and colleagues [121]. They isolated acute myeloid leukemia cells from patients and sorted the leukemic cells with stem and progenitor phenotypes ($CD34^+CD38^-$ and $CD34^+CD38^+$ respectively) [121]. The leukemia stem and progenitor cells had high expression of HO-1 and pharmacological inhibition of HO-1 blocked their growth both *in vitro* and *in vivo* after transplantation in immunocompromised mice. This confirmed that the HO-1 is an important survival factor for leukemia initiating cells.

2.3. Immune cells influence on the tumor growth

The complex interplay between immune system and developing tumor is critical for the growth and expansion of cancer cells [122]. It was evidenced that impaired function of immune system leads to high risk of cancer occurrence. Several genetically modified mouse strains that are immunocompromised have higher frequency of spontaneous and carcinogen-induced tumors (reviewed in [123]). The clinical observations also confirmed this observation. The organ recipients, who receive immunosuppression treatment, are more prone to several types of cancers [124]. Higher incidence of various types of cancer was also observed among patients with AIDS [125].

These observations could be explained by current immunology. The immune system can recognize not only *self* versus *pathogen* or *self* versus *non-self*, but also *self* versus *malignant-self* [123]. Upon recognition of malignant cell, there are specialized cells: natural killer cells, natural killer T cells as well as $CD8^+$ lymphocytes that show direct cytotoxicity against tumor cells [122]. But the participation of immune cell should not be understood only as recognition and killing of tumor cells – the interaction between immune cells and tumor cells is more complex and different at various steps of tumor development. Overall, current view is that immune response against tumor determines its development, by selection of the particular clones of tumor cells [126]. This concept is referred to as tumor immunoediting and it classifies the interactions of immune cells and tumor into three distinct phases [126]. During the first *elimination* phase, the NK, NKT and $CD8^+$ cells recognize and destroy the cancer cells, by means of different mechanisms, e.g. perforins, TRAILs or ROS. These cells create a strong immune pressure what, together with genetic instability of tumor cells, leads to next *equilibrium* phase [126]. In this phase, there is a selection of the tumor clones with the low immunogenicity, in a analogical way to Darwin selection theory. It is thought that this phase lasts the longest and next acquired mutations result in tumor cells with lowest immunogenicity, able to escape immune system [126]. This inevitably ends with the last *escape* phase – fast growth of tumor cells that are not recognized by immune system [126].

2.3.1. Immunosuppressive cell infiltrating tumors

The escape of tumor cells from immune system is not only the result of immunoediting and selection of low-immunogenic tumor cells. The escape phase is also accelerated by immunosuppressive cell populations that inhibit anti-tumor response [122]. This contributes to escape phase and facilitates tumor development. The most studied immunosuppressive populations implicated in tumor development include Tregs [127], myeloid derived suppressive cells (MDSC) [128] and tumor associated macrophages (TAM).

The presence of T cells, that have unique immunosuppressive function, was already proposed in 80's [127]. However, their identification remained problematic for years,

until Tregs were defined in 1995 [129]. It was evidenced that T cells with $CD4^+CD25^+$ phenotype protected the athymic nude mice against immune response from transplanted $CD25^-$ T lymphocytes [129]. Finally, the Tregs were characterized by expression of FOXP3 transcription factor [130].

Further research unambiguously showed that Tregs are indispensable for immune tolerance. Conditional deletion of Foxp3 in mice led to autoimmune diseases [131]. Patients with IPEX (Immunodysregulation, Polyendocrinopathy, Enteropathy, X-linked) syndrome, who have mutations in FOXP3 gene, developed severe autoimmune diseases in early age [132].

The immunosuppressive capabilities of Tregs, that are crucial to sustain tissue homeostasis, in the context of cancer may play a negative, protumorigenic role. There are several evidences that cancer patients have increased numbers of Tregs in peripheral blood, lymph nodes, as well as in tumor infiltrate [127]. After the surgical resection of tumors the number of Tregs decreases, but the tumor reoccurrence is correlated with rebound of Treg numbers [133]. Above observations move towards considering Tregs as biomarker. Indeed, the increased number of Tregs often negatively correlates with patient's survival [133, 134]. The same was observed in case of ratio of Tregs to T effector cells (Treg/Teff) [135].

The cells with immunosuppressive function were also identified among the myeloid lineage and subsequently called myeloid-derived suppressor cells (MDSC) (reviewed in [136]). MDSC is a heterogeneous cell population of myeloid precursors. In homeostatic conditions myeloid progenitor cells differentiate toward granulocytes, monocytes and dendritic cells in the bone marrow and only mature cells are released into circulation. However, during pathological conditions, such as inflammation, malignancy or autoimmunological diseases, the higher numbers of immature myeloid cells in circulation are observed [136].

MDSC populations in mouse models are defined as cells expressing the general myeloid markers, but without expression of markers typical for mature myeloid cells [136]. It was shown that MDSC population could be divided in two phenotypically distinct fractions. One shows granulocyte characteristics (expression of Ly6G) while the second

resembles monocytes (expression of Ly6C) [136, 137]. Several more markers allow to distinguish these subpopulations (Table 1).

Marker	Function	G-MDSC	M-MDSC
CCR2	Receptor for CCL2 (MCP-1)	+	+
CXCR4	Receptor for CXCL12 (SDF-1)	+	+
CXCR2	Receptor for CXCL1 (KC), CXCL2 (MIP-2) and CXCL5 (LIX)	+	+
CD11b	Integrin alpha M (adhesion)	+	+
CD11c	Integrin, alpha X (adhesion)	Subset	Subset
M-CSFR	Receptor for M-CSF	Subset	+
F4/80	Adhesion	-	+
Gr1	Composite epitope between the Ly6C and Ly6G	Bright	Low
Ly6C	Not clear	Low	+
Ly6G	Not clear	+	-
MHC I	Antigen presentation	+	+
MHC II	Antigen presentation	Some models	Some models
Sca-1	Adhesion	Subset	Subset
Tie-2	Angiopoietin receptor	-	-
VEGFR1	Receptor for VEGF	+	+
VEGFR2	Receptor for VEGF	+	+

Table 1. Mouse MDSC subpopulations characteristics (adapted from [137]).

Independently of the heterogeneity, the common feature of MDSC is their biological activity: ability to inhibit adoptive T cell response [136]. Recently, it was evidenced that MDSC may also regulate the innate immunity [138].

Expansion of MDSC in cancer is regulated by factors secreted by tumor cells [139]. Cancer cells produce several factors, which stimulate myelopoiesis, but simultaneously inhibit maturation of myeloid cells. As the result, the number of immature myeloid cells in bone marrow, spleen and tumor is increased. Till now, expansion of MDSC was shown to be driven by IL-6, G-CSF, M-CSF, VEGF and MCP-1 [139].

The numbers of MDSC were also proposed to be used as clinical biomarker in cancer therapy. The melanoma patients had more MDSC in peripheral circulation, but the resection of tumor or treatment with the anti-CTLA-4 antibody ipilimumab did not alter

their numbers [140]. Although the MDSC numbers were not affected during the treatment, their initial number was correlated with effectiveness of ipilimumab administration: the lower MDSC numbers selected patients who better responded to ipilimumab [140].

Macrophages are other myeloid populations that possess immunoregulatory functions. Macrophages are one of the most abundant cell populations in tumor microenvironment and this distinct cell subset is referred to as TAM (reviewed in [141]). Although TAM can be both pro-tumorigenic and anti-tumorigenic, it is thought that their accelerating tumor growth activity prevails [141]. TAM are mainly derived from the generated in BM circulating pool of $Ly6C^+$ monocytes, rather than from tissue-resident macrophages originating from yolk-sac progenitors [142, 143]. The main factor that recruits $Ly6C^+$ monocytes to the tumor niche is M-CSF. Deletion of M-CSF in several tumor models resulted in lower TAM numbers and inhibition of tumor development (reviewed in [141]). Consistently, patients with higher M-CSF levels had worse survival prognosis [144]. The special attention is put to Tie-2 expressing fraction of TAM. $Tie2^+$ TAM are found adjacent to tumor vessels and allow spreading of tumor cells [145]. Genetic ablation of this population inhibits tumor growth, mainly by affecting tumor vascularization [146].

Within the tumor niche macrophages can play both immunosuppressive and immunostimulatory function. The immunoregulatory role is based on inhibition of T, NK and NKT cell cytotoxicity, triggering their apoptosis, as well as recruiting the Tregs [141]. Therefore, the crucial question is what are the factors that drive the immunosuppressive differentiation of TAM against their immunostimulatory fate. Till now, IL-4 was recognized to be involved in promotion of suppressive character of TAM [147]. However, the role of tumor niche is highly complex and some factors, such as GM-CSF (granulocyte-macrophage colony-stimulating factor) may play both immunosuppressive and immunostimulatory role depending on the niche context [148, 149]. Nevertheless, regulation of TAM differentiation to shift them into anti-tumorigenic state remains novel, promising anti-cancer strategy [141].

Finally, it is worth mentioning that both discussed myeloid populations, namely MDSC and TAM, apart from their immune modulatory role, may also promote tumor angiogenesis and therefore further facilitate tumor growth [128, 146].

2.3.2. Role of HO-1 in tumor immunosuppression

HO-1 is recognized as enzyme with immunosuppressive activity. The best characterized immunosuppressive role of HO-1 has been described in transplantation studies [70]. MDSC showed high HO-1 expression, but when HO-1 activity was pharmacologically inhibited, MDSC decreased expression of IL-10 and lost their immunoregulatory abilities, what led to transplant rejection [76].

Therefore, given that HO-1 is important in MDSC biology, it is justified to suppose that HO-1 affects tumor growth in MDSC-dependent mechanism. Indeed, the mouse chimeras that received bone marrow transplantation from HO-$1^{+/-}$ donors had less lung metastasis. This was linked with lower number of myeloid cells in premetastatic niche. However, authors showed the role of general population of $CD11b^{+}$ myeloid cells, and they did not distinguish if the crucial role could be ascribed to MDSC or TAM or both of these populations.

The evidence that HO-1 may be responsible for immunosuppressive function of TAM was presented by Arnold and colleagues [150]. They identified minor subpopulation of $CCR2^{+}F4/80^{hi}CD206^{+}$ TAM that express fibroblast activation protein α (FAP) which was crucial to govern the immune privilege of tumor [150]. FAP^{+} TAM population was the main source of the tumoral HO-1, and the specific deletion of FAP^{+} population using diphtheria toxin receptor system restored the anti-tumor response [150]. Importantly, pharmacological inhibition of HO-1showed similar results as the depletion of FAP^{+} TAM [150]. Thus it is likely that HO-1 activity in FAP^{+} TAM is a crucial factor that maintains immunosuppression of the tumor niche.

2.4. Mobilization of bone marrow cells to peripheral blood

As discussed above tumor occurrence is linked with a higher number of circulating hematopoietic cells. The pool of circulating cells induced by tumor includes those that are absent during physiological conditions. Therefore, much attention was placed on study how these cells translocate from the bone marrow to the peripheral circulation.

2.4.1. Cellular mechanism of mobilization

In steady-state conditions, mature blood cells are released from the bone marrow to the blood to sustain hematological homeostasis [151] (Fig. 4). The process of new blood cells' production and their release from bone marrow is tightly regulated. The bone marrow provides a barrier to limit egress of immature cells to peripheral blood and allows circulation of only small numbers of hematopoietic stem cells [151].

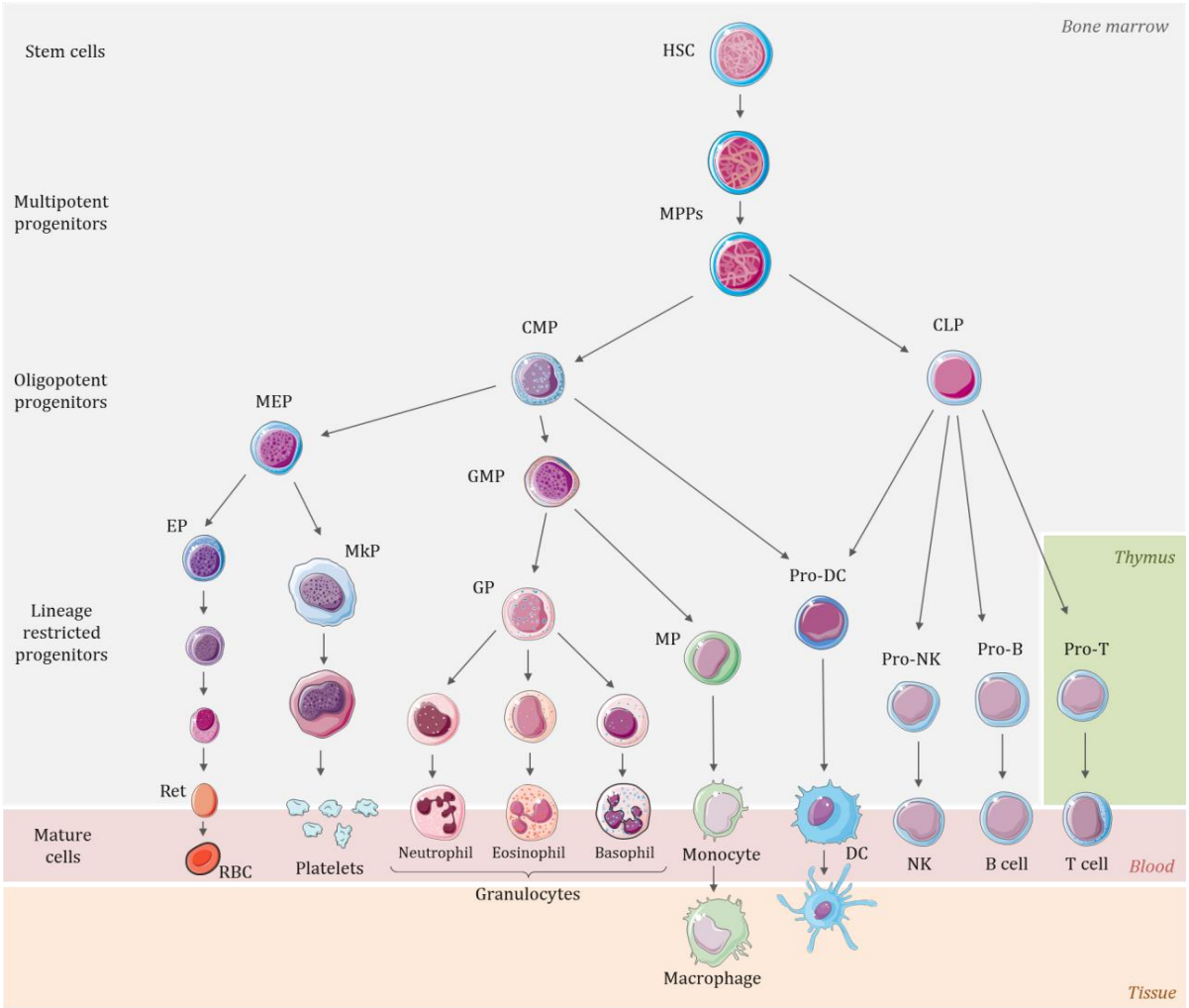

Fig. 4. Scheme of hematopoiesis.

In response to stress stimuli, such as inflammation or neutropenia, as well as in pathological conditions, such as developing tumor, hematopoiesis is accelerated and more cells are released from the bone marrow to the circulation [151] in a process of mobilization [152]. In contrast to steady state conditions, the pool of emergency

mobilized cells includes the increased number of stem and immature hematopoietic cells [153].

Mechanism of mobilization is complex and involves activity of several bone marrow cell populations and cytokine pathways [152, 153]. Upon emergency or pharmacologically-induced mobilization, the BM environment undergoes rapid changes. Concentration of proteolytic enzymes such as cathepsin and elastase increases. Enhanced proteolytic activity leads to cleavage of adhesive molecules that keeps cells in the bone marrow niche [153]. Other components of BM niche: endothelium, macrophages, osteoblasts and sympathetic nerves, all play a crucial role in mobilization. Endothelium barrier becomes more permeable, allowing cells to enter the circulation. Macrophages and osteoblasts activity regulate bone remodeling [153]. Finally, the sympathetic nerves control activity of other cells in BM niche and orchestrate cell egress [154].

2.4.2. Molecular factors regulating mobilization and their application in clinic

Several cytokines regulate mobilization of bone marrow cells. G-CSF is one of the best characterized mobilizing factor [152]. G-CSF acts on the bone marrow myeloid progenitors and drive their proliferation as well as differentiation toward granulocytic lineage [155]. Studies on G-CSF-deficient mice showed that G-CSF is crucial both for basal conditions and emergency granulopoiesis [156–158]. The G-CSF receptor (G-CSFR) involves Janus kinase (Jak) and signal transducers and activators of transcription (STATs) signaling [159]. Although G-CSF administration mobilizes both stem cells and granulocytes, the mobilization of stem cells by G-CSF is independent of G-CSFR as shown in G-CSFR-deficient mice [160]. This suggests some indirect mechanism(s) and involvement of other than G-CSF regulatory factors [161].

Apart from G-CSF and SDF-1α, many other agents, such as SCF (stem cell factor), VEGF, IL-3, IL-6, GM-CSF and M-CSF, can act as mobilizing factors [152]. However, their *in vivo* importance, mutual interactions and mechanism of action are still not fully understood.

Current progress in basic science concerning mobilization has been already successfully translated into clinical practice [162]. Pharmacological mobilization is of outstanding importance to treat neutropenia, that is often a serious side effect of anti-tumor

therapies such as chemotherapy or radiotherapy. Moreover, treating many hematological malignancies involve bone marrow transplantation (BMT) [163]. The success of bone marrow transplantation depends on collection of enough numbers of HSC [164]. Nowadays, the source of transplantable HSC is not necessarily bone marrow itself, but often collected peripheral blood after mobilization of HSC into circulation [162].

The recombinant G-CSF (filgrastim) is used to treat different forms of neutropenia and to mobilize HSC to peripheral blood for subsequent HSC collection by leukapheresis and transplantation [162]. Other clinically approved drug to mobilize HSC is AMD3100 (plerixafor), that blocks CXCR4 signaling [165].

Despite improvement in treating neutropenia and BM transplantation, in some patients application of these drugs is inefficient. Among healthy donors G-CSF mobilization fails in 5%-30%, but in high-risk patients the failure rate reaches even up to 60% [162]. Moreover, production of the recombinant protein is expensive. Therefore, new agents which can induce endogenous G-CSF or provide additional activities are currently investigated for treatment of neutropenia [166]. Better understanding of mechanism underlying the mobilization will help to improve current clinical strategies as well as will contribute to develop new, more efficient mobilizing methods [162].

3. AIM OF THE STUDY

The role of HO-1 in carcinogenesis is still unclear and depends on cancer type. Moreover, different cancer treatments, such as chemo- and radiotherapy, upregulate HO-1 expression. On the other hand, HO-1 is important in the modulation of the immune response, which is now recognized as one of the most important factors in cancer development.

The main aim of our study was to investigate the role of HO-1 in the development and progression of squamous cell carcinoma in two different models. Using chemical carcinogenesis model in mice with different HO-1 expression level we tried to verify the **1st hypothesis, that HO-1 protects against chemical oral carcinogenesis.** We specifically concentrated on evaluating if HO-1 deficient mice will be more susceptible and HO-1-overexpressing mice – protected from 4NQO-induced carcinogenesis.

Next, using a model of subcutaneous injection of HO-1-overexpressing cells into syngeneic mice we aimed to verify the **2nd hypothesis, that HO-1 overexpression in cancer cells facilitates tumor growth, angiogenesis and infiltration with suppressive leukocyte populations.** Moreover we aimed to investigated the systemic effects of HO-1 overexpression in the tumor on leukocyte populations and cytokine concentrations in blood.

During one of the experiments aiming to investigate the effect of pharmacological induction of HO-1 on leukocyte infiltration, we observed unexpectedly that HO-1 inducer, CoPP, increases leukocyte counts and G-CSF concentration in the blood. That led to the additional **3rd hypothesis, that CoPP induces the mobilization of cells from the bone marrow to the blood.** We aimed to verify if CoPP-mobilized granulocytes and HSPC are functional and if effects of CoPP treatment are dependent on HO-1 activity.

4. MATERIALS AND METHODS

4.1. Cell lines

Murine squamous cell carcinoma cell line SCC VII was kindly provided by prof. Lukas Mach, Department of Applied Genetics and Cell Biology, University of Natural Resources and Applied Life Sciences, Vienna, Austria. SCC VII and Phoenix-Eco cells were cultured in Dulbecco Modified Eagle's Medium with 4.5 g/l glucose (DMEM HG, Lonza) with 10% fetal bovine serum (FBS, Lonza), penicillin and streptomycin (100 U/ml and 100 μg/ml, respectively, Sigma).

MBrMEC (FVB), MLuMEC (FVB), MLuMEC (FVB), MPLNHEC (FVB), MSplMEC (FVB) murine endothelial cells were kindly provided by prof. Claudine Kieda, Centre for Molecular Biophysics, Department of Cell Recognition and Glycobiology, Orleans, France. Endothelial cells were cultured in OptiMEM (Gibco), 2% FBS (Lonza), penicillin and streptomycin (100 U/ml and 100 μg/ml, respectively, Sigma). All cell cultures were performed in 37°C, 5% CO_2 and passaged with trypsin with EDTA (Gibco).

4.1.1. Retroviral transduction

Retroviral vectors (RVs) were produced using Phoenix-Eco packaging cells. SCC VII cells were transduced with RVs, generated using pMSCV-Luc plasmid. MSCV Luciferase PGK-hygro, a gift from Dr. Scott Lowe (Addgene plasmid #18782) was provided by prof. Claudine Kieda. SCC VII-Luc cells with stable expression of transgene were selected using hygromycin (0.5 mg/ml, Invitrogen). Next, SCC VII-Luc cells were transduced with RVs, generated using pBABE-puro-HO-1 plasmid and selected with puromycin (5 μg/ml, Sigma-Aldrich). pBABE-puro-HO-1 plasmid was constructed from pBABE-puro [167] and pdAAV-CMV-HO-1 plasmids. pBABE-puro was a gift from Drs. Hartmut Land, Jay Morgenstern & Bob Weinberg (Addgene plasmid # 1764).

4.1.2. Proliferation

SCC VII cells were seeded in 24-well plates (50 000 cells/well). After 48 hours the cells were detached with trypsin and counted using a Burker chamber or Muse Cell Analyzer (Millipore).

4.1.3. Migration/invasion assay

SCC VII cells were stained with PKH26 (Sigma) according to the manufacturer's protocol and seeded in the apical chambers of rehydrated 24-well plates BD BioCoat Tumor Invasion System (BD) with FBS as a chemoattractant (Fig. 5).

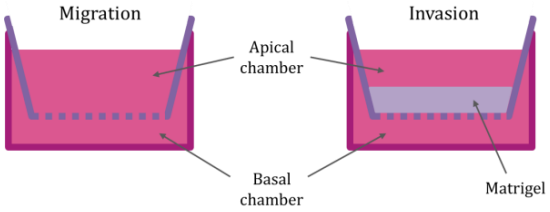

	Migration	Invasion
Cells to seed	50 000/well	50 000/well
Apical chamber	500 µl medium 0% FBS	500µ l medium 0% FBS
Basal chamber	1400 µl medium 10% FBS	750 µl medium 10% FBS

$$\%\ invasion = \frac{Mean\ RFU\ of\ cells\ invaded\ through\ Matrigel - coated\ membrane}{Mean\ RFU\ of\ cells\ migrated\ through\ uncoated\ BD\ FluoroBlock} \times 100$$

Fig. 5. Migration/invasion assay settings.

The plates were incubated for 16 hours and the fluorescence (excitation 551 nm, emission 567 nm) from cells which migrated through the porous membrane was measured using Infinite 200 PRO microplate reader (Tecan).

4.1.4. Adhesion assay

Murine endothelial cells were seeded in 24-well plates and allowed to grow for 48 hours until the confluence reached around 80%. SCC VII cells were detached with EDTA, stained with PKH26 (Sigma) according to the manufacturer's protocol and added to the endothelial cells at the 5:1 ratio. After 20 minutes incubation at 37°C all cells were trypsinized and percentage of $PKH26^+$ cells was analyzed by flow cytometry.

4.2. Mice

Animals were handled in a strict accordance with good animal practice as defined by the relevant national and local animal welfare bodies. All animal work was approved by the Local Ethical Committee for Animal Research at the Jagiellonian University (approval numbers: 106/2007, 180/2014, 8/2015 and 28/2015).

Breeding heterozygote pairs of C57BL/6xFVB HO-$1^{-/-}$ mice were initially provided by Dr. Anupam Agarwal, University of Alabama, Birmingham, USA. Nrf2-deficient C57BL/6 mice ($Nrf2^{-/-}$) were generated by Itoh et al. as described previously [168] and kindly provided by prof. Antonio Cuadrado (Universidad Autonoma de Madrid, Spain) together with control, $Nrf2^{+/+}$ mice. HO-1 transgenic mice overexpressing human HO-1 under keratin 14 promoter [58] were created in the cooperation with dr. Yann Herault at

Centre for Transgenic Animals, CNRS, Orleans, France. Transgene expression was confirmed at mRNA and protein level [58]. C3H mice were purchased from Charles River and Harlan Laboratories. C57BL/6-Tg(UBC-GFP)30Scha/J were bought from the Jackson Laboratories.

Chemical carcinogenesis experiment and CoPP mobilization experiment on HO-1$^{-/-}$ mice were performed in conventional animal facility. All other experiments were performed in specific pathogen free (SPF) conditions.

4.3. Chemical carcinogenesis

One-month old C57BL/6 and C57BL/6xFVB female mice were treated with 4NQO (50 mg/l, Sigma-Aldrich), dissolved in drinking water, for 18 weeks or until we noticed severe weight loss. Control mice received only water. Mice were euthanized by overdosage of xylazine and ketamine. Blood was collected from the vena cava and after clot formation centrifuged for 10 minutes at 1000 *g*. Serum was collected and frozen at -80^{o}C for further analysis. Gastrointestinal tract and other major organs were examined for macroscopically visible lesions. Tongues were cut in half, part for RNA isolation was frozen at -80^{o}C and part for histological analysis fixed in 10% neutral buffered formalin for 24 h.

4.3.1. Tissue processing

Tongue samples fixed in formalin were subsequently passed through increasing ethanol concentrations (70% - 1 h, 90% - 1 h, 99% - 3 h, POCH) and xylene (2 × 30 minutes, POCH). Finally, the samples were soaked and embedded in paraffin (Thermo Fisher).

4.4. Subcutaneous tumor injection

For implantation of tumor cells mice were anesthetized with intraperitoneal (i.p) injection of Avertin aqueous solution (0.25 mg/g of body weight; Sigma-Aldrich) and shaved. SCC VII-Luc and SCC VII-Luc-HO-1 cells were injected subcutaneously into syngeneic C3H mice. 1x10^{6} of cells were injected with 250 µl of Matrigel. Two plugs with the same cell line were injected per mouse and three independent experiments were done. 5-, 7- and 2-month old female C3H mice were used for 1 month, 14 days and 5 days long experiments, respectively.

In 5-day long experiment, some mice were additionally injected with tin protoporphyrin (SnPP) and cobalt protoporphyrin (CoPP) on 1 day before cell injection, then 1 and 3 days after cell injection. CoPP and SnPP (Frontier Scientific) were dissolved in DMSO (Sigma-Aldrich) to achieve the concentration of 0.2 g/ml. The stock solutions were diluted 160x in NaCl. Mice were injected i.p. at the dose of 10 mg/kg (15 μmol/kg). Control mice received DMSO diluted 160x in NaCl.

4.4.1. *In vivo* luciferase measurement

Mice were injected with 200 μl of luciferin (15 mg/ml, Promega) 20 minutes before measurement. After 15 minutes mice were anesthetized with isoflurane (Baxter) and depilated using Veet hair removal cream. Measurements were done using IVIS Lumina (PerkinElmer). Exposure time for bioluminescence measurements was 60 seconds with medium binning mode. Results were calculated from the total photon counts.

4.4.2. Tumor size measurement

Tumor dimensions were measured using caliper. Tumor volume was measured using formula: $V = a \times b \times \frac{b}{2}$, where a is a bigger dimension and b is a smaller dimension.

4.4.3. Sample collection

After 5, 14 or 32 days of experiment the mice were sacrificed, then tumors were dissected and divided into two parts. One part was fixed in 10% neutral buffered formalin for histological analysis. Second part was prepared for flow cytometry analysis. The tumors were fragmented with scalpel blade and digested in 0.5 ml of enzyme mix (37°C, 1 h) consisted of liberase TM 3 U/ml (Roche), hyaluronidase 25 μg/ml (Sigma-Aldrich), DNAse 25 μg/ml (Roche) and dispase 3 U/ml (Sigma-Aldrich). After 1 hour, the reaction was stopped with 0.5 ml of FBS and samples were placed on ice. Cell suspension was filtered through 70 μm strainer (BD Bioscience).

4.4.4. Tissue fixation

Tumor samples were fixed in Shandon Excelsior ES tissue processor (Thermo Scientific) using the following protocol:

	REAGENT	TEMP	TIME	Drain	Vacum	SUPPLIER
1	10% buffered formalin	RT	24 h	60	OFF	Made form POCH reagents
2	H2O	RT	10 min	60	OFF	
3	Ottix Shaper	30°C/RT	30 min	60	OFF	DiaPath
4	Ottix Plus	30°C	1 h	30	ON	DiaPath
5	Ottix Plus	30°C	1 h	30	ON	DiaPath
6	Ottix Plus	30°C	3 h	120	ON	DiaPath
7	Wax	62°C	1 h 30 min	120	ON	Thermo Scientific
8	Wax	62°C	1 h 30 min	120	ON	Thermo Scientific
9	Wax	62°C	overnight	120	ON	Thermo Scientific

Table 2. Tissue fixation protocol.

Next, the specimens were embedded in paraffin using HistoStar embedding workstation (Thermo Scientific).

4.5. Histological analysis

Paraffin blocks were cut with a HM 355S rotary microtome (Thermo Scientific) into 4 µm sections, placed on poly-L-lysine (Sigma)-coated microscope slides and left to dry overnight.

4.5.1. Hematoxyllin and eosin staining

Slides were stained in automatic slide stainer Varistain Gemini ES (Thermo Scientific), using the following protocol:

	REAGENT	TIME	SUPPLIER
1	Heater station	15 min	
2	Ottix Plus	7 min	DiaPath
3	Ottix Plus	7 min	DiaPath
4	Ottix Shaper	7 min	DiaPath
5	dH2O	5 min	
6	Haematoxylin	45 min	Sigma-Aldrich
7	Running water	15 min	
8	Ottix shaper	1 min	
9	Alcoholic eosin	15 sec	Sigma-Aldrich
10	Ottix Shaper	30 sec	DiaPath
11	Ottix Shaper	30 sec	DiaPath
12	Ottix Plus	5 min	DiaPath
13	Ottix Plus	5 min	DiaPath

Table 3. Hematoxyllin and eosin staining protocol.

After staining the slides were covered with histofluid (Marienfeld-Superior) and cover glasses. Pictures were taken using Eclipse Ti microscope (Nikon) and NIS-Elements software.

The analysis of histological changes in the tongues of 4NQO-treated mice was done by Linh Nguyen Tuyet and became the subject of her master thesis *Heme oxygenase-1 increases angiogenic potential of murine squamous carcinoma cells but does not affect induction of carcinogenesis* [169].

4.5.2. Mason's trichrome staining

Slides were stained in automatic slide stainer Varistain Gemini ES (Thermo Scientific), using the following protocol:

	REAGENT	TIME	SUPPLIER
1	Heater station	15 min	
2	Ottix Plus	5 min	DiaPath
3	Ottix Plus	5 min	DiaPath
4	Ottix Shaper	2 min	DiaPath
5	Ottix Shaper	2 min	DiaPath
6	dH2O	wash	
7	Bouin's Solution	overnight	Sigma-Aldrich
8	Running water	10 min	
9	Haematoxylin	5 min	Sigma-Aldrich
10	Running water	5 min	
11	dH2O	30 sec	
12	Biebrich Scarlet-Acid Fucshin	5 sec	Sigma-Aldrich
13	dH2O	30 sec	
14	Phosphotungstic/Phosphomolybdic Acid Solution	5 sec	Sigma-Aldrich
15	Aniline Blue Solution,	5 min	Sigma-Aldrich
16	Acetic acid	2 min	POCH
17	Ottix Shaper	30 sec	DiaPath
18	Ottix Shaper	30 sec	DiaPath
19	Ottix Plus	5 min	DiaPath
20	Ottix Plus	5 min	DiaPath

Table 4. Trichrome staiing protocol.

After staining the slides were covered with histofluid (Marienfeld-Superior) and cover glasses. Pictures taken using Eclipse Ti microscope (Nikon) and NIS-Elements software.

4.6. RNA isolation and real time-PCR

RNA was isolated using modified Chomczyński method. Briefly, tissue samples were lysed using Qiagen Tissue Lyser and QIAzol reagent (Quiagen). Cell cultures were lysed using Fenozol (A&A Biotechnology). RNA was extracted with chloroform (POCH) and precipitated with isopropanol (POCH) at -20˚C overnight. RNA concentration was measured using NanoDrop 1000 spectrophotometer (Thermo Fisher). Reverse transcription of RNA samples from cell culture was performed using M-MuLV Reverse Transcriptase (Finnzymes), dNTP (Promega) and oligo(dT) primers (oligo.pl). Quantitative real-time PCR (qPCR) was performed using SYBR® Green JumpStart™ Taq ReadyMix™ (Sigma-Aldrich). For RNA isolated from tissue samples, reverse transcription and qPCR reaction were prepared using NCode™ VILO™ miRNA cDNA Synthesis Kit (Life Technlogies). qPCR was performed on StepOne Plus thermocycler (Applied Biosystems) and analyzed using StepOne software.

Following primers were used for qPCR reaction:

Gene	NCBI Reference Sequence	Forward (5'-3')	Reverse (5'-3')	Product lenght [nt]	Anealing temp [°C]
Homo sapiens eukaryotic translation elongation factor 2 (***EEF2***)	NM_001961.3	GCGGTCAGCACACTGGCATA	GACATCACCAAGGGTGTGCAG	218	60
Mus musculus heme oxygenase 1 (***Hmox1***)	NM_010442.2	CCTCACTGGCAGGAAATCATC	CCTCGTGGAGACGCTTTACATA	67	60
Homo sapiens heme oxygenase 1 (***HMOX1***)	NM_002133.2	GGAGCTGCTGACCCATGACACC	GCCACCAGAAAGCTGAGTGTAAGG	183	60
Mus musculus superoxide dismutase 1, soluble (***Sod1***)	NM_011434.1	ATGACTTGGGCAAAGGTGGA	ACTGCGCAATCCCAATCACT	90	60
Mus musculus keratin 4 (***Krt4***)	NM_008475.2	GAGCAATGACAAAGGTCGCCTAC	TGCAGCTGTACGCTTGTTGATCT	106	60
Mus musculus keratin 5 (***Krt5***)	NM_027011.2	GCCACCTACAGGAAGCTGCTGG	CTCCTCCGTAGCCAGAAGAGACAC	112	60
Mus musculus keratin 8 (***Krt8***)	NM_031170.2	GCATTCATACGAAGACCACCAGC	CTCATTCCGTAGCTGAAGCCAG	91	60
Mus musculus keratin 14 (***Krt14***)	NM_016958.1	CTCCTCTGGCTCTCAGTCATCCA	AGACCACCTTGCCATCGTGC	92	60

Table 5. Primers used for qPCR reaction.

4.7. Protein isolation

For protein isolation cells were scratched in ice-cold PBS (Lonza), centrifuged (8000 *g*, 5 minutes, 4˚C) and incubated in lysis buffer containing PBS (Lonza), 1% Triton (Sigma-Aldrich) for 30 minutes on ice. Protein concentration was determined with BCA assay or samples were frozen at -20˚C for further analysis.

4.7.1. BCA assay

Protein samples isolated from cell or tissue lysates were incubated with copper sulfate (Sigma) and bicinchonic acid (Sigma) solution (1:50). BSA standards were prepared in proper buffer (reporter lysis buffer, Promega) or lysis buffer for protein isolation. After 15-30 minute incubation at 37˚C the absorbance was measured at wave length of 562 nm using Infinite 200 PRO microplate reader (Tecan).

4.7.2. Western blotting

Protein electrophoresis was done using ready-to-use gels (Bio-Rad). 30 µg of protein sample was loaded in the wells. Electrophoresis was done using Bio-Rad Electrophoresis Chambers, 90 V – 15 minutes and 180 V – 1 h. Protein transfer was done using iBlot Dry Blotting System (Thermo Scientific, 20V, 7 min). Membranes were blocked with 5% milk in PBS, 0.05% Tween. Incubation with primary antibodies (rabbit HO-1 polyclonal antibody, #ADI-SPA-894, Enzo Life Sciences, 1:500; Anti-α-Tubulin Mouse mAb (DM1A), #CP06, Calbiochem, 1:1000) was done at 4˚C, overnight, and with the secondary antibodies (Anti-rabbit IgG, HRP-linked Antibody, #7074, Cell Signaling Technology, 1:5000; HRP Goat Anti-Mouse Ig, #554002, BD Pharmingen; 1:1000) for 2 hours, in room temperature. Signal detection was performed with chemiluminescent substrate reagents SuperSignal West Pico Chemiluminescent Substrate (Thermo Fisher).

4.7.3. Luciferase assay

Luciferase activity in cell and tissue lysates was measured using Luciferase Assay Systems (Promega) according to the manufacturer's protocol. Luminescence was measured in the 96-well OptiPlate (PerkinElmer) using Infinite 200 PRO microplate reader (Tecan).

4.8. Mobilization experiments

Mice were injected with CoPP (10 mg/kg of body weight, Frontier Scientific) prepared as described above or DMSO (Sigma-Aldrich) diluted 160× in NaCl. Recombinant human G-CSF (rhG-CSF, Amgen) was used at the dose of 250 µg/kg of body weight. Compounds were injected i.p. every day for 5 days (except for the experiment with HO-1$^{-/-}$ mice, when animals were injected 3 times, every second day). 6 hours after the last injection mice were euthanized by overdosage of xylazine and ketamine.

4.9. Cytokine concentration analysis

Luminex assays (MILLIPLEX MAP Mouse Cytokine/Chemokine Premixed 32 Plex, Mouse Cytokine/Chemokine Magnetic Bead Premixed 32 Plex and the custom assay panel, Millipore) were performed according to manufacturer's instructions. The samples were diluted 1:1 in Assay Buffer and incubated with Premixed Beads overnight at 4˚C. Signal detection was done using FLEXMAP 3D system (Millipore).

4.10. Heme oxygenase activity measurement

Liver tissue fragments were frozen at -80^{0}C immediately after dissection. HO activity (CO produced within 20 minutes after adding the reaction substrate NADPH) was measured using gas chromatography by Dr. Lucie Muchova (Institute of Clinical Biochemistry and Laboratory Diagnostics, Charles University, Prague, Czech Republic) in a blinded manner.

4.11. Complete blood count

Blood was collected into EDTA-coated test tubes. Complete blood count was done using Vet abc Plus+ hematology analyzer.

4.12. Bone marrow isolation

Bone marrow cells were isolated by cutting the ends of tibias and femurs and flushing the bone marrow cavity with PBS without calcium and magnesium ions (Lonza) with 2% FBS (Lonza).

4.13. Mobilized blood transplantation

2-3-month old female C57BL/6 recipient mice were irradiated with ^{137}Cs γ source at 110 cGy/min (2 × 4.5 Gy at 4 hour intervals) 24 hours before the transplantation at University Children's Hospital of Krakow with help of Dr. Jacek Kijowski.

2-3-month old female C57BL/6-Tg(UBC-GFP)30Scha/J donor mice were treated for 5 consecutive days with CoPP (Frontier Scientific), rhG-CSF (Amgen) or NaCl as described above. 6 hours after the last injection mice were euthanized by overdosage of xylazine and ketamine and blood was collected from the vena cava. Peripheral blood mononuclear cells (PBMC) were isolated using Ficoll-Paque PLUS (GE Healthcare) according to manufacturer's instructions and washed three times with PBS (Lonza). Bone marrow

was isolated from one C57BL/6J mouse as described above. Isolated viable PBMC and BM-derived cells were counted using Muse Cell Analyzer (Millipore).

$5x10^6$ of GFP^+ PBMC with $1x10^5$ GFP^- BM-derived competitor cells were injected into the tail vein of lethally irradiated C57BL/6J mice. The peripheral blood chimerism was evaluated by submandibular bleeding from the mouse cheek and analyzed in B cells, T cells and granulocytes as shown in Fig. 9.

4.14. Flow cytometry

Peripheral blood was collected from the vena cava or from the submandibular vein into the heparin coated syringes. Spleens were dispersed using 70 µm cell strainer (BD). Bone marrow and cells from tumors were isolated as described above. The cell suspensions were filtered with 70 µm cell strainer, depleted of erythrocytes by use of a hypotonic solution, centrifuged (600*g*, 10 minutes, 4°C), resuspended in PBS (Lonza) with 2% FBS, and stained for 20 minutes on ice.

Samples were collected using LSR II and LSRFortessa flow cytometers (BD) and analyzed using BD FACSDiva and FlowJo software. Gating strategies are shown below (Fig. 6-Fig. 9):

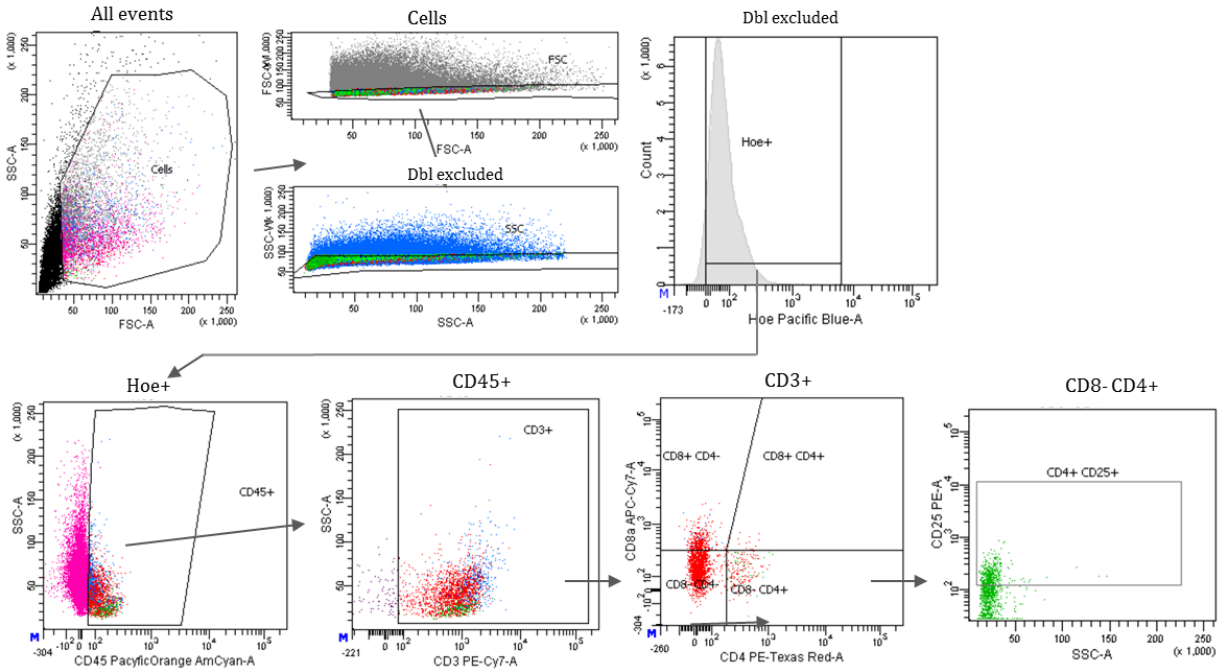

Fig. 6. Example of gating strategy of T lymphocytes.

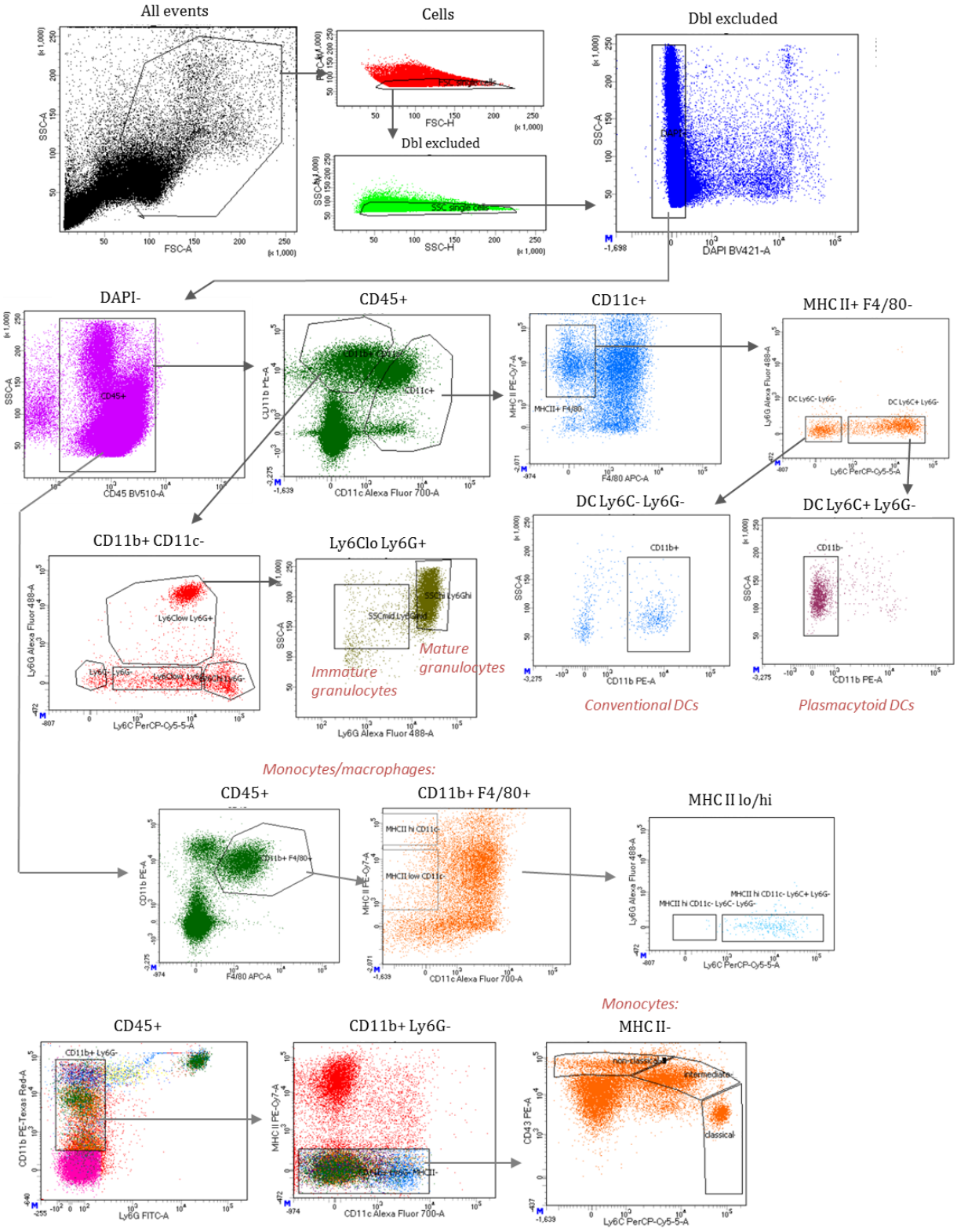

Fig. 7. Example of gating strategy of myeloid cell populations.

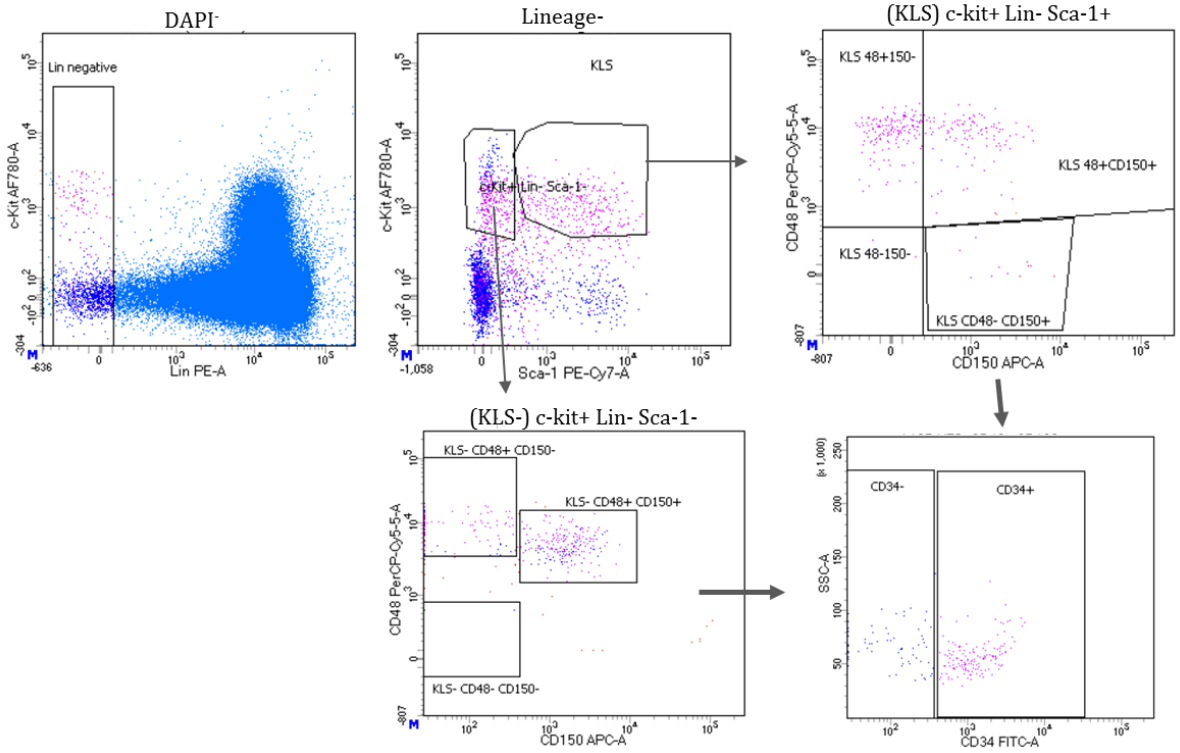

Fig. 8. Example of gating strategy of hematopoietic stem and progenitor cells.

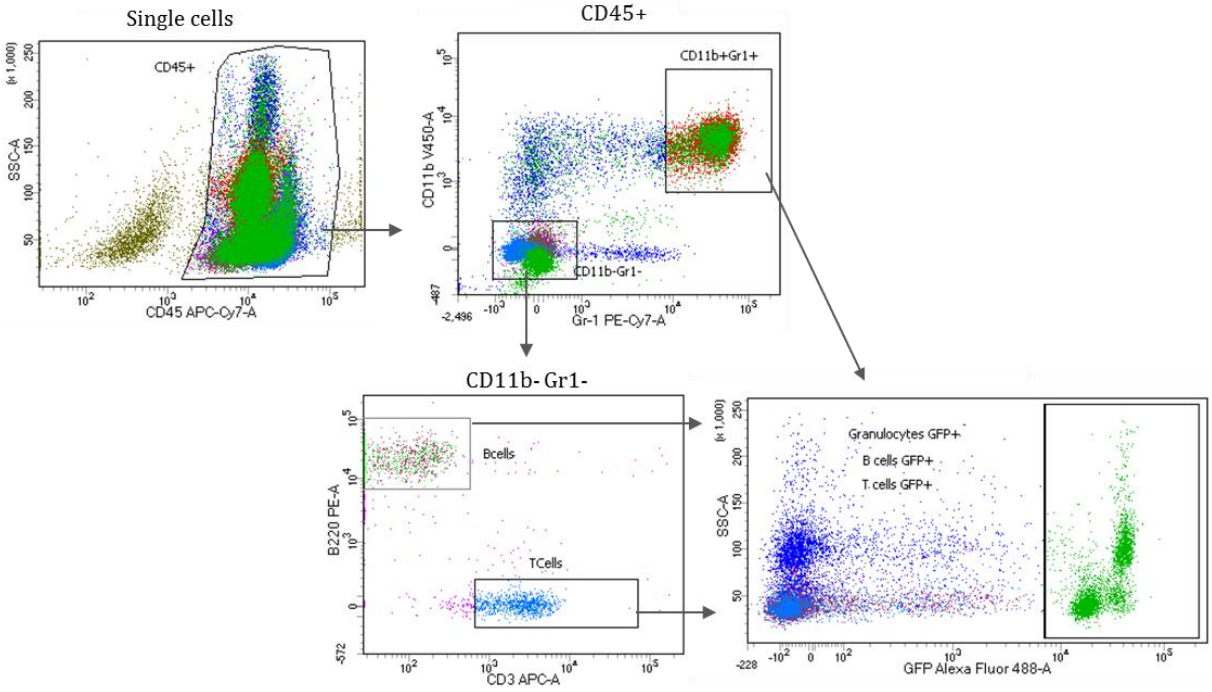

Fig. 9. Example analysis of GFP chimerism.

4.14.1. Reagents for flow cytometry

Following antibodies and dyes for flow cytometry were used:

Antigen	Dye	Clone	Company
CD3e	PE-Cy7	145-2C11	BD Biosciences
CD3e	APC	17A2	BD Biosciences
CD4	PE-CF594	RM4-5	BD Biosciences
CD8a	APC-H7	53-6.7	BD Biosciences
CD8a	APC-Cy7	53-6.7	BD Biosciences
CD11b	PE	M1/70	BD Biosciences
CD11b	V450	M1/70	BD Biosciences
CD11b	PE-CF594	M1/70	BD Biosciences
CD11c	AlexaFluor700	N418	eBioscience
CD14	APC-Cy7	Sa14-2	Biolegend
CD25	PE	PC61	BD Biosciences
CD34	AlexaFluor700	RAM34	BD Biosciences
CD34	FITC	RAM34	BD Biosciences
CD43	FITC	S7	BD Biosciences
CD43	PE	S7	BD Biosciences
CD45	Pacific Orange	30F-10	Invitrogen
CD45	FITC	30F-11	BD Biosciences
CD45	APC	30F-11	BD Biosciences
CD45	APC-Cy7	30F-11	BD Biosciences
CD48	PerCP-Cy5.5	HM-48-1	Biolegend
CD150	APC	TC15-12F12.2	Biolegend
c-Kit	APC-eFluor780	2B8	eBioscience
F4/80	APC	BM8	eBioscience
Gr-1	PE-Cy7	RB6-8C5	BD Bioscience
Ly6C	PerCP-Cy5.5	HK1.4	eBioscience
Ly6C	PerCP-Cy5.5	AL.-21	BD Biosciences
Ly6G	FITC	1A8	BD Biosciences
Ly6G	BV605	1A8	BD Biosciences
MHC II	PE-Cy7	M5/114.15.2	eBioscience
NK1.1	FITC	PK136	BD Biosciences
Sca-1	PE-Cy7	D7	BD Biosciences
Sca-1	PE-Cy5	D7	Biolegend
Tie-2	PE	TEK4	eBioscience
Lineage staining			
B220	PE	RA3-6B2	BD Biosciences
Gr-1	PE	RB6-8C5	BD Biosciences
TCRγδ	PE	GL3	BD Biosciences
TCRβ	PE	H57-597	BD Biosciences
CD11b	PE	M1/70	BD Biosciences
Ter119	PE	TER-119	BD Biosciences
-	DAPI	-	Sigma
-	Hoechst 33342	-	Sigma

Table 6. Antibodies and nuclear dyes used for flow cytometry stainings.

4.14.2. ROS production assay

Mice were treated with CoPP, G-CSF, DMSO and NaCl for 5 consecutive days as described above. Six hours after the last injection blood samples were collected. Phagoburst assay (Glycotope Biotechnology) was performed according to manufacturer's instructions. Briefly, the blood samples were incubated with N-formylmethionyl-leucyl-phenylalanine (fMLP), phorbol 12-myristate 13-acetate (PMA) and opsonized *E. coli* and subsequently with dihydrorhodamine 123. Additionally, samples were stained with anti-Gr-1 antibody. Analysis was performed as shown below:

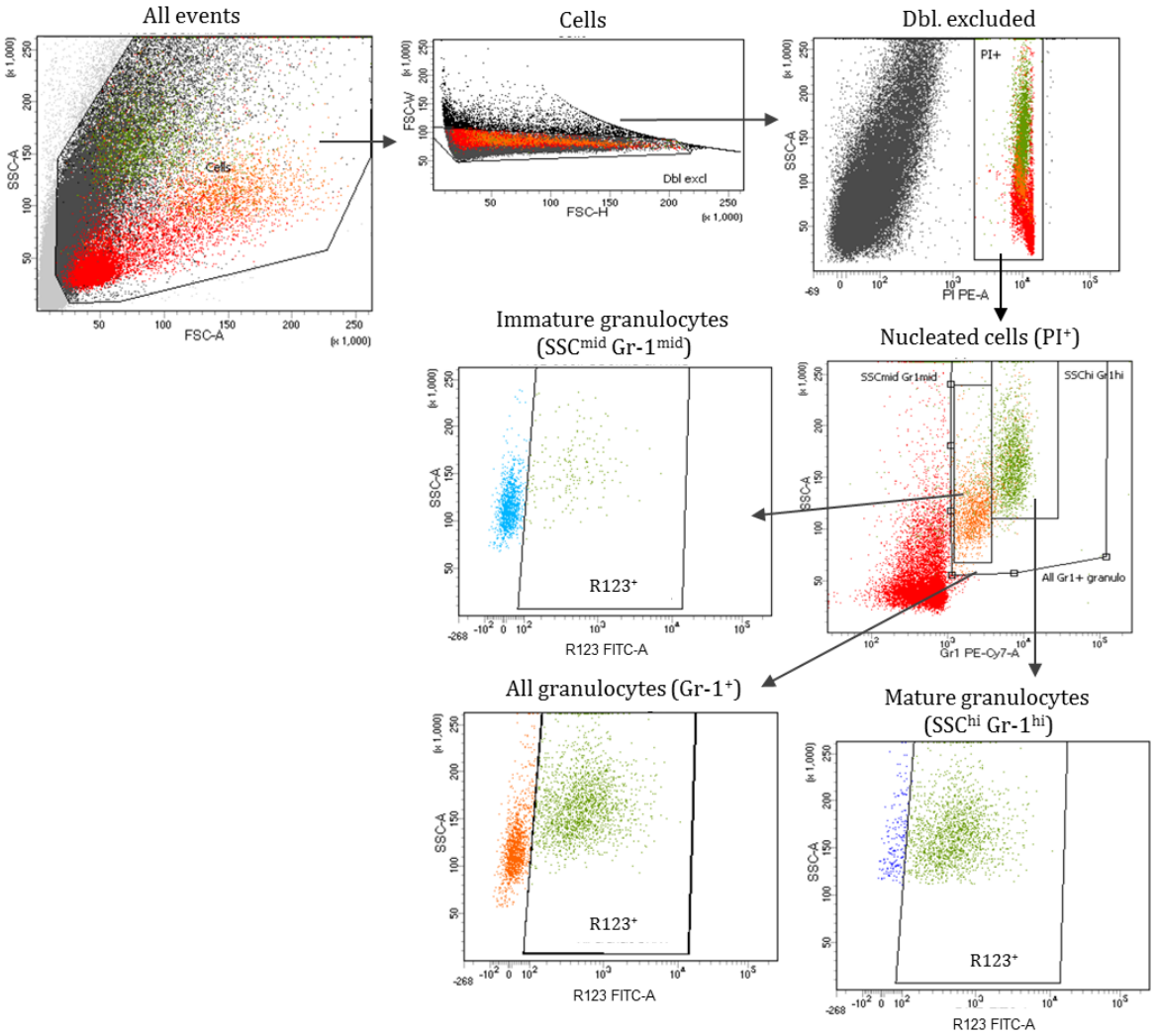

Fig. 10. Gating strategy for Phagoburst assay analysis.

4.15. Statistical analysis

Statistical analysis was done with GraphPad Prism software. Data are presented as mean with SEM or mean with individual values. Two-tailed unpaired T test or Mann-Whitney test were applied when two groups were compared. One-way Anova or two-way Anova with Bonferroni post-hoc test were applied when three or more groups were compared. Kruskal-Wallis with Dunn's post-hoc test were was applied when three or more groups with non-Gaussian distribution were compared. Fisher's exact test was used in the analysis of contingency tables. Results were considered as statistically significant, when $p \leq 0.05$ (* = $p \leq 0.05$; ** = $p \leq 0.01$; *** = $p \leq 0.001$; **** = $p \leq 0.0001$).

4.16. Preparation of figures

The figures were prepared using PowerPoint. Some of the illustrations were created from image bank of Servier Medical Art, available from http://www.servier.com/Powerpoint-image-bank.

5. RESULTS

5.1. HO-1 expression level has little effect on chemical carcinogenesis

Previous studies of our group showed that HO-1$^{-/-}$ mice were more susceptible for chemical skin carcinogenesis [99]. However, tumors developed in HO-1$^{-/-}$ mice were mostly benign in contrast to invasive carcinomas observed in HO-1$^{+/+}$ mice. The aim of our current study was to further investigate the role of HO-1 in the development of squamous cell carcinoma using the model of oral chemical carcinogenesis. In addition to HO-1 deficient C57BL/6xFVB mice we used also C57BL/6 mice with overexpression of HO-1 under the control of keratin 14 promoter. Mice with different levels of HO-1 expression were treated with 4NQO in the drinking water for 4 months.

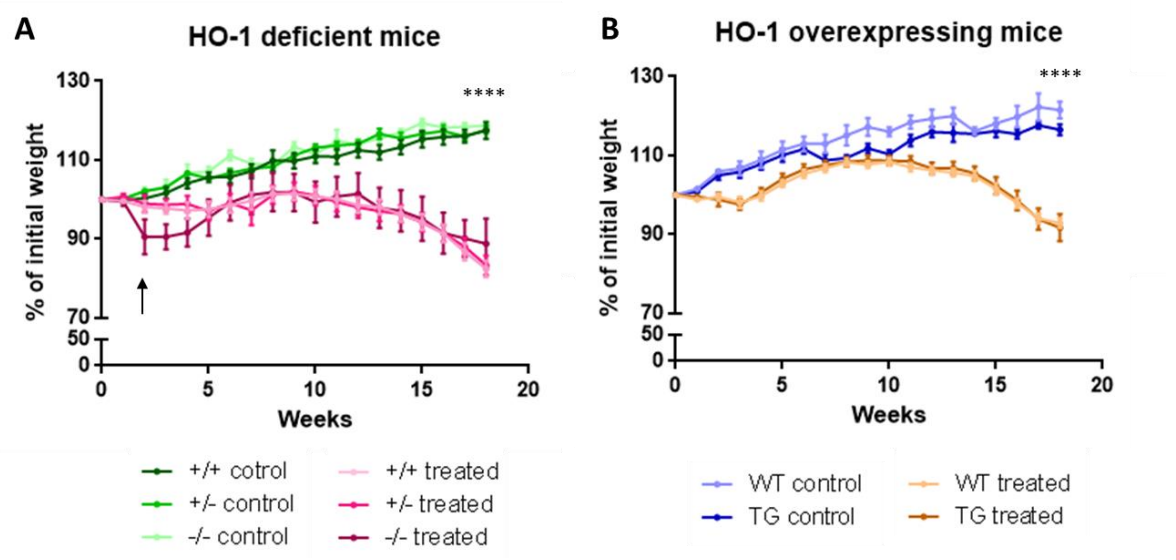

Fig. 11. Weight changes in carcinogen treated animals. A. C57BL/6xFVB mice with normal and lower level of HO-1, arrow indicates decrease of weight in HO-1-/- at the beginning of experiment; **B.** C57BL/6 wild type and HO-1 overexpressing mice (mean + SEM, two-way Anova with Bonferroni post-test; 14-19 4NQO-treated mice per group, 9 HO-1$^{-/-}$ 4NQO-treated mice per group; 5-6 control mice per group; **** is between the 4NQO-treated and control group of the same genotype).

While the control mice were gaining weight throughout the experiment (Fig. 11) , in the treated animals the weight gain was delayed at the beginning. After 10 weeks of treatment mice of all genotypes started to lose weight. In HO-1$^{-/-}$ mice we observed a severe weight loss at the first weeks of 4NQO treatment (Fig. 11A, indicated with an arrow). At this point 10 out if 19 HO-1$^{-/-}$ mice had to be euthanized. Of all other mice, only one HO-1$^{+/+}$ and one HO-1 overexpressing (TG) mouse had to be euthanized (Fisher exact test, HO-1$^{-/-}$ vs. HO-1$^{+/+}$, p = 0.003 and HO-1$^{-/-}$ vs. HO-1$^{+/-}$, p = 0.0004, WT vs. TG,

ns). Of the mice remaining in the experiment we did not observe differences in the weight loss between the 4NQO-treated mice of different genotypes.

5.1.1. HO-1 deficient mice are more susceptible to esophageal, but not to oral carcinogenesis

At the end of experiment all mice were euthanized and we analyzed the presence and number of lesions in the gastrointestinal tract. Lesions were macroscopically visible on the tongues of almost all 4NQO treated mice, regardless of genotype (Fig. 12 A, C).

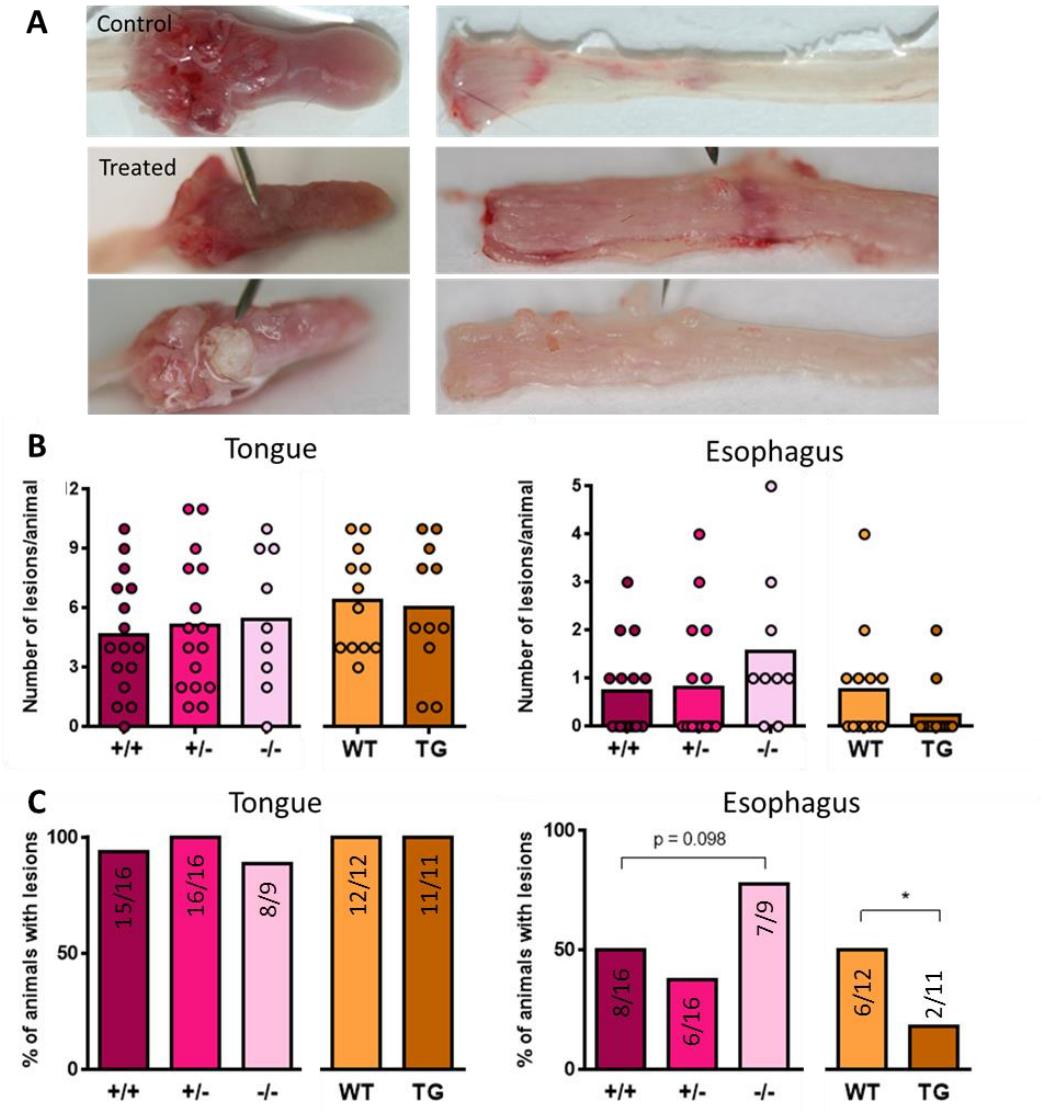

Fig. 12. Carcinogen-induced lesions on tongues and esophagi. A. Macroscopic changes on the tongues (left) and esophagi (right); **B**. Number of lesions per animal (mean + individual values plotted, one-way Anova with Bonferroni post-test; 11-16 4NQO-treated mice per group, 9 HO-1$^{-/-}$ 4NQO-treated mice per group); **C**. Percentage of mice with visible lesions (Fisher exact test; numbers on the bars show number of affected animals/total number of animals in the group).

We did not observe any differences in the number of lesions per mouse between the groups (Fig. 12 B, left). Similarly, we did not observe any differences in the number of esophageal lesions per mouse (Fig. 12 B, right). However, majority of HO-1$^{-/-}$ mice (77.8%) developed lesions on esophagi in comparison to around 50% of the HO-1$^{+/-}$ and HO-1$^{+/+}$ mice. Moreover, less than 20% of TG developed esophageal lesions compared to their control group C57BL/6 wild-type mice (WT) (Fig. 12 C). We did not observe any macroscopic changes in other organs of gastrointestinal system.

Histological analysis of the tongue paraffin sections was the subject of the master thesis of Linh Nguyen Tuyet (*Heme oxygenase-1 increases angiogenic potential of murine squamous carcinoma cells but does not affect induction of carcinogenesis*, Jagiellonian University, Krakow, 2013). Evaluation of hematoxylin and eosin staining of the tongue tissue sections shows the induction of carcinogenesis in the 4NQO-terated mice, however there are no differences between the HO-1 genotypes (Fig. 13).

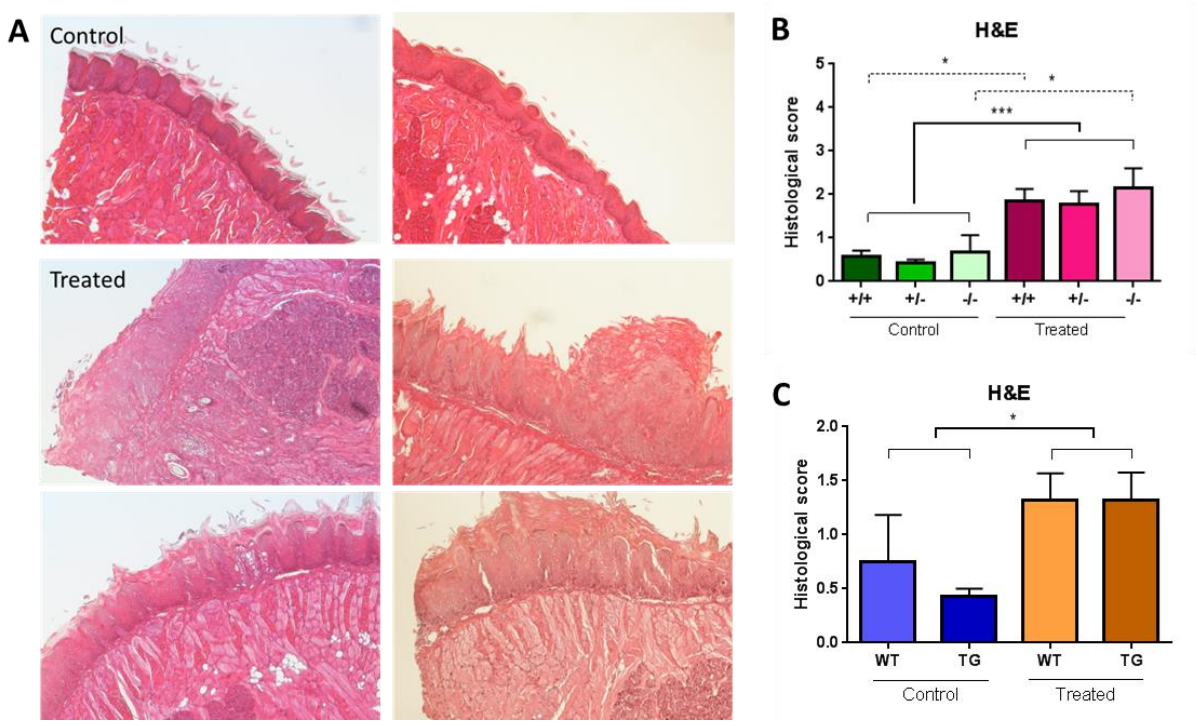

Fig. 13. Histological analysis of tongue paraffin sections from 4NQO-treated mice. A. Representative pictures of hematoxyllin and eosin staining of the tongue tissue sections; **B**, **C**. Analysis of stained specimens from C57BL/6xFVB and C57BL/6, respectively (mean + SEM, two-way Anova with Bonferroni post-test; 8-16 4NQO-treated mice per group; 3-6 control mice per group). Results from the master thesis of Linh Nguyen Tuyet [169], modified.

5.1.2. 4NQO treatment leads to abnormal keratins expression in tongues regardless of HO-1 genotype

Next, we analyzed HO-1 expression in the tongue lysates (Fig. 14). At the mRNA level we observed no difference in murine HO-1 (*Hmox1*) expression between the control and 4NQO-treated C57BL/6xFVB mice. In C57BL/6 mice of both genotypes we observed a decrease of murine HO-1 expression after 4NQO treatment.

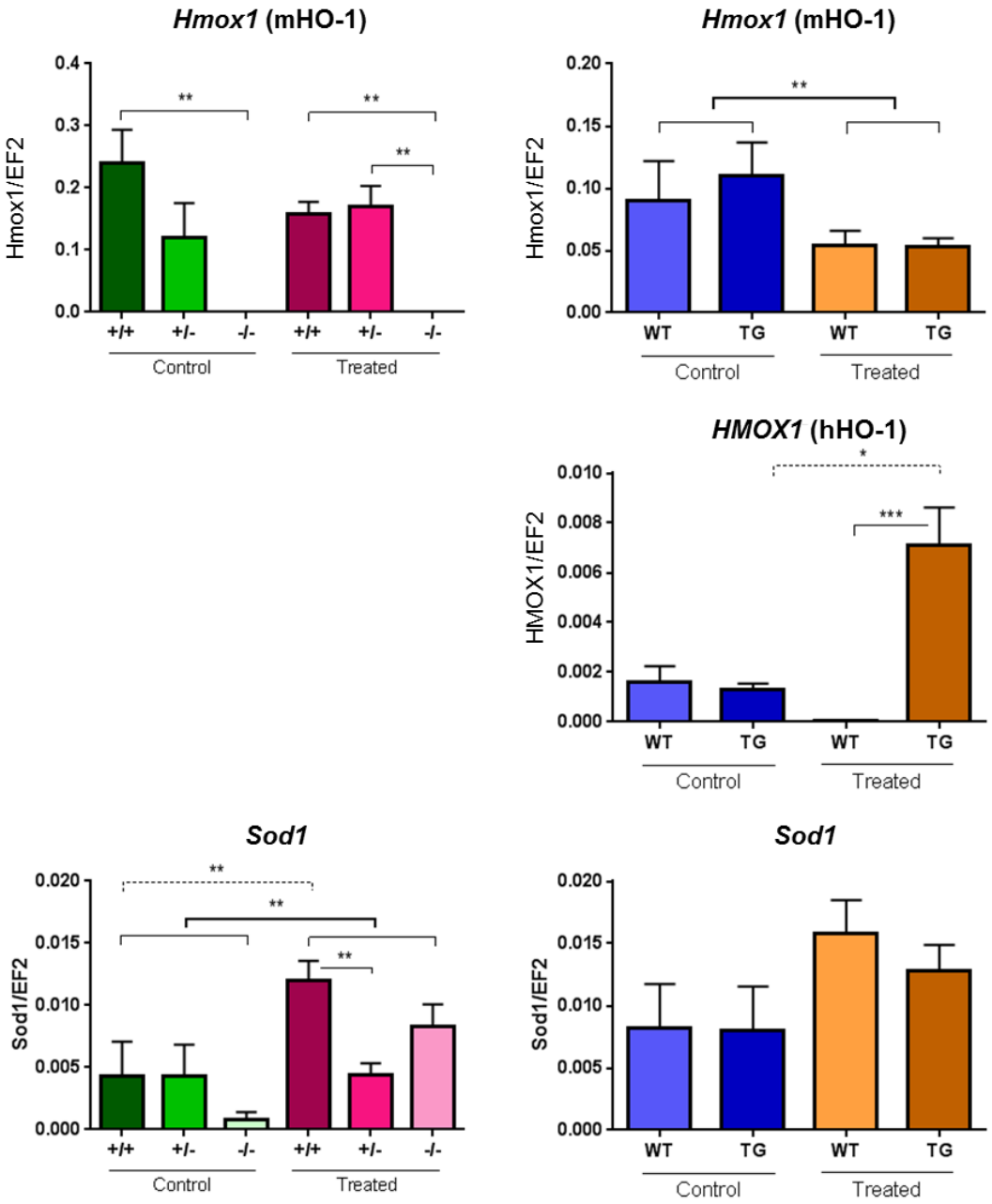

Fig. 14. Expression of antioxidant genes in the tongue lysates from control and 4NQO-treated C57BL/6 (left panel) and C57BL/6 (right panel) mice; bold line indicates the main effect of the treatment, dotted line indicates the effect of the treatment for the given genotype (mean + SEM, two-way Anova with Bonferroni post-test; 8-15 4NQO-treated mice per group; 3-6 control mice per group).

In transgenic (TG) C57BL/6 mice, overexpressing human HO-1 under keratin 14 promoter, there was a strong induction of human HO-1 (*HMOX1*) mRNA after carcinogen treatment. Expression of keratin 14 in the same samples was only slightly upregulated in TG mice after 4NQO treatment (Fig. 15). Expression of another important antioxidant enzyme, superoxide dismutase 1 (*Sod1*) was decreased in the tongues of untreated HO-$1^{-/-}$ mice in comparison to HO-$1^{+/+}$ and HO-$1^{+/-}$ counterparts. Treatment with 4NQO increased *Sod1* expression in HO-$1^{+/+}$ and HO-$1^{-/-}$ mice but not in HO-$1^{+/-}$ mice.

Using the hematoxyllin and eosin staining we observed altered proliferation in the epithelium of the 4NQO-treated mice. To qantitatively assess the effect of 4NQO treatment we analyzed the expression of selected keratins in the tongue lysates. Pair of keratins which are expressed in the mitotically active basal layer of epithelium, namely keratins 5 and 14, were only upregulated in the HO-$1^{+/-}$ mice after 4NQO treatment (Fig. 15). There was also very small and not statistically significant upregulation of keratin 14 in C57BL/6 WT and TG mice. On the other hand, in both mouse strains, there was a downregulation of keratin 4, which is expressed in differentiated layers of epithelium (Fig. 15). This suggests impaired differentiation of the epithelium in the 4NQO-terated mice. Moreover in the tongues of carcinogen-treated mice we observed upregulation of keratin 8, which is not normaly expressed in stratified epithelium (Fig. 15). Expression of keratin 4 was increased in control HO-$1^{-/-}$ mice when compared to HO-$1^{+/+}$ and HO-$1^{+/-}$ mice. Other tested keratins (*Krt5*, *Krt8* and *Krt14*) also tended to be upregulated in HO-$1^{-/-}$ mice in normal conditions.

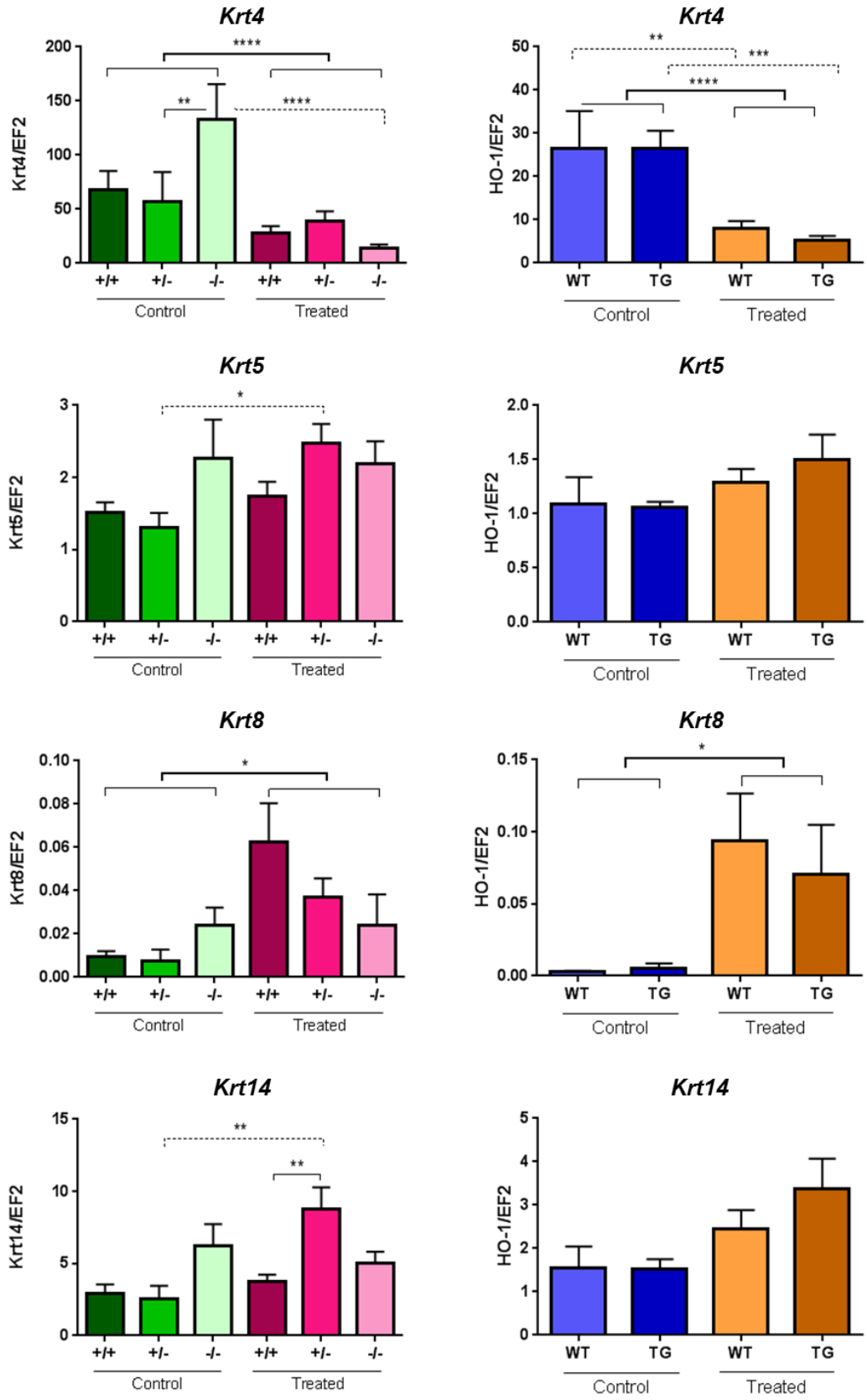

Fig. 15. Expression of keratines in the tongue lysates from control and 4NQO-treated C57BL/6 (left panel) and C57BL/6 (right panel) mice; bold line indicates the main effect of the treatment, dotted line indicates the effect of the treatment for the given genotype (mean + SEM, two-way Anova with Bonferroni post-test; 8-15 4NQO-treated mice per group; 3-6 control mice per group).

5.1.3. HO-1 deficiency affects cytokine concentrations in blood

Results comparing the cytokine concentrations in the samples from wild type C57BL/6JxFVB and C57BL/6J mice were published in the article: A. Szade, W.N. Nowak, K. Szade, A. Gese, R. Czypicki, H. Waś, J. Dulak, A. Józkowicz: Effect of Crossing C57BL6 and FVB Mouse Strains on Basal Cytokine Expression, Mediators of Inflammation, vol. 2015, Article ID 762419, 2015. doi:10.1155/2015/762419.

Inflammation is one of the hallmarks of cancer [36]. Several cytokine pathways were shown to be important in cancer progression and anti-cancer response [170], among them IL-6 [171, 172], IL-10 [173], TNFα [174], various chemokines, like MCP-1 [175, 176] and RANTES [177, 178], and growth factors, such as G-CSF [179, 180], M-CSF [181] or VEGF [182].

HO-1 is known immunomodulatory factor (reviewed in [183, 184]). As described in the chapters 2.2.3 and 2.3.2, HO-1 may influence the cytokine production, immune cell differentiation and their suppressive function. To verify the hypothesis that HO-1 can modulate the immune responses in carcinogenesis, we analyzed the concentrations of cytokines in the sera of mice treated with 4NQO and control mice.

We observed a tendency for increased concentration of IL-6 in HO-1 deficient mice. Treatment with 4NQO led to further increase in IL-6. In the control C67BL/6 mice IL-6 was below the detection limit and rose after treatment with 4NQO. IL-7 concentration increased significantly only in HO-$1^{-/-}$ mice after 4NQO treatment. However we observed also some increase in 4NQO-treated WT C57BL/6 mice. HO-$1^{-/-}$ mice had higher IL-10 concentration than HO-1-expressing mice, regardless of the treatment with 4NQO (Fig. 16).

In C57BL/6xFVB mice we observed higher concentrations of several CCL chemokines in serum after treatment with 4NQO (Fig. 17, left panel). Regardless of *Hmox-1* genotype, 4NQO led to increase in MIP-1 α (CCL3) and eotaxin (CCL11). The increase in MCP-1 (CCL2) concentration was especially pronounced in HO-$1^{-/-}$ mice treated with 4NQO. We did not observe differences in RANTES (CCL5) levels. Concentrations of CCL chemokines in C57BL/6 mice were less affected by 4NQO treatment (Fig. 17, right panel).

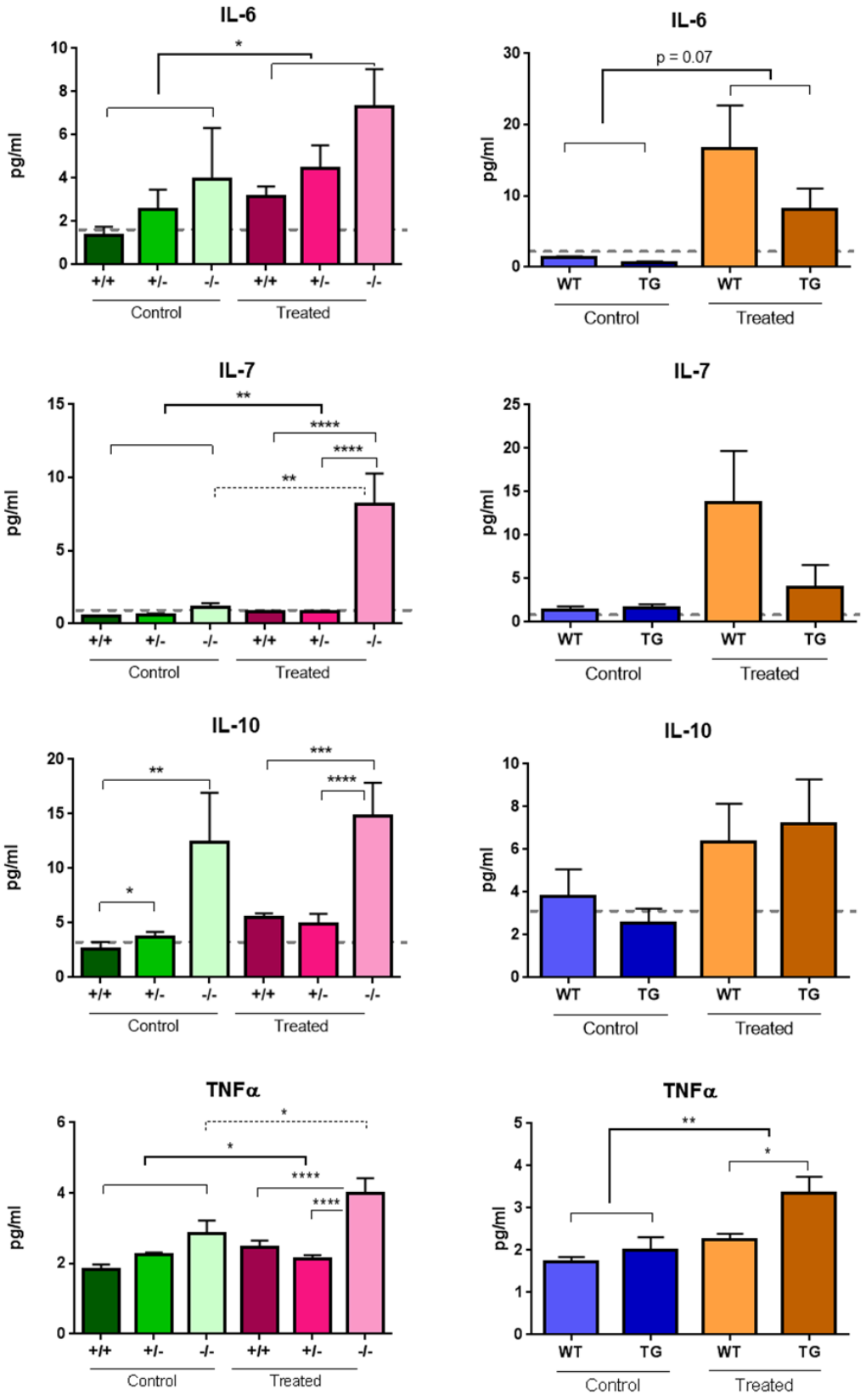

Fig. 16. Concentration of interleukins and TNFα in sera of control and 4NQO-treated C57BL/6 (left panel) and C57BL/6 (right panel) mice; bold line indicates the main effect of the treatment, dotted line indicates the effect of the treatment for the given genotype; dashed line indicates the detection level of the given cytokine (mean + SEM, two-way Anova with Bonferroni post-test; 8-17 4NQO-treated mice per group; 3-6 control mice per group).

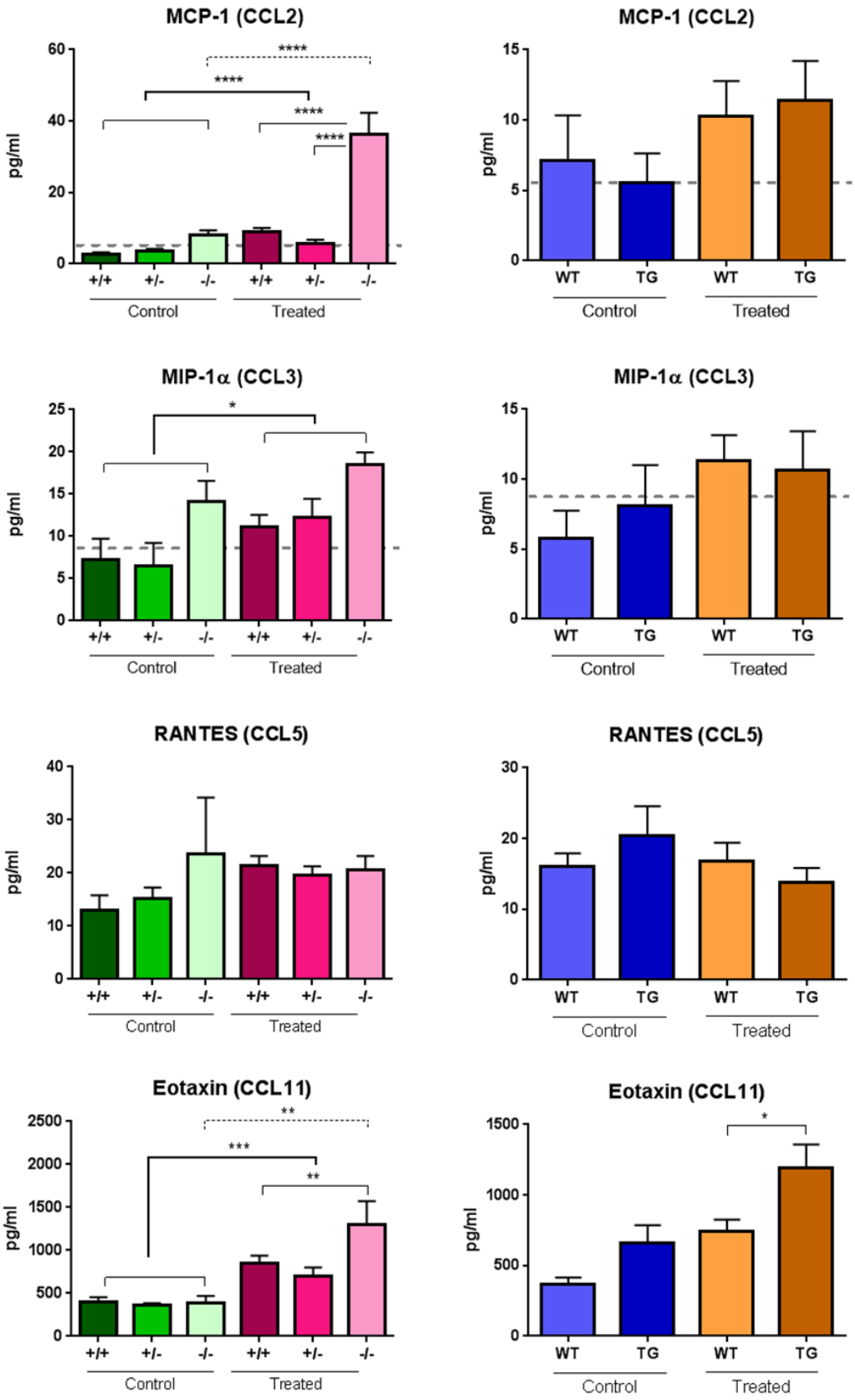

Fig. 17. Concentration of CCL chemokines in sera of control and 4NQO-treated C57BL/6 (left panel) and C57BL/6 (right panel) mice; bold line indicates the main effect of the treatment, dotted line indicates the effect of the treatment for the given genotype; dashed line indicates the detection level of the given cytokine (mean + SEM, two-way Anova with Bonferroni post-test; 8-17 4NQO-treated mice per group; 3-6 control mice per group).

After treatment of mice with 4NQO we did not observe changes in CXCL chemokines: KC (CXCL1), monokine induced by gamma interferon (MIG, CXCL9) and interferon gamma-induced protein 10 (IP-10, CXCL10). Regardless of 4NQO treatment, HO-$1^{-/-}$ mice had higher concentration of IP-10 than HO-$1^{+/+}$ and HO-$1^{+/-}$ mice (Fig. 18). Concentrations of MIP-2 (CXCL2) were below the detection limit.

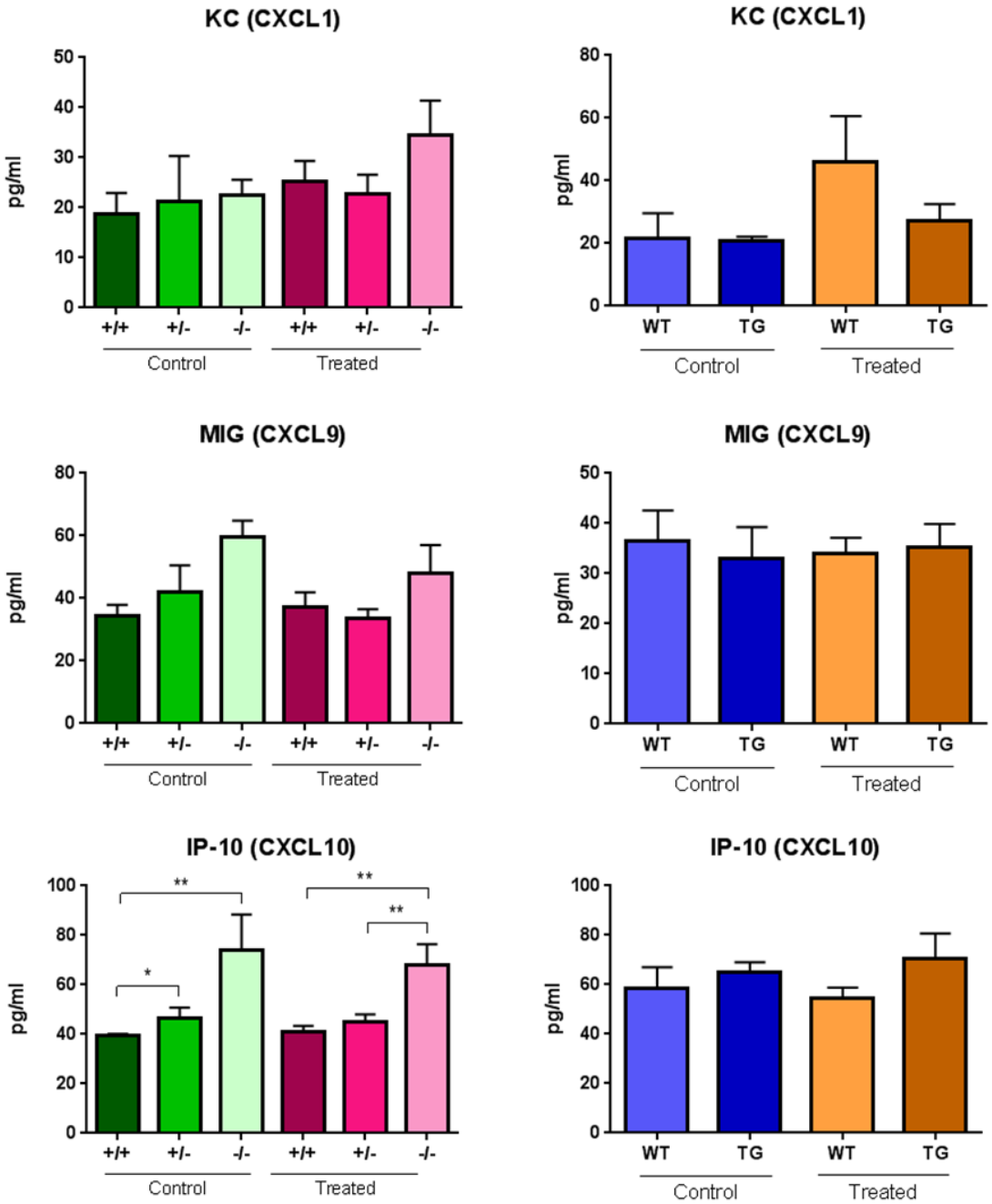

Fig. 18. Concentration of CXCL chemokines in sera of control and 4NQO-treated C57BL/6J (left panel) and C57BL/6J (right panel) mice; bold line indicates the main effect of the treatment, dotted line indicates the effect of the treatment for the given genotype; dashed line indicates the detection level of the given cytokine (mean + SEM, two-way Anova with Bonferroni post-test; 8-17 4NQO-treated mice per group; 3-6 control mice per group).

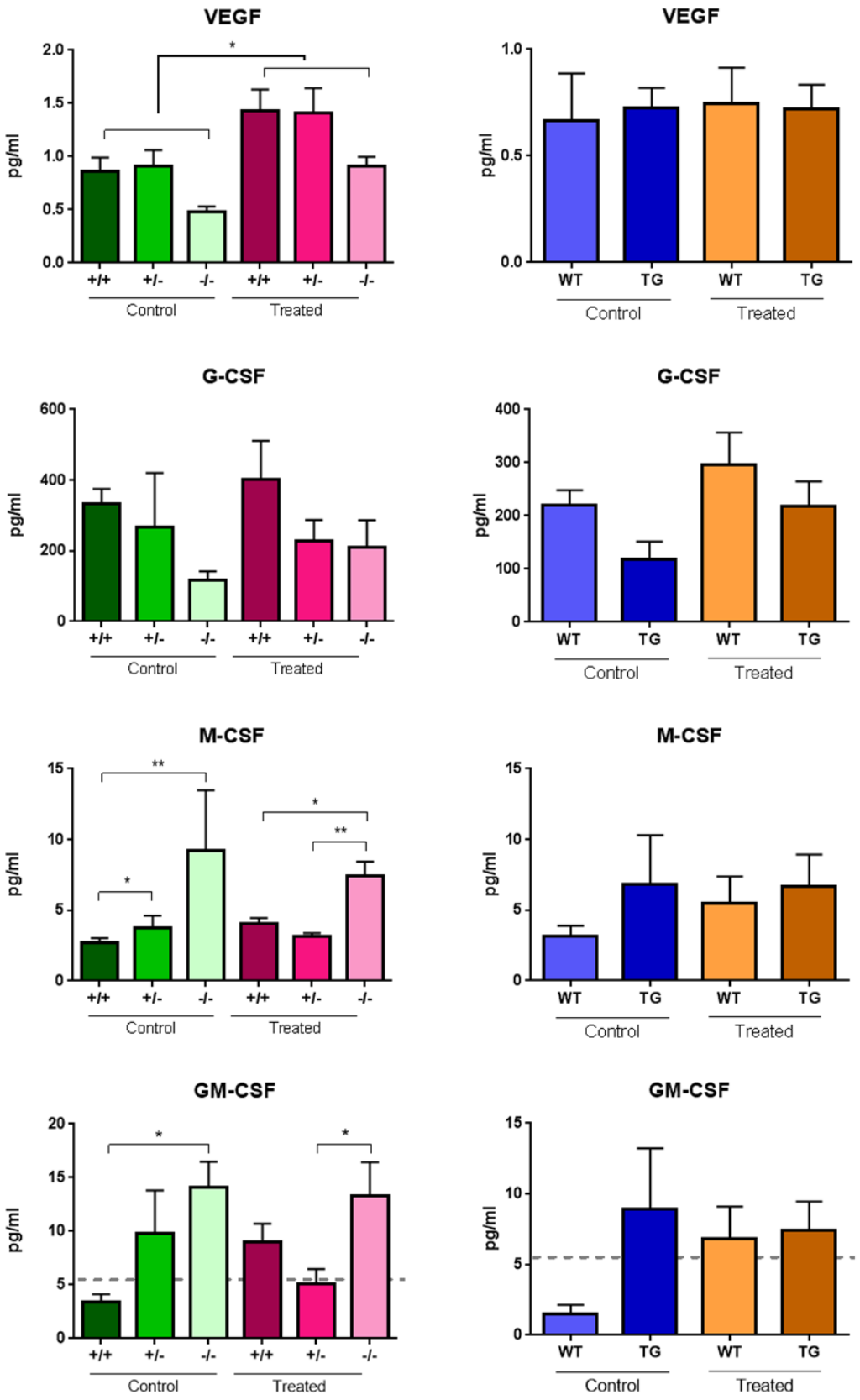

Fig. 19. Concentration of growth factors in sera of control and 4NQO-treated C57BL/6 (left panel) and C57BL/6 (right panel) mice; bold line indicates the main effect of the treatment, dotted line indicates the effect of the treatment for the given genotype; dashed line indicates the detection level of the given cytokine (mean + SEM, two way Anova with Bonferroni post-test; 8-17 4NQO-treated mice per group; 3-6 control mice per group).

Of the growth factors analyzed, only the concentration of VEGF was affected by 4NQO treatment in C57BL/6xFVB. VEGF level in serum was slightly lower in HO-$1^{-/-}$ mice than in HO-1 expressing mice. After treatment with 4NQO, VEGF concentration increased in the same manner in all HO-1 genotypes (Fig. 19, top left). We did not observe any differences in VEGF concentration in C57BL/6 HO-1 WT and TG mice (Fig. 19, top right). Concentrations of hematopoietic growth factors were not affected by 4NQO treatment in both the mouse strains. However, in the control C57BL/6xFVB mice, we observed a trend for decreased concentration of G-CSF and, at the same time, an increased concentrations of M-CSF and GM-CSF in HO-$1^{-/-}$ mice in comparison to HO-$1^{+/+}$ mice (Fig. 19, left).

Carcinogenic treatment of the wild type mice, with normal HO-1 expression level, did not influence the concentrations of majority of the cytokines tested. However, HO-$1^{-/-}$ mice not only had different cytokine profile at the basal conditions, but also responded differently to the carcinogen exposure. This suggests, that HO-1 might influence the response of immune system to carcinogenesis.

5.2. Overexpression of HO-1 in SCC VII cells affects the immune system response

In the experiments with chemical carcinogenesis we observed that HO-1 deficient mice had more lesions in the esophagi and produced different amounts of cytokines in response to 4NQO treatment. To further evaluate the role of HO-1 in tumor growth and tumor-induced immune response, we analyzed the syngeneic tumor model with HO-1 overexpressing cell line.

We transduced murine squamous cell carcinoma cell line SCC VII with retroviral vectors (RVs) to stably express luciferase (Fig. 20 A, B) in order to be able to monitor the tumor growth *in vivo*. Next, we transduced the established SCC VII-Luc cell line with RVs containing human *HMOX1* gene (Fig. 20 A). HO-1 overexpression was confirmed at the mRNA and protein level (Fig. 20 C, D).

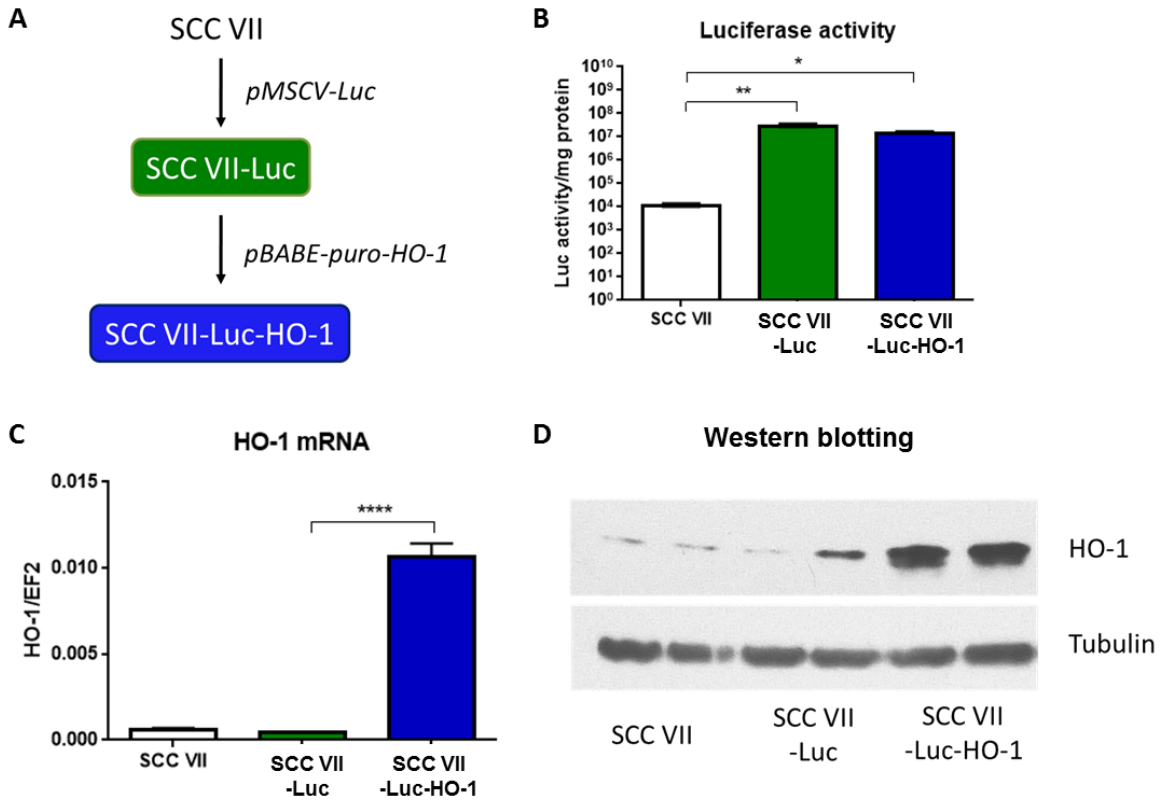

Fig. 20. Establishment of SCC VII genetically modified cell lines. A. Scheme of retroviral transductions; **B.** *In vitro* luciferase activity measurement (unpaired T-test, 2 samples per group); **C.** Expression of HO-1 at mRNA level measured by real time-PCR (unpaired T-test between SCC VII-Luc and SCC VII-Luc-HO-1, 2-3 samples per group); **D.** Expression of HO-1 at protein level evaluated by western blotting.

Before starting *in vivo* experiments, we compared SCC VII-Luc and SCC VII-Luc-HO-1 cell lines *in vitro*. We did not observe HO-1 influence on proliferation (Fig. 21 A), migration and invasion through the Matrigel matrix (Fig. 21 B). HO-1 overexpression did not influence the adhesion of the SCC VII to murine endothelial cell lines. However we observed the increased adhesion of both SCC VII-Luc and SCC VII-Luc-HO-1 to the high endothelial cells from peripheral lymph node (MPLNHEC) in comparison to the microvascular endothelial cells deried from spleen (MSplMEC), brain (MBrMEC) and lung (MLuMEC) (Fig. 21 C).

Next we measured the concentrations of several cytokines and growth factors which can be important in the regulation of tumor infiltration with immune cells. Both SCC VII-Luc and SCC VII-Luc-HO-1 produced similarly high levels of M-CSF, VEGF, leukemia inhibitory factor (LIF), MCP-1, RANTES and IP-10 (Fig. 22). Neither SCC VII-Luc nor SCC VII-Luc-HO-1 produced G-CSF, IL-6 and eotaxin (data not shown).

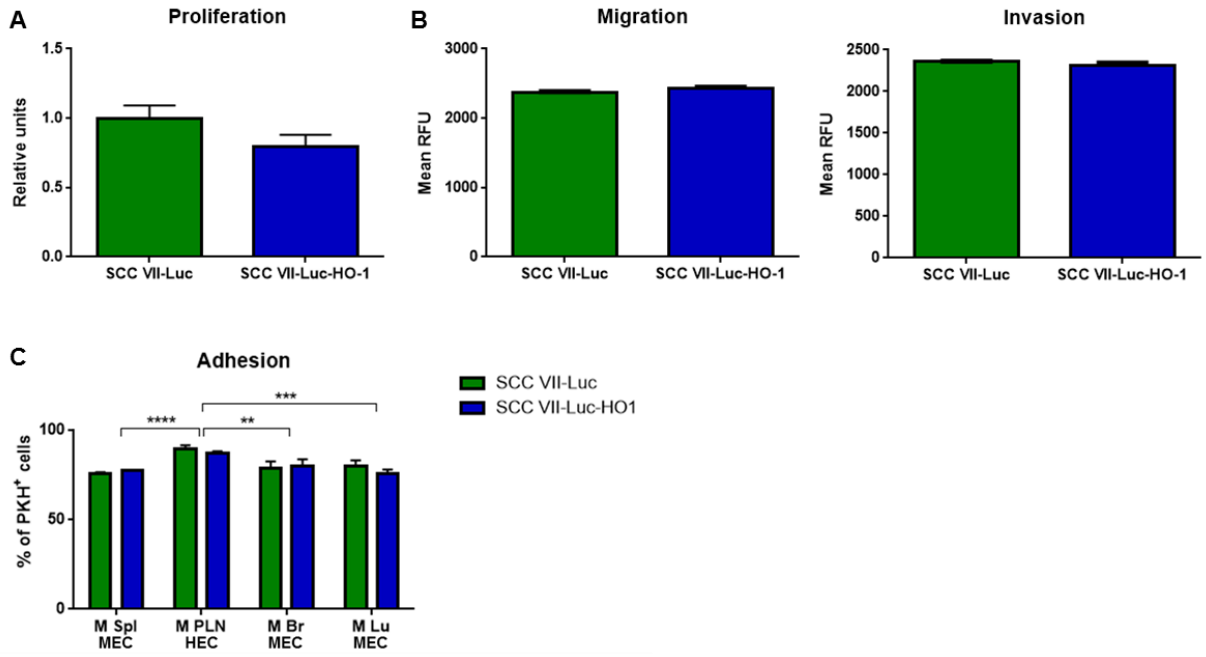

Fig. 21. SCC VII *in vitro* functional assays. A. Proliferation calculated as SCC VII-Luc-HO-1 cell number/well relative to SCC VII-Luc cell number/well 48 h after seeding equal number of cells (mean of 4 independent experiments + SEM); **B.** Migration/invasion through an empty transwell and transwell with Matrigel, respectively, measured as the mean fluorescence of PKH26 labelled cells (mean + SEM, 3 samples per group); **C.** Adhesion of SCC VII-Luc and SCC VII-Luc-HO-1 to murine endothelial cells (mean + SEM; 2 independent experiments, 3 samples per group; two-way Anova + Bonferroni post-test).

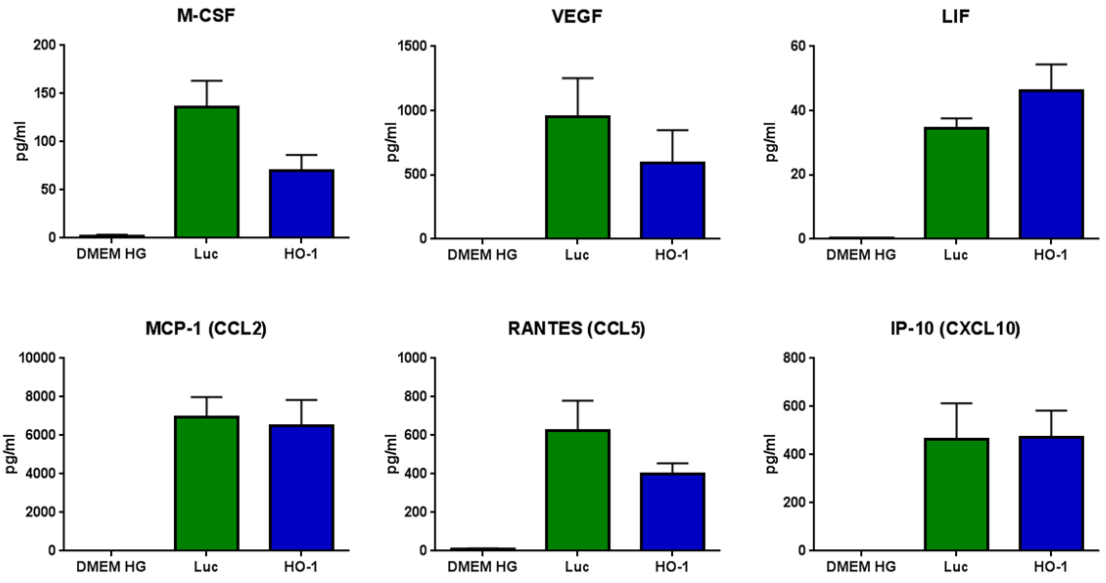

Fig. 22. Concentration of cytokines in culture supernatants from SCC VII cells with normal expression of HO-1 (Luc) or overexpression of HO-1 (HO-1). DMEM HG means empty medium. Supernatants collected after 24 h of cell culture and analyzed with Luminex assay (results from 4 independent experiments pooled together, mean + SEM, one-way Anova with Bonferroni post-test, 12-14 samples per group).

5.2.1. HO-1 overexpression in SCC VII cells increases tumor infiltration and affects systemic cytokine production one month after subcutaneous injection

Having characterized control SCC VII-Luc and HO-1-overexpressing (SCC VII-Luc-HO-1) cell lines *in vitro*, we injected them subcutaneously in the Matrigel matrix into syngeneic C3H mice (Fig. 23).

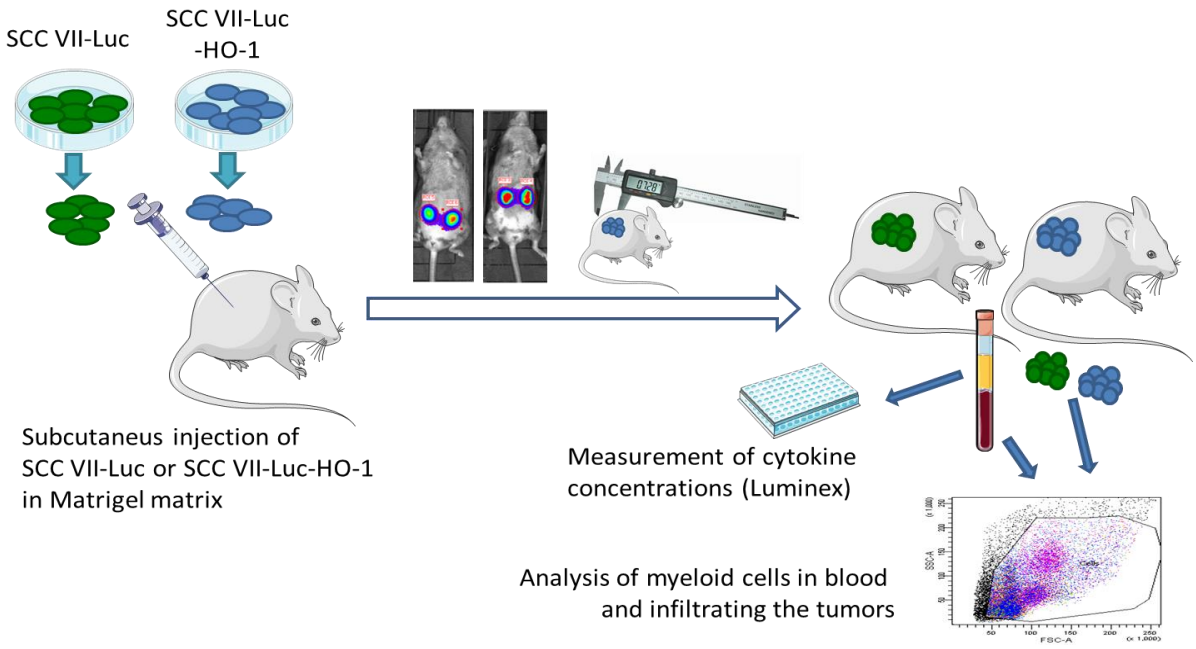

Fig. 23. Scheme of the experiment with HO-1 overexpressing tumor cells injected into syngeneic mice.

We analyzed the tumor growth by *in vivo* luciferase activity measurements using IVIS. Luciferase activity initially decreased in mice with SCC VII-Luc-HO-1, but not in mice with SCC VII-Luc. From day 7 luciferase activity was increasing in both groups of mice, but in mice which received HO-1 overexpressing cells the signal increase was much higher (Fig. 24 A). The increase of luciferase activity did not reflect the tumor size measured by the caliper. After 4 weeks, tumors formed by SCC VII-Luc were smaller than tumors from SCC VII-Luc-HO-1 (Fig. 24 B). At the end of experiment (32 days) the difference was still visible, but smaller, as few mice with the biggest tumors had to be euthanized due to scratches.

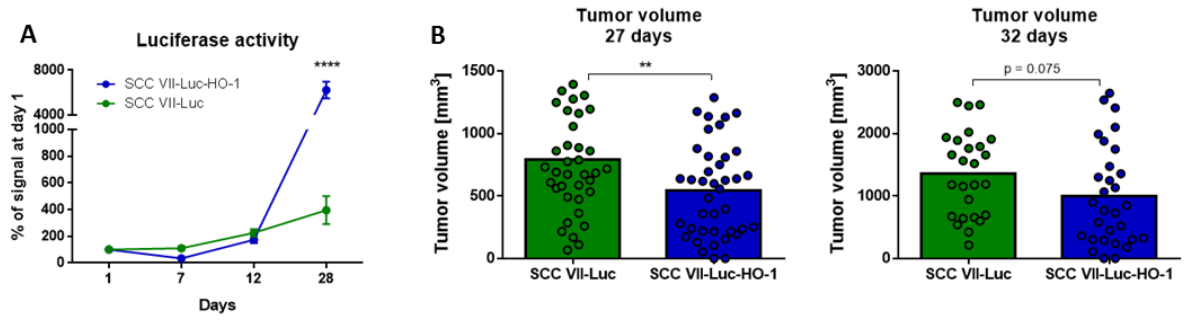

Fig. 24. Growth of tumors from subcutaneously injected SCC VII cells. A. *In vivo* bioluminescence measurements of luciferase activity (mean + SEM, two-way Anova with Bonferroni post-test, 40 measurements per group, 20 mice per group, 2 plugs per mouse); **B.** Tumor volume measured by caliper (mean + individual values plotted, unpaired T-test, 26-40 measurements per group).

To investigate the possible reasons for the discrepancy between *in vivo* luciferase activity measurements and tumor size, we measured the luciferase activity in the tumor lysates. In concordance with the *in vivo* luciferase measurements, SCC VII-Luc-HO-1 tumors had much higher luciferase activity per mg of protein than SCC VII-Luc tumors (Fig. 25 A). This excludes the possibility that SCC VII-Luc tumors gave the lower luciferase signal due to the insufficient substrate delivery.

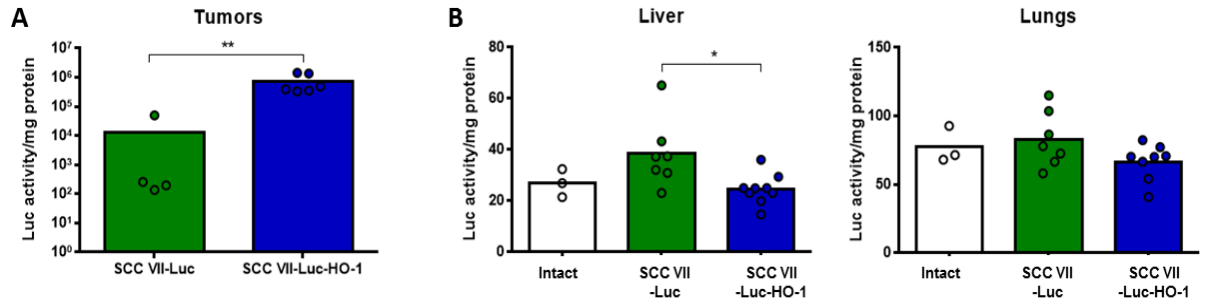

Fig. 25. Luciferase activity in tissue lysates from mice injected with SCC VII-Luc and SCC VII-Luc-HO-1 cells one month after tumor cells injection A. Luciferase activity in tumors (mean + individual values plotted, Mann-Whitney test 4-6 samples per group); **B**. Luciferase activity in livers and lungs (mean + individual values plotted, one-way Anova with Bonferroni post-test, 3-7 samples per group). Intact – negative controls, showing the assay background signal.

Having observed significantly higher luciferase activity in SCC VII-Luc-HO-1 tumors, we wanted to exclude the possibility of the difference in luciferase activity in both cell lines cultured *in vitro*. As shown on Fig. 20 A, luciferase gene was introduced to SCC VII cells before HO-1, thus luciferase activity should be comparable. Indeed, at the time when SCC VII-Luc-HO-1 cell line was established, the luciferase activity was similar in SCC CII-Luc

and SCC VII-Luc-HO-1 (Fig. 20 B). Unexpectedly, newly obtained lysates from SCC VII-Luc-HO-1 had higher luciferase activity than lysates from SCC VII-Luc (Fig. 26 A). Next, we wanted to verify the hypothesis that luciferase signal increases in the same in both SCC VII cell lines. We seeded various numbers of cells in the 96-well plate and measured luciferase activity after 48 hours. Luciferase signal was higher in SCC VII-Luc-HO-1 than in SCC VII-Luc in all tested densities, and the difference was increasing with the cell number until certain threshold. However, when we calculated the results as the percentage of signal at the lowest density, the relative luciferase activity was increasing almost linearly in SCC VII-Luc, and quickly reached plateau in SCC VII-Luc-HO-1 (Fig. 26 B).

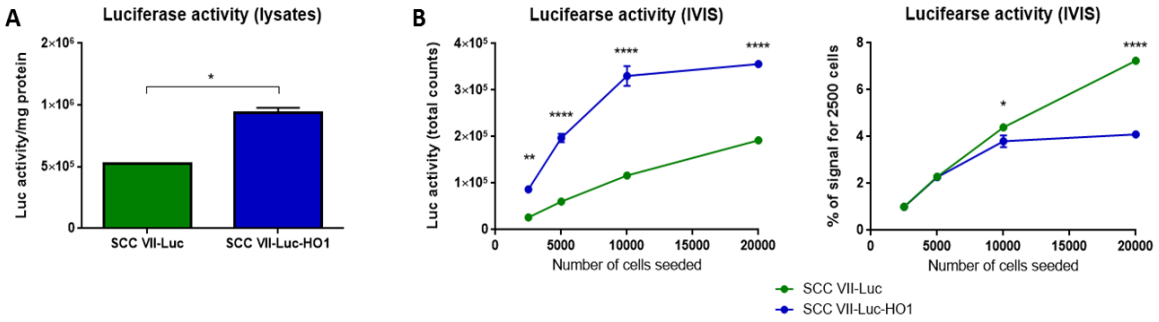

Fig. 26. Luciferase activity in SCC VII cells cultured *in vitro*. A. Luciferase activity measured in SCC VII cell lysates with the microplate reader (mean + SEM, 2 samples per group, unpaired T-test); **B.** Luciferase activity in live cells measured using IVIS, 48 hours after seeding of indicated number of cells (mean + SEM, 2 samples per group, two-way Anova with Bonferroni post-test).

As we did not find any macroscopically visible secondary tumors in the liver and lungs, in order to detect potential metastases, we measured luciferase activity in tissue lysates. We did not observe any difference in the luciferase activity in the lungs. However, some mice bearing SCC VII-Luc tumors had increased luciferase activity in the liver (Fig. 25 B). Concerning the fact that SCC VII-Luc-HO-1 give much higher luciferase signal both *in vitro* and from the tumor lysates, increased luciferase activity in liver in SCC VII-Luc group suggest the possible micrometastases.

The discrepancy between the luciferase measurement and tumor size can be explained by the fact, that tumor mass does not only contain the tumor cells, but also a variety of other components forming tumor niche. Bigger in size but having less viable cancer cells with active luciferase, SCC VII-Luc tumors could have the higher infiltration with

immune cells, connective tissue content and necrosis. To find the possible explanation, we performed the trichrome staining of the tumor sections (Fig. 27 A). Unexpectedly, semi-quantitative analysis of the specimens revealed that SCC VII-Luc tumors have smaller amount of connective tissue (Fig. 27 B). We did not observe differences in the blood vessel and necrosis content between control and HO-1-overexpressing tumors. In most of the specimens, the necrosis was not present.

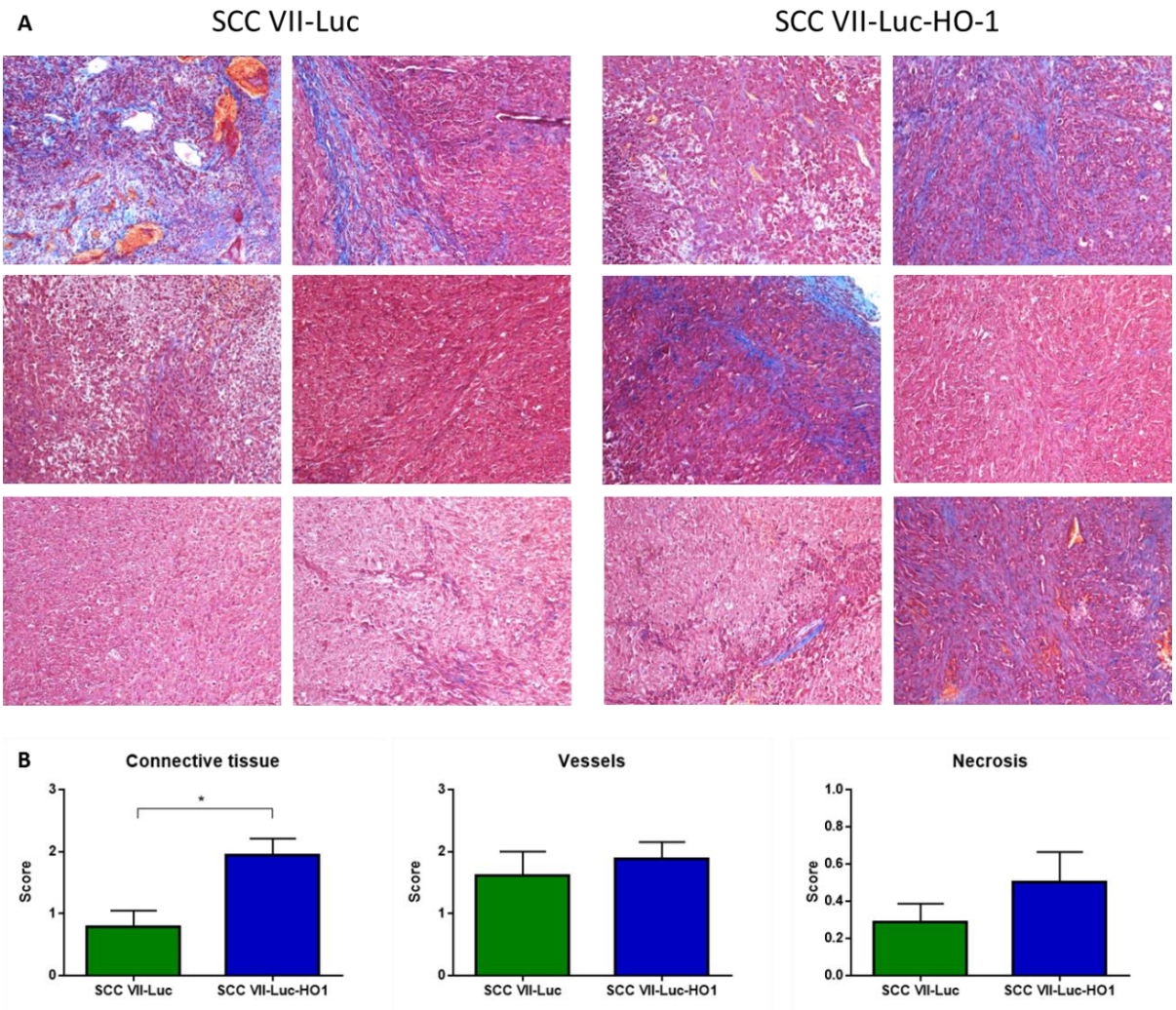

Fig. 27. Histological analysis of tumor samples 1 month after subcutaneous injection of C3H mice with SCC VII cells. A. Representative pictures of Trichrome staining; **B.** Results of analysis of the staining, pictures were assessed using the scale from 0 to 3 (mean + SEM, unpaired T-test, 7-8 samples per group).

To elucidate if the bigger, SCC VII-Luc derived tumors were more heavily infiltrated with leukocytes and to evaluate if HO-1 overexpression in the tumor influenced the phenotype of infiltrating cells, we analyzed them by flow cytometry.

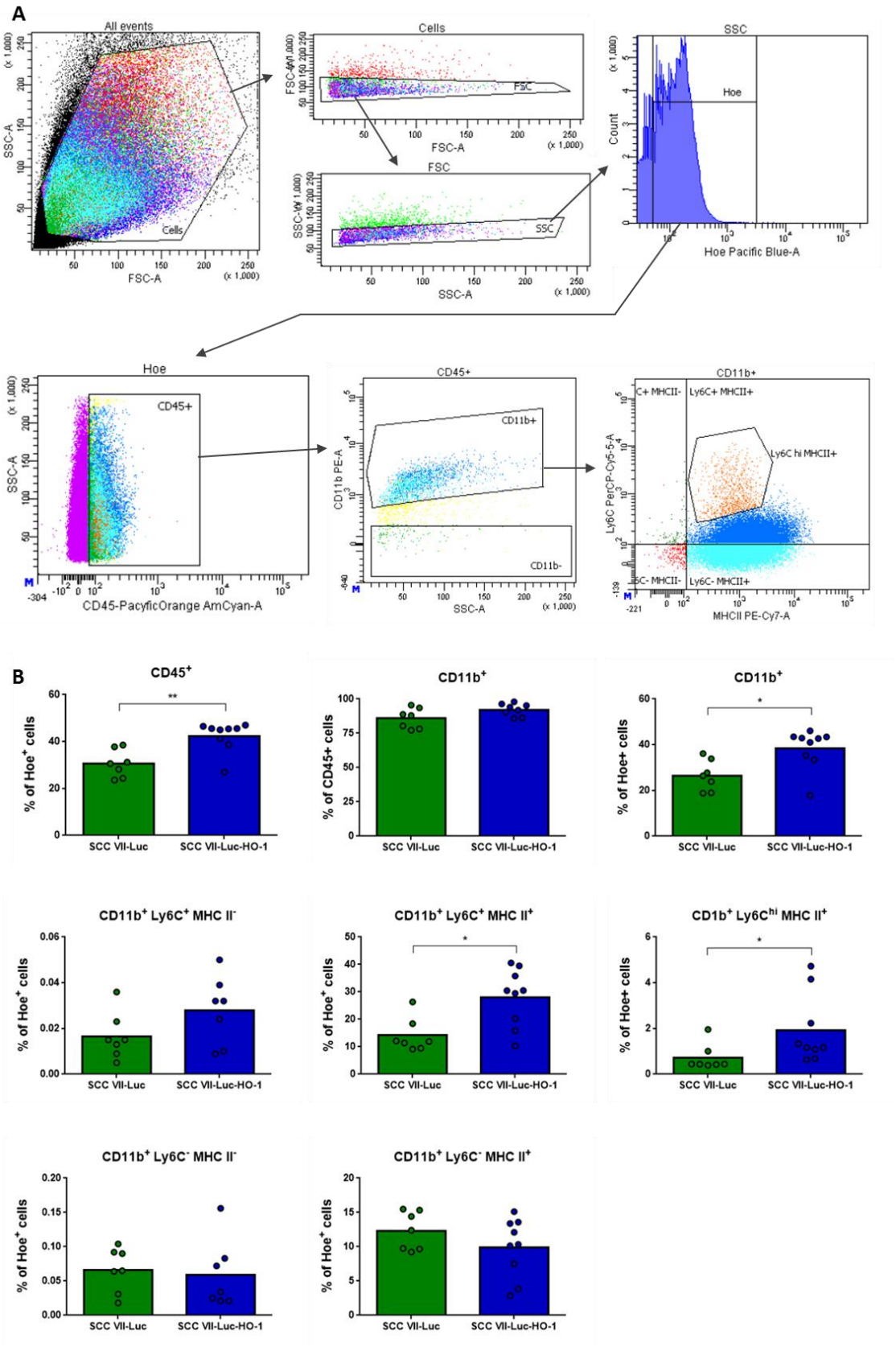

Fig. 28. Flow cytometry analysis of myeloid cells infiltrating the tumors 1 month after subcutaneous injection of C3H mice with SCC VII cells. A. Gating strategy; **B.** Percentages of myeloid cells ($CD11b^+$) infiltrating the tumors characterized basing on Ly6C and MHC type II expression (mean + individual values plotted, Mann-Whitney test, 7-9 samples per group).

As the SCC VII-Luc tumors were bigger but had lower increase in luciferase activity, we expected the higher infiltration with leukocytes of the SCC VII-Luc tumors than SCC VII-Luc-HO-1 ones. Oppositely to expectations, we observed a higher number of $CD45^+$ cells infiltrating the tumors from SCC VII-Luc-HO-1 cells. The majority of infiltrating leukocytes were $CD11b^+$ myeloid cells (Fig. 28).

The cells were next characterized using Ly6C and MHC type II (MHC II) markers, which were shown to classify tumor infiltrating cells into functional subsets [185]. Ly6C and MHC II did not separate well the infiltrating myeloid subpopulations, however, we were able to see difference between control and HO-1 overexpressing tumors. SCC VII–Luc-HO-1 tumors had higher percentage of infiltrating $Ly6C^+$ and $Ly6C^{hi}$, MHC II expressing myeloid cells. Proportions of $Ly6C^-$ cells were similar in both groups (Fig. 28). MHC II expressing cells were much more abundant than MHC II negative cells.

One month after subcutaneous injection of SCC VII cells we observed differences in myeloid cell infiltration in the HO-1 overexpressing tumors. However when the tumors were growing for such a long time, distinct populations of infiltrating cells were difficult to distinguish with certain markers, for example with MHC II and Ly6C. As characterization of infiltrating cells with MHC II and Ly6C can reflect functional diversity of different subpopulations [185], we decided to performed similar experiment, but the tumors were growing for a shorter time.

After 2 weeks we did not observe the difference in the percentage of $CD45^+$ cells infiltrating the SCC VII-Luc and SCC VII-Luc-HO-1 tumors but, similarly to the previous experiment, SCC VII-Luc-HO-1 tumors were more heavily infiltrated with myeloid cells. Basing on Ly6C and MHC II expression we distinguished 5 populations of myeloid cells infiltrating the tumors. SCC VII-Luc-HO-1 tumors had a higher percentage of $Ly6C^{lo}$ MHC II^{hi} and MHC II^{lo} infiltrating cells. Percentage of $Ly6C^{mid}$ MHC II^{lo} cells as well as of $Ly6C^{hi}$ cells, regardless of MHC II expression, was similar in SCC VII-Luc and SCC VII-Luc-HO-1 tumors. HO-1-overexpressing tumors were, however, more heavily infiltrated with $CD11b^+$ $F4/80^+$ $Tie\text{-}2^+$ cells (Fig. 29).

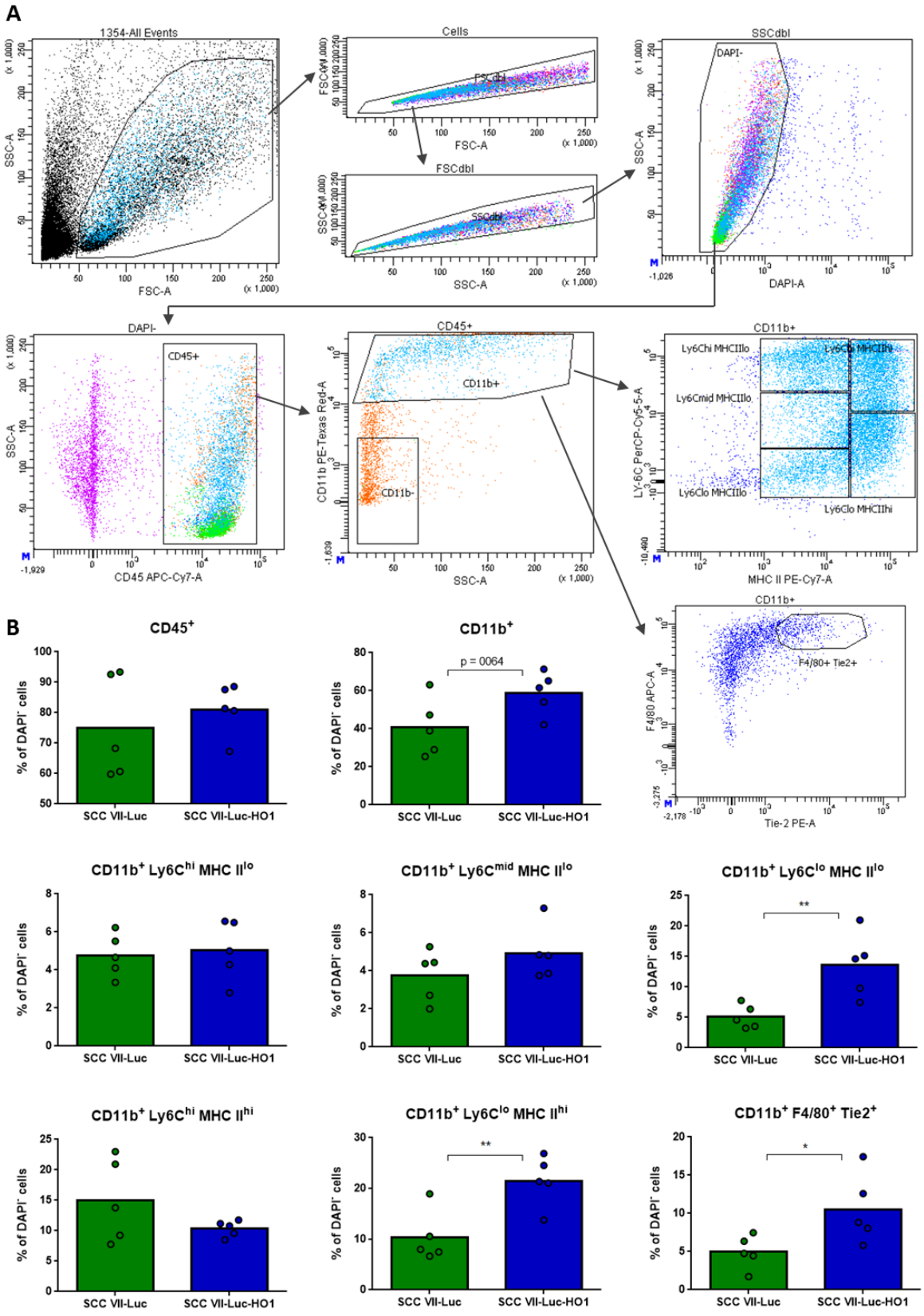

Fig. 29. Flow cytometry analysis of myeloid cells infiltrating the tumors, 2 weeks after subcutaneous injection of C3H mice with SCC VII cells. A. Gating strategy; **B.** Percentages of myeloid cells ($CD11b^+$) infiltrating the tumors, characterized basing on Ly6C/MHC type II and F4/80/Tie-2 expression (mean + individual values plotted, unpaired T- test, 5 samples per group).

Tie-2-expressing monocytes/macrophages (TEM) are regarded as very important subset of myeloid cells, especially in tumor angiogenesis. We therefore analyzed the Tie-2 and F4/80 expression among the myeloid cell populations divided according to Ly6C and MHC II markers. F4/80^{+} Tie-2^{+} cells were mainly present in both MHC II^{hi} populations, regardless of Ly6C expression. There were no significant differences in F4/80+ Tie-2+ percentages of parent populations between SCC VII-Luc and SCC VII-Luc-HO-1 tumors. However, percentages of Ly6C^{lo} MHC II^{lo} F4/80^{+} Tie-2^{+} and Ly6C^{lo} MHC II^{hi} F4/80^{+} Tie-2^{+} subsets among all cells in the tumor were higher in HO-1 overexpressing tumors than in the control ones (Fig. 30).

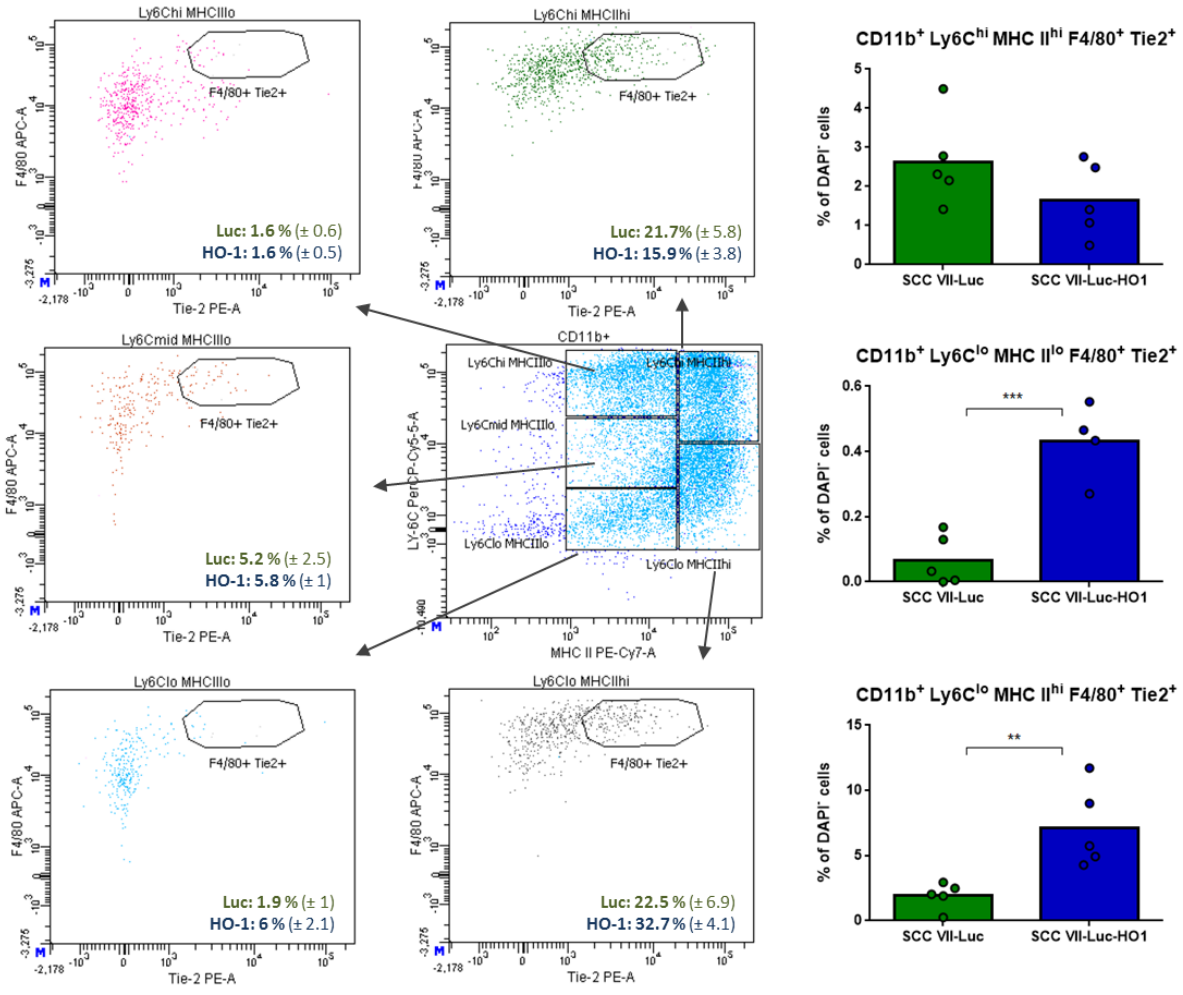

Fig. 30. Further characterization of the main myeloid cells populations, based on F4/80 and Tie-2 expression (mean + individual values plotted, unpaired T- test, 5 samples per group); the mean percentages of F4/80^{+} Tie-2^{+} cells among the parent population are shown on the plots.

Next, we analyzed the infiltration of tumors with MDSC. After 2 weeks of tumor growth among MDSC infiltrating the tumors, Ly6C^{low} Ly6G^{+} granulocytic MDCS (G-MDSC) were more abundant than Ly6C^{hi} Ly6G^{-} monocytic-MDSC (M-MDSC), and there were no

differences in percentages of MDSC populations between SCC VII-Luc and SCC VII-Luc-HO-1 tumors (Fig. 31 A).

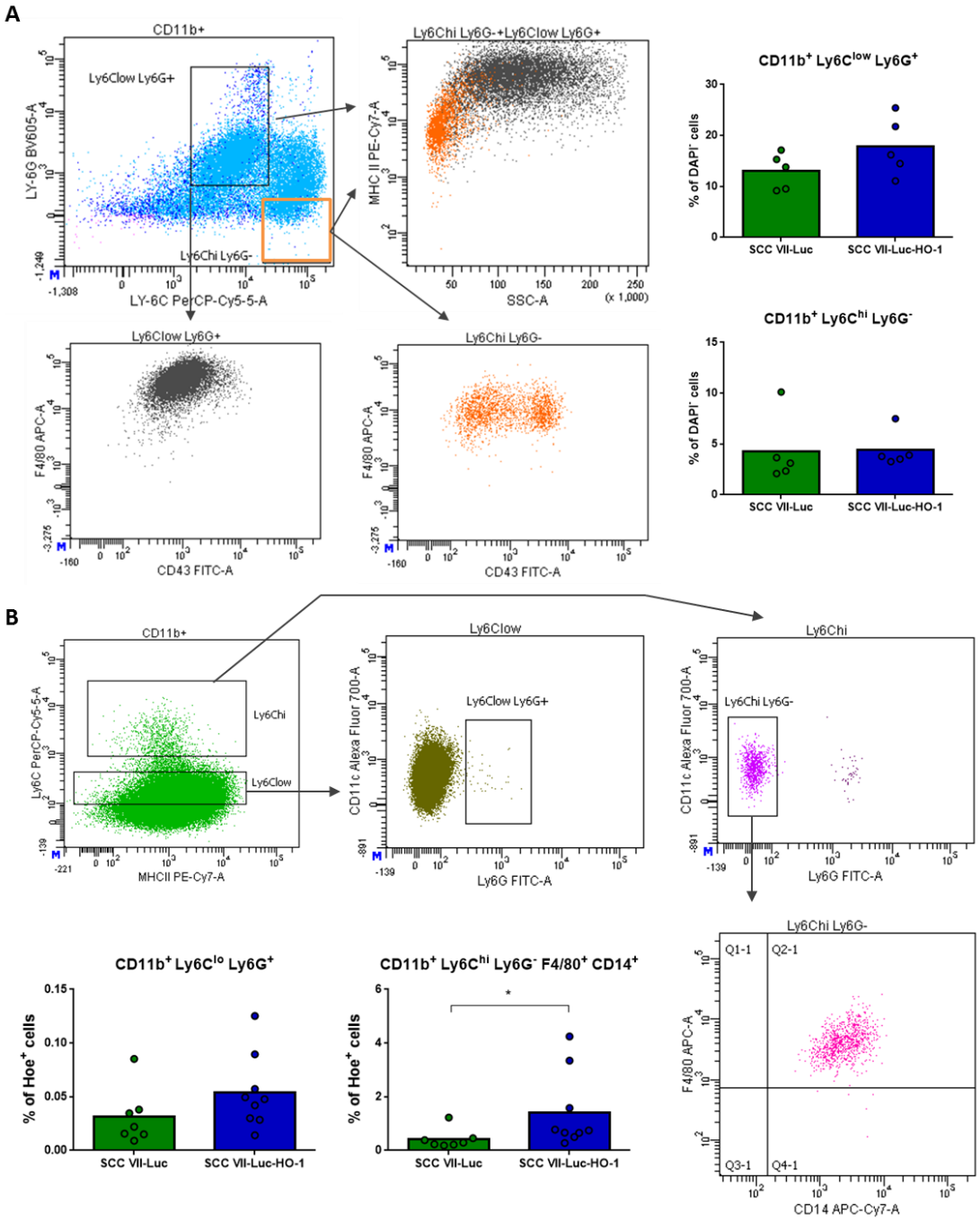

Fig. 31. Flow cytometry analysis of myeloid-derived suppressor cells (MDCS) infiltrating the SCC VII tumors; A. 2 weeks after subcutaneous injection of C3H mice with SCC VII cells (mean + individual values plotted, unpaired T- test, 5 samples per group)**; B.** 1 month after subcutaneous injection of C3H mice with SCC VII cells (mean + individual values plotted, Mann-Whitney test, 7-9 samples per group).

When tumors were grown for 1 month, there was a very low percentage of G-MDSC, similar between both groups. M-MDSC were more abundant and their percentage was higher in the SCC VII-Luc-HO-1 tumors than in SCC VII-Luc tumors. Almost all infiltrating M-MDSC were F4/80 and CD14 positive (Fig. 31 B).

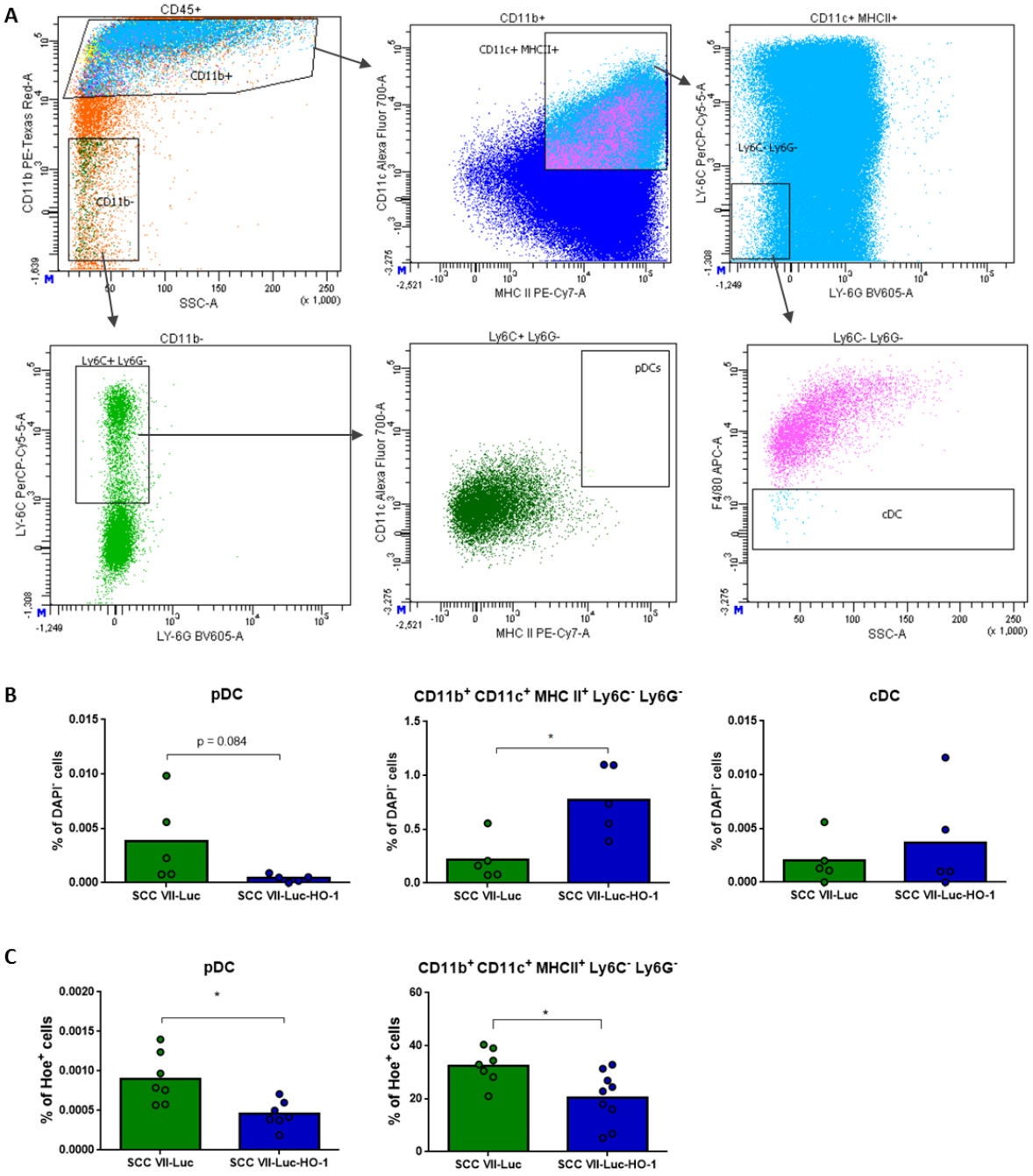

Fig. 32. Flow cytometry analysis of dendritic cells (DC) infiltrating the SCC VII tumors; A. Gating strategy for analysis of dendritic cells; **B.** Analysis of DC 2 weeks after subcutaneous injection of C3H mice with SCC VII cells (mean + individual values plotted, unpaired T- test, 5 samples per group); **C.** Analysis of DC 1 month after subcutaneous injection of C3H mice with SCC VII cells (mean + individual values plotted, Mann-Whitney test, 7-9 samples per group).

Dendritic cells comprised a very low percent of cells in the SCC VII tumors. After 2 weeks of tumor growth pDC were only present in SCC VII-Luc tumors and cDC were similarly infiltrating both SCC VII-Luc and SCC VII-Luc-HO-1 tumors. However, $CD11b^+$ $CD11c^+$ MHC II^+ $Ly6C^-$ $Ly6G^-$ cells, mostly positive for F4/80 marker, were more abundant in SCC VII tumors and their amount was higher in HO-1-overexpressing tumors than in the control ones (Fig. 32 B). When the tumors were growing for 1 month, the percentage of plasmacytoid dendritic cells (pDC) infiltrating the SCC VII tumors was very low, but it was higher in SCC VII-Luc than in SCC VII-Luc-HO-1 tumors (Fig. 32 C).

We analyzed also the lymphoid infiltration into the SCC VII tumors. SCC VII-Luc-HO-1 had lower CD4/CD8 ratio of tumor infiltrating lymphocytes after 1 month of tumor growth (Fig. 33). Moreover, HO-1 overexpressing tumors were less infiltrated with cells of Treg phenotype ($CD4^+$ $CD25^+$).

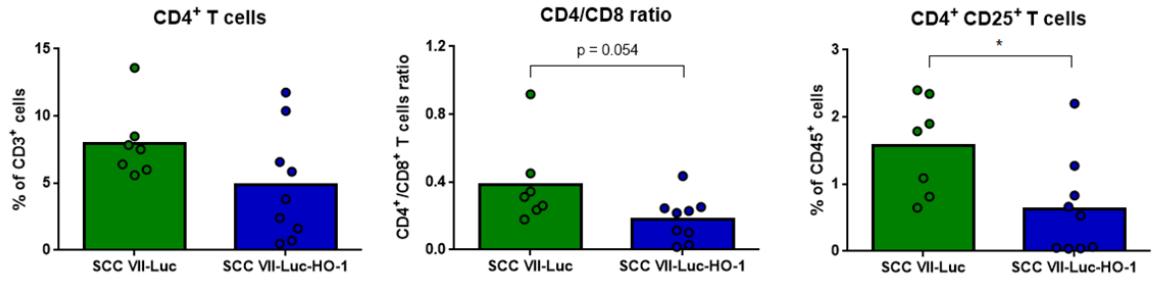

Fig. 33. Flow cytometry analysis of T lymphocytes infiltrating the tumors 1 month after subcutaneous injection of C3H mice with SCC VII cells (mean + individual values plotted, unpaired T-test, 7-9 samples per group).

We did not observe any differences in total WBC number and percentage of lymphocytes in peripheral blood between mice with SCC VII-Luc and SCC VII-Luc-HO-1 tumors (Fig. 34 A). However, after one month of tumor growth flow cytometry analysis of blood lymphocytes showed increased CD4/CD8 ratio in mice with control (SCC VII-Luc) tumors, which was at the normal level in mice with HO-1-overexpressing tumors. The number of $CD4^+$ $CD25^{hi}$ Treg cells was decreased in tumor-bearing mice, however there were no differences between SCC VII-Luc and SCC VII-Luc-HO-1 groups (Fig. 34 B). Mice with the control tumors had decreased number of RBC in blood (Fig. 34 A).

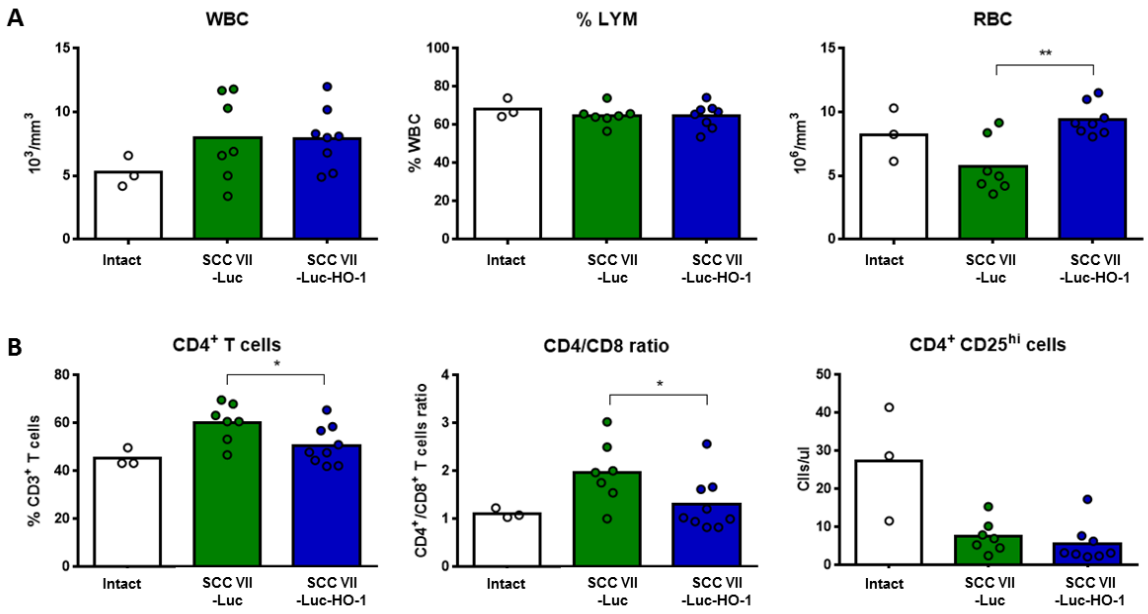

Fig. 34. Peripheral blood from mice injected subcutaneously with SCC VII cells for 1 month. A. Complete blood count; **B.** Flow cytometry-based T cell analysis (mean + individual values plotted, Mann-Whitney test between SCC VII-Luc and SCC VII-Luc-HO-1 injected mice, 7-9 samples per compered groups and 3 control samples). Intact – control, untreated mice.

Having observed the influence of HO-1 overexpression in tumor cells on circulating blood lymphocytes, we expected to find differences in the cytokine concentrations. Therefore, we analyzed the plasma samples by Luminex assay. We especially looked at the cytokines which were differentially expressed in mice with different HO-1 genotype upon the 4NQO treatment and cytokines produced in high amounts by SCC VII cells *in vitro*.

After 2 weeks of tumor growth we did not find the differences in concentrations of MCP-1, RANTES, eotaxin, KC, LIX, MIG, IP-10 and G-CSF (Fig. 35 A). Similarly 1 month after tumor cells injection, there were no differences in MCP-1, RANTES, KC and IL-6 concentrations between plasma samples from mice with SCC VII-Luc and SCC VII-Luc-HO-1 tumors. However, levels of eotaxin, LIX, MIG and IP-10 were lower in mice with SCC VII-Luc tumors than in mice with SCC VII-Luc-HO-1 tumors (Fig. 35 B). Concentration of VEGF was at the border of detection in SCC VII-Luc group and slightly lower in SCC VII-Luc-HO-1 group. Concentrations of IL-4, IL-5, IL-7, IL-10, IL-15, INFγ, TNFα and GM-CSF were below the detection limit.

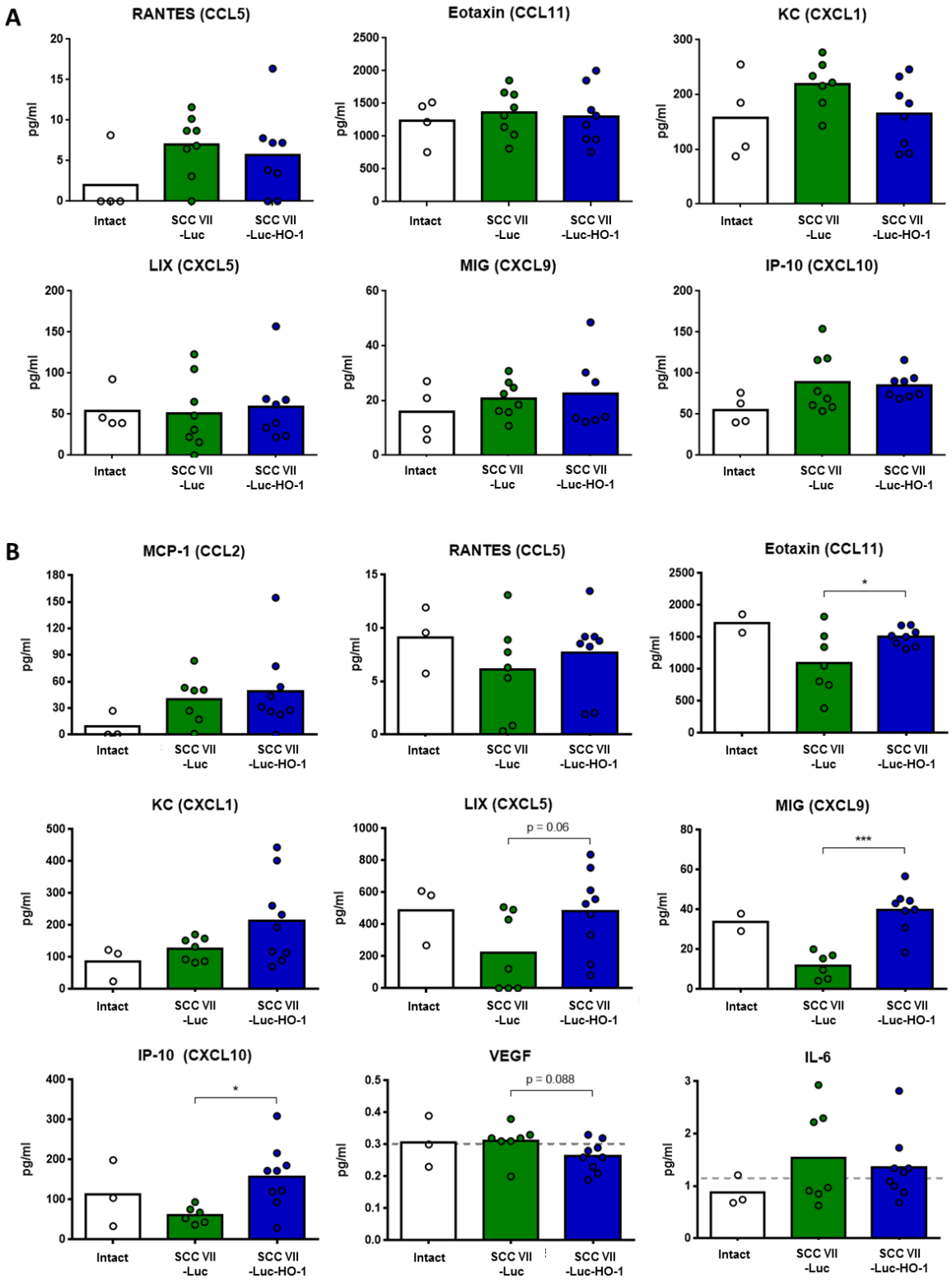

Fig. 35. Cytokine concentrations in the plasma of SCC VII tumor bearing mice. A. 2 weeks after subcutaneous injection of C3H mice with SCC VII cells (mean + individual values plotted, unpaired T-test between SCC VII-Luc and SCC VII-Luc-HO-1 injected mice, 8 samples per compered groups and 4 control samples). **B.** 1 month after subcutaneous injection of C3H mice with SCC VII cells (mean + individual values plotted, Mann-Whitney test between SCC VII-Luc and SCC VII-Luc-HO-1 injected mice, 7-9 samples per compered groups and 3 control samples). Intact – control, untreated mice.

SCC VII cell injection into syngeneic C3H mice showed that HO-1 overexpression in SCC VII cells increased tumor infiltration with leukocytes and affected the phenotype of infiltrating cells. Moreover, HO-1 expression in tumor cells had systemic effect on cytokine concentration in plasma and T cell populations in peripheral blood when tumors were growing for 1 month.

5.2.2. CoPP treatment affects the infiltration of Matrigel plugs with myeloid cells, plasma cytokine concentrations and leukocyte counts

Having observed the different infiltration of control and HO-1-overexpressing tumors with the immune cells we decided to pharmacologically induce and inhibit HO-1 activity together with SCC VII cells injection (Fig. 36).

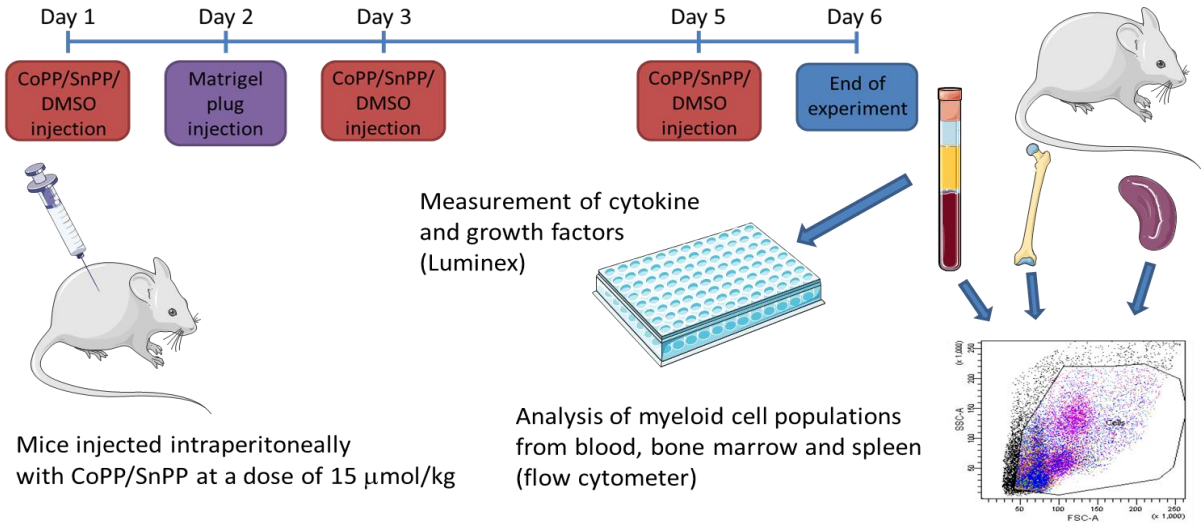

Fig. 36. Scheme of the experiment aiming to investigate the effect of pharmacological HO-1 induction for the tumor infiltration with myeloid cells.

We injected the mice with Matrigel plugs containing SCC VII-Luc or SCC VII-Luc-HO-1 cells. Empty Matrigel plugs were used as a control. Mice with empty plugs or plugs with SCC VII-Luc cells were additionally injected with HO-1 inducer (CoPP), HO-1 inhibitor (SnPP) or proper solvent controls, one day before, one day after and three days after the Matrigel plug injection. CoPP ans SnPP were dissolved in DMSO further diluted in NaCl. As DMSO itself can have anti-inflammatory properties, both Nacl and DMSO were used as controls. We analyzed the myeloid cell populations in the blood, bone marrow and spleen (Fig. 36).

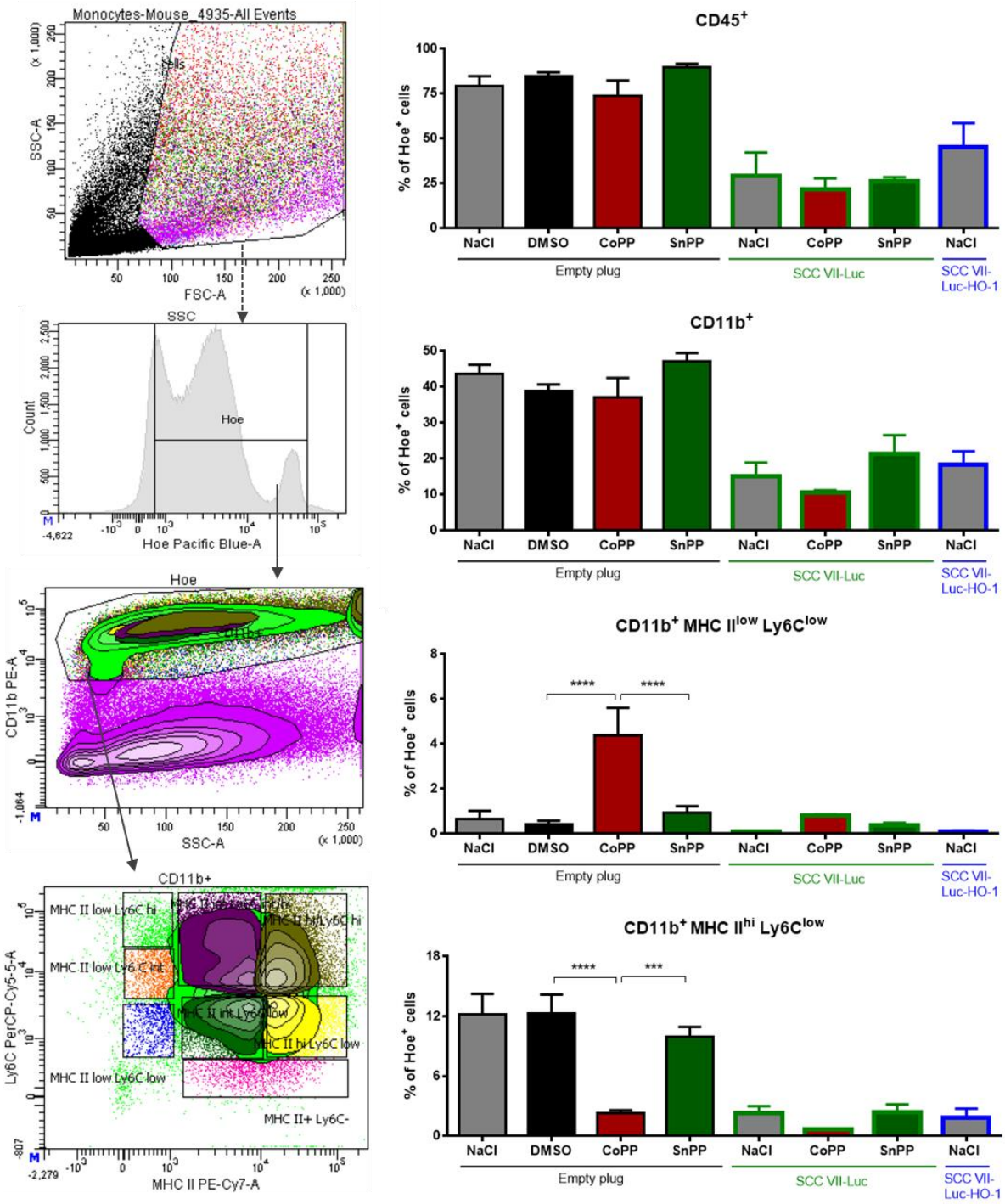

Fig. 37. Flow cytometry analysis of myeloid cells infiltrating the tumors, 5 days after subcutaneous injection of SCC VII cells: gating strategy (left panel) and percentages of cells infiltrating the tumor (right panel) (mean + SEM, one-way Anova with Bonferroni post-test, 5 mice per group).

There were no differences in early infiltration of Matrigel plugs containing SCC VII-Luc and SCC VII-Luc-HO-1 cells with total CD45$^+$ or CD11b$^+$ myeloid cells. Analysis of MHC II and Ly6C expression allowed us to distinguish few distinct populations of myeloid cells. In CoPP treated mice, we observed altered phenotype of CD11b$^+$ Ly6C^{low} plug-infiltrating cells - higher percentage of MHC II^{low} an lower percentage of MHC II^{hi} cells

(Fig. 37). Effects of HO-1 pharmacological induction by CoPP were not achieved by HO-1 overexpression in tumor cells. Moreover, HO-1 inhibition by SnPP did not have opposite effect to HO-1 upregulation by CoPP. Those observations may suggest that CoPP acts on immune system independently of HO-1.

Additional analysis of flow cytometry data allowed for identification of several cell populations that were more heavily infiltrating SCC VII-Luc-HO-1-containing Matrigel plugs than plugs with control SCC VII-Luc cells. In plugs with HO-1 overexpressing cells we observed increased percentage of $CD11b^{+}$ $F4/80^{+}$ $Ly6C^{hi}$ $Ly6G^{-}$ TAMs with high or low expression of MHC II. pDC were present in small numbers plugs with SCC VII-Luc-HO-1 cells, but not in plugs with SCC VII-Luc cells. We observed no differences in the percentage of G-MDSCs, Mo-MDSCs and cDC between plugs with SCC VII-Luc and SCC VII-Luc-HO-1 (Fig. 38).

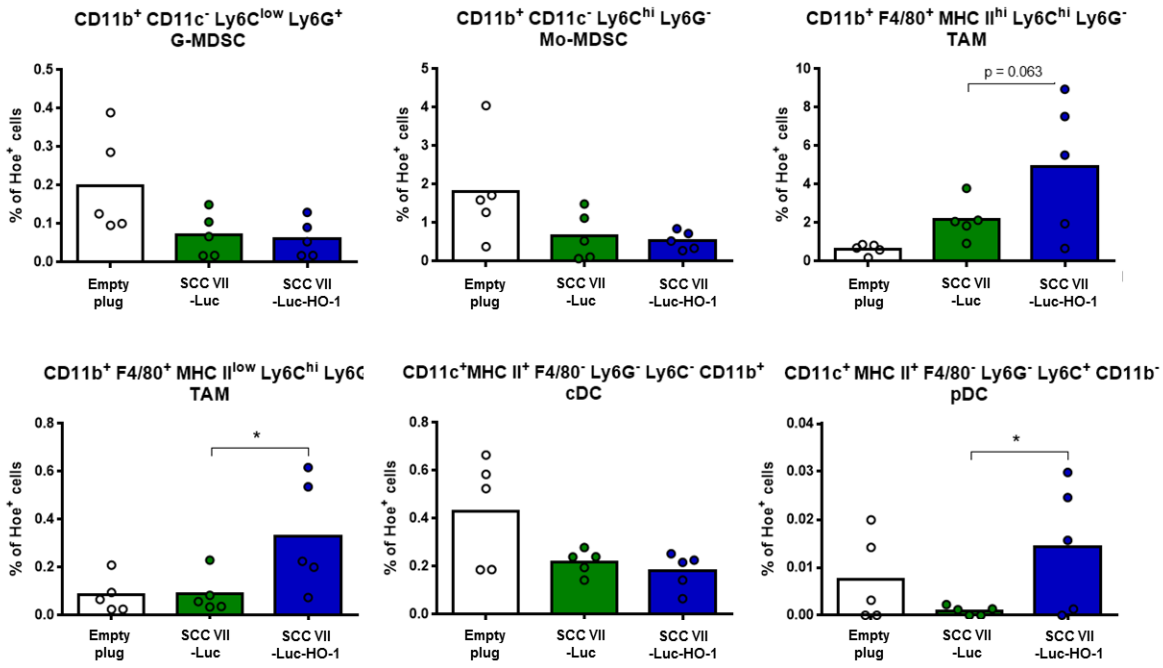

Fig. 38. Further characterization of cells infiltrating the tumors, 5 days after subcutaneous injection of SCC VII cells (mean + individual values plotted, one-way Anova with Bonferroni post-test between SCC VII-Luc and SCC VII-Luc-HO-1, 5 mice per group).

There were no differences in the complete blood cell count parameters between SCC VII-Luc- and SCC VII-Luc-HO-1-bearing mice. However, we observed increased number of WBC, increased percentage of granulocytes and decreased percentage of lymphocytes in mice treated with CoPP. Treatment of mice with SnPP did not have any effect of blood parameters (Fig. 39).

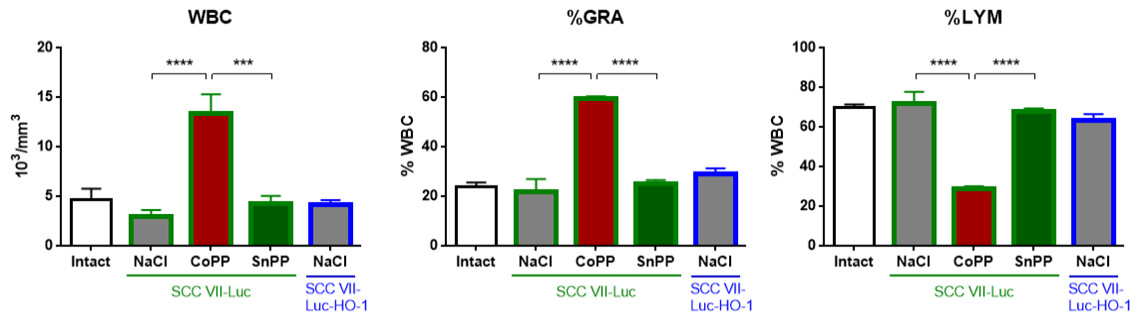

Fig. 39. Complete blood cell count in the C3H mice, 5 days after subcutaneous injection of SCC VII cells (mean + SEM, one-way Anova with Bonferroni post-test, 5 mice per group).

Among cytokines tested, there were no differences in plasma concentrations between mice with Matrigel plugs containing the SCC VII-Luc or SCC VII-Luc-HO-1 cells. However, in the plasma of CoPP-treated mice, we observed increased concentrations of G-CSF, M-CFS, IL-6 and IP-10. Treatment with SnPP did not affect any cytokine levels (Fig. 40).

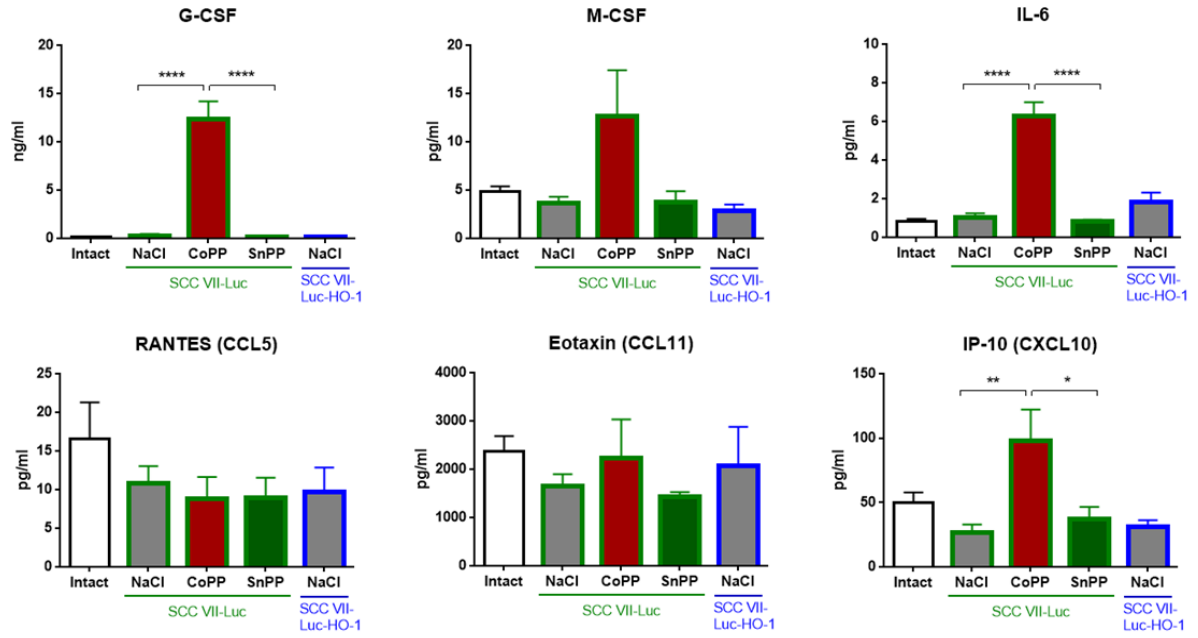

Fig. 40. Cytokine concentrations in plasma of C3H mice, 5 days after subcutaneous injection of SCC VII cells (mean + SEM, one-way Anova with Bonferroni post-test, 5 mice per group).

HO-1 overexpression in SCC VII cells did not have a profound effect on Matrigel plug infiltration with leukocytes 5 days after subcutaneous injection. However, treatment with HO-1 inducer, CoPP affected Matrigel plug infiltration, leukocyte counts in blood and cytokine concentration in plasma.

5.3. CoPP treatment induces mobilization of cells from the bone marrow to blood

5.3.1. CoPP treatment increases leukocyte numbers in blood

Treatment of SCC VII tumor-bearing mice with CoPP increased the number of white blood cells and the concentrations of G-CSF, IL-6 and IP-10 in plasma (Fig. 39, Fig. 40).

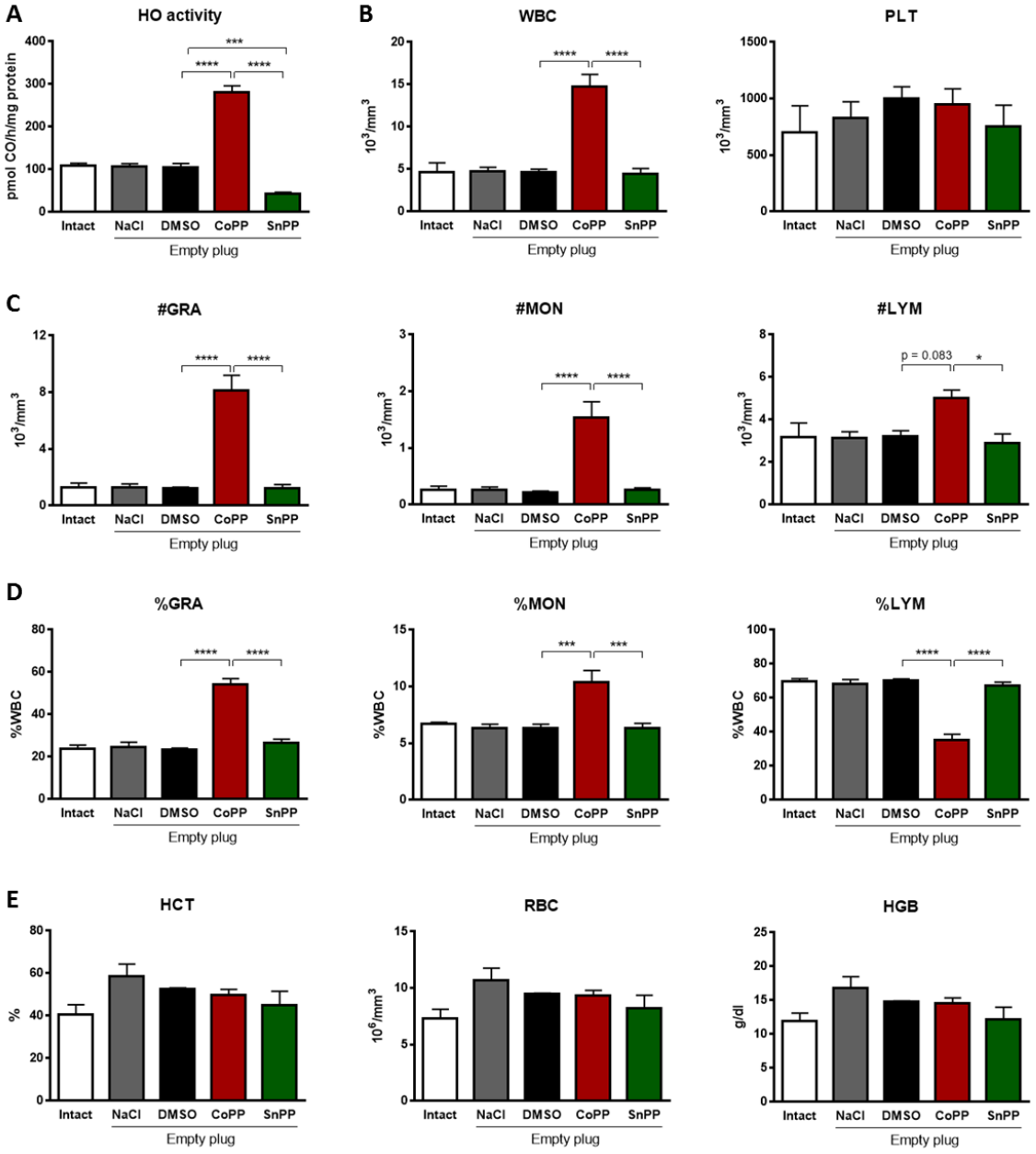

Fig. 41. Effects CoPP and SnPP on HO-1 activity and complete blood count in C3H mice (mean + SEM, one-way Anova with Bonferroni post-test, 5 mice per group). **A.** HO-1 activity in the liver (measured by dr Lucie Muchova, Charles University in Prague); **B.** Numbers of white blood cells and platelets; **C.** Numbers of granulocytes, monocytes and lymphocytes; **D.** Percentages of granulocytes, monocytes and lymphocytes; **E.** Hematocrit, red blood cell number and hemoglobin content; WBC - white blood cells, PLT - platelets, #GRA – number of granulocytes, #MON – number of monocytes, #LYM – number of lymphocytes, %GRA – percentage of granulocytes, %MON – percentage of monocytes, %LYM – percentage of lymphocytes, HCT – hematocrit, RBC – red blood cells, HGB – hemoglobin.

Administration of CoPP resulted in 2.6-fold increase in HO-1 activity (measured in the liver), whereas SnPP decreased HO-1 activity by 2.4 times (Fig. 41 A). Mice treated with CoPP had increased number of all types of leukocytes in blood (Fig. 41 B, C). However there is a visible shift towards myeloid lineage, as the percentage of lymphocytes decreases in favor of granulocytes and monocytes (Fig. 41 D). Number of platelets, as well as erythrocyte parameters, were unaffected by CoPP treatment (Fig. 41 E). In contrast, SnPP did not have any effect of complete blood count.

5.3.2. Treatment with CoPP increases concentrations of G-CSF and IL-6 in plasma

We analyzed a panel of cytokines in plasma of mice treated with CoPP and SnPP.

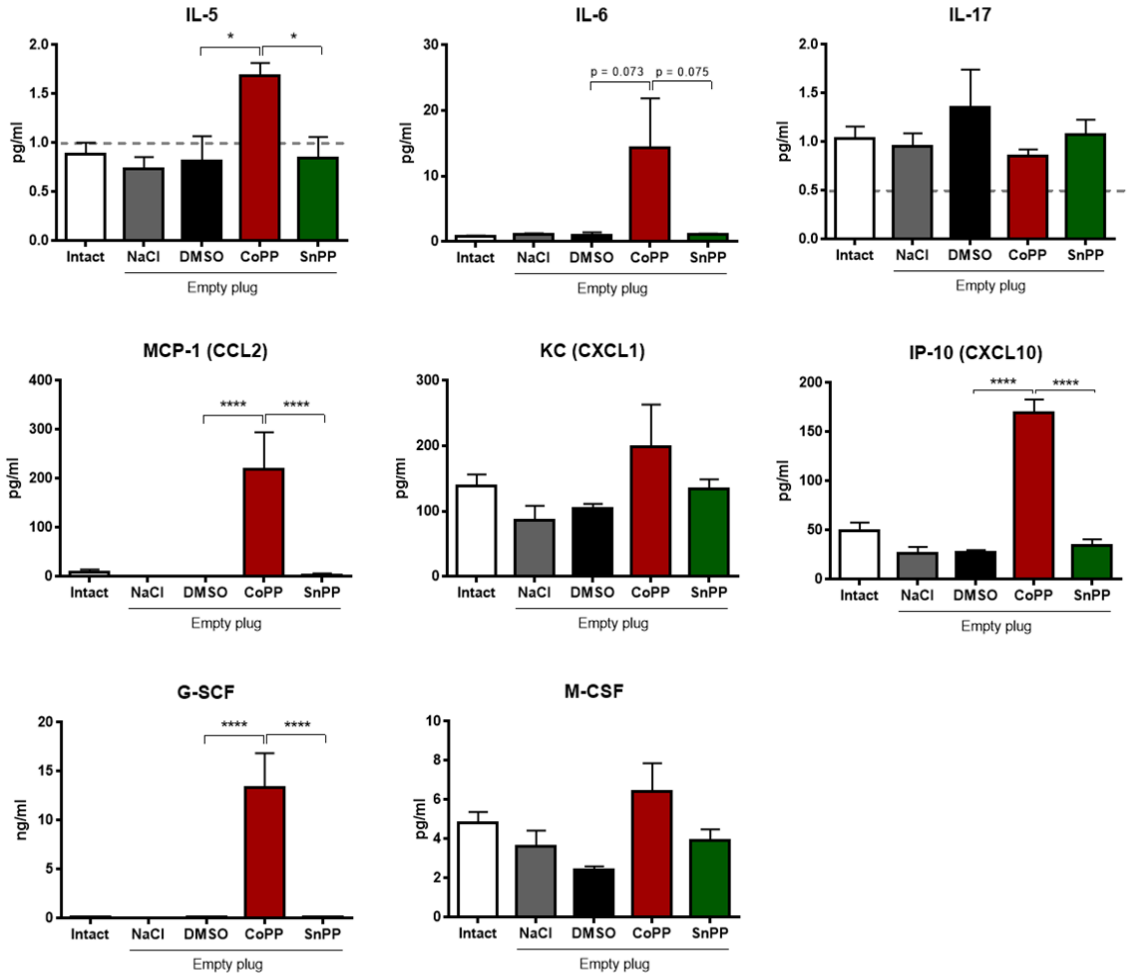

Fig. 42. Concentrations of selected cytokine in the plasma of C3H mice treated with CoPP or SnPP (mean + SEM, one-way Anova with Bonferroni post-test, 5 mice per group).

Concentrations of IL-5 and IL-6 were increased in response to CoPP administration (Fig. 42). Concentrations of IL-1α, IL-1β, IL-2, IL-3, IL-4, IL-7, IL-9, IL-10, IL-12p40, IL-12p70, IL-13 and IL-15 were below the detection limit. CoPP increased the level of chemokines,

MCP-1 and IP-10, not affecting KC (Fig. 42). MIP-1α, mIP-1β and MIP-2 were not detectable. We observed a strong increase of G-CSF, but other colony stimulating factors were unchanged (M-CSF) (Fig. 42) or not detectable (GM-CSF). We could not detect TNFα, INFγ and VEGF in the plasma. Surprisingly, SnPP did not have any influence on any of the analyzed cytokines.

Flow cytometry analysis of bone marrow shows decrease in CD11b$^+$ F4/80$^+$ MHC II^{hi} macrophages. More frequent subpopulation of CD11b$^+$ F4/80$^+$ MHC II^{low} cells was not affected (Fig. 43 A). At the same time, number of CD11b$^+$ F4/80$^+$ MHC II^{hi} and MHC II^{low} macrophages in the spleen was increased (Fig. 43 B). Both in the bone marrow and spleen we observed an increase in CD11b$^+$ CD11c$^-$ Ly6C$^{low/+}$ Ly6G$^+$ cells (Fig. 43 A, B).

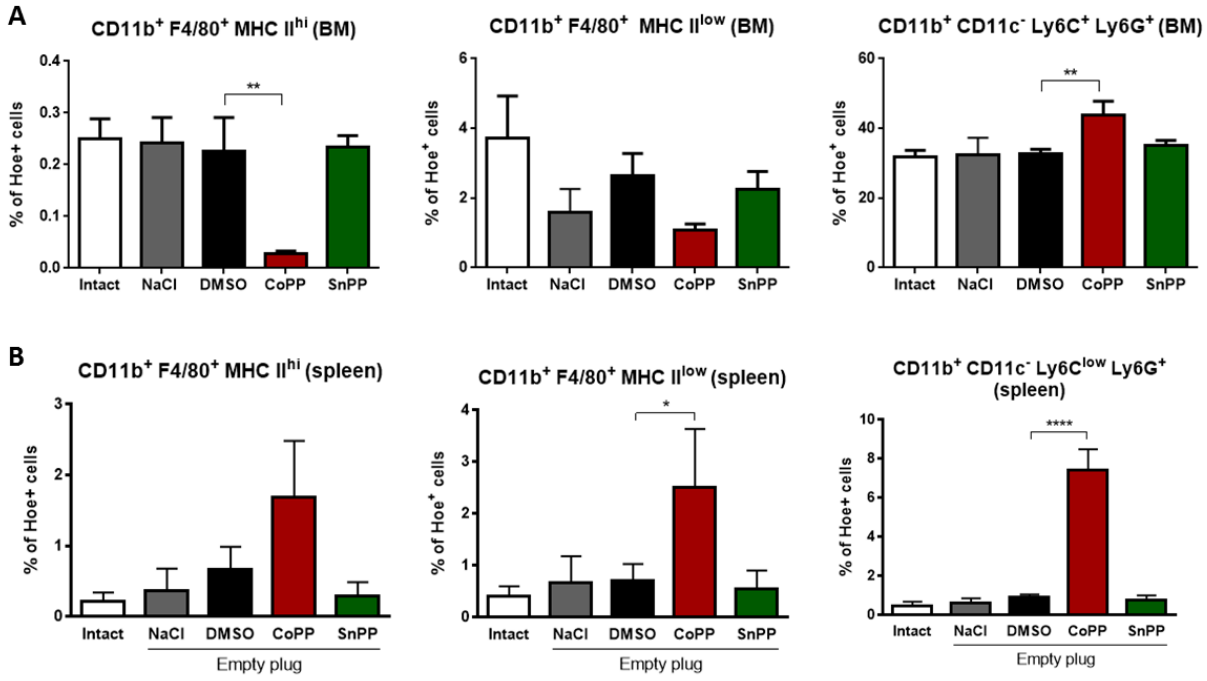

Fig. 43. Macrophage populations in the bone marrow (A) and spleen (B) of C3H mice treated with CoPP or SnPP (mean + SEM, one-way Anova with Bonferroni post-test, 5 mice per group).

5.3.3. CoPP exerts similar effects to G-CSF treatment

As treatment of mice with CoPP increased G-CSF concentration in plasma, we directly compared the effect of G-CSF and CoPP administration (Fig. 44 A). C57BL/6xFVB mice were injected with rhG-CSF, CoPP or appropriate vehicle controls (NaCl and DMSO, respectively), once a day for 5 days. Six hours after the last injection the peripheral blood and bone marrow samples were collected. We analyzed myeloid and hematopoietic stem/progenitor cells by flow cytometry.

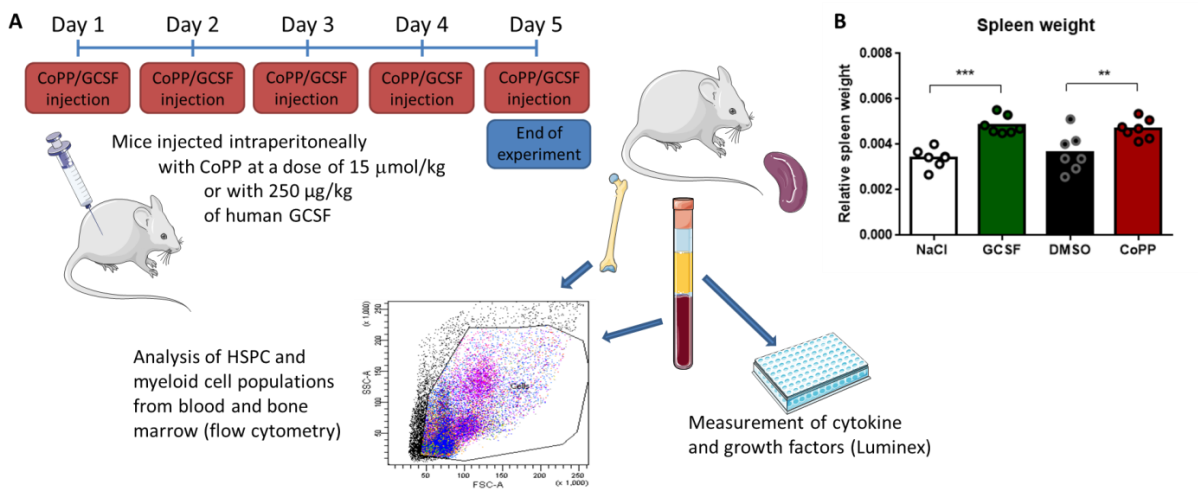

Fig. 44. Experiment comparing the effects of G-CSF and CoPP treatment. A. Scheme of the experiment; **B.** Relative spleen weight in mice treated with G-CSF or CoPP (mean + individual values plotted, one-way Anova with Bonferroni post-test, 7 mice per group).

Mice treated with G-CSF and CoPP had enlarged spleens, when compared to the vehicle controls (Fig. 44 B). Main leukocyte populations were counted basing on the flow cytometry analysis using Trucount tubes. We observed increased number of $CD45^+$ cells, especially granulocytes, in the peripheral blood of mice treated with G-CSF and CoPP, however, the increase was higher after G-CSF (Fig. 45). The numbers of monocytes and NK cells were similarly increased after G-CSF and CoPP. Only G-CSF treatment led to the increase in lymphocytes, mainly T cells.

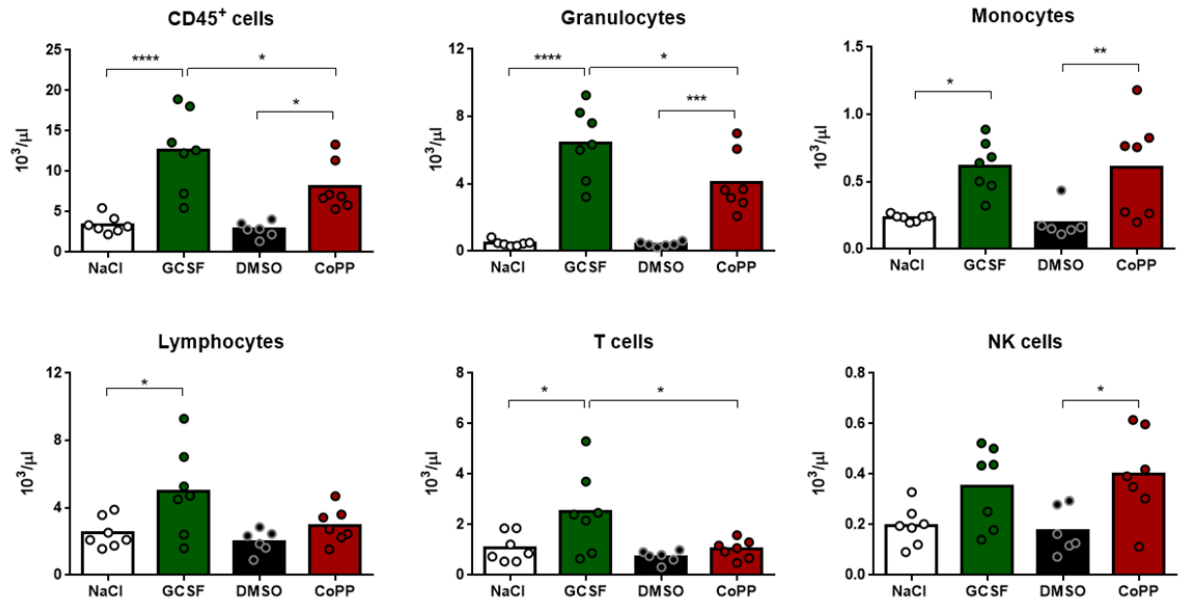

Fig. 45. Numbers of cells of basic hematopoietic cell populations in blood of C57BL/6xFVB mice treated with G-CSF or CoPP (mean + individual values plotted, one-way Anova with Bonferroni post-test, 7 mice per group).

Further analysis of myeloid cells by flow cytometry shows the differences in phenotype between granulocytes mobilized by CoPP and G-CSF. CD11b$^+$ CD11c$^-$ Ly6C$^-$ Ly6G$^+$ cells mobilized by CoPP are more granular (higher SCC parameter) and have higher expression of Ly6G (Fig. 46). They resemble more the granulocytes of the control mice than that mobilized by G-CSF.

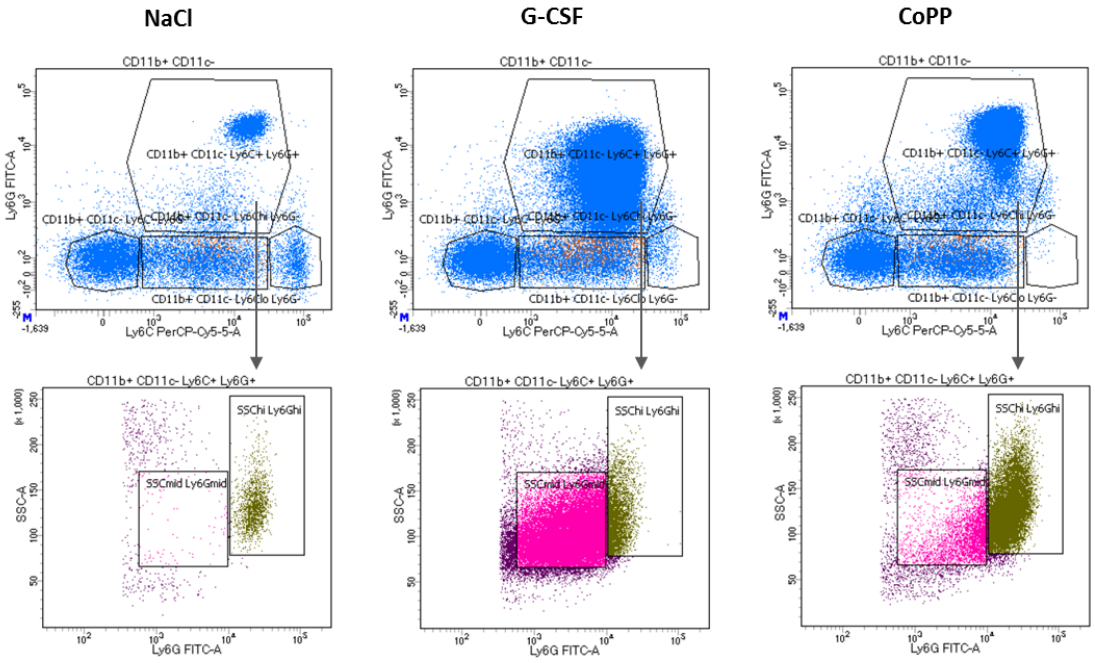

Fig. 46. Representative plots from the flow cytometry analysis of granulocytes in the blood of CoPP and G-CSF treated mice.

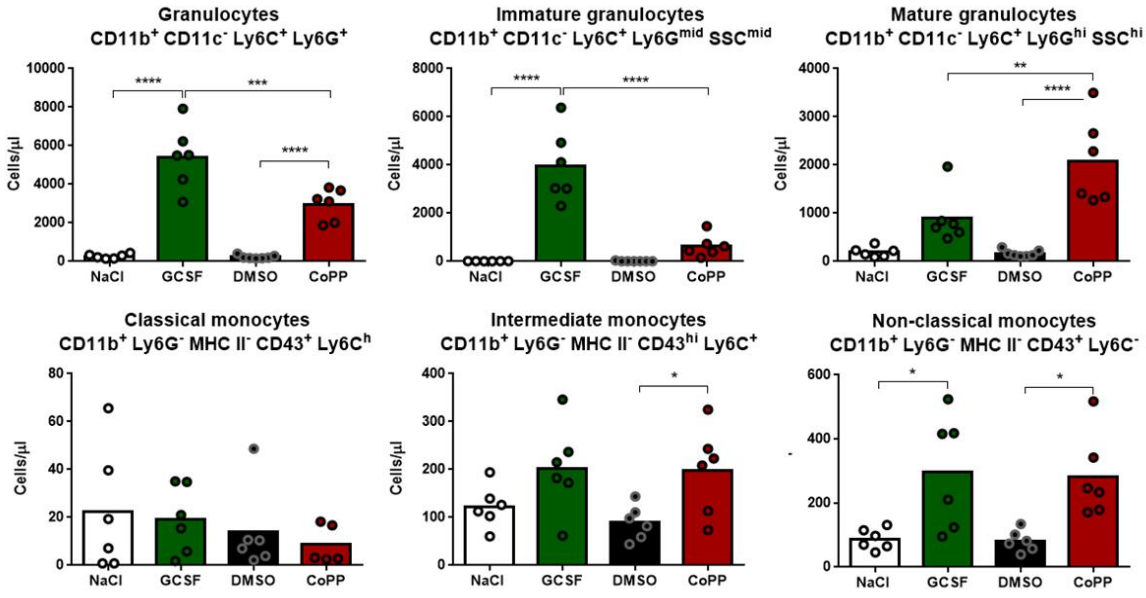

Fig. 47. Flow cytometry analysis of myeloid cells in peripheral blood of C57BL/6xFVB mice treated with G-CSF and CoPP (mean + individual values plotted, one-way Anova with Bonferroni post-test, 7 mice per group).

Although mice treated with G-CSF had the higher total number of granulocytes in blood, these were mainly immature granulocytes (Ly6G^{mid} SCC^{mid}), whereas CoPP treatment increased the number of mature cells (Ly6G^{hi} SCC^{hi}) (Fig. 47, upper panel). Both G-CSF and CoPP increased the numbers of non-classical and intermediate monocytes, without classical monocytes population being affected (Fig. 47, bottom panel).

Having observed an increase in granulocyte numbers and G-CSF concentration in blood after CoPP treatment, we analyzed the composition of the myeloid cell populations in the bone marrow (Fig. 48 upper panel). Percentage of CD11b$^+$ CD11c$^-$ Ly6C^{low} Ly6G$^+$ and CD11b$^+$ CD11c$^-$ Ly6C^{low} SSC^{med} Ly6G^{med} cells was increased after G-CSF and CoPP treatment, but the increase after G-CSF was more pronounced. Percentage of CD11b$^+$ CD11c$^-$ Ly6C^{low} SSC^{hi} Ly6G^{hi} was decreased after G-CSF, but not affected by CoPP. Although there was no difference in the percentage of CD11b$^+$ F4/80$^+$ cells, we observed a decrease in CD11b$^+$ F4/80$^+$ CD11c$^-$ macrophages expressing low and high levels of MHC class II both after G-CSF and CoPP treatment (Fig. 48).

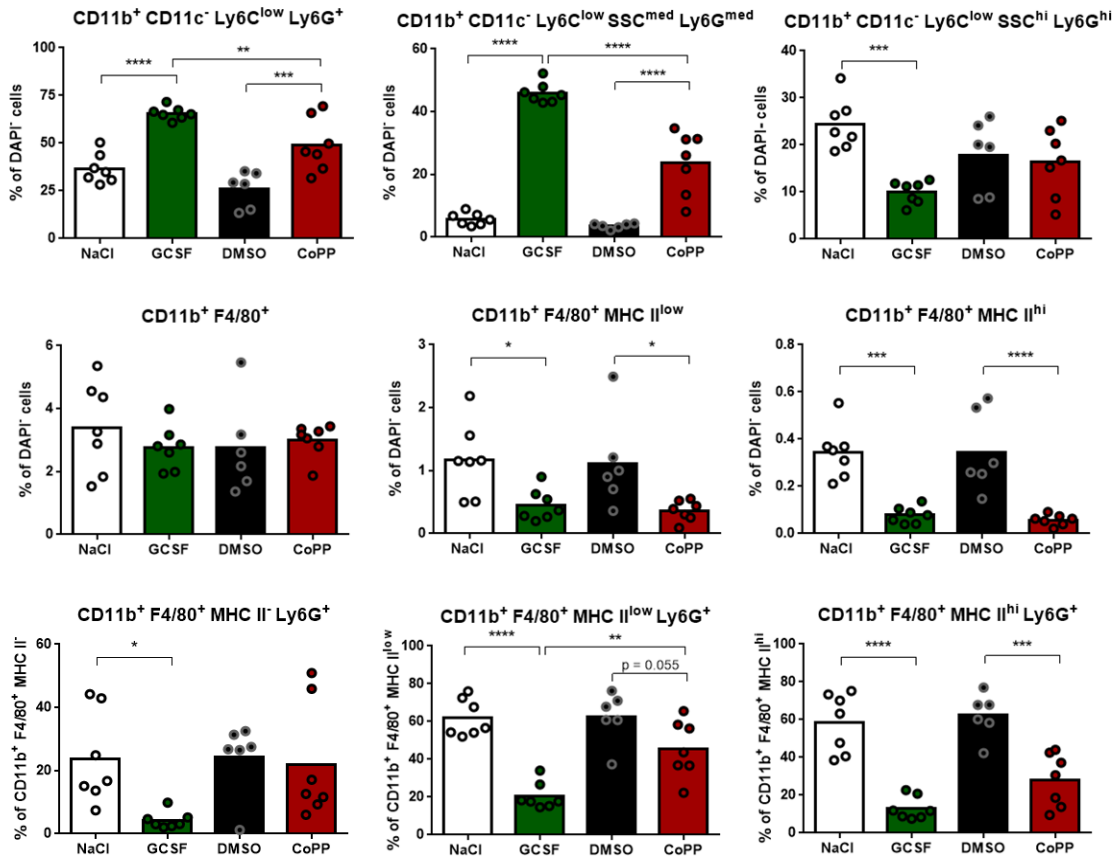

Fig. 48. Flow cytometry analysis of myeloid cells in bone marrow of C57BL/6xFVB mice treated with G-CSF or CoPP (mean + individual values plotted, one-way Anova with Bonferroni post-test, 6-7 mice per group).

Majority of MHC II expressing myeloid cells in the bone marrow were also positive for Ly6G marker. Percentage of Ly6G$^+$ cells among F4/80$^+$ MHC II^{low} or MHC II^{hi} cells decreased after CoPP and G-CSF treatment. In the population of MHC II negative cells, percentage of Ly6G$^+$ cells decreased only after G-CSF treatment (Fig. 48).

As G-CSF is a known mobilizer of hematopoietic stem and progenitor cells (HSPC), we analyzed HSPC populations in the blood and bone marrow of mice treated with CoPP and G-CSF. We found that mice treated with CoPP had increased percentage and number of KLS (c-Kit$^+$ Lin$^-$ Sca-1$^+$) cells in blood. In animals treated with G-CSF increase in KLS cells was visible, although it was not statistically significant.

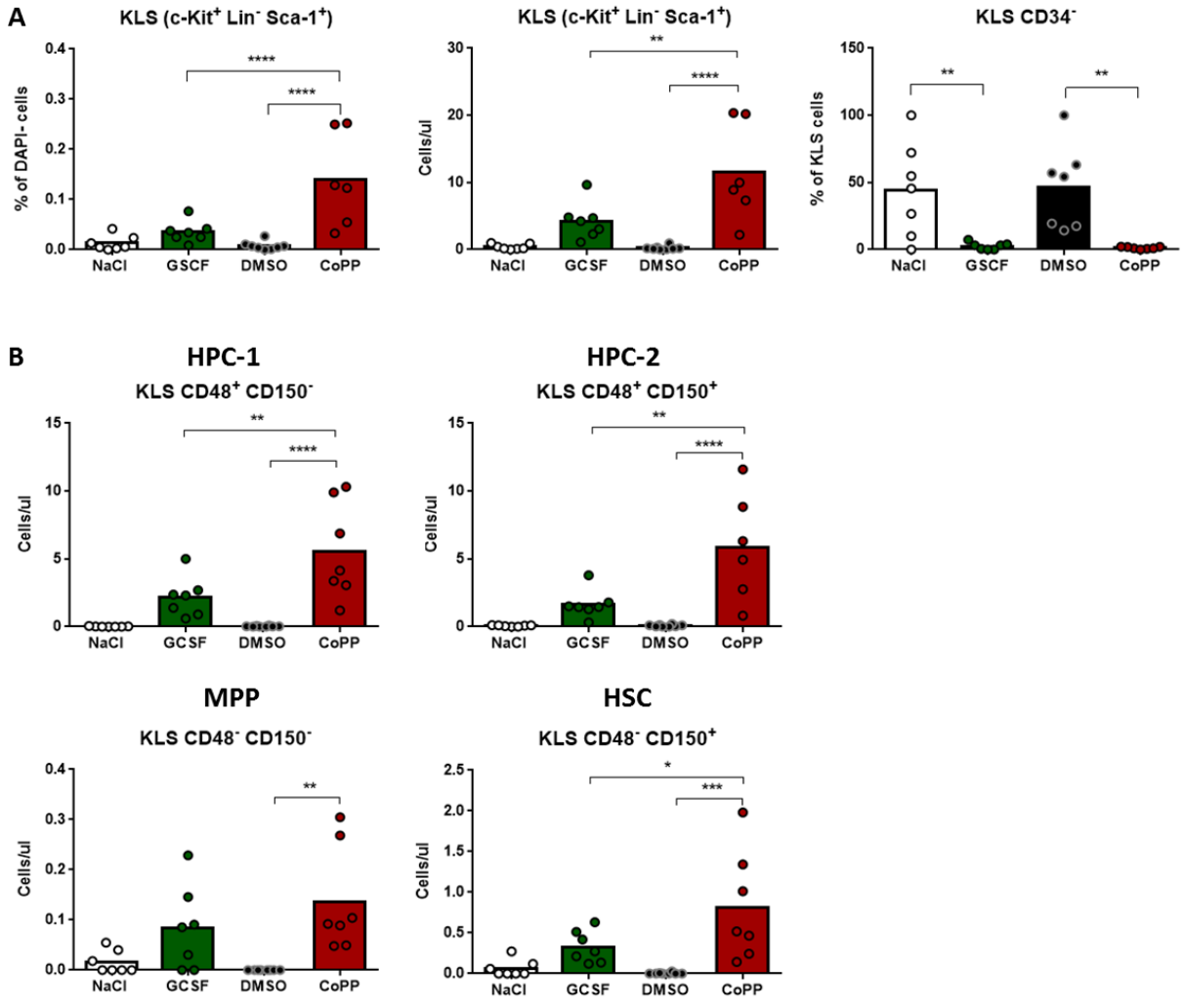

Fig. 49. Flow cytometry analysis of HSPC populations in blood of C57BL/6xFVB mice treated with G-CSF or CoPP (mean + individual values plotted, one-way Anova with Bonferroni post-test, 7 mice per group). **A.** Percentage and numbers of KLS (c-Kit+ Lin- Sca-1+) in blood, percentage of CD34- cells among KLS population **B.** Characterization of KLS population using CD48 and CD150 markers.

Mobilized KLS cells were further characterized using CD34 and SLAM markers CD48 and CD150, which enable to define HSC (KLS CD48$^-$ CD150$^+$), MPP (multipotent progenitors, KLS CD48$^-$ CD150$^-$) and HPC (hematopoietic progenitors, KLS CD48$^+$ CD150$^-$ and KLS CD48$^+$ CD150$^+$) populations [186]. CoPP treatment led to the higher increase in cells of HSC, MPP and HPC phenotypes than treatment with G-CSF [186]. Of note, only small proportion of KLS cells mobilized by G-CSF and CoPP were CD34 negative (Fig. 49).

Next we analyzed more differentiated, but still immature hematopoietic cells. Oligopotent, granulocyte-macrophage progenitor (GMP) and megakaryocyte-erythroid progenitor (MEP) numbers were more higher in the blood of mice treated with CoPP than in the mice treated by G-CSF. The increase in erythroid progenitors (EP) number was similar in both groups (Fig. 50).

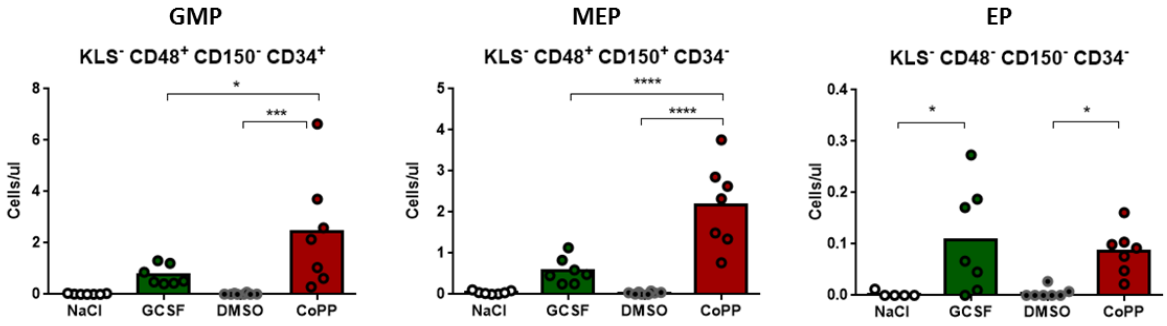

Fig. 50. Flow cytometry analysis of oligopotent and lineage-restricted progenitors in the blood of C57BL/6xFVB mice treated with G-CSF or CoPP (mean + individual values plotted, one-way Anova with Bonferroni post-test, 7 mice per group).

CoPP treatment led to the increase in KLS percentage in the bone marrow (Fig. 51). In contrast, percentage of committed progenitors (KLS$^-$) was decreased after G-CSF and CoPP, however the decrease after CoPP was less pronounced than after G-CSF. Further characterization of committed progenitors with CD34 and SLAM markers shows, that MEP and EP are similarly decreased after G-CSF and CoPP. Only G-CSF treatment leads to the decrease in GMP percentage in the bone marrow, there is no change visible after CoPP (Fig. 51).

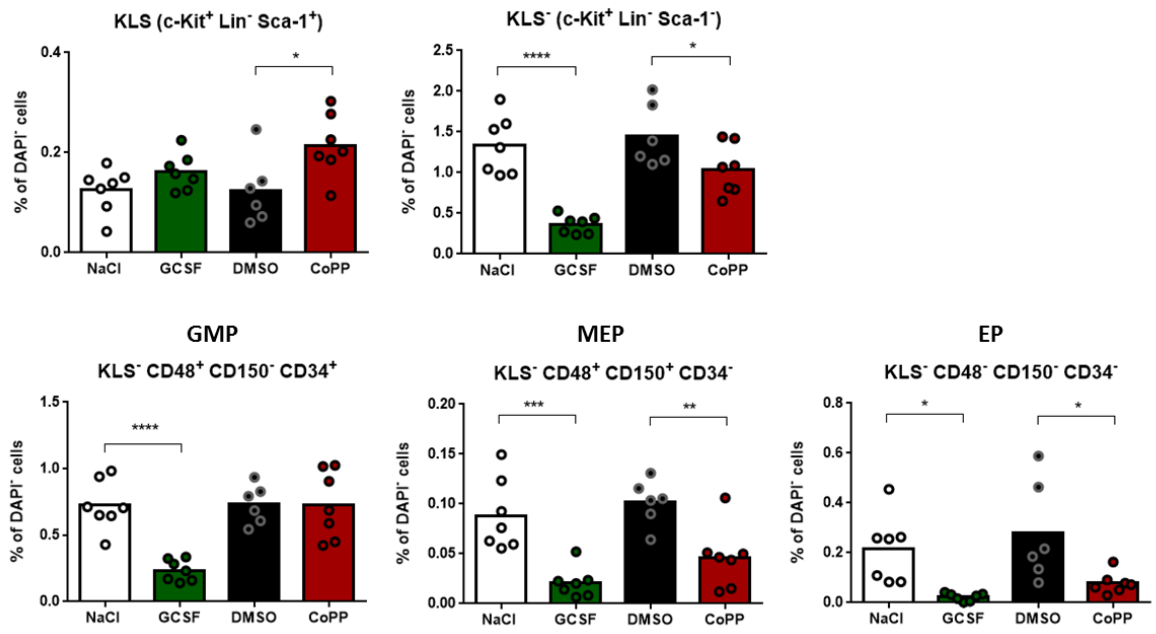

Fig. 51. Flow cytometry analysis of HSPC populations in bone marrow of C57BL/6xFVB mice treated with G-CSF or CoPP (mean + individual values plotted, one-way Anova with Bonferroni post-test, 7 mice per group).

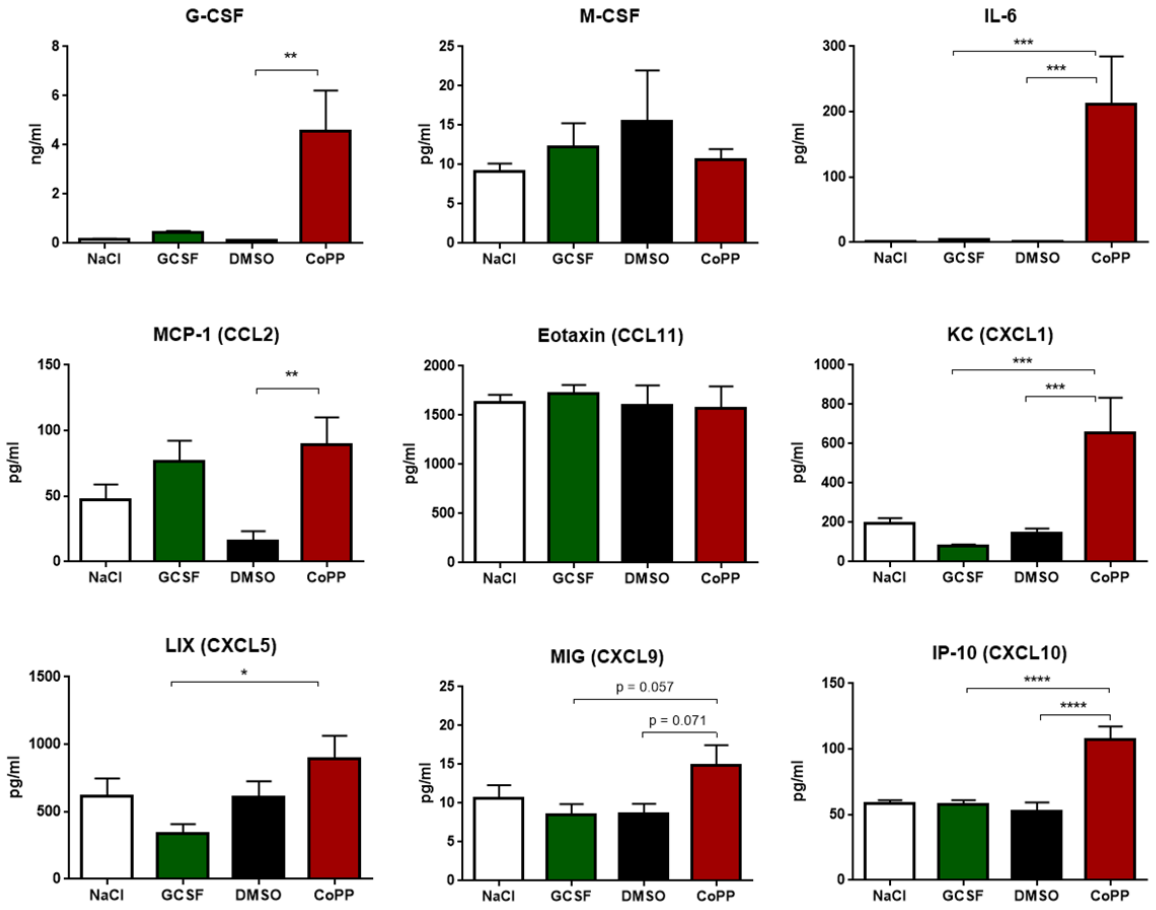

Fig. 52. Cytokine concentrations in the plasma of C57BL/6xFVB mice treated with G-CSF or CoPP (mean + SEM, one-way Anova with Bonferroni post-test, 7 mice per group).

By Luminex assay we confirmed the increase in G-CSF concentration after CoPP treatment. Additionally, we observed a 5-fold increase in IL-6 concentration after G-CSF administration, however, it was not comparable to the 160-fold increase in IL-6 concentration after CoPP. MCP-1 was upregulated by CoPP, while the increase after G-CSF was very small. Only CoPP treatment led to the increase in KC, IP-10 and MIG concentrations. Neither G-CSF nor CoPP increased concentrations of M-CSF and eotaxin. Concentration of LIX was slightly higher after CoPP than after G-CSF, however the increase after CoPP in comparison to DMSO control was not significant (Fig. 52).

The results of comparison between G-CSF and CoPP show that, although these two factors exert similar effects, some of the observed properties (e.g. increase in certain cytokine concentrations) are unique for CoPP. This suggests, that CoPP may work not only through G-CSF induction, but also other cytokines might be involved in its action.

5.3.4. CoPP mobilizes functional granulocytes

As shown in the previous section, treatment of mice with CoPP resulted in mobilization of the granulocytes of more mature phenotype, than treatment with G-CSF (Fig. 46 and Fig. 47). To investigate if more mature phenotype would correlate with the increased phagocytic function, we treated the mice with G-CSF or CoPP and measured reactive oxygen species (ROS) production after incubation of blood samples with different stimuli.

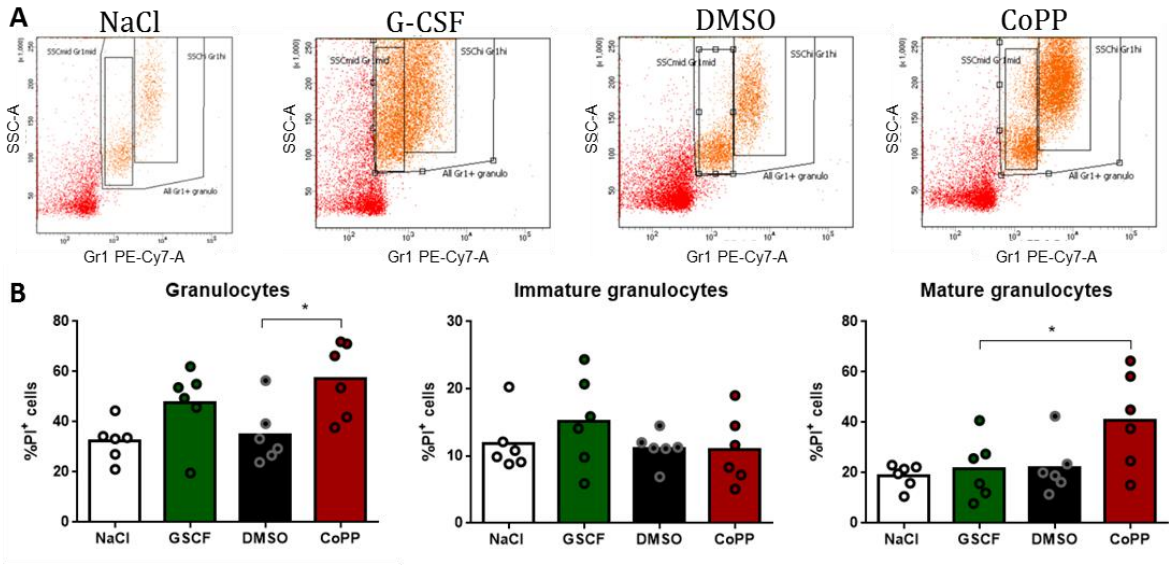

Fig. 53. Analysis of granulocyte phenotypes from the peripheral blood of mice treated with G-CSF and CoPP for Phagoburst assay. A. Representative plots from the flow cytometry analysis; **B.** Calculation of the results (mean + individual values plotted, one-way Anova with Bonferroni post-test, 6 samples per group).

We observed the higher percentage of granulocytes in blood after treatment of mice with G-CSF and CoPP (Fig. 53). However, the increase was much lower comparing to the previous experiment. In all groups we were able to distinguish two populations of granulocytes - SSC^{mid} $Gr1^{mid}$ immature granulocytes and SSC^{hi} $Gr1^{hi}$ mature granulocytes. There were no differences in the percentage of immature granulocytes between the groups, but the percentage of mature granulocytes was the highest in the blood of CoPP-treated mice.

The blood samples from G-CSF- and CoPP-treated mice were incubated with N-formylmethionyl-leucyl-phenylalanine (fMLP), phorbol 12-myristate 13-acetate (PMA) and opsonized *E. coli*. Conversion of dihydrorhodamine 123 (DHR 123) to fluorescent rhodamine 123 (R123) was used to assess the production of ROS by stimulated cells.

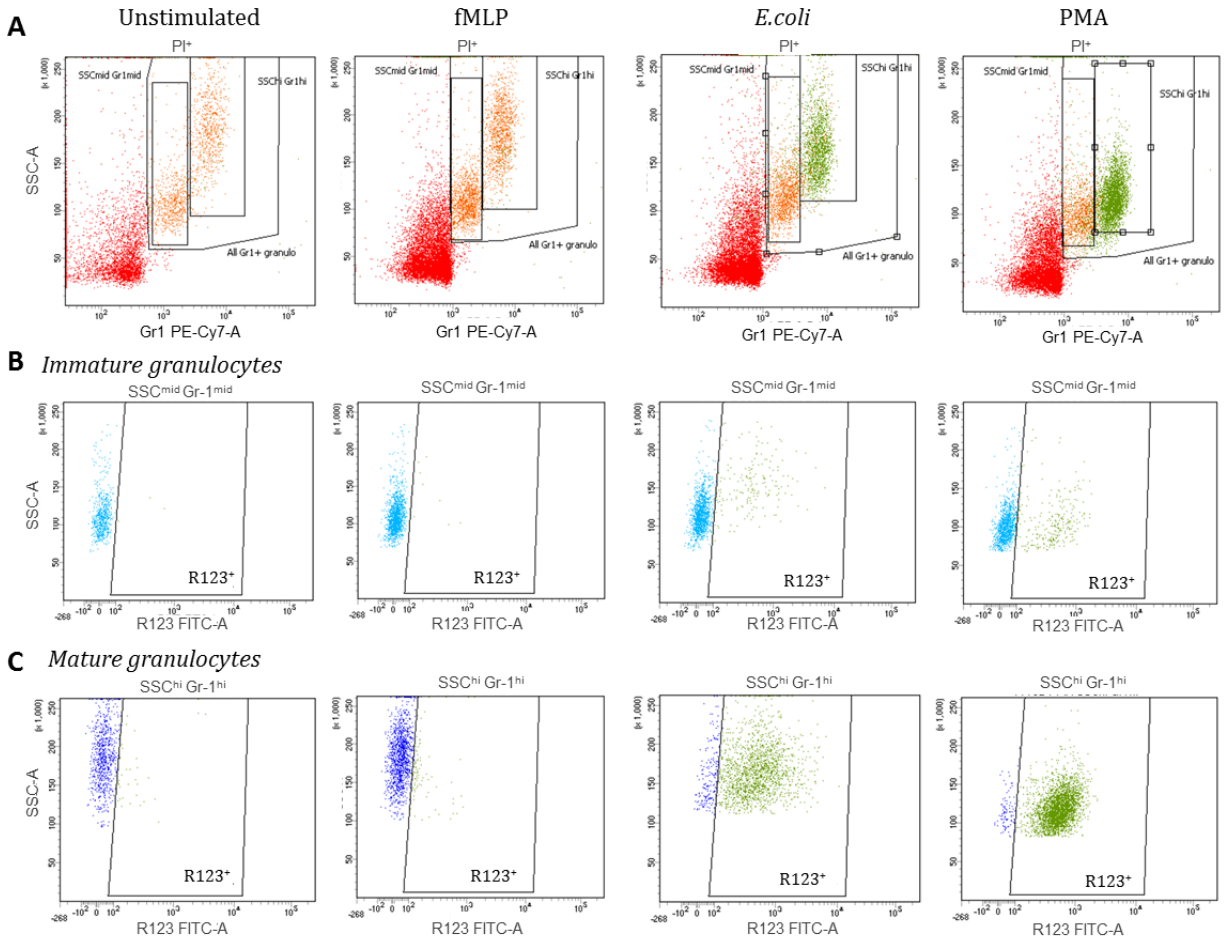

Fig. 54. Representative plots from flow cytometry analysis of granulocytes from peripheral blood samples (control NaCl injected mouse) incubated with indicated stimuli. A. Ly6G expression and granularity; **B.** Rhodamine 123 fluorescence in the immature granulocytes (SSC^{mid} $Gr\text{-}1^{mid}$); **C.** Rhodamine 123 fluorescence in the mature granulocytes (SSC^{hi} $Gr\text{-}1^{hi}$).

We analyzed both the percentage of ROS producing cells and the activity of cells among the selected populations – all PI^+ (nucleated) cells, granulocytes and their two subpopulations – SSC^{mid} $Gr1^{mid}$ immature granulocytes and SSC^{hi} $Gr1^{hi}$ mature granulocytes.

Cells incubated with fMLP or *E. coli* did not change their morphology. After the incubation with PMA, the cells became less granular, as evidenced by decreased SSC values. After incubation with *E. coli* or PMA mostly mature granulocytes became R123 positive (Fig. 54).

When all cells were analyzed, there was a higher percentage of ROS-producing cells in the blood samples from G-CSF and CoPP treated mice stimulated with *E. coli* or PMA. Exposure to *E. coli* or PMA resulted in similar increase of percentage of $R123^+$ cells among granulocytes in samples from mice of all experimental groups. Percentage of $R123^+$ cells among immature granulocytes from G-CSF-treated mice increased both after *E. coli* and PMA stimulation, whereas in the samples from CoPP-treated mice the increase was only observed after PMA. Percentage of $R123^+$ cells among mature granulocytes from G-CSF and CoPP-treated mice was smaller than among mature granulocytes from the control mice (Fig. 55).

Apart from the percentage of ROS producing cells we also assessed their ROS-producing activity by measuring the mean fluorescence intensity (MFI) of R123 among the $R123^+$ populations. We observed an increase in ROS-producing activity in unstimulated cells from G-SCF- and CoPP-treated mice. R123 MFI in the population of R123+ granulocytes was the highest after stimulation with *E. coli*, especially in the samples from the control, NaCl-injected mice. There were no major differences in R123 MFI among the immature granulocytes. Only in the population of mature granulocytes the activity of cells highly increased after stimulation with *E. coli* and PMA comparing to unstimulated and fMLP-stimulated cells, however there were no differences between the samples from control and G-CSF- or CoPP-treated mice (Fig. 56).

Results of ROS production measurement show that granulocytes mobilized by G-CSF and CoPP are similarly efficient in phagocytic activity as the granulocytes from the control mice.

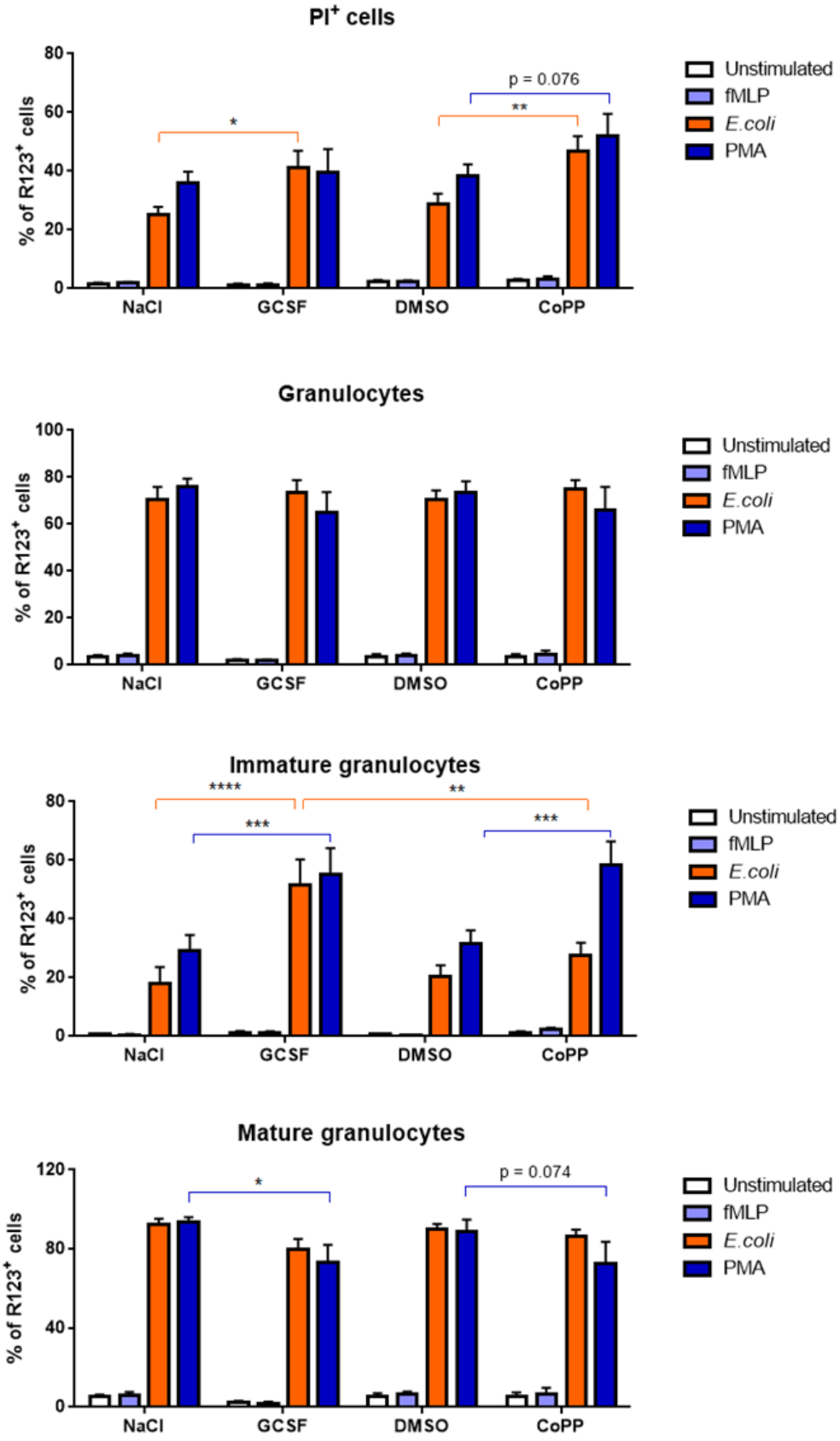

Fig. 55. The percentage of cells isolated from C57BL/6xFVB mice treated with G-CSF or CoPP that are producing reactive oxygen species after incubation with indicated stimuli (mean + SEM, two-way Anova with Bonferroni post-test, 6 mice per group).

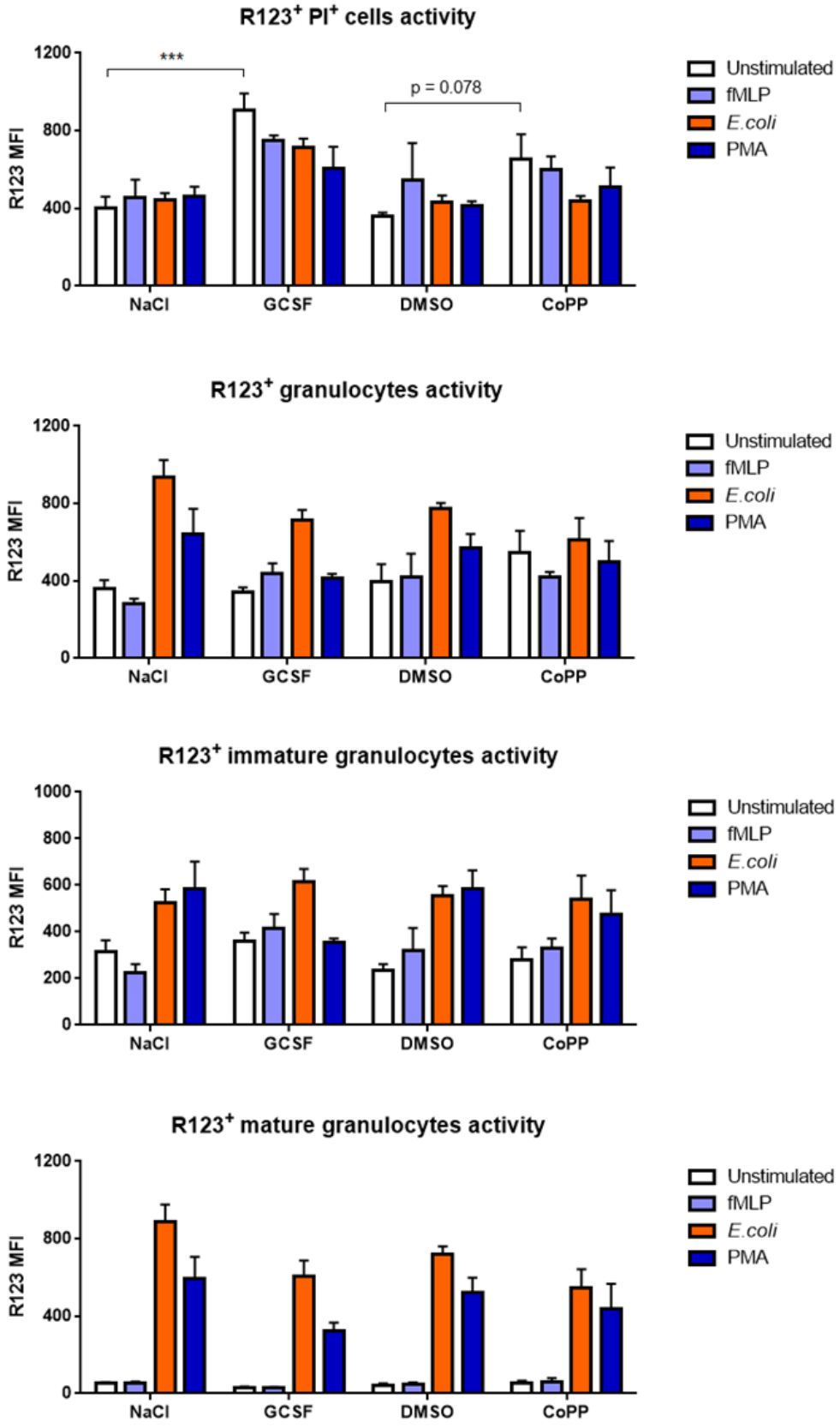

Fig. 56. Activity of cells (measured as mean fluorescence intensity of the probe) isolated from C57BL/6xFVB mice treated with G-CSF or CoPP after incubation with indicated stimuli (mean + SEM, one-way Anova with Bonferroni post-test, 6 mice per group).

5.3.5. CoPP mobilizes functional HSPC

As shown in Fig. 49, treatment of mice with CoPP increased the number of cells with HSPC phenotype in the blood more efficiently than treatment with G-CSF. To prove that CoPP indeed induces mobilization of functional HSPC, we performed transplantation of mobilized peripheral blood mononuclear cells (PBMC).

We treated the green fluorescent protein (GFP)-expressing mice with CoPP, G-CSF or NaCl as a control. At the 5^{th} day of treatment we isolated the PBMC and then transplanted $5x10^6$ of isolated PBMC to the lethally irradiated GFP^- recipient mice, together with 10^5 GFP^- bone marrow-derived competitor cells (Fig. 57 A). Unexpectedly, the mean numbers of isolated PBMC from NaCl- and CoPP-treated mice were similar, whereas the number of PBMC isolated from G-CSF-treated mice was almost two times lower (Fig. 57 B). In most cases, cells from two GFP^+ donors were pooled for injection to one recipient. We monitored the complete blood cell count and GFP chimerism in blood. After 18 or 20 weeks we sacrificed the primary recipients, isolated the bone marrow cells and transplanted them to lethally irradiated secondary recipients (Fig. 57 A). The experiment is ongoing, the results will be analyzed 12-16 weeks after the secondary transplantation.

At the day of isolation of PBMC for transplantation, we collected blood samples for flow cytometry analysis to assess the numbers of mobilized cells. As in the previous experiment (chapter 5.3.3, Fig. 49 A), CoPP mobilized higher number of KLS cells than G-SCF (Fig. 57 C). CoPP mobilized also higher number of $CD45^+$ cells (Fig. 57 C). Both in mice treated with G-CSF and CoPP we observed increased number of granulocytes, however the increase after CoPP was higher. G-CSF and CoPP treatments similarly increased the numbers of immature granulocytes in blood, but only CoPP treatment increased the number of mature granulocytes (Fig. 57 D). As can be seen on graphs showing KLS (Fig. 57 C) and granulocyte numbers (Fig. 57 D), among the G-CSF-treated mice there is a bimodal distribution, where only 4 mice that mobilized well KLS cells and granulocytes in response to G-CSF.

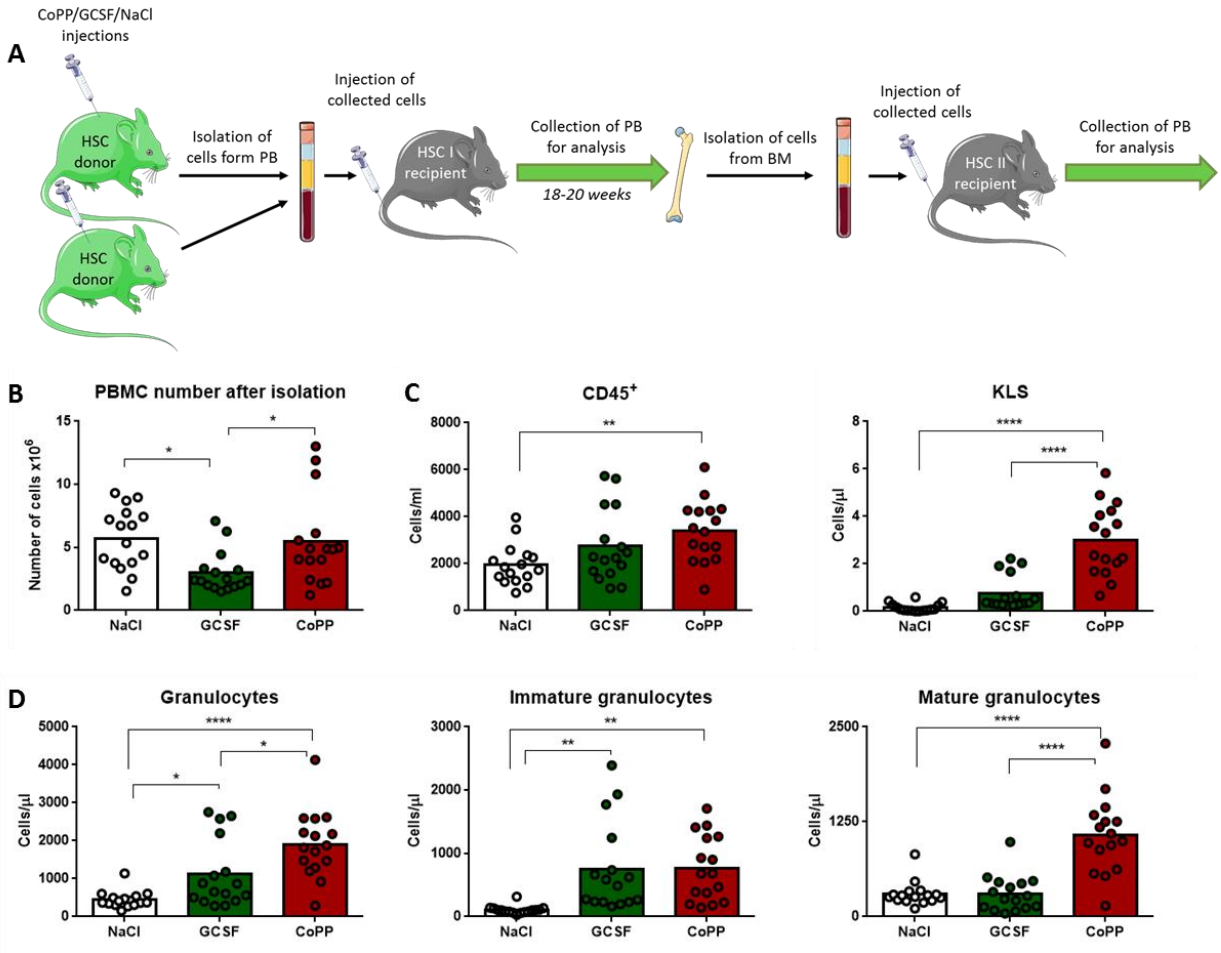

Fig. 57. Mobilized blood transplantation. A. Scheme of the experiment; **B, C, D:** Mobilization in C57BL/6-Tg(UBC-GFP)30Sch/J donor mice (mean + individual values, one-way Anova with Bonferroni post-test, 16 mice per group) **B.** Number of isolated PBMCs; **C.** Numbers of total CD45+ cells and KLS cells after mobilization; **D.** Numbers of granulocyte populations.

At selected time points after the PBMC transplantation we collected the blood samples to analyze the complete blood count and GFP chimerism in the recipient mice. Two weeks after transplantation, all recipient mice had WBC numbers much below the normal range. Number of platelets was also decreased in majority of mice. Mean numbers of WBC and platelets were the highest in mice which received CoPP-mobilized PBMC (Fig. 58). RBC number and hematocrit (HCT) were within the normal range already 2 weeks after PBMC transplantation. After four weeks, all parameters were normalized, except the number of lymphocytes which was slightly increased. There were no differences between the experimental groups at this time point (Fig. 58).

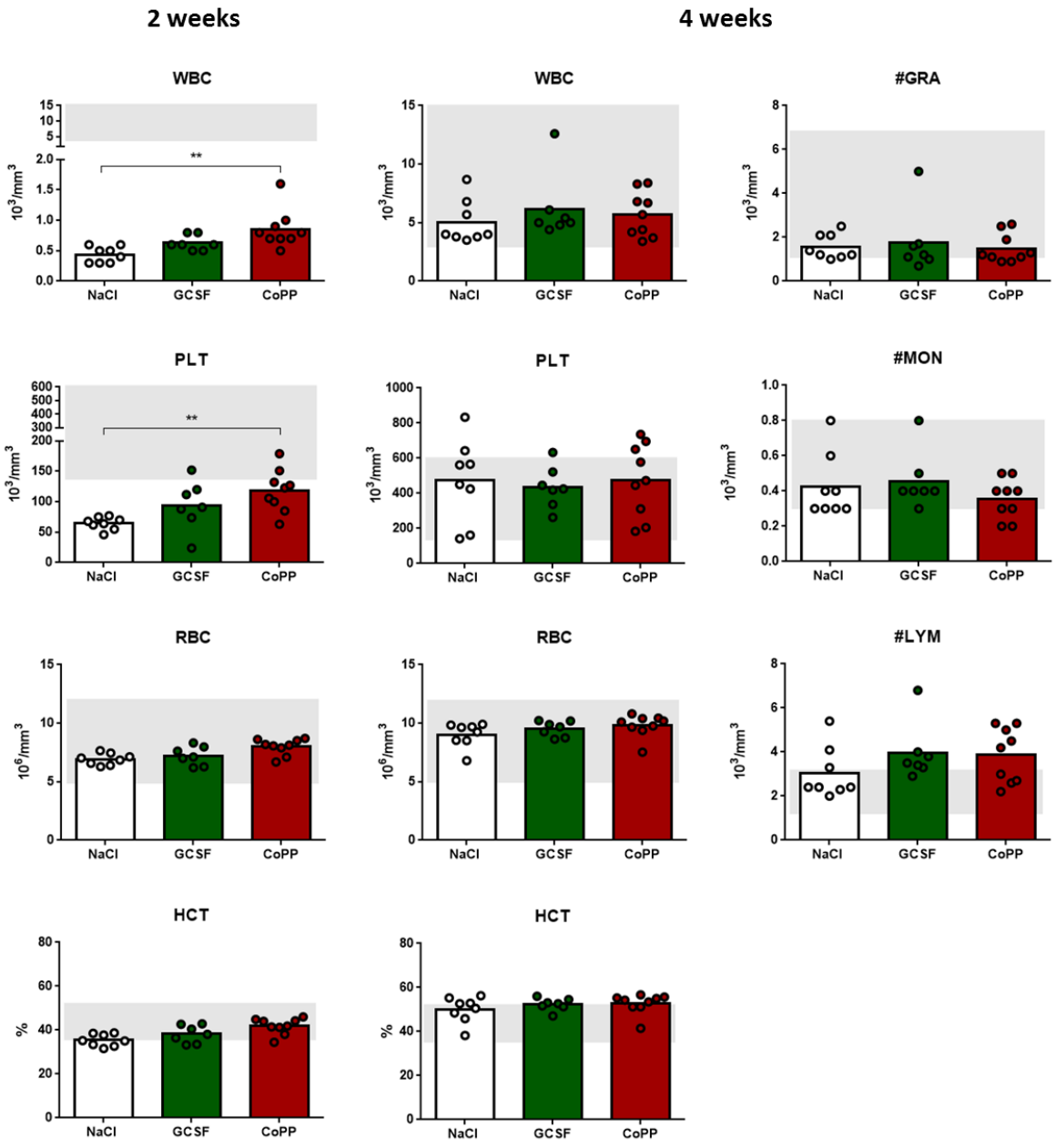

Fig. 58. Complete blood count of C57BL/6 recipient mice 2 and 4 weeks after mobilized blood transplantation (mean + individual values plotted, one-way Anova with Bonferroni post-test, 7-9 mice per group; grey area indicates the reference values for each parameter).

To assess the potential of transplanted PBMC to repopulate the bone marrow and rescue hematopoiesis of irradiated recipients, we analyzed the GFP chimerism in the blood. At all investigated time points, the GFP chimerism among all CD45$^+$ peripheral blood cells, granulocytes and B cells was the highest in mice which received CoPP-mobilized PBMC (Fig. 59).

In all experimental groups the number of GFP+ CD45+ cells was the highest 2 weeks after the PBMC transplantation, and decreased after 4 weeks, reaching the plateau (Fig. 59, Fig. 60). Number of GFP+ B cells was increasing up to 4 weeks, and stayed at the same level or slightly decreased in mice that received G-CSF- and CoPP-mobilized PBMC, respectively.

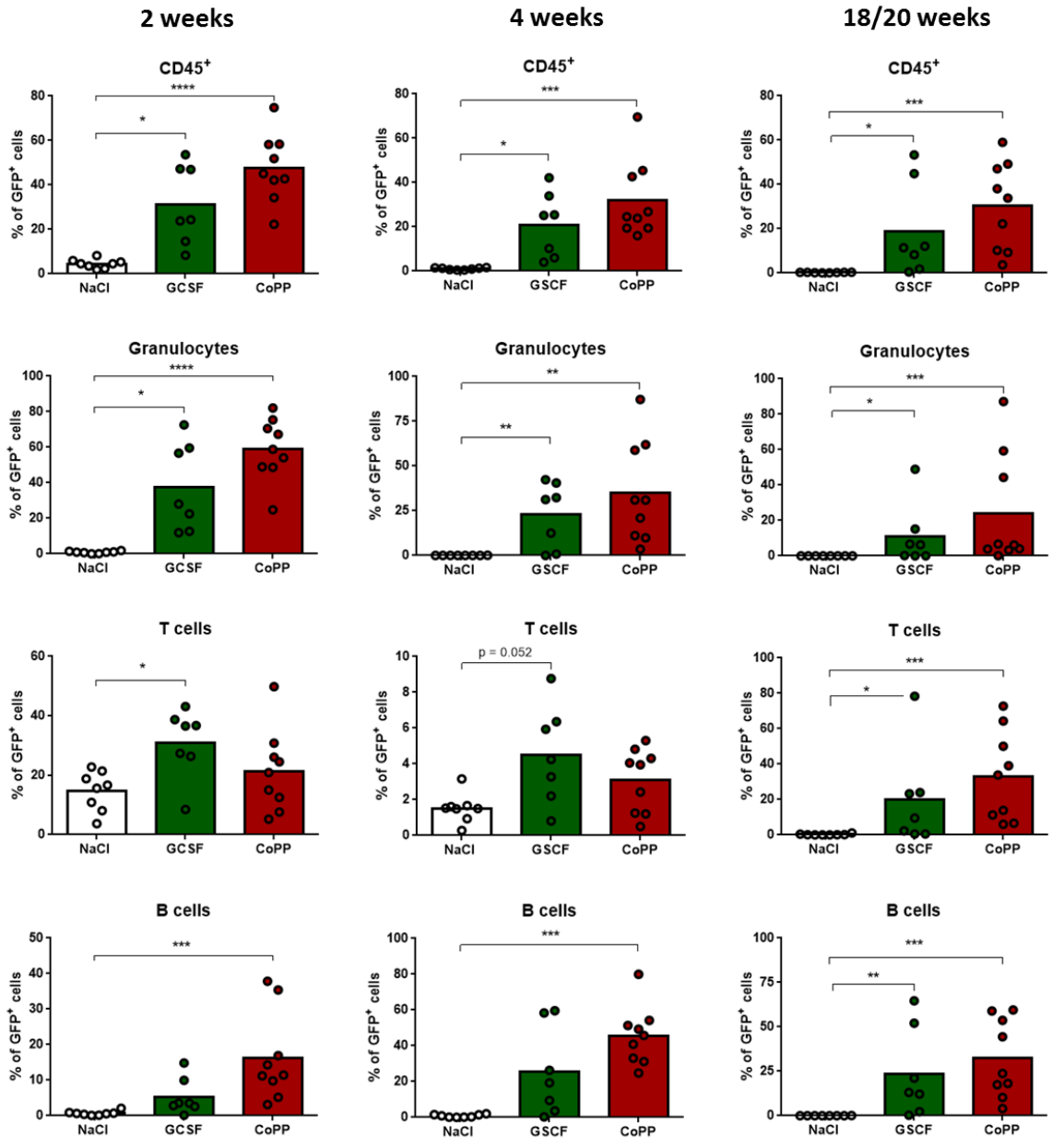

Fig. 59. GFP chimerism in the blood of C57BL/6 recipient mice 2, 4 and 18/20 weeks after mobilized blood transplantation (mean + individual values plotted, one-way Anova with Bonferroni post-test, 7-9 mice per group).

GFP chimerism among granulocytes was the highest 2 weeks after transplantation and decreased in both, G-CSF and CoPP, groups throughout the experiment. Two and four

weeks after transplantation, the GFP chimerism was the highest in mice that received G-CSF-mobilized PBMC (Fig. 59). Number of GFP+ T cells decreased between 2 and 4 weeks in all groups and subsequently increased up to 18-20 weeks in G-CSF and CoPP groups, reaching the highest values in CoPP group at the last time point (Fig. 59, Fig. 60).

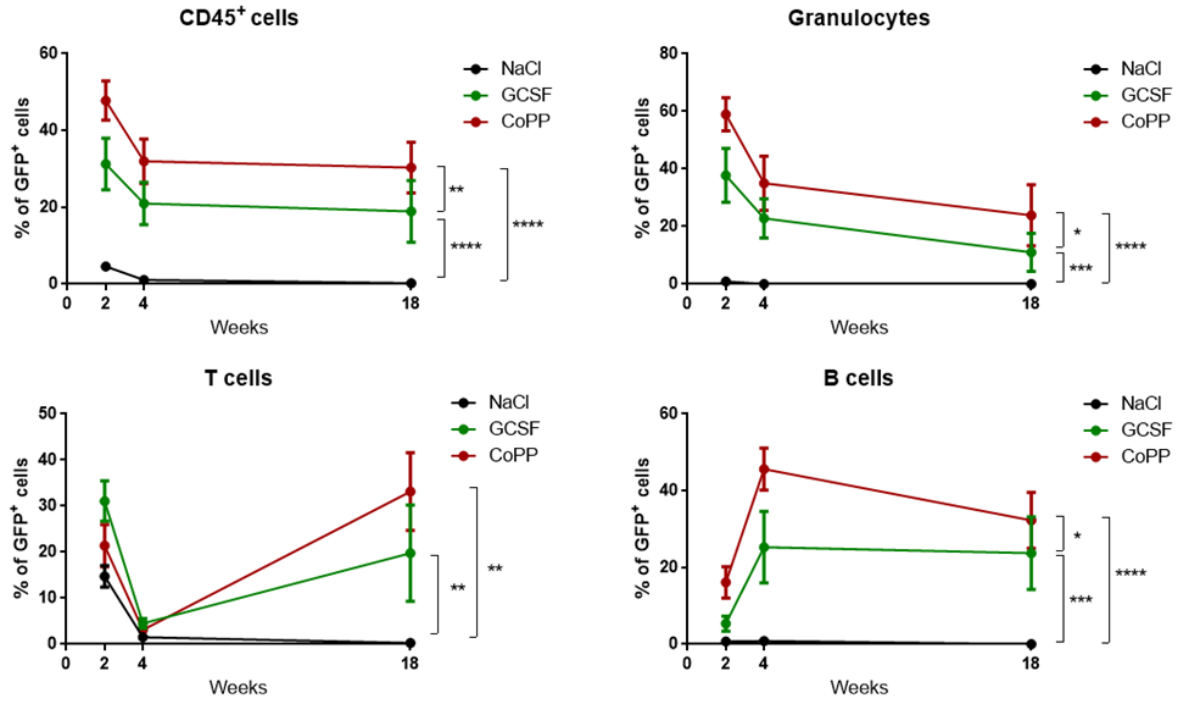

Fig. 60. GFP chimerism in peripheral blood of recipient C57BL/6 mice transplanted with mobilized PBMC; main effect of the mobilizer is indicated (mean + SEM, two-way Anova with Bonferroni post-test, 7-9 mice per group).

Our mobilized PBMC transplantation experiment show that treatment of mice with CoPP induces mobilization of functional HSPC which rescue hematopoiesis when injected to lethally-irradiated mice. Moreover, CoPP-mobilized cells seem to be more effective than G-CSF-mobilized cells in restoring hematopoiesis after engraftment.

5.3.6. Single injection of CoPP induces multiple cytokine expressions

To elucidate which cytokines might be directly induced by CoPP, we treated mice with a single injection of CoPP and collected the blood samples at selected time points (3 to 24 hours after injection). Luminex analysis of the plasma samples shows the upregulation of G-CSF with the peak of expression at 6 hours after single CoPP injection (Fig. 61 A). The maximal concentration of G-CSF is 55 times higher than the basal concentration in the untreated mice (Fig. 61 B). Other CoPP-upregulated cytokines: IL-6, MCP-1, and KC peak at 3 hours after injection (Fig. 61 A). Maximal concentration of IL-6 is 92 times

higher than the basal level and the pattern of IL-6 induction is the same as for KC (Fig. 61 A, B). We observed also a 2-fold induction of IP-10 at 3 and 6 hours after CoPP injection. Concentration of M-CSF was not changed between 3-24 hours after CoPP treatment (Fig. 61 A). Percentage of granulocytes increased after 3 hours, but was the highest 6 hours after CoPP injection (Fig. 61 C).

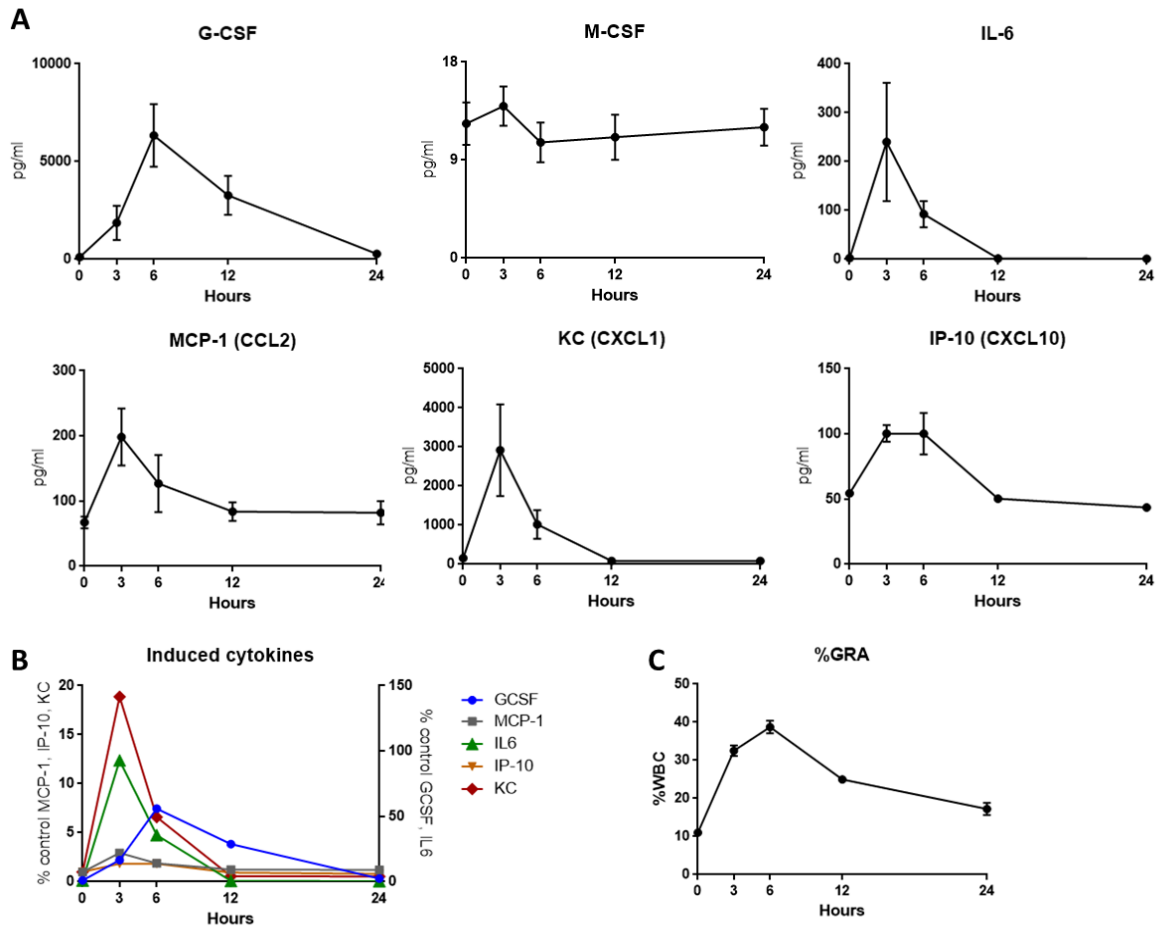

Fig. 61. Cytokine concentrations in plasma of mice treated with a single injection of CoPP (3 samples per group, mean + SEM). **A.** Concentrations measured by Luminex; **B.** Data from A, normalized to the concentration at time point 0 (error bars not shown for better visibility); **C.** Percentage of granulocytes among the WBC.

The results of experiment with a single CoPP injection show that expression of IL-6, MCP-1 and KC is induced by CoPP faster than expression of G-CSF.

5.3.7. Effect of CoPP on leukocytes does not depend either on HO-1 or on Nrf2

Although CoPP is a known inducer of HO-1 expression, not all of its activities are mediated by HO-1. As the inhibition of HO-1 by SnPP did not have any effect on the parameters affected by CoPP (chapters 5.3.1 and 5.3.2), we hypothesized that HO-1 may

not be involved in the CoPP-induced mobilization. To verify this hypothesis, we treated HO-$1^{+/+}$ and HO-$1^{-/-}$ mice with CoPP and measured leukocyte numbers and cytokine concentrations in their blood.

As HO-$1^{-/-}$ individuals have increased susceptibility to the toxic effect of many compounds (e.g. 4NQO, as shown in the chapter 5.1), in the experiment with HO-$1^{+/+}$ and HO-$1^{-/-}$ mice we injected them with CoPP three times, every second day (instead of everyday for 5 days). Nevertheless, 2 out of 6 HO-$1^{-/-}$ mice treated with CoPP had to be euthanized before the end of experiment.

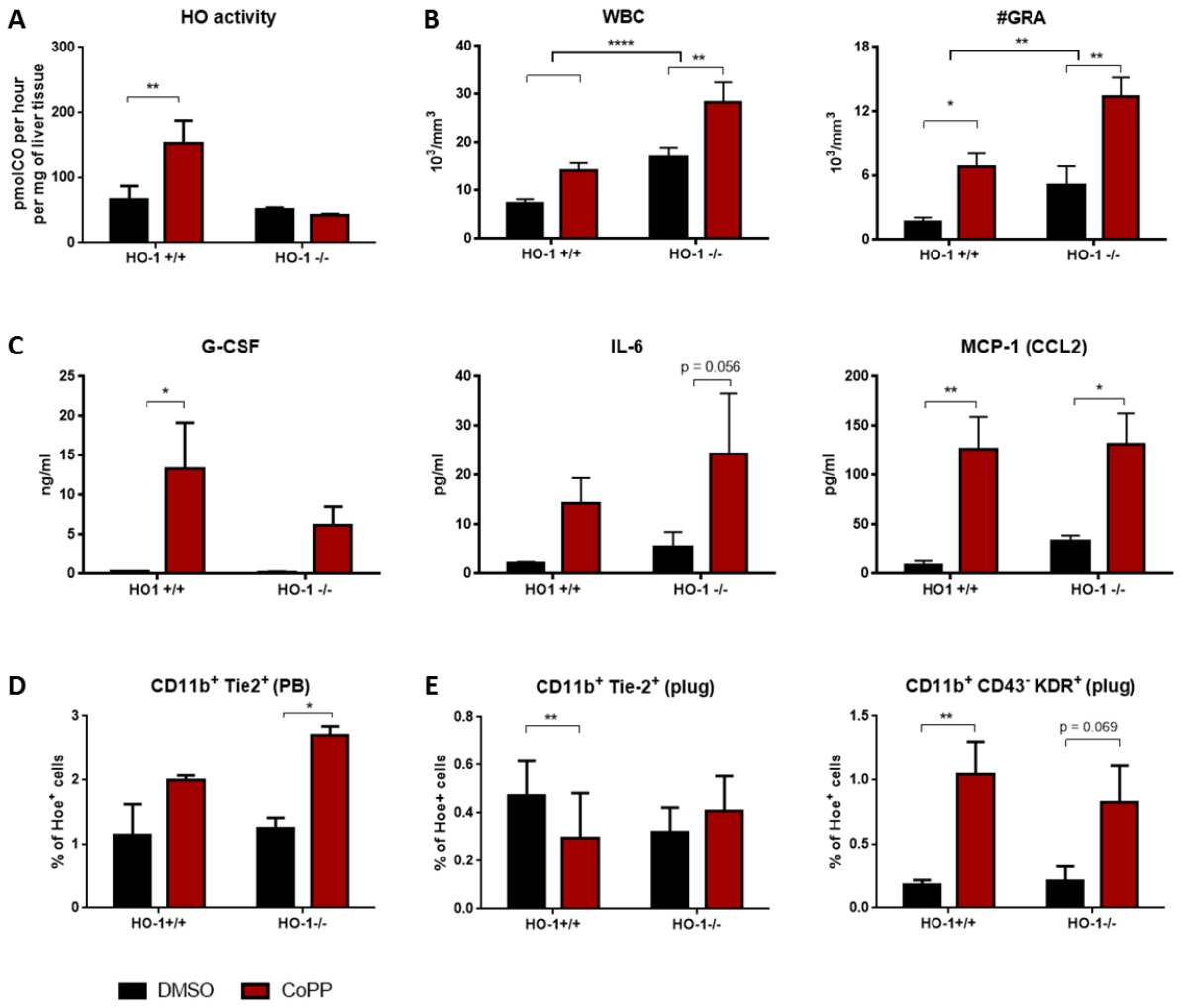

Fig. 62. Effects of CoPP administration in HO-$1^{+/+}$ and HO-$1^{-/-}$ mice. A. HO activity in the liver (measured by dr Lucie Muchova, Charles University in Prague; mean + SEM, two-way Anova with Bonferroni post-test, 2-4 samples per group); **B.** Number of all white blood cells and granulocytes (mean + SEM, two-way Anova with Bonferroni post-test, 4-6 samples per group); **C.** Cytokine concentrations in plasma of HO-$1^{+/+}$ and HO-$1^{-/-}$ mice treated with CoPP (mean + SEM, two-way Anova with Bonferroni post-test, 3-5 samples per group); **D.** and **E.** Percentage of proangiogenic cells in the blood (**D**) and in the Matrigel plug (**E**) of HO-$1^{+/+}$ and HO-$1^{-/-}$ mice treated with CoPP (mean + SEM, two-way Anova with Bonferroni post-test, 4-5 samples per group).

As expected, treatment of mice with CoPP increased HO activity in HO-1$^{+/+}$ but not in HO-1$^{-/-}$ mice (Fig. 62 A). Although the total WBC and granulocyte numbers were higher in the control, DMSO-treated HO-1$^{-/-}$ mice than in their HO-1$^{+/+}$ counterparts, administration of CoPP increased the leukocyte numbers in both groups (Fig. 62 B). Both HO-1$^{+/+}$ and HO-1$^{-/-}$ mice had increased concentrations of G-CSF, IL-6 and MCP-1 in the plasma after treatment with CoPP (Fig. 62 C). As HO-1 was shown to be involved in the regulation of angiogenesis, we investigated the influence of CoPP administration on proangiogenic cells. CoPP led to the increase in TEM percentage in the blood, but not in the Matrigel plug (Fig. 62 D, E). However, treatment of mice with CoPP increased the percentage of KDR^{+} myeloid cells infiltrating the plug (Fig. 62 E).

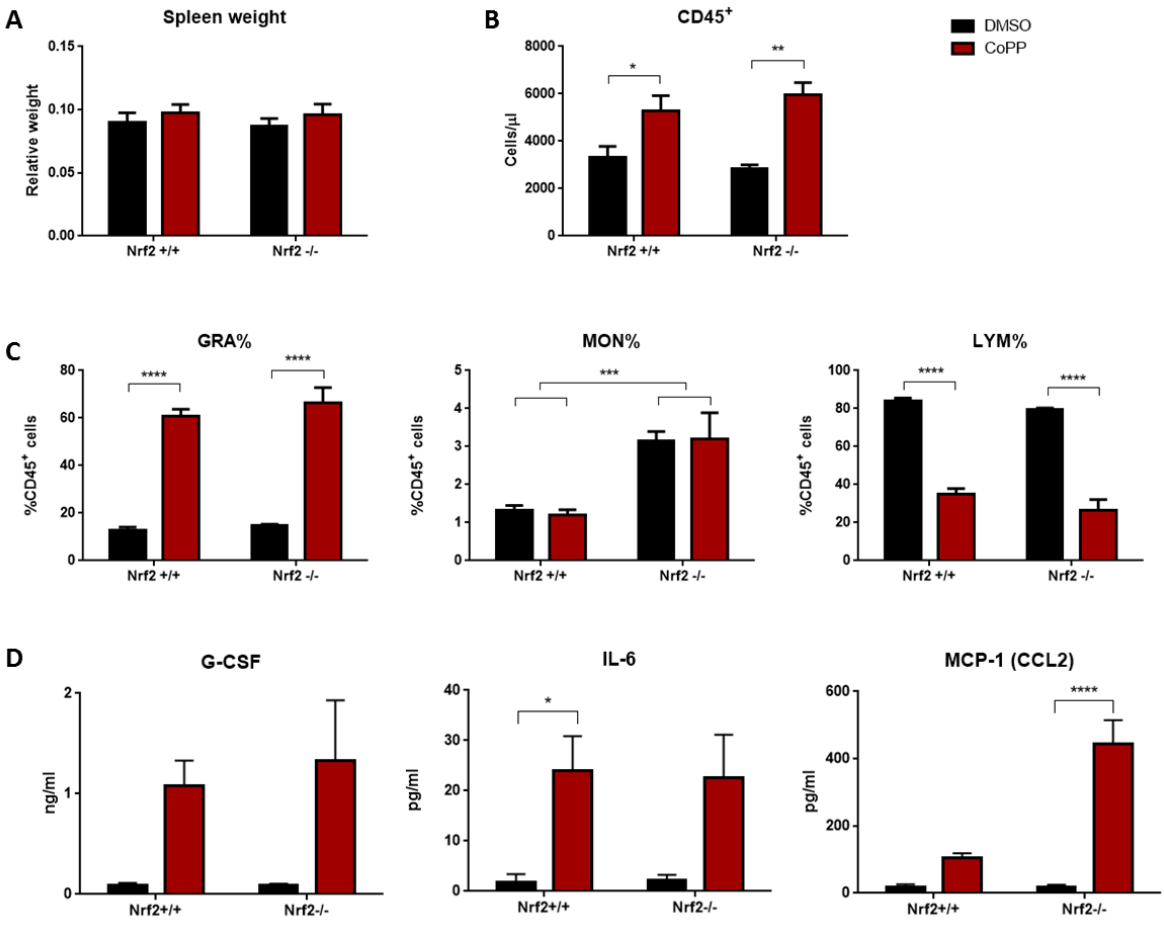

Fig. 63. Effects of CoPP treatment in Nrf2$^{+/+}$ and Nrf2$^{-/-}$ mice (mean + SEM, two-way Anova with Bonferroni post-test, 4-5 mice per group). **A.** Relative spleen weight; **B.** Number of CD45^{+} leukocytes in blood; **C.** Basic hematopoietic cell population numbers in blood calculated from flow cytometry data; D. Cytokine concentration in plasma.

Having excluded involvement of HO-1 in CoPP-induced mobilization, we examined the upstream signaling. Transcription of *Hmox1* gene in response to CoPP is regulated by Nrf2 transcription factor. To verify if Nrf2 is involved in the mobilization of cells after CoPP treatment, we treated $Nrf2^{+/+}$ and $Nrf2^{-/-}$ mice with CoPP. We observed no enlargement of the spleen in C57BL/6J mice regardless of Nrf2 genotype (Fig. 63 A).

Mice of both genotypes had increased number of $CD45^{+}$ leukocytes in blood after treatment with CoPP (Fig. 63 B). Among the leukocytes, there was increased percentage of granulocytes and decreased percentage of lymphocytes. Percentage of monocytes was not affected by CoPP, however regardless of the treatment, it was higher in $Nrf2^{-/-}$ mice than in $Nrf2^{+/+}$ mice (Fig. 63 C). We observed similar increase in concentrations of G-CSF and IL-6 in plasma of CoPP-treated $Nrf2^{+/+}$ and $Nr2^{-/-}$ mice. Increase in MCP-1 concentration after CoPP administration was higher in $Nrf2^{-/-}$ mice than in $Nrf2^{+/+}$ mice (Fig. 63 D).

The results of experiments performed in $HO\text{-}1^{-/-}$ and $Nrf2^{-/-}$ mice indicate, that the effect of CoPP on cell mobilization from the bone marrow to the blood depends neither on HO-1 nor on Nrf2.

6. DISCUSSION

Our primary aim was to investigate the role of HO-1 in squamous cell carcinoma. We used two distinct mouse cancer models. First, we applied 4NQO carcinogen in mice with different HO-1 expression levels. Next, we injected subcutaneously control or HO-1-overexpressing SCC-VII squamous cell carcinoma cell lines into syngeneic mice. The obtained results indicate that HO-1 prevents animals from toxic effects of carcinogen and then modulates the immune response induced by tumors.

Moreover, we used pharmacological HO-1 inducer, CoPP, to evaluate the influence of systemic HO-1 upregulation on immune cell infiltration into the growing tumors. Unexpectedly, we found that administration of CoPP induces cell mobilization from the bone marrow to the blood. This observation indicates that CoPP may mimic or even surpass the activity of G-CSF, the protein commonly used in clinic, especially in patients suffering from chemotherapy-induced neutropenia. As that phenomenon may be of clinical relevance, in the last part of the study we concentrated on its more detailed characterization.

6.1. HO-1 deficiency has moderate effect on oral chemical carcinogenesis

Previous experiments of our group with DMBA/PMA-induced skin carcinogenesis in mice expressing different HO-1 levels showed that HO-$1^{-/-}$ individuals were developing tumors earlier than their HO-$1^{+/+}$ counterparts [99]. However, while in the HO-$1^{-/-}$ mice most of the tumors were benign papillomas, HO-$1^{+/+}$ mice formed invasive carcinomas [99]. In the present study, to further investigate the role of HO-1 in the tumor initiation and progression, we subjected mice of different HO-1 genotype to 4NQO-induced oral carcinogenesis.

Carcinogenesis in the oral cavity caused by 4NQO resembles better the human HNSCC characteristics than other models, such as DMBA-induced cancers [187]. It was also shown that 4NQO in drinking water results in a higher and more rapid cancer incidence than the topical application few times a week [188]. Therefore, we treated HO-$1^{+/+}$, HO-$1^{+/-}$ and HO-$1^{-/-}$ C57BL/6xFVB mice with 4NQO in drinking water. In addition to HO-1 deficient mice, we employed also a new model of transgenic mice harboring human HO-

1 cDNA under the control of keratin 14 promoter, with specific overexpression of HO-1 in proliferating epithelial cells. After 18 weeks of treatment almost all mice developed lesions on their tongues, but we did not observe any differences in tumor incidence and lesion numbers between the mice with different HO-1 genotypes. The number of lesions on the esophagi per animal was not significantly changed between the groups, however the number of affected animals was higher in HO-$1^{-/-}$ group and lower in HO-1-overexpressing mice compared to the control group. Majority of HO-$1^{-/-}$ mice developed lesions on esophagi, whereas HO-1-overexpressing TG mice seemed to be protected – only 20% in the group were affected.

Protective effect of HO-1 expression is in concordance with majority of the previously published human studies. The role of HO-1 in oral carcinogenesis was mainly investigated in the human populations of Asia, where the incidence of HNSCC is relatively higher than in Western countries. According to Taiwanese study by Chang et al. HO-1 promoter polymorphism is associated with the risk of oral carcinogenesis in areca chewers [189]. Lower number of GT repeats was associated with decreased risk of OSCC development [189]. As lower number of GT repeats results in higher HO-1 expression [190], HO-1 seems to play a beneficial role in oral carcinogenesis.

While the protective effect of HO-1 in initial carcinogenesis has been documented, there is no consistent notion on its role in more advanced tumor stages. It was suggested that HO-1 might be protective not only during first steps of OSCC, but also in more advanced stages of tumor development. Japanese study by Tsuji et al. correlates high HO-1 expression in OSCC with low risk of lymph node metastasis [191]. Later study by the same group confirms the previous observation on the larger and more uniform group of patients [192]. Namely, lower expression of HO-1 was associated with higher incidence of lymph node metastasis and higher percentage of poorly differentiated samples [192].

On the other hand, Lee et al. reported that expression of HO-1 was increased in OSCC specimens from areca chewers in comparison to normal epithelium samples from non-areca quid chewers, and high HO-1 levels were associated with metastatic tumors [193]. However, the results were not compared to the control group of the healthy areca chewers. In the same study HO-1 upregulation by major areca nut alkaloid, arecoline, has been shown [193]. Thus, the higher HO-1 expression in OSCC specimens might be a result of areca chewing itself, rather than distinctive features of OSCC cells. Other study

shows correlation between HO-1 level, PCNA (proliferating cell nuclear antigen) expression, and disease progression in oral dysplasia and SCC [194].

Although some of the results obtained by various groups may seem to be contradictory, the differences might be explained, among others, by the different mechanisms of carcinogenesis and variable environmental factors. Moreover, HO-1 expression might be modulated by carcinogens, as shown in areca studies, what makes the interpretation of HO-1 role in tumor development even more complicated.

Taking this observation into consideration, we also monitored how the 4NQO treatment affects the HO-1 expression. As regulation of HO-1 occurs mainly at the transcriptional level (reviewed in [40]), we used the real time-PCR method to quantify HO-1 mRNA. Expression of endogenous HO-1 in the tongues after the 4NQO administration was not changed in C57BL/6xFVB HO-$1^{+/+}$ and HO-$1^{+/-}$ mice and decreased in C57BL/6 WT and TG mice. It was already shown, that various mouse strains respond differently to chemical carcinogenesis [195]. We have previously reported, that mice form mixed strain C57BL/6xFVB have different serum concentrations of several cytokines than parental C57BL/6 strain [56]. Moreover, differences in the level of HO-1 induction in various mouse strains have already been shown. HO-1 was more strongly upregulated in the liver of C57BL/6 than in C3H/HeJ mice fed with atherogenic diet [196]. Induction of HO-1 was also higher in the lungs of C57BL/6 mice infected with influenza virus, compared to C3H/HeJ [197].

In contrast to endogenous murine gene, expression of human HO-1 transgene in TG mice was strongly upregulated after the treatment with 4NQO. This could be expected, as in the TG mice hHO-1 transgene is located under control of keratin 14 promoter, known to be activated in proliferating epithelial cells [198]. Accordingly, keratin 14 expression was also upregulated by 4NQO treatment, although not to such high extent, as was hHO-1.

Apart from HO-1 we checked expression of another antioxidant enzyme, Sod1. In our experiment 4NQO treatment increased expression of Sod1 in the tongue. In contrast, Viswanadha at al. reported decreased SOD activity in the livers and kidneys of 4NQO treated rats [199]. Apparently, the mechanisms of regulation of antioxidant genes can vary between different organs. Moreover, the assay used by Viswanadha at al. measures

total SOD activity [200], which results from the enzymatic activity of a few SOD isoforms. Our group has previously reported the increased Sod1 expression in the liver of mice treated locally with DMBA/PMA [99]. These results suggest that as an antioxidant enzyme induced by carcinogens, Sod1 might play a protective role in chemical carcinogenesis.

When analyzing the HO-1 expression at mRNA level, it has to be noticed, that HO-1 activity is modulated also by posttranscriptional modifications. Among them, the truncation of C-terminus and subsequent translocation to the nucleus has been evidenced as important for tumor development. Wegiel and colleagues showed that nuclear HO-1 may play different role in cancer progression than the active cytoplasmic HO-1 [113]. Furthermore, it was shown that HO-1 expression and nuclear translocation were higher in the tumor tissue than in the adjacent healthy tissue in the study with HNSCC [117]. However, the nuclear HO-1 did not seem to be involved in 4NQO carcinogenesis model. Although we did not compare immunohistological stainings of the tongue tissue sections systemically, in the few tested specimens we did not observe any HO-1 translocation to the nucleus (data not shown).

The valuable information about HO-1 role in carcinogenesis may be gained not only from the endpoint analysis, but also from the kinetics of acquired changes during the 4NQO administration. However, due to the nature of the model used, we were not able to monitor the tumor appearance in 4NQO-treated mice during the course of experiment. The parameter which could indirectly demonstrate the pathological changes in the gastrointestinal tract of mice, was the weight loss. In the first few weeks of experiment, 4NQO treatment inhibited the weight gain in all groups, with exception of HO-1$^{-/-}$ mice, which showed significant decrease of the weight. Inhibition of weight gain in rats [201, 202] or slight weight loss in mice [188] were reported after treatment with 4NQO. A study by Barcessat et al. shows that the weight gain inhibition after 4NQO treatment is not caused by decreased food intake, but rather by catabolic effect induced by 4NQO [202]. Moreover, Barcessat et al. described the systemic toxic effect of 4NQO affecting the liver, kidneys and WBC number [202]. Importantly, these changes were not associated with carcinogenesis, but they were rather of degenerative or inflammatory characteristics [202]. 4NQO decreases the levels of antioxidant enzymes (SOD, catalase, glutathione peroxidase, glutathione-S-transferase) in the kidney and liver of rats [199].

This might explain the weight loss and decreased survival of HO-1$^{-/-}$ mice at the beginning of 4NQO treatment. More than half (10 out of 19) of the HO-1$^{-/-}$ mice and only two mice from other groups had to be euthanized in the first few weeks of experiment. HO-1 was shown to protect mice from cisplatin-mediated acute kidney injury [203] and LPS-mediated hepatic necrosis [46]. Thus in our study HO-1-deficient mice were most probably more sensitive to 4NQO toxicity than HO-1-expressing mice, as they have decreased antioxidant capacity in the basal conditions. Therefore, in our study the 4NQO model did not allow us to compare kinetics of the carcinogenesis in HO-1$^{-/-}$ mice, due to acute proinflammatory toxicity.

The malignant transformation of squamous epithelium is linked with alteration of cell differentiation. Therefore, we analyzed if HO-1 can modulate this process. As the markers of 4NQO-induced dysregulation of epithelial differentiation, we checked the expression of keratins at mRNA level in the tissue lysates form the tongues of control mice and mice treated with 4NQO.

Specific pairs of keratins, consisting of acidic and basic forms, are expressed in certain types of epithelium and heterodimerize to form intermediate filaments (reviewed in [204]). Importantly, characteristic pattern of aberrantly expressed keratins allows the identification of the cancer type [204]. Normal non-keratinized stratified squamous epithelium expresses keratins pairs 5/14 in basal layer, where cells proliferate, whereas more differentiated cells express keratins 4/13 [198, 205]. Expression of *Krt5* was elevated in oral mucosa of rats treated with 4NQO [206]. Though, in our study *Krt5* mRNA was only upregulated in HO-1$^{+/-}$ mice after 4NQO treatment, in all other genotypes it was not affected. We observed significant increase of *Krt14* expression only in HO-1$^{+/-}$ mice, however *Krt14* was also slightly increased in HO-1 TG mice, where HO-1 is under *Krt14* promoter. Treatment with 4NQO downregulated *Krt4* expression in all treated genotypes, but the effect was the strongest in HO-1$^{-/-}$ mice. This shows that treatment with 4NQO decreases cell differentiation in oral epithelium and that HO-1 deficient mice are the most susceptible for the 4NQO-induced inhibition of proper epithelial maturation.

Keratins 8/18 are not found in stratified epithelia and their aberrant expression is associated with induction of cell motility and tumorigenicity [207]. Expression of keratin 8/18 was associated with decreased survival in OSCC [207]. In concordance with the

literature data, we observed increased expression of keratin 8 mRNA in mice treated with 4NQO in comparison to controls, except for HO-1$^{-/-}$ mice.

Expression of all tested keratins (4, 5, 8 and 14) tended to be higher in HO-1$^{-/-}$ mice than in HO-1$^{+/+}$ and HO-1$^{+/-}$ individuals. Thus, based on the altered keratins' expression we suppose that HO-1 may affect the epithelial differentiation in the 4NQO model. Nevertheless, this should by confirmed by histological examinations in future analyses.

The systemic effect of 4NQO treatment is reflected by changes in concentration of cytokines. Indeed, we observed significant influence of HO-1 genotype on the cytokines in sera of mice exposed to 4NQO. Namely, HO-1$^{-/-}$ mice treated with 4NQO had increased concentration of IL-7 and MCP-1. Concentration of IL-7 and MCP-1 in serum of mice of other genotypes, both control and 4NQO-treated, as well as control HO-1$^{-/-}$ mice, was at the border of detection. Consistently with our study, IL-7 and IL-12 proteins were detected in the HNSCC tumor samples [208]. Level of IL-7 and IL-12 expression was not related to the tumor stage, however high IL-7 was associated with better survival [208].

In another study, Luminex analysis of the panel of cytokines and growth factors revealed elevated concentration of IL-6, IL-7, MIG, RANTES, HGF and EGF in the sera of patients with HNSCC compared to healthy smokers [209]. We did not observe any effect of 4NQO treatment on the concentrations of MIG and RANTES, while IL-6 was elevated similarly in all HO-1 genotypes. Regardless of 4NQO treatment IL-6 concentration tended to increase in HO-1 deficient mice and decrease in HO-1 overexpressing mice.

MCP-1 was shown to be upregulated in the HO-1$^{-/-}$ mice in comparison to HO-1$^{+/+}$ mice, both in control and stressing conditions [210]. Peritoneal macrophages isolated from HO-1$^{-/-}$ mice produced higher amounts of IL-6 and MCP-1, than macrophages isolated from HO-1$^{+/+}$ counterparts [211]. However, CO treated mice had increased concentration of IL-6, MCP-1 and IP-10 in plasma, in comparison to the mice breathing air [74].

We also found that 4NQO treatment led to increase in MIP-1α and eotaxin concentrations in the sera of C57BL/6xFVB mice, regardless of Hmox1 genotype. Noteworthy, eotaxin upregulates MMP3 (matrix metalloproteinase 3) expression and promotes prostate cancer invasiveness [212]. Moreover, eotaxin can also stimulate angiogenesis [213], which is one of the crucial hallmarks of cancer.

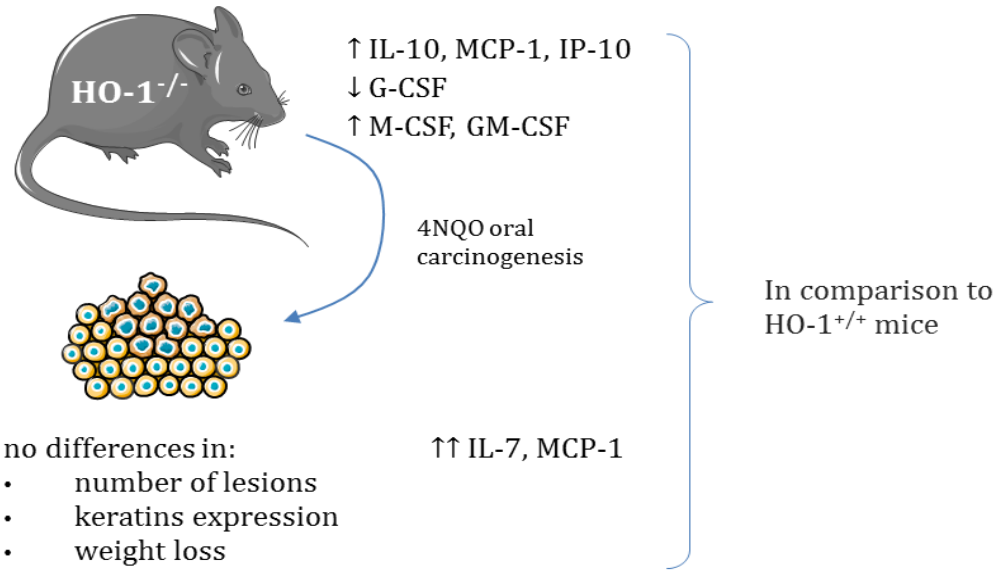

Fig. 64. Blood cytokines concentration in control and carcinogen-treated HO-1 deficient mice.

Given the changes in cytokine concentrations after 4NQO treatment between the mice with different HO-1 genotypes, it is justified to suspect that the numbers and phenotypes of the immune cells in blood may be also affected.

To sum up, neither HO-1 deficiency, nor overexpression affects 4NQO-induced oral carcinogenesis, however HO-1 expression seems to have a protective effect on esophageal carcinogenesis. HO-1 deficiency increased the percentage of affected animals, while HO-1 overexpression protected from esophageal changes. HO-1 deficiency modifies the concentration of cytokines that regulate immune response in 4NQO model (Fig. 64)**.**

6.2. HO-1 overexpression in cancer cells influences tumor infiltration with immune cells

The importance of immune cells infiltrating the tumors has been shown in many studies (reviewed in [136, 214]). Tumor infiltrating leukocytes have profound influence on the cancer cell behavior, and oppositely - cancer cells affect the infiltrating immune cells. Various subpopulations of myeloid cells are attracted to the tumor site and regulate tumor growth, angiogenesis and metastasis [215, 216]. Tumor microenvironment modifies myeloid cells which infiltrate the tumor causing the shift towards the immunosuppressive phenotype (reviewed in [217]). As HO-1 is an immunomodulatory

enzyme, and we found that HO-1 influences the cytokines regulating immune response, next we investigated if HO-1 overexpression in cancer cells might influence the tumor infiltrating leukocytes.

We transduced murine SCC VII cell line with retroviral vectors containing *HMOX1* gene. In the *in vitro* experiments we did not observe any significant differences between the cells with normal and increased HO-1 level. Overexpression of HO-1 did not affect SCC VII proliferation, migration, invasion or adhesion to endothelial cells. Both, control and HO-1 overexpressing cell lines produced cytokines which are chemoattractants for the immune cells, also those involved in the regulation of tumor growth: M-CSF, VEGF, MCP-1, RANTES, IP-10.

Apart from being a hematopoietic growth factor, M-CSF is also a chemoattractant for monocytes and macrophages [218, 219]. VEGF, in addition to its direct proangiogenic effects, is one of the factors which induce expansion of MDSC (reviewed in [136]). MCP-1, a well-known monocyte/macrophage chemoattractant, is also important for myeloid cells-induced tumor angiogenesis [220]. In accordance, MCP-1 receptor, CCR2 is necessary for recruitment of myeloid suppressor cells to the tumor site [221]. RANTES was shown to induce monocyte migration to breast cancer [178], whereas IP-10 may stimulate the recruitment of Tregs into the tumor [222]. Thus, SCC VII cells provide a good model to study the migration of various immune cells to the tumor.

To assess if HO-1 can modulate the immune cell recruitment into the tumor, we injected control and HO-1-overexpressing cells into syngeneic mice. The tumors were growing for 5, 14 and 32 days. Importantly, due to technical limitations connected with numbers of accessible mice, these were 3 independent experiments, not the 3 time-points of the same experiment. Therefore, it has to be taken into consideration that several factors, mainly changes in SCC VII cell lines and different age of mice could have influenced the obtained results.

Firstly, we compared the growth kinetics of tumors derived from SCC VII-Luc and SCC VII-Luc-HO-1 cells. We employed *in vivo* luciferase activity measurements as the method of monitoring the tumor growth in time. As the tumor cells were injected subcutaneously in the Matrigel matrix, the measurement with caliper might not reflect the tumor growth, especially at initial time points. Namely, the initial volume comes

from the plug itself and lateron it depends not only on tumor cells proliferation, but also on the Matrigel degradation. Therefore, we used the caliper to assess tumor size only in the later phase of tumor growth.

However, we encountered some difficulties in interpretation of the luciferase activity measurements. First, while measuring the luciferase activity in SCC VII cells *in vitro* we observed higher activity in SCC VII-Luc-HO-1 than in SCC VII-Luc. This was unexpected, as the HO-1-overexpressing cells were derived from the established SCC VII-Luc cell line. Moreover, at the time when modified SCC VII cell lines were created, luciferase activity was similar in both of the lines. Nevertheless, this hindrance could be solved by normalization of the signal to initial values, as we tested that both cell lines produced signal above the detection limit.

Second, we observed that luciferase activity in tumors did not correlate with the actual tumor size. We excluded some possible reasons for such discrepancy – differences in vasculature and substrate delivery into tumors. *In vitro* test performed in tumor lysate samples showed much higher luciferase activity in those from SCC VII-Luc-HO-1 tumors than from SCC VII-Luc tumors. What could explain this observation is the different content of necrosis in tumors . We recently showed that that the ratio of luciferase signal to volume of the tumor may be used as indicator of necrosis [223]. Thus, it could be possible that bigger SCC VII-Luc were more necrotic and therefore were not able to produce the luciferase signal comparable to smaller SCC VII-Luc-HO-1 tumors. However the trichrome staining did not show significant areas of necrosis in any examined tumor specimen.

Apart from monitoring the growth of primary tumors we tried to evaluate the presence of potential metastases. We observed a possible formation of micrometastases in the liver only in mice with the control SCC VII tumors and not in that with HO-1 overexpressing tumors. Similar association was found in the discussed earlier human studies on OSCC, where tumors with higher expression of HO-1 in OSCC specimens were associated with lower risk of lymph node metastasis [191, 192]. On the other hand, HO-1 deficiency in myeloid cells reduced metastasis of subcutaneously grown tumors [224], so HO-1 expression in different cell types seems to affect metastasis in opposite ways.

The main aim of the experiment was not only to compare how SCC VII cells with different HO-1 levels grow, but also to verify if HO-1 level in cancer cells affects tumor infiltration with immune cells. It is well evidenced that HO-1 plays an important role in hematopoietic cells. HO-1 is an essential factor in myeloid cells differentiation. It was shown that deletion of HO-1 in myeloid lineage inhibits differentiation to macrophages, as evidenced by decreased expression of CD14, Mac3 and M-CSFR markers [74]. CO produced by HO-1 increases M-CSFR expression on myeloid cells and enhances their differentiation toward macrophages [74]. Recently, study by Nemeth et al. revealed that HO-1 plays an important role in TAMs in the prostate cancer [225]. Specific deletion of HO-1 in myeloid cells was associated with suppressed tumor growth but, at the same time, with increased epithelial to mesenchymal transition (EMT) [225]. HO-$1^{+/+}$ bone marrow derived macrophages (BMDM) expressed higher level of VEGF and IL-10 at mRNA level, than did HO-$1^{+/-}$ BMDM [224]. HO-$1^{+/-}$ myeloid cells were recruited to the premetastatic niche in lower numbers than HO-$1^{+/+}$ myeloid cells [224]. However, it is poorly understood how HO-1 expression in tumor cells regulates infiltration of immune cells.

After 2 weeks, the HO-1 overexpressing tumors were more heavily infiltrated with $Ly6C^{lo}$ MHC II^{hi} and $Ly6C^{lo}$ MHC II^{lo} TAM. Both TAM subsets were shown to have proangiogenic activities [185]. Interestingly, HO-1 overexpressing tumors were also more heavily infiltrated with $CD11b^{+}$ $F4/80^{+}$ $Tie\text{-}2^{+}$ myeloid cells. Tie-2 expressing monocytes (TEM) were identified as the most important proangiogenic myeloid cells recruited to tumors [146]. TEM were found in healthy human blood and tumor samples, but not in non-malignant tissues other than blood [226]. Higher infiltration of SCC VII-Luc-HO-1 tumors with TAM and TEM cells might suggest the higher degree of angiogenesis than in the control tumors. Indeed, in concordance with higher content of proangiogenic cells, tumors from SCC VII-Luc-HO-1 cells tended to be more vascularized than control tumors, assessed by 3D USG Power Doppler examination (Witold Nowak, unpublished data).

Apart from the myeloid cells, we also analyzed selected lymphoid populations. We observed lower CD4/CD8 T cell ratio and smaller percentage of $CD4^{+}$ $CD25^{+}$ T cells of Treg phenotype in the HO-1 overexpressing tumors than in control tumors. CD4/CD8 ratio of tumor infiltrating lymphocytes (TIL) was shown to be an important

characteristics in several human studies. Shah et al. described higher 5-year survival in the group of cervical cancer patients with high CD4/CD8 ratio of TIL than in patients with low CD4/CD8 ratio [227]. Higher CD4/CD8 ratio of TIL was observed in cervical cancer patients without lymph node metastasis, but there was no difference in CD4/CD8 ratio in PBMC between the groups [228]. However Piersma et al. reported lower CD4/CD8 ratio in cervical cancer patients without lymph node metastasis compared to patients with lymph node metastasis [229]. Interestingly, we observed the influence of HO-1 overexpression in tumor on peripheral T cell phenotypes. Mice with SCC VII-Luc tumors had higher CD4/CD8 ratio in blood than mice with SCC VII-Luc-HO-1 tumors. However, we did not observe the difference in Treg numbers in peripheral blood.

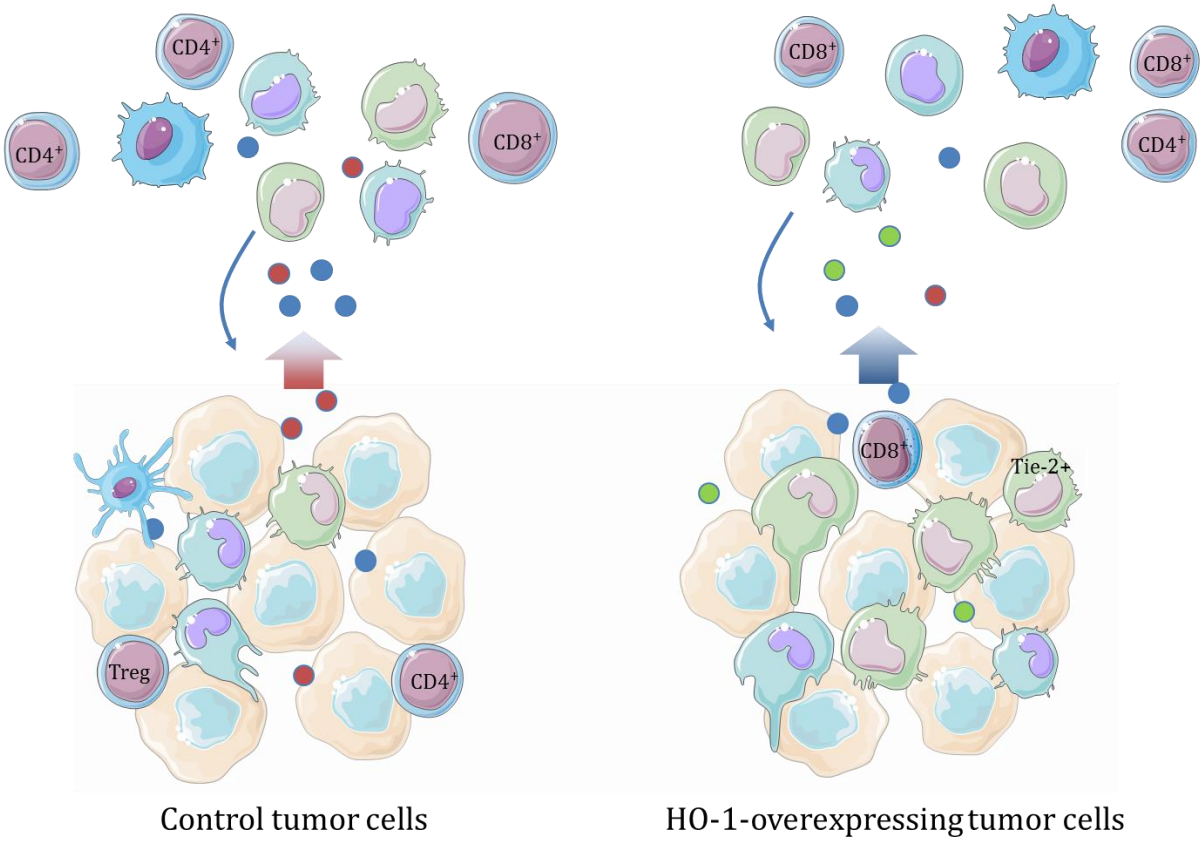

Fig. 65. Effects of HO-1 overexpression in tumor cells on peripheral blood and tumor infiltrating leukocytes.

To indicate the possible mechanism that mediates differential infiltration and mobilization of leukocytes by SCC VII-Luc and SCC VII-Luc-HO-1 cells we analyzed the cytokine concentrations in blood. One month, but not at earlier time points, after SCC VII cell line injection we observed systemic effects of HO-1 overexpression in tumor cells.

Mice harboring SCC VII-Luc-HO-1 tumors had increased concentrations of eotaxin, LIX, MIG and IP-10. As discussed earlier, increase in eotaxin concentration is associated with carcinogenesis, also in the 4NQO model that we used. Of note, MIG and IP-10 signal through the same receptor, CXCR3, which is present on activated T cells and regulates their trafficking [230].

Finally, we decided to study the effect of systemic pharmacological induction or inhibition of HO-1 on tumor infiltration. In our experiment, CoPP (commonly applied HO-1 inducer) did not influence the overall leukocyte infiltration to empty or SCC VII cells-containing Matrigel plugs. However, CoPP affected the structure of infiltrating cell populations – percentage of MHC II^{low} $Ly6C^{low}$ cells was increased and, at the same time, percentage of MHC II^{hi} $Ly6C^{low}$ cells was decreased in both plug types in mice treated with CoPP.

Previously, CoPP was shown to possess proangiogenic properties. Bussolati *et al.* proposed that CoPP, used to upregulate HO-1, induces the non-inflammatory angiogenesis by increasing endothelial cell proliferation and, at the same time, may reduce inflammatory angiogenesis due to inhibition of leukocyte infiltration [63]. However, it has to be stated that CoPP may also exert HO-1-independent effects [231]. On the other hand, authors of this study used LPS as the proinflammatory stimulus [63], and the role of HO-1 in attenuation of acute inflammatory response might have a different effect than upregulation of HO-1 alone, as in our experimental setting.

To sum up, HO-1 overexpression in tumor cells increased the tumor infiltration with myeloid cells and affected the types of infiltrating cells (Fig. 65)**.**

6.3. CoPP mobilizes cells form the bone marrow to blood

In one of the experiments we aimed to investigate how pharmacological modulation of HO-1 affects immune cell infiltration of tumors. We injected the mice with HO-1 inducer, CoPP and HO-1 inhibitor, SnPP. Unexpectedly, we noticed that mice injected with CoPP have increased number of WBC in the blood. Among WBC, the percentage of granulocytes and monocytes significantly increased, whereas that of lymphocytes decreased. Moreover, treatment of mice with CoPP increased the blood concentration of several cytokines, IL-5, IL-6, IP-10, MCP-1 and, most notably, G-CSF. We found these

observations to be potentially important in the hematological field and decided to study more deeply the phenomenon of CoPP-induced mobilization and its potential application.

G-CSF is one of the most important hematopoietic growth factors. It regulates granulopoiesis and neutrophil survival, but also plays a role in development and migration of other myeloid cells (reviewed in [232]). Although different mobilizing factors can induce cell release form the bone marrow to the blood, G-CSF is essential for neutrophil mobilization [233]. It also mediates mobilization of HSC (reviewed in [234]).

It has not escaped our attention that cytokines other than G-CSF, which were also induced by CoPP, could have mobilizing properties. IL-5 is a cytokine produced by T cells, which, together with IL-3 and GM-CSF, is important for terminal differentiation of eosinophils [235], but was also shown to influence basophil functions [236]. Most importantly, IL-5 induces mobilization of eosinophils from the bone marrow [237]. However, the increase in IL-5 concentration was relatively small and eosinophils constitute only a small percentage of all granulocytes. Although mobilization of eosinophils by CoPP can contribute to the total granulocyte increase, the most important mobilized cell type seems to be neutrophils.

IL-6 appears to be an important effector of CoPP-induced mobilization. IL-6 was shown to be crucial cytokine produced by HPSC responsible for myeloid differentiation [238]. IL-6 alone is able to induce mobilization of granulocytes into the blood [239]. Finally, MCP-1 is mainly responsible for recruitment of monocytes [240], while IP-10 is important for recruitment of T cells [230] and chemotaxis of NK cells [241]. Of the other cytokines important in the differentiation pathway from HSC to granulocytes that we investigated, GM-CSF and IL-3 were unaffected by the CoPP treatment.

We hypothesized, that CoPP increases G-CSF concentration in the blood, and thereby induces mobilization of cells from the bone marrow. To assess if the effects of CoPP treatment resemble treatment with G-CSF, we directly compared both factors. We injected C57BL/6xFVB mice with recombinant human G-CSF, CoPP or appropriate control vehicles, NaCl and DMSO, respectively. We observed increased number of $CD45^+$ cells in peripheral blood after both tested compounds, however, the increase caused by G-CSF was more pronounced. Monocytes and NK cells increased similarly after G-CSF

and CoPP, whereas only G-CSF increased number of lymphocytes. Those results suggested that, in general, G-CSF and CoPP cause similar mobilization of cells, but their mechanisms of action are not identical.

Furthermore, detailed flow cytometry characterization revealed that granulocytes mobilized by CoPP are more granular and have higher expression of Ly6G antigen, so they phenotypically resemble mature granulocytes found in the control mice, rather than granulocytes from G-CSF treated mice. To evaluate the functional maturity of CoPP- and G-CSF-mobilized granulocytes we measured the ROS production after *in vitro* stimulation of cells with *E. coli.* We found, however, no major differences in ROS production in response to bacteria between the cells isolated from G-CSF- and CoPP-treated mice. Nevertheless, it has to be noted, that here the flow cytometry analysis showed lower increase in percentage of granulocytes in mice treated with G-CSF and CoPP in comparison to controls, than observed in the previous experiments. Thus, we cannot exclude the possibility that with the higher mobilization rate, some differences in ROS production could be observed.

To look for the possible reason for different mobilization of granulocytes by G-CSF and CoPP, we examined the lineage restricted progenitors in the bone marrow. The whole population of lineage restricted progenitors is characterized by c-Kit^{+} Lin^{-} Sca-1^{-} phenotype (KLS^{-}). Percentage of KLS^{-} cells in the bone marrow was more decreased after G-CSF than after CoPP. Using CD34 and SLAM markers, CD48 and CD150, we were able to distinguish three different subsets of KLS- population: MEP, EP and GMP [242]. Percentage of MEP and EP in the bone marrow were similarly decreased in G-CSF- and CoPP-treated mice in comparison to controls, whereas in peripheral blood number of MEP was more increased after CoPP than after G-CSF.

G-CSF, but not CoPP treatment caused the decrease in GMP percentage in the bone marrow. This might suggest, that G-CSF, but not CoPP causes release of GMP from the bone marrow to the blood. However, this is inconsistent with observation that mice mobilized with CoPP had higher number of GMP in the peripheral blood than mice treated with G-CSF. This could mean that CoPP accelerates myelopoiesis at earlier stages of hematopoiesis, e.g. through acting on hematopoietic stem cells, or regulating differentiation of GMP differently than G-CSF. These hypotheses have to be verified experimentally during next studies.

One of the most important applications of G-CSF in therapy is the mobilization of HSC for their subsequent isolation and transplantation, either auto- or allogenic (reviewed in [162]). We wanted to verify if mobilization of HCS could be achieved by treatment of mice with CoPP. We showed that CoPP mobilized higher number of HSPC than G-CSF, both KLS and KLS$^-$. Importantly, also KLS CD48$^-$ CD150$^+$ cells of HSC phenotype were also better mobilized by CoPP than by G-CSF.

KLS CD48$^-$ CD150$^+$ cells were shown to be a true HSC population, capable of long-term multilineage reconstitution [186]. To prove the stem cell characteristics of HSC cells mobilized by CoPP, we transplanted PBMC mobilized by CoPP and G-CSF to lethally irradiated mice. Mice which received CoPP-mobilized cells recovered faster after transplantation, as evidenced by higher WBC and platelet numbers. The donor chimerism in WBC, granulocytes and B cells was higher from 2 to 16-18 weeks after transplantation in CoPP group in comparison to G-CFS. Only in T cells, the donor chimerism was initially higher in G-CSF than in CoPP group, but after 18 weeks it was reversed. These results prove that CoPP mobilizes functional HSC from the bone marrow to blood. Moreover, CoPP mobilizes higher number of functional HSC than G-CSF. To confirm the long term repopulating potential of HSC mobilized by CoPP, bone marrow cells isolated from primary recipients were further transplanted to secondary recipients. However, this experiment is still in progress.

Our initial hypothesis was that CoPP increases G-CSF concentration, and this is a direct trigger to mobilize the neutrophils into peripheral blood, which in turn produce a set of other cytokines. However, when we treated the mice with a single injection of CoPP, it were IL-6, MCP-1 or KC that were induced first. The maximal increase in G-CSF concentration was observed later than peaks of IL-6, MCP-1 or KC. Moreover, when we measured cytokine concentration in the plasma of mice treated with G-CSF and CoPP, only CoPP increased concentrations of MIG, KC and IP-10. G-CSF elevated IL-6, but the level of induction was very low, compared to the IL-6 induction by CoPP.

Concentration of MCP-1 was increased in mice treated with CoPP in comparison to those treated with the solvent, DMSO, but was not changed significantly in response to administration of G-CSF. MCP-1 regulates IL-6 and G-CSF expression. Accordingly, MCP-1 deficient mice have impaired IL-6 and G-CSF expression, accompanied by reduced neutrophil influx into the ischemic area after stroke [243]. MCP-1, MCP-3 and their

receptor, CCR2 are crucial for monocyte regress from the bone marrow and their recruitment to the inflammatory site [240].

Another cytokine elevated after CoPP, but not after G-CSF treatment was KC. The receptor for KC is CXCR2 and its expression on neutrophils is necessary for G-CSF-induced release of neutrophils from the bone marrow to the blood [244]. Nevertheless, there are more CXCR2 ligands and those responsible for neutrophil egress have not been identified [245]. Among them, MIP-2 is likely to play a role in CXCR2-dependent mobilization as bone marrow stromal cells produce MIP-2 after stimulation with G-CSF [244].

Of other CXCR2 ligands that we investigated were LIX and MIP-2. Concentration of LIX was not significantly affected by CoPP or G-CSF in comparison to their solvent controls, however it was slightly higher in the plasma of mice treated with CoPP than those treated with G-CSF. MIP-2 was not detected in the plasma of mice treated with CoPP, but we did not measure MIP-2 concentration in mice treated with G-CSF.

Altogether, we think that the main factor which drives the CoPP-induced mobilization is G-CSF. However, there are several other potential mediators: IL-6, MIG, KC, and IP-10 that are upregulated by CoPP, but not by GCSF. It is likely that these cytokines are responsible for the differences between mobilization induced by CoPP and G-CSF.

Nevertheless, our observation that injection of CoPP upregulates G-CSF, IL-6 and other cytokines and thereby mobilizes the cells, is still pure correlative. We considered how to verify if G-CSF or IL-6 have a mechanistic role in the CoPP induced mobilization. A way to prove it would be to inject the G-CSF or IL-6 deficient mice with CoPP. These genetic mouse models are elegant scientific tools, but in our case possess some important limitations. Although mature and functional neutrophils develop in G-CSFR$^{-/-}$ mice [157], the G-CSF$^{-/-}$ mice have a reduced number of neutrophil precursors in the bone marrow and do not respond to the mobilization as do the wild type counterparts [156]. Similarly, IL-6$^{-/-}$ mice fail to increase neutrophil counts in response to *Listeria monocytogenes* [246] and *Candida albicans* [247] infections. Therefore, in our opinion, the employment of IL-6 or G-CSF/G-CSFR deficient mice would not prove that the effect of CoPP depends on IL-6 and/or G-CSF.

Moreover, the signaling involved in mobilization of cells comprises many different cell types. Lulu et al. generated various G-CSFR^{+} and G-CSF^{-} chimeras using bone marrow transplantation, in which they studied HPC mobilization with G-CSF [160]. Their results show that expression of G-CSFR neither on HPC surface nor on the stromal cells is necessary for mobilization with G-CSF [160]. The authors concluded that G-CSF signals in trans to induce mobilization of HPC [160]. It is likely, that CoPP-induced mobilization is based on several interplaying pathways. Thus, mouse model deficient in only one of these pathways would not help us to understand the mechanism of CoPP action.

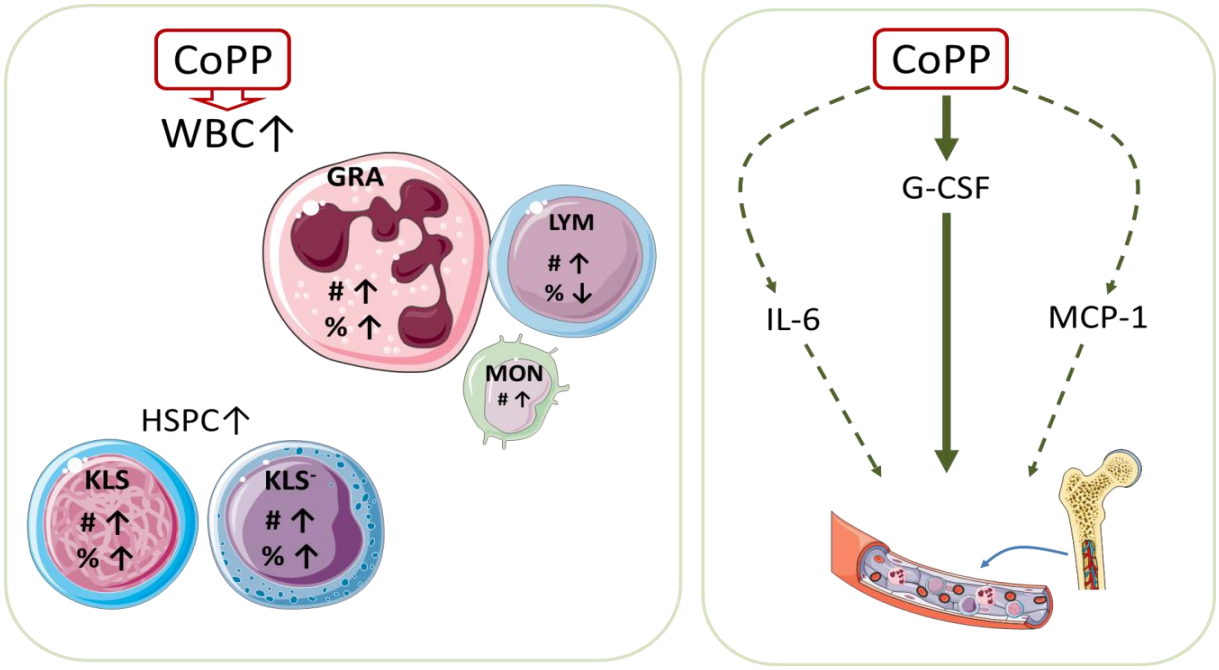

Fig. 66. Effect of CoPP on mobilization of cells from the bone marrow to blood.

When discussing the molecular factors underlying the CoPP action, one may ask what is the effect induced by the CoPP solvent, DMSO, itself. It can have anti-inflammatory properties. For example, DMSO inhibited the LPS-induced MCP-1 expression, but did not influence IL-6 and TNFα expression in the whole blood and PBMC [248]. However, both MCP-1 and IL-6 were shown to be inhibited by DMSO in Caco-2 intestinal cells [249]. Furthermore, it was reported that DMSO downregulated HO-1 expression in human promyelocytic leukemia cell line, HL-60 [250]. Downregulation of HO-1 activity by DMSO or ZnPP led to increased differentiation of HL-60, as evidenced by upregulation of

CD11b expression [250]. In contrast, CoPP treatment decreased CD11b expression [250].

Recently, it was shown that G-CSF treatment depletes certain macrophage populations from the bone marrow niches, facilitating HSC egress from the bone marrow [251]. Treatment of mice with clodronate depleted $CD11b^+$ $F4/80^+$ $Ly6G^+$ macrophages, leading to HSC mobilization into the blood [251]. We observed decreased number of macrophages, among them $CD11b^+$ $F4/80^+$ macrophages with high or low expression of MHC II, in the bone marrow of mice treated with G-CSF and CoPP. Moreover, among these macrophages, $Ly6G^+$ subpopulation was decreased after G-CSF or CoPP administration. This suggests, that the effect of G-CSF and CoPP on the bone marrow niche, specifically on macrophages, is similar.

The initial purpose why we injected the mice with CoPP was to investigate the effect of HO-1 induction on immune cells migration to the Matrigel plug containing tumor cells. CoPP is a known HO-1 inducer, used in many *in vitro* and *in vivo* studies and the majority of effects of CoPP have been attributed to HO-1 activity. It is known that HO-$1^{-/-}$ mice have increased leukocytosis [46] and MCP-1 concentration in plasma [210]. Despite the fact, that we observed similar elevation in control, DMSO-injected HO-$1^{-/-}$ mice, CoPP was able to further increase WBC and granulocyte counts, as well as G-CSF, IL-6 and MCP-1 concentrations. This shows, that effect of CoPP on mobilization of cells from the bone marrow does not depend on HO-1.

CoPP activates HO-1 expression by destabilization of Bach1 repressor and stabilization of the Nrf2 transcription factor [252]. Hmox1 is only one of many genes activated by Nrf2, thus we wanted to verify if CoPP acts on the hematopoietic system through Nrf2. We treated the Nrf$2^{-/-}$ mice with CoPP. Such a treatment affected the blood parameters in Nrf$2^{+/+}$ and Nrf$2^{-/-}$ mice in the same way. This proves that CoPP-induced mobilization of cells from the bone marrow to blood is independent of Nrf2 transcription factor.

Spleen enlargement is one of the known side effects of G-CSF treatment [253]. We observed a similar increase in relative spleen weight in C57BL/6JxFVB mice treated with G-CSF and CoPP. However, the spleen weight was unaffected by CoPP treatment of C57BL/6J Nrf$2^{+/+}$ and Nrf$2^{-/-}$ mice regardless of genotype. It is known that the spleen enlargement after G-CSF treatment can vary between the mouse strains [254].

Moreover, small effect of G-CSF treatment was accompanied by lower rate of mobilization of WBC [254]. C57BL/6 mice are regarded as poor mobilizers in comparison to other strains. In majority of our experiments C57BL/6xFVB mice mobilized WBC better than did C57BL/6. Our results may indicate that crossing of C57BL/6 with FVB improved the C57BL/6 mice ability to mobilize cells in response to CoPP. However, we did not perform the direct comparison between the two strains at the same time, so this has to be confirmed.

In majority of C57BL/6 mice the level of G-CSF-induced mobilization was very low. After tratment of mice with G-CSF, two groups of mice could be distinguished according to the numbers of mobilized granulocytes and KLS cells: one group showed no response while the second group, consisting of less than a half of mice, mobilized efficiently granulocytes and KLS cells. However, such division was not visible in mice treated with CoPP. CoPP-treated mice efficiently mobilizaed both cell types in majority of mice.

It is known that there is a number of patients who do not respond to G-CSF treatment [162]. Thus, the obtained results after G-CSF mobilization in C57BL/6 mice are similar to clinical practice. Given that CoPP was an efficient mobilizing agent in C57BL/6 mice, where G-CSF failed, there is a possibility, that also patients who do not respond to G-CSF treatment could be successfully treated with CoPP or its derivative.

Although CoPP is not found in normal conditions in the organism, it may be formed in vivo after $CoCl_2$ injection [255]. Metalloporphyrins in which iron is replaced by other metals, are able to induce HO-1 expression at mRNA and protein level, just as heme does [256, 257]. However, non-heme porphyrins inhibit the enzyme activity [256, 257]. The increase of HO-1 expression CoPP prevails over the transient inhibitory effect of CoPP on HO-1 activity [256]. Oppositely, SnPP inhibits HO-1 activity more strongly than CoPP and at the same time less potently upregulates HO-1 expression [256]. In overall, concerning the final effect, CoPP is used as HO-1 inducer and SnPP as HO-1 inhibitor, but one has to remember that both can exert similar activities.

Ghoreschi et al. elucidated the mechanism of cytokine expression regulation by HO-1 [258]. Their study shows that fumarate treatment of DC upregulates HO-1, which is cleaved and translocated to the nucleus. In the nucleus HO-1 associates with AP-1 or NFκB binding sites in the IL-23p19 promoter, where it interferes with transcriptional

activity. As a result, HO-1 decreases IL12p19 transcription [258]. Expression of MCP-1 in liver DC at mRNA level was decreased in mice treated with CoPP, while RANTES and IP-10 were unaffected [259]. However, the inhibitory effect of CoPP on dendritic cell maturation was shown to be independent of HO-1 [231].

The possibility that porphyrins may possess several activities that are independent of their HO-1 modulatory function was already proposed by Blumenthal and coworkers [257]. They showed that both CoPP and SnPP, can directly inhibit caspase-3 and -8 activity, independently of HO-1 [257]. Both of these caspases were shown to play a role in hematopoiesis [260]. Inhibition of caspase-3 and -8 decreases human neutrophil apoptosis [261].

Two other studies indicate the HO-1-independent modulation of immune reaction by CoPP. One of them shows that CoPP inhibited LPS-stimulated activation of inducible nitric synthase (iNOS) in RAW264.7 macrophages by blocking JNK phosphorylation [262]. Silencing of HO-1 with siRNA did not affect iNOS inhibition by CoPP [262]. Similarly, cyclooxygenase-2 (COX-2) upregulation by CoPP in microglia was proved to be HO-1-independent by the use of HO-1 siRNA [263].

CoPP has also been reported to regulate myeloid differentiation – it induced differentiation of monocytic THP-1 cell line into macrophages [264]. Treatment of THP-1 cells with CoPP led to increased expression of CD11b, MMP9, CD14 and ICAM-1 and was correlated with the decrease of redox factor-1 (Ref-1) [264].

There are two studies showing that HO-1 decreases mobilization of cells from the bone marrow. However, both of those studies demonstrate only how HO-1 modulates the effect of other mobilizing factors. In the study by Konrad et al. CoPP or CoPP with SnPP were injected to the mice before injection of LPS [265]. Pretreatment of mice with CoPP decreased mobilization of neutrophils from the bone marrow and their migration to the lungs. In this case, HO-1 attenuated the inflammatory response evoked by LPS [265]. In the study by Wysoczynski et al., SnPP was injected with G-CSF or AMD3100 [266]. SnPP potentiated the mobilizing effect of G-CSF and AMD3100 on HSPC, but given alone did not affect the mobilization of WBC [266]. In our study, CoPP increases the mobilization of both leukocytes and HSPCs, whereas SnPP does not have any effect on measured parameters. However, the effect of CoPP or SnPP injection alone can differ from the

combination of CoPP or SnPP with other factors. Therefore, our results do not contradict the data obtained by others [265, 266]. SnPP is an inhibitor of HO-1 enzymatic activity, but it also upregulates HO-1 expression at protein level [256]. Some observed effects of SnPP administration may be though related to the possible non-enzymatic activity of HO-1, e.g. as the regulator of transcription.

We demonstrated that Nrf2 and HO-1 do not mediate the CoPP-induced mobilization of cells. There are, however, some other transcription factors that could possibly be involved in this process. Bach1 and Bach2 are DNA-binding proteins, which work mainly as transcriptional repressors [267]. Heme regulates *Bach1* expression by binding to Bach1 protein and inducing its nuclear export [268]. Furthermore, heme was shown to induce the ubiquitination and proteasomal degradation of Bach1 [269].

Expression of *Bach1* mRNA is the highest in various HSPC populations: HSC, MEP and GMP. Its continues to be very high in monocytes and granulocytes, but also in T-cell lineage (Fig. 67, [270]). In contrast, *Bach1* mRNA level is very low in the CLP, and in the cells from B-cell development pathway [270]. Also *Bach2* mRNA is expressed in various HSPC populations, with the highest level in the B-cell lineage and mature T cells, and much lower in MEP, GMP, monocytes and granulocytes (Fig. 67, [270]).

Bach2$^{-/-}$ and *Bach1*$^{-/-}$*Bach2*$^{-/-}$ mice have increased number of CD11b^{+} and Gr1^{+} cells in peripheral blood [271]. It was shown that Bach2 is repressing myeloid genes by direct binding to their promoters [271]. On the other hand, Bach1 and Bach2 redundantly repress *Hmox1* expression [272]. As heme binds to Bach1 and Bach2 and inhibits their activity, this provides the negative feedback loop for the control of Hmox1 expression. Because heme binds to both Bach1 and Bach2 [272], and CoPP binds to Bach2, it is possible that CoPP could inhibit also Bach2. We can thus suspect that CoPP binds to the Bach2 and by this way derepresses myeloid genes. This in turn could move the balance of hematopoiesis towards myeloid lineage. However, this hypothesis has to be verified experimentally.

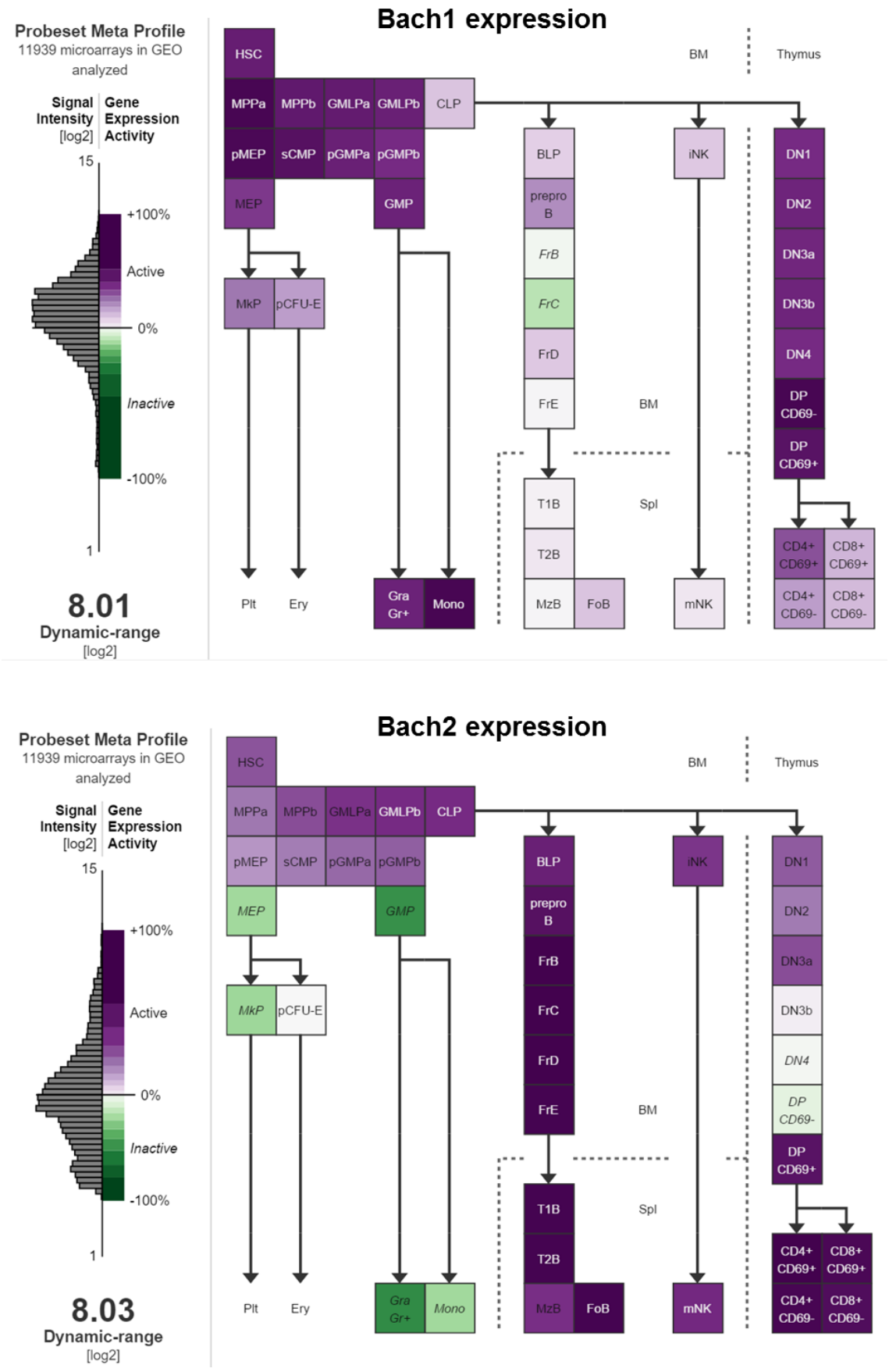

Fig. 67. *Bach1* and *Bach2* expression during hematopoietic cell differentiation (graphs generated form the database Gene Expression Commons, Mouse Hematopoiesis model, [270]).

One of the potential mechanisms of CoPP-induced cell mobilization could be an activation of STAT3, the positive regulator of expression of both IL-6 and G-CSF [273]. Using a dominant negative STAT3 Shimozaki et al. showed that STAT3 is important for the G-CSF induced morphological changes during the differentiation of neutrophils, but not for the MPO expression [274]. However, it was later reported, that STAT3 is not needed for G-SCF-induced neutrophil differentiation, but rather functions as a negative regulator of granulopoieis, allowing for the control of the proper neutrophil number [273]. It was shown, that G-CSF and IL-6 increase expression and phosphorylation of STAT3 in neutrophils in bone marrow, what leads to increased expression of *Mmp9* and *Bv8* [180]. These changes were associated with proangiogenic and protumorigenic function of neutrophils [180]. Importantly, it was shown, that CoPP treatment induces the expression of STAT3 in the liver [231]. Increased expression of STAT3 in the liver could result from CoPP-induced production of G-CSF and IL-6, but on the other hand, it may also suggest, that STAT3 mediates CoPP-induced mobilization of cells.

Another possible transcription factor that could mediate the CoPP activity in hematopoietic system is FoxO1, which has already been shown to take part in upregulation of HO-1 expression by CoPP [275]. CoPP increases FoxO1 expression and increases FoxO1 binding to *Hmox1* promoter [275]. FoxO transcription factors are important in protecting HSC from oxidative stress [276]. However, FoxO1, FoxO3 and FoxO4 deficiency did not alter myeloid differentiation of HSC [276]. In the end, *FoxO1* mRNA expression is very low in the cells of myeloid lineage [270], so it seems unlikely that FoxO1 mediates CoPP effects on mobilization of granulocytes.

Along with investigation of molecular mechanism beyond CoPP-induced mobilization and its connection with GCSF, our studies indicate that CoPP may have a potential clinical application.

Currently, G-CSF is widely used in clinical practice for mobilization of HSC for further transplantation, as well as for the treatment of neutropenias of various origin, especially in prevention of neutropenia as a side effect of chemotherapy. However, G-CSF-induced HSC mobilization fails in 5-30% of healthy donors and up to 60% of high-risk patients [162]. Moreover, although G-CSF therapy reduces incidence of neutropenia, it does not significantly decrease infection-related mortality [277]. That is why new therapeutic options are needed, which will further reduce the incidence and duration of

neutropenia, leading to decreased mortality [166] and increase the yield of mobilized HSC for transplantations [162]. Of advantage would be a drug that could activate the G-CSF receptor/induce endogenous ligand and have additional activities [166]. CoPP possesses such characteristics – it upregulates endogenous G-CSF, but also induces other cytokines, among them IL-6. One of the CoPP advantage over the G-CSF are potentially lower costs: G-CSF is a recombinant protein, while CoPP is well-known molecule with established synthesis methods.

Given that various metalloporphyrins (Mps) were considered for the therapeutic applications already in the early 80's, the potential application of CoPP is tempting. For example, SnPP was proposed to be a drug for neonatal hyperbilirubinemia [278]. Since then, many clinical trials were conducted using SnPP or tin mesoporphyrin (SnMP) (reviewed in [279]).

Metalloporphyrins are usually administered i.v. in the *in vivo* setting. Some studies show no difference in HO-1 activity after oral administration of Mps [280, 281]. However, certain Mps were shown to be orally absorbed and able to modulate HO-1 activity in mice [282]. Moreover, lipid-based formulation of ZnPP was recently reported to be orally absorbed in neonatal mice [283]. It is important, though, to notice, that majority of the studies on oral administration of Mps were aimed to inhibit HO-1 activity. Increase of *Hmox1* gene expression could be much easier than inhibition of enzymatic activity, thus, there is a possibility that CoPP-based drug could also be administered orally. However this issue is still to be investigated and confirmed experimentally. Moreover, toxicity testing is needed to confirm the safety of potential use of CoPP as a drug.

To sum up, administration of CoPP results in the mobilization of functional granulocytes and HSPC into the blood, what correlates with increased plasma concentrations of G-CSF, IL-6 and MCP-1 (Fig. 66)**. This effect is independent of HO-1 and Nrf2.**

7. SUMMARY

The aim of this study was to investigate the role of HO-1 in the development and progression of squamous cell carcinoma. Basing on the literature data we formulated two hypotheses, which we tried to verify experimentally.

We did not confirm our **1st hypothesis, that HO-1 protects against chemical oral carcinogenesis.** Using 4NQO-induced carcinogenesis we showed that endogenous HO-1 deficiency did not affect oral carcinogenesis. However, HO-1 deficiency increased susceptibility for esophageal carcinogenesis and HO-1 overexpression seemed to have a protective effect. Moreover, HO-1 deficiency affected the cytokine production in response to 4NQO.

Next, using the model of subcutaneous tumor injection into syngeneic mice we partially confirmed the **2nd hypothesis, that HO-1 overexpression in cancer cells facilitates tumor growth, angiogenesis and infiltration with suppressive leukocyte populations.** Although results concerning the tumor growth were inconclusive and need further investigation, HO-1 overexpressing tumors were more heavily infiltrated with certain population of leukocytes. HO-1 overexpression in tumor affected also peripheral T cells phenotype and cytokine concentrations.

Finally, we were able to confirm the additional, **3rd hypothesis, that CoPP induces the mobilization of cells from the bone marrow to blood.** We showed that CoPP induces mobilization of functional, ROS-producing granulocytes and HSC, which are able to rescue hematopoiesis in lethally irradiated mice. Those effects are probably mediated manly by G-CSF and IL-6, but other cytokines such as MCP-1, KC or IP-10 might also be involved. Finally, we show that effects of CoPP-induced mobilization are HO-1- and Nrf2-independent.

In conclusion, HO-1 might affect both esophageal squamous cell carcinogenesis and immune response to the growing tumor. CoPP could be used as a mobilizing agent.

8. FUNDING

Presented work was supported by Polish Ministry of Science and Higher Education (grant: NN301144336) and structural funds from the EU (grant: 01.02.00-069/09).

The Faculty of Biochemistry, Biophysics and Biotechnology of the Jagiellonian University was beneficiary of the structural funds from the European Union (grants POIG.02.01.00-12-064/08 and POIG.02.02.00-014/08).

The Faculty of Biochemistry, Biophysics and Biotechnology of Jagiellonian University is a partner of the Leading National Research Center (KNOW) supported by the Ministry of Science and Higher Education.

During the PhD studies I was receiving a scholarship within the project "Doctus - Malopolska scholarship fund for graduate students" co-financed by the European Union under the European Social Fund.

9. POTENTIAL CONFLICT OF INTEREST

A. Szade, K. Szade, A. Józkowicz and J.Dulak are authors of pending patent application no PCT/PL2015/050014 entitled *The use of cobalt porphyrins.*

10. BIBLIOGRAPHY

1. Young B, O'Dowd G, Woodford P: *Wheater's Functional Histology. A Text and Colour Atlas. Fifth Edition.* Elsevier; 2006.

2. Jenkins G, Tortora GJ: *Anatomy and Physiology From Science to Life 3rd Edition*. John Wiley & Sons, Ltd; 2013.

3. Marieb EN, Hoehn K: *Human Anatomy & Physiology. 7th Ed.* San Francisco Pearson Benjamin Cummings; 2007.

4. Squier CA, Kremer MJ: **Biology of Oral Mucosa and Esophagus**. *JNCI Monogr* 2001, **2001**:7–15.

5. Shetty S: **Keratinization and its Disorders**. *Oman Med J* 2012, **27**:348–357.

6. Kumar V, Cotran RS, Robbins SL: *Robbins Patologia*. Wrocław: Elsevier Urban & Partner; 2005.

7. Marks R: **Squamous cell carcinoma**. *The Lancet* 1996, **347**:735–738.

8. Ferlay J, Shin H-R, Bray F, Forman D, Mathers C, Parkin DM: **Estimates of worldwide burden of cancer in 2008: GLOBOCAN 2008**. *Int J Cancer* 2010, **127**:2893–2917.

9. Parkin DM, Bray F, Ferlay J, Pisani P: **Global Cancer Statistics, 2002**. *CA Cancer J Clin* 2005, **55**:74–108.

10. Carvalho AL, Nishimoto IN, Califano JA, Kowalski LP: **Trends in incidence and prognosis for head and neck cancer in the United States: a site-specific analysis of the SEER database**. *Int J Cancer J Int Cancer* 2005, **114**:806–816.

11. Toner M, O'Regan EM: **Head and neck squamous cell carcinoma in the young: a spectrum or a distinct group? Part 1**. *Head Neck Pathol* 2009, **3**:246–248.

12. Ferri FF: *Ferri's Clinical Advisor 2013,5 Books in 1, Expert Consult - Online and Print,1: Ferri's Clinical Advisor 2013*. Elsevier Health Sciences; 2012.

13. Arnold M, Soerjomataram I, Ferlay J, Forman D: **Global incidence of oesophageal cancer by histological subtype in 2012**. *Gut* 2015, **64**:381–387.

14. Kachala R: **Systematic review: epidemiology of oesophageal cancer in Sub-Saharan Africa**. *Malawi Med J J Med Assoc Malawi* 2010, **22**:65–70.

15. Lewin F, Norell SE, Johansson H, Gustavsson P, Wennerberg J, Biörklund A, Rutqvist LE: **Smoking tobacco, oral snuff, and alcohol in the etiology of squamous cell carcinoma of the head and neck: a population-based case-referent study in Sweden**. *Cancer* 1998, **82**:1367–1375.

16. Fan Y, Yuan J-M, Wang R, Gao Y-T, Yu MC: **Alcohol, Tobacco and Diet in Relation to Esophageal Cancer: The Shanghai Cohort Study**. *Nutr Cancer* 2008, **60**:354–363.

17. Walker DM, Boey G, McDonald L: **The pathology of oral cancer**. *Pathology (Phila)* 2003, **35**:376–383.

18. Fakhry C, Westra WH, Li S, Cmelak A, Ridge JA, Pinto H, Forastiere A, Gillison ML: **Improved Survival of Patients With Human Papillomavirus–Positive Head and Neck Squamous Cell Carcinoma in a Prospective Clinical Trial**. *J Natl Cancer Inst* 2008, **100**:261–269.

19. Marur S, D'Souza G, Westra WH, Forastiere AA: **HPV-associated head and neck cancer: a virus-related cancer epidemic**. *Lancet Oncol* 2010, **11**:781–789.

20. Baselga J, Pfister D, Cooper MR, Cohen R, Burtness B, Bos M, D'Andrea G, Seidman A, Norton L, Gunnett K, Falcey J, Anderson V, Waksal H, Mendelsohn J: **Phase I studies of anti-epidermal growth factor receptor chimeric antibody C225 alone and in combination with cisplatin**. *J Clin Oncol Off J Am Soc Clin Oncol* 2000, **18**:904–914.

21. Bonner JA, Harari PM, Giralt J, Azarnia N, Shin DM, Cohen RB, Jones CU, Sur R, Raben D, Jassem J, Ove R, Kies MS, Baselga J, Youssoufian H, Amellal N, Rowinsky EK, Ang KK: **Radiotherapy plus cetuximab for squamous-cell carcinoma of the head and neck**. *N Engl J Med* 2006, **354**:567–578.

22. Vermorken JB, Trigo J, Hitt R, Koralewski P, Diaz-Rubio E, Rolland F, Knecht R, Amellal N, Schueler A, Baselga J: **Open-label, uncontrolled, multicenter phase II study to evaluate the efficacy and toxicity of cetuximab as a single agent in patients with recurrent and/or metastatic squamous cell carcinoma of the head and neck who failed to respond to platinum-based therapy**. *J Clin Oncol Off J Am Soc Clin Oncol* 2007, **25**:2171–2177.

23. Yamazaki M, Yamashita Y, Kubo N, Yashiro M, Ohira M, Ako E, Tanaka H, Muguruma K, Sawada T, Hirakawa K: **Concurrent biological targeting therapy of squamous cell carcinoma of the esophagus with cetuximab and trastuzumab**. *Oncol Rep* 2012, **28**:49–54.

24. Cohen EEW, Rosen F, Stadler WM, Recant W, Stenson K, Huo D, Vokes EE: **Phase II trial of ZD1839 in recurrent or metastatic squamous cell carcinoma of the head and neck**. *J Clin Oncol Off J Am Soc Clin Oncol* 2003, **21**:1980–1987.

25. Stewart JSW, Cohen EEW, Licitra L, Van Herpen CML, Khorprasert C, Soulieres D, Vodvarka P, Rischin D, Garin AM, Hirsch FR, Varella-Garcia M, Ghiorghiu S, Hargreaves L, Armour A, Speake G, Swaisland A, Vokes EE: **Phase III study of gefitinib compared with intravenous methotrexate for recurrent squamous cell carcinoma of the head and neck [corrected]**. *J Clin Oncol Off J Am Soc Clin Oncol* 2009, **27**:1864–1871.

26. Argiris A, Ghebremichael M, Gilbert J, Lee J-W, Sachidanandam K, Kolesar JM, Burtness B, Forastiere AA: **Phase III randomized, placebo-controlled trial of docetaxel with or without gefitinib in recurrent or metastatic head and neck cancer: an eastern cooperative oncology group trial**. *J Clin Oncol Off J Am Soc Clin Oncol* 2013, **31**:1405–1414.

27. Pollack VA, Savage DM, Baker DA, Tsaparikos KE, Sloan DE, Moyer JD, Barbacci EG, Pustilnik LR, Smolarek TA, Davis JA, Vaidya MP, Arnold LD, Doty JL, Iwata KK, Morin MJ:

Inhibition of epidermal growth factor receptor-associated tyrosine phosphorylation in human carcinomas with CP-358,774: dynamics of receptor inhibition in situ and antitumor effects in athymic mice. *J Pharmacol Exp Ther* 1999, **291**:739–748.

28. Hidalgo M, Siu LL, Nemunaitis J, Rizzo J, Hammond LA, Takimoto C, Eckhardt SG, Tolcher A, Britten CD, Denis L, Ferrante K, Von Hoff DD, Silberman S, Rowinsky EK: **Phase I and pharmacologic study of OSI-774, an epidermal growth factor receptor tyrosine kinase inhibitor, in patients with advanced solid malignancies**. *J Clin Oncol Off J Am Soc Clin Oncol* 2001, **19**:3267–3279.

29. Harrington KJ, El-Hariry IA, Holford CS, Lusinchi A, Nutting CM, Rosine D, Tanay M, Deutsch E, Matthews J, D'Ambrosio C, Turner SJ, Pandeshwara JS, Bourhis J: **Phase I study of lapatinib in combination with chemoradiation in patients with locally advanced squamous cell carcinoma of the head and neck**. *J Clin Oncol Off J Am Soc Clin Oncol* 2009, **27**:1100–1107.

30. Machiels J-PH, Henry S, Zanetta S, Kaminsky M-C, Michoux N, Rommel D, Schmitz S, Bompas E, Dillies A-F, Faivre S, Moxhon A, Duprez T, Guigay J: **Phase II study of sunitinib in recurrent or metastatic squamous cell carcinoma of the head and neck: GORTEC 2006-01**. *J Clin Oncol Off J Am Soc Clin Oncol* 2010, **28**:21–28.

31. **Antitumor activity of cediranib in patients with metastatic or recurrent head and neck cancer (HNC) or recurrent non-small cell lung cancer (NSCLC): An open-label exploratory study.** *J Clin Oncol* .

32. Koster MI: **Making an epidermis**. *Ann N Y Acad Sci* 2009, **1170**:7–10.

33. Halprin KM: **Epidermal "turnover time"--a re-examination**. *Br J Dermatol* 1972, **86**:14–19.

34. Potten CS, Saffhill R, Maibach HI: **Measurement of the transit time for cells through the epidermis and stratum corneum of the mouse and guinea-pig**. *Cell Tissue Kinet* 1987, **20**:461–472.

35. Reya T, Morrison SJ, Clarke MF, Weissman IL: **Stem cells, cancer, and cancer stem cells**. *Nature* 2001, **414**:105–111.

36. Hanahan D, Weinberg RA: **Hallmarks of Cancer: The Next Generation**. *Cell* 2011, **144**:646–674.

37. Prince ME, Sivanandan R, Kaczorowski A, Wolf GT, Kaplan MJ, Dalerba P, Weissman IL, Clarke MF, Ailles LE: **Identification of a subpopulation of cells with cancer stem cell properties in head and neck squamous cell carcinoma**. *Proc Natl Acad Sci U S A* 2007, **104**:973–978.

38. Tenhunen R, Marver HS, Schmid R: **The enzymatic conversion of heme to bilirubin by microsomal heme oxygenase.** *Proc Natl Acad Sci U S A* 1968, **61**:748–755.

39. Tenhunen R, Ross ME, Marver HS, Schmid R: **Reduced nicotinamide-adenine dinucleotide phosphate dependent biliverdin reductase: partial purification and characterization**. *Biochemistry (Mosc)* 1970, **9**:298–303.

40. Ryter SW, Alam J, Choi AMK: **Heme oxygenase-1/carbon monoxide: from basic science to therapeutic applications**. *Physiol Rev* 2006, **86**:583–650.

41. Morse D, Choi AMK: **Heme oxygenase-1: the "emerging molecule" has arrived**. *Am J Respir Cell Mol Biol* 2002, **27**:8–16.

42. Maines MD, Trakshel GM, Kutty RK: **Characterization of two constitutive forms of rat liver microsomal heme oxygenase. Only one molecular species of the enzyme is inducible**. *J Biol Chem* 1986, **261**:411–419.

43. Exner M, Minar E, Wagner O, Schillinger M: **The role of heme oxygenase-1 promoter polymorphisms in human disease**. *Free Radic Biol Med* 2004, **37**:1097–1104.

44. Radhakrishnan N, Yadav SP, Sachdeva A, Pruthi PK, Sawhney S, Piplani T, Wada T, Yachie A: **Human heme oxygenase-1 deficiency presenting with hemolysis, nephritis, and asplenia**. *J Pediatr Hematol Oncol* 2011, **33**:74–78.

45. Radhakrishnan N, Yadav SP, Sachdeva A, Wada T, Yachie A: **An interesting tetrad of asplenia, inflammation, hemolysis, and nephritis**. *Pediatr Hematol Oncol* 2011, **28**:723–726.

46. Poss KD, Tonegawa S: **Heme oxygenase 1 is required for mammalian iron reutilization**. *Proc Natl Acad Sci* 1997, **94**:10919–10924.

47. Taguchi K, Motohashi H, Yamamoto M: **Molecular mechanisms of the Keap1–Nrf2 pathway in stress response and cancer evolution**. *Genes Cells Devoted Mol Cell Mech* 2011, **16**:123–140.

48. Kansanen E, Kuosmanen SM, Leinonen H, Levonen A-L: **The Keap1-Nrf2 pathway: Mechanisms of activation and dysregulation in cancer**. *Redox Biol* 2013, **1**:45–49.

49. Wagener FADTG, Volk H-D, Willis D, Abraham NG, Soares MP, Adema GJ, Figdor CG: **Different faces of the heme-heme oxygenase system in inflammation**. *Pharmacol Rev* 2003, **55**:551–571.

50. Florczyk UM, Jozkowicz A, Dulak J: **Biliverdin reductase: new features of an old enzyme and its potential therapeutic significance**. *Pharmacol Rep PR* 2008, **60**:38–48.

51. Loboda A, Jazwa A, Grochot-Przeczek A, Rutkowski AJ, Cisowski J, Agarwal A, Jozkowicz A, Dulak J: **Heme oxygenase-1 and the vascular bed: from molecular mechanisms to therapeutic opportunities**. *Antioxid Redox Signal* 2008, **10**:1767–812.

52. Naito Y, Takagi T, Yoshikawa T: **Heme oxygenase-1: a new therapeutic target for inflammatory bowel disease**. *Aliment Pharmacol Ther* 2004, **20 Suppl 1**:177–184.

53. Wang WP, Guo X, Koo MW, Wong BC, Lam SK, Ye YN, Cho CH: **Protective role of heme oxygenase-1 on trinitrobenzene sulfonic acid-induced colitis in rats**. *Am J Physiol Gastrointest Liver Physiol* 2001, **281**:G586–594.

54. Nakahira K, Kim HP, Geng XH, Nakao A, Wang X, Murase N, Drain PF, Wang X, Sasidhar M, Nabel EG, Takahashi T, Lukacs NW, Ryter SW, Morita K, Choi AMK: **Carbon monoxide differentially inhibits TLR signaling pathways by regulating ROS-induced trafficking of TLRs to lipid rafts**. *J Exp Med* 2006, **203**:2377–2389.

55. Foresti R, Bani-Hani MG, Motterlini R: **Use of carbon monoxide as a therapeutic agent: promises and challenges**. *Intensive Care Med* 2008, **34**:649–658.

56. Szade A, Grochot-Przeczek A, Florczyk U, Jozkowicz A, Dulak J: **Cellular and molecular mechanisms of inflammation-induced angiogenesis**. *IUBMB Life* 2015, **67**:145–159.

57. Dulak J, Deshane J, Jozkowicz A, Agarwal A: **Heme Oxygenase-1 and Carbon Monoxide in Vascular Pathobiology Focus on Angiogenesis**. *Circulation* 2008, **117**:231–241.

58. Grochot-Przeczek A, Lach R, Mis J, Skrzypek K, Gozdecka M, Sroczynska P, Dubiel M, Rutkowski A, Kozakowska M, Zagorska A, Walczynski J, Was H, Kotlinowski J, Drukala J, Kurowski K, Kieda C, Herault Y, Dulak J, Jozkowicz A: **Heme oxygenase-1 accelerates cutaneous wound healing in mice**. *PloS One* 2009, **4**:e5803.

59. Jazwa A, Stepniewski J, Zamykal M, Jagodzinska J, Meloni M, Emanueli C, Jozkowicz A, Dulak J: **Pre-emptive hypoxia-regulated HO-1 gene therapy improves post-ischaemic limb perfusion and tissue regeneration in mice**. *Cardiovasc Res* 2013, **97**:115–124.

60. Suzuki M, Iso-o N, Takeshita S, Tsukamoto K, Mori I, Sato T, Ohno M, Nagai R, Ishizaka N: **Facilitated angiogenesis induced by heme oxygenase-1 gene transfer in a rat model of hindlimb ischemia**. *Biochem Biophys Res Commun* 2003, **302**:138–143.

61. Lin H-H, Chen Y-H, Chang P-F, Lee Y-T, Yet S-F, Chau L-Y: **Heme oxygenase-1 promotes neovascularization in ischemic heart by coinduction of VEGF and SDF-1**. *J Mol Cell Cardiol* 2008, **45**:44–55.

62. Lakkisto P, Siren J-M, Kytö V, Forsten H, Laine M, Pulkki K, Tikkanen I: **Heme oxygenase-1 induction protects the heart and modulates cellular and extracellular remodelling after myocardial infarction in rats**. *Exp Biol Med* 2011, **236**:1437–1448.

63. Bussolati B, Ahmed A, Pemberton H, Landis RC, Carlo FD, Haskard DO, Mason JC: **Bifunctional role for VEGF-induced heme oxygenase-1 in vivo: induction of angiogenesis and inhibition of leukocytic infiltration**. *Blood* 2004, **103**:761–766.

64. Deshane J, Chen S, Caballero S, Grochot-Przeczek A, Was H, Li Calzi S, Lach R, Hock TD, Chen B, Hill-Kapturczak N, Siegal GP, Dulak J, Jozkowicz A, Grant MB, Agarwal A: **Stromal cell-derived factor 1 promotes angiogenesis via a heme oxygenase 1-dependent mechanism**. *J Exp Med* 2007, **204**:605–618.

65. Dulak J, Józkowicz A, Foresti R, Kasza A, Frick M, Huk I, Green CJ, Pachinger O, Weidinger F, Motterlini R: **Heme oxygenase activity modulates vascular endothelial growth factor synthesis in vascular smooth muscle cells**. *Antioxid Redox Signal* 2002, **4**:229–240.

66. Florczyk U, Józkowicz A, Dulak J: **Nrf2 Transcription Factor and Heme Oxygenase-1 as Modulators of Vascular Injury and Angiogenesis**. In *Angiogenesis and Vascularisation*. Edited by Dulak J, Józkowicz A, Łoboda A. Springer Vienna; 2013:213–239.

67. Wei Y, Gong J, Thimmulappa RK, Kosmider B, Biswal S, Duh EJ: **Nrf2 acts cell-autonomously in endothelium to regulate tip cell formation and vascular branching**. *Proc Natl Acad Sci U S A* 2013, **110**:E3910–3918.

68. Florczyk U, Jazwa A, Maleszewska M, Mendel M, Szade K, Kozakowska M, Grochot-Przeczek A, Viscardi M, Czauderna S, Bukowska-Strakova K, Kotlinowski J, Jozkowicz A, Loboda A, Dulak J: **Nrf2 regulates angiogenesis: effect on endothelial cells, bone marrow-derived proangiogenic cells and hind limb ischemia**. *Antioxid Redox Signal* 2014, **20**:1693–1708.

69. Ichihara S, Yamada Y, Liu F, Murohara T, Itoh K, Yamamoto M, Ichihara G: **Ablation of the transcription factor Nrf2 promotes ischemia-induced neovascularization by enhancing the inflammatory response**. *Arterioscler Thromb Vasc Biol* 2010, **30**:1553–1561.

70. Blancou P, Tardif V, Simon T, Rémy S, Carreño L, Kalergis A, Anegon I: **Immunoregulatory properties of heme oxygenase-1**. *Methods Mol Biol Clifton NJ* 2011, **677**:247–268.

71. Deshmane SL, Kremlev S, Amini S, Sawaya BE: **Monocyte Chemoattractant Protein-1 (MCP-1): An Overview**. *J Interferon Cytokine Res* 2009, **29**:313–326.

72. Otterbein LE, Bach FH, Alam J, Soares M, Tao Lu H, Wysk M, Davis RJ, Flavell RA, Choi AM: **Carbon monoxide has anti-inflammatory effects involving the mitogen-activated protein kinase pathway**. *Nat Med* 2000, **6**:422–428.

73. Lee T-S, Chau L-Y: **Heme oxygenase-1 mediates the anti-inflammatory effect of interleukin-10 in mice**. *Nat Med* 2002, **8**:240–246.

74. Wegiel B, Hedblom A, Li M, Gallo D, Csizmadia E, Harris C, Nemeth Z, Zuckerbraun BS, Soares M, Persson JL, Otterbein LE: **Heme oxygenase-1 derived carbon monoxide permits maturation of myeloid cells**. *Cell Death Dis* 2014, **5**:e1139.

75. Condamine T, Gabrilovich DI: **Molecular mechanisms regulating myeloid-derived suppressor cell differentiation and function**. *Trends Immunol* 2011, **32**:19–25.

76. De Wilde V, Van Rompaey N, Hill M, Lebrun JF, Lemaître P, Lhommé F, Kubjak C, Vokaer B, Oldenhove G, Charbonnier LM, Cuturi MC, Goldman M, Le Moine A: **Endotoxin-Induced Myeloid-Derived Suppressor Cells Inhibit Alloimmune Responses via Heme Oxygenase-1**. *Am J Transplant* 2009, **9**:2034–2047.

77. Tzima S, Victoratos P, Kranidioti K, Alexiou M, Kollias G: **Myeloid heme oxygenase–1 regulates innate immunity and autoimmunity by modulating IFN-β production**. *J Exp Med* 2009, **206**:1167–1179.

78. Herrada AA, Llanos C, Mackern-Oberti JP, Carreño LJ, Henriquez C, Gómez RS, Gutierrez MA, Anegon I, Jacobelli SH, Kalergis AM: **Haem oxygenase 1 expression is altered in monocytes from patients with systemic lupus erythematosus**. *Immunology* 2012, **136**:414–424.

79. Chora AA, Fontoura P, Cunha A, Pais TF, Cardoso S, Ho PP, Lee LY, Sobel RA, Steinman L, Soares MP: **Heme oxygenase-1 and carbon monoxide suppress autoimmune neuroinflammation**. *J Clin Invest* 2007, **117**:438–447.

80. Chauveau C, Rémy S, Royer PJ, Hill M, Tanguy-Royer S, Hubert F-X, Tesson L, Brion R, Beriou G, Gregoire M, Josien R, Cuturi MC, Anegon I: **Heme oxygenase-1 expression inhibits dendritic cell maturation and proinflammatory function but conserves IL-10 expression**. *Blood* 2005, **106**:1694–1702.

81. Rémy S, Blancou P, Tesson L, Tardif V, Brion R, Royer PJ, Motterlini R, Foresti R, Painchaut M, Pogu S, Gregoire M, Bach JM, Anegon I, Chauveau C: **Carbon monoxide inhibits TLR-induced dendritic cell immunogenicity**. *J Immunol Baltim Md 1950* 2009, **182**:1877–1884.

82. Pae H-O, Oh G-S, Choi B-M, Chae S-C, Chung H-T: **Differential expressions of heme oxygenase-1 gene in CD25- and CD25+ subsets of human CD4+ T cells**. *Biochem Biophys Res Commun* 2003, **306**:701–705.

83. Choi B-M, Pae H-O, Jeong Y-R, Kim Y-M, Chung H-T: **Critical role of heme oxygenase-1 in Foxp3-mediated immune suppression**. *Biochem Biophys Res Commun* 2005, **327**:1066–1071.

84. Zelenay S, Chora A, Soares MP, Demengeot J: **Heme oxygenase-1 is not required for mouse regulatory T cell development and function**. *Int Immunol* 2007, **19**:11–18.

85. George JF, Braun A, Brusko TM, Joseph R, Bolisetty S, Wasserfall CH, Atkinson MA, Agarwal A, Kapturczak MH: **Suppression by CD4+CD25+ regulatory T cells is dependent on expression of heme oxygenase-1 in antigen-presenting cells**. *Am J Pathol* 2008, **173**:154–160.

86. Hori R, Kashiba M, Toma T, Yachie A, Goda N, Makino N, Soejima A, Nagasawa T, Nakabayashi K, Suematsu M: **Gene Transfection of H25A Mutant Heme Oxygenase-1 Protects Cells against Hydroperoxide-induced Cytotoxicity**. *J Biol Chem* 2002, **277**:10712–10718.

87. Lin Q, Weis S, Yang G, Weng Y-H, Helston R, Rish K, Smith A, Bordner J, Polte T, Gaunitz F, Dennery PA: **Heme Oxygenase-1 Protein Localizes to the Nucleus and Activates Transcription Factors Important in Oxidative Stress**. *J Biol Chem* 2007, **282**:20621 –20633.

88. Linnenbaum M, Busker M, Kraehling JR, Behrends S: **Heme oxygenase isoforms differ in their subcellular trafficking during hypoxia and are differentially modulated by cytochrome P450 reductase**. *PloS One* 2012, **7**:e35483.

89. Was H, Dulak J, Jozkowicz A: **Heme oxygenase-1 in tumor biology and therapy**. *Curr Drug Targets* 2010, **11**:1551–1570.

90. Marinissen MJ, Tanos T, Bolós M, de Sagarra MR, Coso OA, Cuadrado A: **Inhibition of heme oxygenase-1 interferes with the transforming activity of the Kaposi sarcoma herpesvirus-encoded G protein-coupled receptor**. *J Biol Chem* 2006, **281**:11332–11346.

91. Mayerhofer M, Florian S, Krauth M-T, Aichberger KJ, Bilban M, Marculescu R, Printz D, Fritsch G, Wagner O, Selzer E, Sperr WR, Valent P, Sillaber C: **Identification of heme oxygenase-1 as a novel BCR/ABL-dependent survival factor in chronic myeloid leukemia**. *Cancer Res* 2004, **64**:3148–3154.

92. Fang J, Sawa T, Akaike T, Greish K, Maeda H: **Enhancement of chemotherapeutic response of tumor cells by a heme oxygenase inhibitor, pegylated zinc protoporphyrin**. *Int J Cancer J Int Cancer* 2004, **109**:1–8.

93. Shi L, Fang J: **Implication of heme oxygenase-1 in the sensitivity of nasopharyngeal carcinomas to radiotherapy**. *J Exp Clin Cancer Res CR* 2008, **27**:13.

94. Nowis D, Legat M, Grzela T, Niderla J, Wilczek E, Wilczynski GM, Głodkowska E, Mrówka P, Issat T, Dulak J, Józkowicz A, Waś H, Adamek M, Wrzosek A, Nazarewski S, Makowski M, Stokłosa T, Jakóbisiak M, Gołab J: **Heme oxygenase-1 protects tumor cells against photodynamic therapy-mediated cytotoxicity**. *Oncogene* 2006, **25**:3365–3374.

95. Andersen MH, Sørensen RB, Brimnes MK, Svane IM, Becker JC, thor Straten P: **Identification of heme oxygenase-1–specific regulatory CD8+ T cells in cancer patients**. *J Clin Invest* 2009, **119**:2245–2256.

96. Loboda A, Jozkowicz A, Dulak J: **HO-1/CO system in tumor growth, angiogenesis and metabolism - Targeting HO-1 as an anti-tumor therapy**. *Vascul Pharmacol* 2015.

97. Chang K-W, Lee T-C, Yeh W-I, Chung M-Y, Liu C-J, Chi L-Y, Lin S-C: **Polymorphism in heme oxygenase-1 (HO-1) promoter is related to the risk of oral squamous cell carcinoma occurring on male areca chewers**. *Br J Cancer* 2004, **91**:1551–1555.

98. Chau L-Y: **Heme oxygenase-1: emerging target of cancer therapy**. *J Biomed Sci* 2015, **22**:22.

99. Was H, Sokolowska M, Sierpniowska A, Dominik P, Skrzypek K, Lackowska B, Pratnicki A, Grochot-Przeczek A, Taha H, Kotlinowski J, Kozakowska M, Mazan A, Nowak W, Muchova L, Vitek L, Ratajska A, Dulak J, Jozkowicz A: **Effects of heme oxygenase-1 on induction and development of chemically induced squamous cell carcinoma in mice**. *Free Radic Biol Med* 2011, **51**:1717–1726.

100. Alaoui-Jamali MA, Bismar TA, Gupta A, Szarek WA, Su J, Song W, Xu Y, Xu B, Liu G, Vlahakis JZ, Roman G, Jiao J, Schipper HM: **A Novel Experimental Heme Oxygenase-1–Targeted Therapy for Hormone-Refractory Prostate Cancer**. *Cancer Res* 2009, **69**:8017–8024.

101. Rushworth SA, MacEwan DJ: **HO-1 underlies resistance of AML cells to TNF-induced apoptosis**. *Blood* 2008, **111**:3793–801.

102. Kim H-R, Kim S, Kim E-J, Park J-H, Yang S-H, Jeong E-T, Park C, Youn M-J, So H-S, Park R: **Suppression of Nrf2-driven heme oxygenase-1 enhances the chemosensitivity of lung cancer A549 cells toward cisplatin**. *Lung Cancer Amst Neth* 2008, **60**:47–56.

103. Chen GG, Liu ZM, Vlantis AC, Tse GMK, Leung BCH, van Hasselt CA: **Heme oxygenase-1 protects against apoptosis induced by tumor necrosis factor-alpha and cycloheximide in papillary thyroid carcinoma cells**. *J Cell Biochem* 2004, **92**:1246–1256.

104. Liu Z-M, Chen GG, Ng EKW, Leung W-K, Sung JJY, Chung SCS: **Upregulation of heme oxygenase-1 and p21 confers resistance to apoptosis in human gastric cancer cells**. *Oncogene* 2004, **23**:503–513.

105. Busserolles J, Megías J, Terencio MC, Alcaraz MJ: **Heme oxygenase-1 inhibits apoptosis in Caco-2 cells via activation of Akt pathway**. *Int J Biochem Cell Biol* 2006, **38**:1510–1517.

106. Was H, Cichon T, Smolarczyk R, Rudnicka D, Stopa M, Chevalier C, Leger JJ, Lackowska B, Grochot A, Bojkowska K, Ratajska A, Kieda C, Szala S, Dulak J, Jozkowicz A: **Overexpression of heme oxygenase-1 in murine melanoma: increased proliferation and viability of tumor cells, decreased survival of mice**. *Am J Pathol* 2006, **169**:2181–2198.

107. Lee PJ, Alam J, Wiegand GW, Choi AM: **Overexpression of heme oxygenase-1 in human pulmonary epithelial cells results in cell growth arrest and increased resistance to hyperoxia.** *Proc Natl Acad Sci U S A* 1996, **93**:10393–10398.

108. Hill M, Pereira V, Chauveau C, Zagani R, Remy S, Tesson L, Mazal D, Ubillos L, Brion R, Ashgar K, Mashreghi MF, Kotsch K, Moffett J, Doebis C, Seifert M, Boczkowski J, Osinaga E, Anegon I: **Heme oxygenase-1 inhibits rat and human breast cancer cell proliferation: mutual cross inhibition with indoleamine 2,3-dioxygenase**. *FASEB J* 2005, **19**:1957–1968.

109. Gueron G, Siervi AD, Ferrando M, Salierno M, Luca PD, Elguero B, Meiss R, Navone N, Vazquez ES: **Critical Role of Endogenous Heme Oxygenase 1 as a Tuner of the Invasive Potential of Prostate Cancer Cells**. *Mol Cancer Res* 2009, **7**:1745–1755.

110. Skrzypek K, Tertil M, Golda S, Ciesla M, Weglarczyk K, Collet G, Guichard A, Kozakowska M, Boczkowski J, Was H, Gil T, Kuzdzal J, Muchova L, Vitek L, Loboda A, Jozkowicz A, Kieda C, Dulak J: **Interplay between heme oxygenase-1 and miR-378 affects non-small cell lung carcinoma growth, vascularization, and metastasis**. *Antioxid Redox Signal* 2013, **19**:644–660.

111. Doi K, Akaike T, Fujii S, Tanaka S, Ikebe N, Beppu T, Shibahara S, Ogawa M, Maeda H: **Induction of haem oxygenase-1 by nitric oxide and ischaemia in experimental solid tumours and implications for tumour growth**. *Br J Cancer* 1999, **80**:1945–1954.

112. Hirai K, Sasahira T, Ohmori H, Fujii K, Kuniyasu H: **Inhibition of heme oxygenase-1 by zinc protoporphyrin IX reduces tumor growth of LL/2 lung cancer in C57BL mice**. *Int J Cancer* 2007, **120**:500–505.

113. Wegiel B, Gallo D, Csizmadia E, Harris C, Belcher J, Vercellotti GM, Penacho N, Seth P, Sukhatme V, Ahmed A, Pandolfi PP, Helczynski L, Bjartell A, Persson JL, Otterbein LE: **Carbon Monoxide Expedites Metabolic Exhaustion to Inhibit Tumor Growth**. *Cancer Res* 2013.

114. Hsu F-F, Yeh C-T, Sun Y-J, Chiang M-T, Lan W-M, Li F-A, Lee W-H, Chau L-Y: **Signal peptide peptidase-mediated nuclear localization of heme oxygenase-1 promotes cancer cell proliferation and invasion independent of its enzymatic activity**. *Oncogene* 2015, **34**:2360–2370.

115. Sacca P, Meiss R, Casas G, Mazza O, Calvo JC, Navone N, Vazquez E: **Nuclear translocation of haeme oxygenase-1 is associated to prostate cancer**. *Br J Cancer* 2007, **97**:1683–1689.

116. Degese MS, Mendizabal JE, Gandini NA, Gutkind JS, Molinolo A, Hewitt SM, Curino AC, Coso OA, Facchinetti MM: **Expression of heme oxygenase-1 in non-small cell lung cancer (NSCLC) and its correlation with clinical data**. *Lung Cancer Amst Neth* 2012, **77**:168–175.

117. Gandini NA, Fermento ME, Salomón DG, Blasco J, Patel V, Gutkind JS, Molinolo AA, Facchinetti MM, Curino AC: **Nuclear localization of heme oxygenase-1 is associated with tumor progression of head and neck squamous cell carcinomas**. *Exp Mol Pathol* 2012, **93**:237–245.

118. Tibullo D, Barbagallo I, Giallongo C, La Cava P, Parrinello N, Vanella L, Stagno F, Palumbo GA, Li Volti G, Di Raimondo F: **Nuclear translocation of heme oxygenase-1 confers resistance to imatinib in chronic myeloid leukemia cells**. *Curr Pharm Des* 2013, **19**:2765–2770.

119. Frezza C, Zheng L, Folger O, Rajagopalan KN, MacKenzie ED, Jerby L, Micaroni M, Chaneton B, Adam J, Hedley A, Kalna G, Tomlinson IPM, Pollard PJ, Watson DG, Deberardinis RJ, Shlomi T, Ruppin E, Gottlieb E: **Haem oxygenase is synthetically lethal with the tumour suppressor fumarate hydratase**. *Nature* 2011, **477**:225–228.

120. Kreso A, Dick JE: **Evolution of the cancer stem cell model**. *Cell Stem Cell* 2014, **14**:275–291.

121. Herrmann H, Kneidinger M, Cerny-Reiterer S, Rülicke T, Willmann M, Gleixner KV, Blatt K, Hörmann G, Peter B, Samorapoompichit P, Pickl W, Bharate GY, Mayerhofer M, Sperr WR, Maeda H, Valent P: **The Hsp32 inhibitors SMA-ZnPP and PEG-ZnPP exert major growth-inhibitory effects on D34+/CD38+ and CD34+/CD38- AML progenitor cells**. *Curr Cancer Drug Targets* 2012, **12**:51–63.

122. Dunn GP, Old LJ, Schreiber RD: **The Immunobiology of Cancer Immunosurveillance and Immunoediting**. *Immunity* 2004, **21**:137–148.

123. Dunn GP, Bruce AT, Ikeda H, Old LJ, Schreiber RD: **Cancer immunoediting: from immunosurveillance to tumor escape**. *Nat Immunol* 2002, **3**:991–998.

124. Penn I: **Occurrence of cancers in immunosuppressed organ transplant recipients**. *Clin Transpl* 1998:147–158.

125. Grulich AE, van Leeuwen MT, Falster MO, Vajdic CM: **Incidence of cancers in people with HIV/AIDS compared with immunosuppressed transplant recipients: a meta-analysis**. *The Lancet* 2007, **370**:59–67.

126. Koebel CM, Vermi W, Swann JB, Zerafa N, Rodig SJ, Old LJ, Smyth MJ, Schreiber RD: **Adaptive immunity maintains occult cancer in an equilibrium state**. *Nature* 2007, **450**:903–907.

127. Mougiakakos D, Choudhury A, Lladser A, Kiessling R, Johansson CC: **Regulatory T cells in cancer**. *Adv Cancer Res* 2010, **107**:57–117.

128. Nagaraj S, Gabrilovich DI: **Tumor Escape Mechanism Governed by Myeloid-Derived Suppressor Cells**. *Cancer Res* 2008, **68**:2561–2563.

129. Sakaguchi S, Sakaguchi N, Asano M, Itoh M, Toda M: **Immunologic self-tolerance maintained by activated T cells expressing IL-2 receptor alpha-chains (CD25). Breakdown of a single mechanism of self-tolerance causes various autoimmune diseases**. *J Immunol Baltim Md 1950* 1995, **155**:1151–1164.

130. Brunkow ME, Jeffery EW, Hjerrild KA, Paeper B, Clark LB, Yasayko SA, Wilkinson JE, Galas D, Ziegler SF, Ramsdell F: **Disruption of a new forkhead/winged-helix protein, scurfin, results in the fatal lymphoproliferative disorder of the scurfy mouse**. *Nat Genet* 2001, **27**:68–73.

131. Williams LM, Rudensky AY: **Maintenance of the Foxp3-dependent developmental program in mature regulatory T cells requires continued expression of Foxp3**. *Nat Immunol* 2007, **8**:277–284.

132. Bennett CL, Christie J, Ramsdell F, Brunkow ME, Ferguson PJ, Whitesell L, Kelly TE, Saulsbury FT, Chance PF, Ochs HD: **The immune dysregulation, polyendocrinopathy, enteropathy, X-linked syndrome (IPEX) is caused by mutations of FOXP3**. *Nat Genet* 2001, **27**:20–21.

133. Kono K, Kawaida H, Takahashi A, Sugai H, Mimura K, Miyagawa N, Omata H, Fujii H: **CD4(+)CD25high regulatory T cells increase with tumor stage in patients with gastric and esophageal cancers**. *Cancer Immunol Immunother CII* 2006, **55**:1064–1071.

134. Sasada T, Kimura M, Yoshida Y, Kanai M, Takabayashi A: **CD4+CD25+ regulatory T cells in patients with gastrointestinal malignancies: possible involvement of regulatory T cells in disease progression**. *Cancer* 2003, **98**:1089–1099.

135. Sato E, Olson SH, Ahn J, Bundy B, Nishikawa H, Qian F, Jungbluth AA, Frosina D, Gnjatic S, Ambrosone C, Kepner J, Odunsi T, Ritter G, Lele S, Chen Y-T, Ohtani H, Old LJ, Odunsi K: **Intraepithelial CD8+ tumor-infiltrating lymphocytes and a high CD8+/regulatory T cell ratio are associated with favorable prognosis in ovarian cancer**. *Proc Natl Acad Sci U S A* 2005, **102**:18538–18543.

136. Gabrilovich DI, Nagaraj S: **Myeloid-derived-suppressor cells as regulators of the immune system**. *Nat Rev Immunol* 2009, **9**:162–174.

137. Talmadge JE, Gabrilovich DI: **History of myeloid derived suppressor cells (MDSCs) in the macro- and micro-environment of tumour-bearing hosts**. *Nat Rev Cancer* 2013, **13**:739–752.

138. Ostrand-Rosenberg S, Sinha P: **Myeloid-Derived Suppressor Cells: Linking Inflammation and Cancer**. *J Immunol Baltim Md 1950* 2009, **182**:4499–4506.

139. Gabrilovich DI, Bronte V, Chen S-H, Colombo MP, Ochoa A, Ostrand-Rosenberg S, Schreiber H: **The Terminology Issue for Myeloid-Derived Suppressor Cells**. *Cancer Res* 2007, **67**:425–425.

140. Meyer C, Cagnon L, Costa-Nunes CM, Baumgaertner P, Montandon N, Leyvraz L, Michielin O, Romano E, Speiser DE: **Frequencies of circulating MDSC correlate with clinical outcome of melanoma patients treated with ipilimumab**. *Cancer Immunol Immunother* 2013, **63**:247–257.

141. Noy R, Pollard JW: **Tumor-Associated Macrophages: From Mechanisms to Therapy**. *Immunity* 2014, **41**:49–61.

142. Shand FHW, Ueha S, Otsuji M, Koid SS, Shichino S, Tsukui T, Kosugi-Kanaya M, Abe J, Tomura M, Ziogas J, Matsushima K: **Tracking of intertissue migration reveals the origins of tumor-infiltrating monocytes**. *Proc Natl Acad Sci U S A* 2014, **111**:7771–7776.

143. Franklin RA, Liao W, Sarkar A, Kim MV, Bivona MR, Liu K, Pamer EG, Li MO: **The cellular and molecular origin of tumor-associated macrophages**. *Science* 2014, **344**:921–925.

144. Qian B-Z, Pollard JW: **Macrophage diversity enhances tumor progression and metastasis**. *Cell* 2010, **141**:39–51.

145. Wyckoff JB, Wang Y, Lin EY, Li J, Goswami S, Stanley ER, Segall JE, Pollard JW, Condeelis J: **Direct visualization of macrophage-assisted tumor cell intravasation in mammary tumors**. *Cancer Res* 2007, **67**:2649–2656.

146. De Palma M, Venneri MA, Galli R, Sergi LS, Politi LS, Sampaolesi M, Naldini L: **Tie2 identifies a hematopoietic lineage of proangiogenic monocytes required for tumor vessel formation and a mesenchymal population of pericyte progenitors**. *Cancer Cell* 2005, **8**:211–226.

147. Gocheva V, Wang H-W, Gadea BB, Shree T, Hunter KE, Garfall AL, Berman T, Joyce JA: **IL-4 induces cathepsin protease activity in tumor-associated macrophages to promote cancer growth and invasion**. *Genes Dev* 2010, **24**:241–255.

148. Pyonteck SM, Akkari L, Schuhmacher AJ, Bowman RL, Sevenich L, Quail DF, Olson OC, Quick ML, Huse JT, Teijeiro V, Setty M, Leslie CS, Oei Y, Pedraza A, Zhang J, Brennan CW, Sutton JC, Holland EC, Daniel D, Joyce JA: **CSF-1R inhibition alters macrophage polarization and blocks glioma progression**. *Nat Med* 2013, **19**:1264–1272.

149. Su S, Liu Q, Chen J, Chen J, Chen F, He C, Huang D, Wu W, Lin L, Huang W, Zhang J, Cui X, Zheng F, Li H, Yao H, Su F, Song E: **A positive feedback loop between mesenchymal-like cancer cells and macrophages is essential to breast cancer metastasis**. *Cancer Cell* 2014, **25**:605–620.

150. Arnold JN, Magiera L, Kraman M, Fearon DT: **Tumoral Immune Suppression by Macrophages Expressing Fibroblast Activation Protein-α and Heme Oxygenase-1**. *Cancer Immunol Res* 2014, **2**:121–126.

151. Weiss L, Geduldig U: **Barrier cells: stromal regulation of hematopoiesis and blood cell release in normal and stressed murine bone marrow**. *Blood* 1991, **78**:975–990.

152. Lapid K, Glait-Santar C, Gur-Cohen S, Canaani J, Kollet O, Lapidot T: **Egress and Mobilization of Hematopoietic Stem and Progenitor Cells: A Dynamic Multi-facet Process**. In *StemBook*. Cambridge (MA): Harvard Stem Cell Institute; 2008.

153. Lapidot T, Petit I: **Current understanding of stem cell mobilization: the roles of chemokines, proteolytic enzymes, adhesion molecules, cytokines, and stromal cells**. *Exp Hematol* 2002, **30**:973–981.

154. Benschop RJ, Rodriguez-Feuerhahn M, Schedlowski M: **Catecholamine-Induced Leukocytosis: Early Observations, Current Research, and Future Directions**. *Brain Behav Immun* 1996, **10**:77–91.

155. Beekman R, Touw IP: **G-CSF and its receptor in myeloid malignancy**. *Blood* 2010, **115**:5131–5136.

156. Lieschke GJ, Grail D, Hodgson G, Metcalf D, Stanley E, Cheers C, Fowler KJ, Basu S, Zhan YF, Dunn AR: **Mice lacking granulocyte colony-stimulating factor have chronic neutropenia, granulocyte and macrophage progenitor cell deficiency, and impaired neutrophil mobilization**. *Blood* 1994, **84**:1737–1746.

157. Liu F, Wu HY, Wesselschmidt R, Kornaga T, Link DC: **Impaired production and increased apoptosis of neutrophils in granulocyte colony-stimulating factor receptor-deficient mice**. *Immunity* 1996, **5**:491–501.

158. Basu S, Hodgson G, Zhang H-H, Katz M, Quilici C, Dunn AR: **"Emergency" granulopoiesis in G-CSF–deficient mice in response to Candida albicans infection**. *Blood* 2000, **95**:3725–3733.

159. Avalos BR, Parker JM, Ware DA, Hunter MG, Sibert KA, Druker BJ: **Dissociation of the Jak kinase pathway from G-CSF receptor signaling in neutrophils**. *Exp Hematol* 1997, **25**:160–168.

160. Liu F, Poursine-Laurent J, Link DC: **Expression of the G-CSF receptor on hematopoietic progenitor cells is not required for their mobilization by G-CSF**. *Blood* 2000, **95**:3025–3031.

161. Christopher MJ, Rao M, Liu F, Woloszynek JR, Link DC: **Expression of the G-CSF receptor in monocytic cells is sufficient to mediate hematopoietic progenitor mobilization by G-CSF in mice**. *J Exp Med* 2011, **208**:251–260.

162. To LB, Levesque J-P, Herbert KE: **How I treat patients who mobilize hematopoietic stem cells poorly**. *Blood* 2011, **118**:4530–4540.

163. Koreth J, Schlenk R, Kopecky KJ, et al: **Allogeneic stem cell transplantation for acute myeloid leukemia in first complete remission: Systematic review and meta-analysis of prospective clinical trials**. *JAMA* 2009, **301**:2349–2361.

164. Kondo M, Wagers AJ, Manz MG, Prohaska SS, Scherer DC, Beilhack GF, Shizuru JA, Weissman IL: **BIOLOGY OF HEMATOPOIETIC STEM CELLS AND PROGENITORS: Implications for Clinical Application**. *Stem Cells* 2008, **1**:759–806.

165. Liles WC, Broxmeyer HE, Rodger E, Wood B, Hübel K, Cooper S, Hangoc G, Bridger GJ, Henson GW, Calandra G, Dale DC: **Mobilization of hematopoietic progenitor cells in healthy volunteers by AMD3100, a CXCR4 antagonist**. *Blood* 2003, **102**:2728–2730.

166. Hoggatt J, Pelus LM: **New G-CSF agonists for neutropenia therapy**. *Expert Opin Investig Drugs* 2014, **23**:21–35.

167. Morgenstern JP, Land H: **Advanced mammalian gene transfer: high titre retroviral vectors with multiple drug selection markers and a complementary helper-free packaging cell line**. *Nucleic Acids Res* 1990, **18**:3587–3596.

168. Itoh K, Wakabayashi N, Katoh Y, Ishii T, Igarashi K, Engel JD, Yamamoto M: **Keap1 represses nuclear activation of antioxidant responsive elements by Nrf2 through binding to the amino-terminal Neh2 domain**. *Genes Dev* 1999, **13**:76–86.

169. Linh Nguyen Tuyet: **Heme oxygenase-1 increases angiogenic potential of murine squamous carcinoma cells but does not affect induction of carcinogenesis**. Jagiellonian University; 2013.

170. Dranoff G: **Cytokines in cancer pathogenesis and cancer therapy**. *Nat Rev Cancer* 2004, **4**:11–22.

171. Guo Y, Xu F, Lu T, Duan Z, Zhang Z: **Interleukin-6 signaling pathway in targeted therapy for cancer**. *Cancer Treat Rev* 2012, **38**:904–910.

172. Chang Q, Bournazou E, Sansone P, Berishaj M, Gao SP, Daly L, Wels J, Theilen T, Granitto S, Zhang X, Cotari J, Alpaugh ML, de Stanchina E, Manova K, Li M, Bonafe M,

Ceccarelli C, Taffurelli M, Santini D, Altan-Bonnet G, Kaplan R, Norton L, Nishimoto N, Huszar D, Lyden D, Bromberg J: **The IL-6/JAK/Stat3 Feed-Forward Loop Drives Tumorigenesis and Metastasis**. *Neoplasia N Y N* 2013, **15**:848–862.

173. Mocellin S, Marincola FM, Young HA: **Interleukin-10 and the immune response against cancer: a counterpoint**. *J Leukoc Biol* 2005, **78**:1043–1051.

174. Balkwill F: **Tumour necrosis factor and cancer**. *Nat Rev Cancer* 2009, **9**:361–371.

175. Brown CE, Vishwanath RP, Aguilar B, Starr R, Najbauer J, Aboody KS, Jensen MC: **Tumor-Derived Chemokine MCP-1/CCL2 Is Sufficient for Mediating Tumor Tropism of Adoptively Transferred T Cells**. *J Immunol* 2007, **179**:3332–3341.

176. Ji W-T, Chen H-R, Lin C-H, Lee J-W, Lee C-C: **Monocyte Chemotactic Protein 1 (MCP-1) Modulates Pro-Survival Signaling to Promote Progression of Head and Neck Squamous Cell Carcinoma**. *PLoS ONE* 2014, **9**:e88952.

177. Aldinucci D, Colombatti A, Aldinucci D, Colombatti A: **The Inflammatory Chemokine CCL5 and Cancer Progression, The Inflammatory Chemokine CCL5 and Cancer Progression**. *Mediat Inflamm Mediat Inflamm* 2014, **2014, 2014**:e292376.

178. Azenshtein E, Luboshits G, Shina S, Neumark E, Shahbazian D, Weil M, Wigler N, Keydar I, Ben-Baruch A: **The CC Chemokine RANTES in Breast Carcinoma Progression Regulation of Expression and Potential Mechanisms of Promalignant Activity**. *Cancer Res* 2002, **62**:1093–1102.

179. Waight JD, Hu Q, Miller A, Liu S, Abrams SI: **Tumor-Derived G-CSF Facilitates Neoplastic Growth through a Granulocytic Myeloid-Derived Suppressor Cell-Dependent Mechanism**. *PLoS ONE* 2011, **6**:e27690.

180. Yan B, Wei J-J, Yuan Y, Sun R, Li D, Luo J, Liao S-J, Zhou Y-H, Shu Y, Wang Q, Zhang G-M, Feng Z-H: **IL-6 Cooperates with G-CSF To Induce Protumor Function of Neutrophils in Bone Marrow by Enhancing STAT3 Activation**. *J Immunol* 2013, **190**:5882–5893.

181. Chockalingam S, Ghosh SS: **Macrophage colony-stimulating factor and cancer: a review**. *Tumour Biol J Int Soc Oncodevelopmental Biol Med* 2014, **35**:10635–10644.

182. Carmeliet P: **VEGF as a key mediator of angiogenesis in cancer**. *Oncology* 2005, **69 Suppl 3**:4–10.

183. Paine A, Eiz-Vesper B, Blasczyk R, Immenschuh S: **Signaling to heme oxygenase-1 and its anti-inflammatory therapeutic potential**. *Biochem Pharmacol* 2010, **80**:1895–1903.

184. Araujo JA, Zhang M, Yin F: **Heme oxygenase-1, oxidation, inflammation, and atherosclerosis**. *Drug Metab Transp* 2012, **3**:119.

185. Movahedi K, Laoui D, Gysemans C, Baeten M, Stangé G, Van den Bossche J, Mack M, Pipeleers D, In't Veld P, De Baetselier P, Van Ginderachter JA: **Different tumor**

microenvironments contain functionally distinct subsets of macrophages derived from Ly6C(high) monocytes. *Cancer Res* 2010, **70**:5728–5739.

186. Oguro H, Ding L, Morrison SJ: **SLAM family markers resolve functionally distinct subpopulations of hematopoietic stem cells and multipotent progenitors**. *Cell Stem Cell* 2013, **13**:102–116.

187. Nauta JM, Roodenburg JL, Nikkels PG, Witjes MJ, Vermey A: **Comparison of epithelial dysplasia--the 4NQO rat palate model and human oral mucosa**. *Int J Oral Maxillofac Surg* 1995, **24**(1 Pt 1):53–58.

188. Tang X-H, Knudsen B, Bemis D, Tickoo S, Gudas LJ: **Oral Cavity and Esophageal Carcinogenesis Modeled in Carcinogen-Treated Mice**. *Clin Cancer Res* 2004, **10**:301–313.

189. Chang K-W, Lee T-C, Yeh W-I, Chung M-Y, Liu C-J, Chi L-Y, Lin S-C: **Polymorphism in heme oxygenase-1 (HO-1) promoter is related to the risk of oral squamous cell carcinoma occurring on male areca chewers**. *Br J Cancer* 2004, **91**:1551–1555.

190. Taha H, Skrzypek K, Guevara I, Nigisch A, Mustafa S, Grochot-Przeczek A, Ferdek P, Was H, Kotlinowski J, Kozakowska M, Balcerczyk A, Muchova L, Vitek L, Weigel G, Dulak J, Jozkowicz A: **Role of heme oxygenase-1 in human endothelial cells - lesson from the promoter allelic variants**. *Arterioscler Thromb Vasc Biol* 2010, **30**:1634–1641.

191. Tsuji MH, Yanagawa T, Iwasa S, Tabuchi K, Onizawa K, Bannai S, Toyooka H, Yoshida H: **Heme oxygenase-1 expression in oral squamous cell carcinoma as involved in lymph node metastasis**. *Cancer Lett* 1999, **138**:53–59.

192. Yanagawa T, Omura K, Harada H, Nakaso K, Iwasa S, Koyama Y, Onizawa K, Yusa H, Yoshida H: **Heme oxygenase-1 expression predicts cervical lymph node metastasis of tongue squamous cell carcinomas**. *Oral Oncol* 2004, **40**:21–27.

193. Lee S-S, Yang S-F, Tsai C-H, Chou M-C, Chou M-Y, Chang Y-C: **Upregulation of heme oxygenase-1 expression in areca-quid-chewing-associated oral squamous cell carcinoma**. *J Formos Med Assoc Taiwan Yi Zhi* 2008, **107**:355–363.

194. Lee J, Lee S-K, Lee B-U, Lee H-J, Cho N-P, Yoon J-H, Choi H-R, Lee S-K, Kim E-C: **Upregulation of heme oxygenase-1 in oral epithelial dysplasias**. *Int J Oral Maxillofac Surg* 2008, **37**:287–292.

195. Abel EL, Angel JM, Kiguchi K, DiGiovanni J: **Multi-stage chemical carcinogenesis in mouse skin: Fundamentals and applications**. *Nat Protoc* 2009, **4**:1350–1362.

196. Liao F, Andalibi A, deBeer FC, Fogelman AM, Lusis AJ: **Genetic control of inflammatory gene induction and NF-kappa B-like transcription factor activation in response to an atherogenic diet in mice.** *J Clin Invest* 1993, **91**:2572–2579.

197. Choi AM, Knobil K, Otterbein SL, Eastman DA, Jacoby DB: **Oxidant stress responses in influenza virus pneumonia: gene expression and transcription factor activation**. *Am J Physiol* 1996, **271**(3 Pt 1):L383–391.

198. Lloyd C, Yu QC, Cheng J, Turksen K, Degenstein L, Hutton E, Fuchs E: **The basal keratin network of stratified squamous epithelia: defining K15 function in the absence of K14**. *J Cell Biol* 1995, **129**:1329–1344.

199. Viswanadha VP, Sivan S, Rajendra Shenoi R: **Protective effect of Spirulina against 4-nitroquinoline-1-oxide induced toxicity**. *Mol Biol Rep* 2011, **38**:309–317.

200. Kakkar P, Das B, Viswanathan PN: **A modified spectrophotometric assay of superoxide dismutase**. *Indian J Biochem Biophys* 1984, **21**:130–132.

201. Ribeiro DA, Salvadori DMF: **Gingival Changes in Wistar Rats after Oral Treatment with 4-Nitroquinoline 1-Oxide**. *Eur J Dent* 2007, **1**:152–157.

202. Barcessat ARR, Huang I, Rabelo GD, Rosin FCP, Ferreira LGV, de Cerqueira Luz JG, Corrêa L: **Systemic toxic effects during early phases of topical 4-NQO-induced oral carcinogenesis in rats**. *J Oral Pathol Med Off Publ Int Assoc Oral Pathol Am Acad Oral Pathol* 2014, **43**:770–777.

203. Bolisetty S, Traylor AM, Kim J, Joseph R, Ricart K, Landar A, Agarwal A: **Heme Oxygenase-1 Inhibits Renal Tubular Macroautophagy in Acute Kidney Injury**. *J Am Soc Nephrol JASN* 2010, **21**:1702–1712.

204. Chu PG, Weiss LM: **Keratin expression in human tissues and neoplasms**. *Histopathology* 2002, **40**:403–439.

205. van der Velden LA, Manni JJ, Ramaekers FC, Kuijpers W: **Expression of intermediate filament proteins in benign lesions of the oral mucosa**. *Eur Arch Oto-Rhino-Laryngol Off J Eur Fed Oto-Rhino-Laryngol Soc EUFOS Affil Ger Soc Oto-Rhino-Laryngol - Head Neck Surg* 1999, **256**:514–519.

206. Kanojia D, Sawant SS, Borges AM, Ingle AD, Vaidya MM: **Alterations in keratins and associated proteins during 4- Nitroquinoline-1-oxide induced rat oral carcinogenesis**. *J Carcinog* 2012, **11**.

207. Fillies T, Werkmeister R, Packeisen J, Brandt B, Morin P, Weingart D, Joos U, Buerger H: **Cytokeratin 8/18 expression indicates a poor prognosis in squamous cell carcinomas of the oral cavity**. *BMC Cancer* 2006, **6**:10.

208. Paleri V, Pulimood A, Davies GR, Birchall MA: **Interleukins 7 and 12 are expressed in head and neck squamous cancer**. *Clin Otolaryngol Allied Sci* 2001, **26**:302–306.

209. Linkov F, Lisovich A, Yurkovetsky Z, Marrangoni A, Velikokhatnaya L, Nolen B, Winans M, Bigbee W, Siegfried J, Lokshin A, Ferris RL: **Early Detection of Head and Neck Cancer: Development of a Novel Screening Tool Using Multiplexed Immunobead-Based Biomarker Profiling**. *Cancer Epidemiol Biomarkers Prev* 2007, **16**:102–107.

210. Pittock ST, Norby SM, Grande JP, Croatt AJ, Bren GD, Badley AD, Caplice NM, Griffin MD, Nath KA: **MCP-1 is up-regulated in unstressed and stressed HO-1 knockout mice: Pathophysiologic correlates**. *Kidney Int* 2005, **68**:611–622.

211. Orozco LD, Kapturczak MH, Barajas B, Wang X, Weinstein MM, Wong J, Deshane J, Bolisetty S, Shaposhnik Z, Shih DM, Agarwal A, Lusis AJ, Araujo JA: **Heme oxygenase-1 expression in macrophages plays a beneficial role in atherosclerosis**. *Circ Res* 2007, **100**:1703–11.

212. Zhu F, Liu P, Li J, Zhang Y: **Eotaxin-1 promotes prostate cancer cell invasion via activation of the CCR3-ERK pathway and upregulation of MMP-3 expression**. *Oncol Rep* 2014, **31**:2049–2054.

213. Salcedo R, Young HA, Ponce ML, Ward JM, Kleinman HK, Murphy WJ, Oppenheim JJ: **Eotaxin (CCL11) Induces In Vivo Angiogenic Responses by Human CCR3+ Endothelial Cells**. *J Immunol* 2001, **166**:7571–7578.

214. Gajewski TF, Schreiber H, Fu Y-X: **Innate and adaptive immune cells in the tumor microenvironment**. *Nat Immunol* 2013, **14**:1014–1022.

215. Doseff A, Parihar A: **Monocyte Subsets and Their Role in Tumor Progression**. In *Tumor Microenvironment and Myelomonocytic Cells*. Edited by Biswas S. InTech; 2012.

216. Coffelt SB, Lewis CE, Naldini L, Brown JM, Ferrara N, De Palma M: **Elusive Identities and Overlapping Phenotypes of Proangiogenic Myeloid Cells in Tumors**. *Am J Pathol* 2010, **176**:1564–1576.

217. Gabrilovich DI, Ostrand-Rosenberg S, Bronte V: **Coordinated regulation of myeloid cells by tumours**. *Nat Rev Immunol* 2012, **12**:253–268.

218. Pierce JH, Di Marco E, Cox GW, Lombardi D, Ruggiero M, Varesio L, Wang LM, Choudhury GG, Sakaguchi AY, Di Fiore PP: **Macrophage-colony-stimulating factor (CSF-1) induces proliferation, chemotaxis, and reversible monocytic differentiation in myeloid progenitor cells transfected with the human c-fms/CSF-1 receptor cDNA.** *Proc Natl Acad Sci U S A* 1990, **87**:5613–5617.

219. Pixley FJ: **Macrophage Migration and Its Regulation by CSF-1, Macrophage Migration and Its Regulation by CSF-1**. *Int J Cell Biol Int J Cell Biol* 2012, **2012, 2012**:e501962.

220. Gazzaniga S, Bravo AI, Guglielmotti A, van Rooijen N, Maschi F, Vecchi A, Mantovani A, Mordoh J, Wainstok R: **Targeting tumor-associated macrophages and inhibition of MCP-1 reduce angiogenesis and tumor growth in a human melanoma xenograft**. *J Invest Dermatol* 2007, **127**:2031–2041.

221. Huang B, Lei Z, Zhao J, Gong W, Liu J, Chen Z, Liu Y, Li D, Yuan Y, Zhang G-M, Feng Z-H: **CCL2/CCR2 pathway mediates recruitment of myeloid suppressor cells to cancers**. *Cancer Lett* 2007, **252**:86–92.

222. Lunardi S, Jamieson NB, Lim SY, Griffiths KL, Carvalho-Gaspar M, Al-Assar O, Yameen S, Carter RC, McKay CJ, Spoletini G, D'Ugo S, Silva MA, Sansom OJ, Janssen K-P, Muschel RJ, Brunner TB: **IP-10/CXCL10 induction in human pancreatic cancer stroma influences lymphocytes recruitment and correlates with poor survival**. *Oncotarget* 2014, **5**:11064–11080.

223. Szade K, Zukowska M, Szade A, Collet G, Kloska D, Kieda C, Jozkowicz A, Dulak J: **Spheroid-plug model as a tool to study tumor development, angiogenesis, and heterogeneity in vivo**. *Tumour Biol J Int Soc Oncodevelopmental Biol Med* 2015.

224. Lin H-H, Chiang M-T, Chang P-C, Chau L-Y: **Myeloid heme oxygenase-1 promotes metastatic tumor colonization in mice**. *Cancer Sci* 2015, **106**:299–306.

225. Nemeth Z, Li M, Csizmadia E, Döme B, Johansson M, Persson JL, Seth P, Otterbein L, Wegiel B: **Heme oxygenase-1 in macrophages controls prostate cancer progression**. *Oncotarget* 2015.

226. Venneri MA, Palma MD, Ponzoni M, Pucci F, Scielzo C, Zonari E, Mazzieri R, Doglioni C, Naldini L: **Identification of proangiogenic TIE2-expressing monocytes (TEMs) in human peripheral blood and cancer**. *Blood* 2007, **109**:5276–5285.

227. Shah W, Yan X, Jing L, Zhou Y, Chen H, Wang Y: **A reversed CD4/CD8 ratio of tumor-infiltrating lymphocytes and a high percentage of CD4+FOXP3+ regulatory T cells are significantly associated with clinical outcome in squamous cell carcinoma of the cervix**. *Cell Mol Immunol* 2011, **8**:59–66.

228. Sheu BC, Hsu SM, Ho HN, Lin RH, Torng PL, Huang SC: **Reversed CD4/CD8 ratios of tumor-infiltrating lymphocytes are correlated with the progression of human cervical carcinoma**. *Cancer* 1999, **86**:1537–1543.

229. Piersma SJ, Jordanova ES, Poelgeest MIE van, Kwappenberg KMC, Hulst JM van der, Drijfhout JW, Melief CJM, Kenter GG, Fleuren GJ, Offringa R, Burg SH van der: **High Number of Intraepithelial CD8+ Tumor-Infiltrating Lymphocytes Is Associated with the Absence of Lymph Node Metastases in Patients with Large Early-Stage Cervical Cancer**. *Cancer Res* 2007, **67**:354–361.

230. Loetscher M, Gerber B, Loetscher P, Jones SA, Piali L, Clark-Lewis I, Baggiolini M, Moser B: **Chemokine receptor specific for IP10 and mig: structure, function, and expression in activated T-lymphocytes**. *J Exp Med* 1996, **184**:963–969.

231. Mashreghi M-F, Klemz R, Knosalla IS, Gerstmayer B, Janssen U, Buelow R, Jozkowicz A, Dulak J, Volk H-D, Kotsch K: **Inhibition of Dendritic Cell Maturation and Function Is Independent of Heme Oxygenase 1 but Requires the Activation of STAT3**. *J Immunol* 2008, **180**:7919–7930.

232. Liongue C, Wright C, Russell AP, Ward AC: **Granulocyte colony-stimulating factor receptor: stimulating granulopoiesis and much more**. *Int J Biochem Cell Biol* 2009, **41**:2372–2375.

233. Semerad CL, Liu F, Gregory AD, Stumpf K, Link DC: **G-CSF is an essential regulator of neutrophil trafficking from the bone marrow to the blood**. *Immunity* 2002, **17**:413–423.

234. Greenbaum AM, Link DC: **Mechanisms of G-CSF-mediated hematopoietic stem and progenitor mobilization**. *Leukemia* 2011, **25**:211–217.

235. Yamaguchi Y, Suda T, Suda J, Eguchi M, Miura Y, Harada N, Tominaga A, Takatsu K: **Purified interleukin 5 supports the terminal differentiation and proliferation of murine eosinophilic precursors**. *J Exp Med* 1988, **167**:43–56.

236. Hirai K, Yamaguchi M, Misaki Y, Takaishi T, Ohta K, Morita Y, Ito K, Miyamoto T: **Enhancement of human basophil histamine release by interleukin 5**. *J Exp Med* 1990, **172**:1525–1528.

237. Palframan RT, Collins PD, Severs NJ, Rothery S, Williams TJ, Rankin SM: **Mechanisms of Acute Eosinophil Mobilization from the Bone Marrow Stimulated by Interleukin 5: The Role of Specific Adhesion Molecules and Phosphatidylinositol 3-Kinase**. *J Exp Med* 1998, **188**:1621–1632.

238. Zhao JL, Ma C, O'Connell RM, Mehta A, DiLoreto R, Heath JR, Baltimore D: **Conversion of danger signals into cytokine signals by hematopoietic stem and progenitor cells for regulation of stress-induced hematopoiesis**. *Cell Stem Cell* 2014, **14**:445–459.

239. Pojda Z, Tsuboi A: **In vivo effects of human recombinant interleukin 6 on hemopoietic stem and progenitor cells and circulating blood cells in normal mice**. *Exp Hematol* 1990, **18**:1034–1037.

240. Tsou C-L, Peters W, Si Y, Slaymaker S, Aslanian AM, Weisberg SP, Mack M, Charo IF: **Critical roles for CCR2 and MCP-3 in monocyte mobilization from bone marrow and recruitment to inflammatory sites**. *J Clin Invest* 2007, **117**:902–909.

241. Maghazachi AA, Skalhegg BS, Rolstad B, Al-Aoukaty A: **Interferon-inducible protein-10 and lymphotactin induce the chemotaxis and mobilization of intracellular calcium in natural killer cells through pertussis toxin-sensitive and -insensitive heterotrimeric G-proteins**. *FASEB J Off Publ Fed Am Soc Exp Biol* 1997, **11**:765–774.

242. Gentner B, Visigalli I, Hiramatsu H, Lechman E, Ungari S, Giustacchini A, Schira G, Amendola M, Quattrini A, Martino S, Orlacchio A, Dick JE, Biffi A, Naldini L: **Identification of hematopoietic stem cell-specific miRNAs enables gene therapy of globoid cell leukodystrophy**. *Sci Transl Med* 2010, **2**:58ra84.

243. Strecker J-K, Minnerup J, Gess B, Ringelstein EB, Schäbitz W-R, Schilling M: **Monocyte Chemoattractant Protein-1-Deficiency Impairs the Expression of IL-6, IL-1β and G-CSF after Transient Focal Ischemia in Mice**. *PLoS ONE* 2011, **6**:e25863.

244. Eash KJ, Greenbaum AM, Gopalan PK, Link DC: **CXCR2 and CXCR4 antagonistically regulate neutrophil trafficking from murine bone marrow**. *J Clin Invest* 2010, **120**:2423–2431.

245. Mei J, Liu Y, Dai N, Hoffmann C, Hudock KM, Zhang P, Guttentag SH, Kolls JK, Oliver PM, Bushman FD, Worthen GS: **Cxcr2 and Cxcl5 regulate the IL-17/G-CSF axis and neutrophil homeostasis in mice**. *J Clin Invest* 2012, **122**:974–986.

246. Dalrymple SA, Lucian LA, Slattery R, McNeil T, Aud DM, Fuchino S, Lee F, Murray R: **Interleukin-6-deficient mice are highly susceptible to Listeria monocytogenes**

infection: correlation with inefficient neutrophilia. *Infect Immun* 1995, **63**:2262–2268.

247. Romani L, Mencacci A, Cenci E, Spaccapelo R, Toniatti C, Puccetti P, Bistoni F, Poli V: **Impaired neutrophil response and CD4+ T helper cell 1 development in interleukin 6-deficient mice infected with Candida albicans.** *J Exp Med* 1996, **183**:1345–1355.

248. Xing L, Remick DG: **MECHANISMS OF OXIDANT REGULATION OF MONOCYTE CHEMOTACTIC PROTEIN 1 PRODUCTION IN HUMAN WHOLE BLOOD AND ISOLATED MONONUCLEAR CELLS:** *Shock* 2007, **28**:178–185.

249. Hollebeeck S, Raas T, Piront N, Schneider Y-J, Toussaint O, Larondelle Y, During A: **Dimethyl sulfoxide (DMSO) attenuates the inflammatory response in the in vitro intestinal Caco-2 cell model**. *Toxicol Lett* 2011, **206**:268–275.

250. Noh E-M, Cho D-H, Lee Y-R, Jeong Y-J, Kim J-H, Chae HS, Park J, Jung W-S, Park S-J, Kim J-S: **Dimethylsulfoxide (DMSO) induces downregulation of heme oxygenase-1 (HO-1) in HL-60 cells: involvement of HO-1 in HL-60 cell differentiation**. *BMB Rep* 2011, **44**:753–757.

251. Winkler IG, Sims NA, Pettit AR, Barbier V, Nowlan B, Helwani F, Poulton IJ, Rooijen N van, Alexander KA, Raggatt LJ, Lévesque J-P: **Bone marrow macrophages maintain hematopoietic stem cell (HSC) niches and their depletion mobilizes HSCs**. *Blood* 2010, **116**:4815–4828.

252. Shan Y, Lambrecht RW, Donohue SE, Bonkovsky HL: **Role of Bach1 and Nrf2 in up-regulation of the heme oxygenase-1 gene by cobalt protoporphyrin**. *FASEB J Off Publ Fed Am Soc Exp Biol* 2006, **20**:2651–2653.

253. Roberts AW, Hasegawa M, Metcalf D, Foote SJ: **Identification of a genetic locus modulating splenomegaly induced by granulocyte colony-stimulating factor in mice**. *Leukemia* 2000, **14**:657–661.

254. Roberts AW, Foote S, Alexander WS, Scott C, Robb L, Metcalf D: **Genetic Influences Determining Progenitor Cell Mobilization and Leukocytosis Induced by Granulocyte Colony-Stimulating Factor**. *Blood* 1997, **89**:2736–2744.

255. Sinclair P, Gibbs AH, Sinclair JF, de Matteis F: **Formation of cobalt protoporphyrin in the liver of rats. A mechanism for the inhibition of liver haem biosynthesis by inorganic cobalt**. *Biochem J* 1979, **178**:529–538.

256. Sardana MK, Kappas A: **Dual control mechanism for heme oxygenase: tin(IV)-protoporphyrin potently inhibits enzyme activity while markedly increasing content of enzyme protein in liver**. *Proc Natl Acad Sci* 1987, **84**:2464–2468.

257. Blumenthal SB, Kiemer AK, Tiegs G, Seyfried S, Höltje M, Brandt B, Höltje H-D, Zahler S, Vollmar AM: **Metalloporphyrins inactivate caspase-3 and -8**. *FASEB J* 2005, **19**:1272–1279.

258. Ghoreschi K, Brück J, Kellerer C, Deng C, Peng H, Rothfuss O, Hussain RZ, Gocke AR, Respa A, Glocova I, Valtcheva N, Alexander E, Feil S, Feil R, Schulze-Osthoff K, Rupec RA, Lovett-Racke AE, Dringen R, Racke MK, Röcken M: **Fumarates improve psoriasis and multiple sclerosis by inducing type II dendritic cells**. *J Exp Med* 2011, **208**:2291–2303.

259. Gu Q, Wu Q, Jin M, Xiao Y, Xu J, Mao C, Zhao F, Zhang Y, Zhang Y: **Heme Oxygenase-1 Alleviates Mouse Hepatic Failure through Suppression of Adaptive Immune Responses**. *J Pharmacol Exp Ther* 2012, **340**:2–10.

260. Droin N, Cathelin S, Jacquel A, Guéry L, Garrido C, Fontenay M, Hermine O, Solary E: **A role for caspases in the differentiation of erythroid cells and macrophages**. *Biochimie* 2008, **90**:416–422. [*Cellular Proteolysis*]

261. Alvarado-Kristensson M, Melander F, Leandersson K, Rönnstrand L, Wernstedt C, Andersson T: **p38-MAPK Signals Survival by Phosphorylation of Caspase-8 and Caspase-3 in Human Neutrophils**. *J Exp Med* 2004, **199**:449–458.

262. Lin H-Y, Shen S-C, Lin C-W, Wu M-S, Chen Y-C: **Cobalt protoporphyrin inhibition of lipopolysaccharide or lipoteichoic acid-induced nitric oxide production via blocking c-Jun N-terminal kinase activation and nitric oxide enzyme activity**. *Chem Biol Interact* 2009, **180**:202–210.

263. Lin H-Y, Tsai C-H, Lin C, Yeh W-L, Tsai C-F, Chang P-C, Wu L-H, Lu D-Y: **Cobalt Protoporphyrin Upregulates Cyclooxygenase-2 Expression Through a Heme Oxygenase-Independent Mechanism**. *Mol Neurobiol* 2015.

264. Song JD, Lee SK, Park SE, Kim KM, Kim K, Park YM, Park YC: **Cobalt protoporphyrin induces differentiation of monocytic THP-1 cells through regulation of cytoplasmic Ref-1-related NADPH oxidase activity**. *Int J Mol Med* 2011, **28**:841–845.

265. Konrad FM, Braun S, Ngamsri K-C, Vollmer I, Reutershan J: **Heme oxygenase-1 attenuates acute pulmonary inflammation by decreasing the release of segmented neutrophils from the bone marrow**. *Am J Physiol Lung Cell Mol Physiol* 2014, **307**:L707–717.

266. Wysoczynski M, Ratajczak J, Pedziwiatr D, Rokosh G, Bolli R, Ratajczak MZ: **Identification of heme oxygenase 1 (HO-1) as a novel negative regulator of mobilization of hematopoietic stem/progenitor cells**. *Stem Cell Rev* 2015, **11**:110–118.

267. Oyake T, Itoh K, Motohashi H, Hayashi N, Hoshino H, Nishizawa M, Yamamoto M, Igarashi K: **Bach proteins belong to a novel family of BTB-basic leucine zipper transcription factors that interact with MafK and regulate transcription through the NF-E2 site.** *Mol Cell Biol* 1996, **16**:6083–6095.

268. Suzuki H, Tashiro S, Hira S, Sun J, Yamazaki C, Zenke Y, Ikeda-Saito M, Yoshida M, Igarashi K: **Heme regulates gene expression by triggering Crm1-dependent nuclear export of Bach1**. *EMBO J* 2004, **23**:2544–2553.

269. Zenke-Kawasaki Y, Dohi Y, Katoh Y, Ikura T, Ikura M, Asahara T, Tokunaga F, Iwai K, Igarashi K: **Heme Induces Ubiquitination and Degradation of the Transcription Factor Bach1**. *Mol Cell Biol* 2007, **27**:6962–6971.

270. Seita J, Sahoo D, Rossi DJ, Bhattacharya D, Serwold T, Inlay MA, Ehrlich LIR, Fathman JW, Dill DL, Weissman IL: **Gene Expression Commons: an open platform for absolute gene expression profiling**. *PloS One* 2012, **7**:e40321.

271. Itoh-Nakadai A, Hikota R, Muto A, Kometani K, Watanabe-Matsui M, Sato Y, Kobayashi M, Nakamura A, Miura Y, Yano Y, Tashiro S, Sun J, Ikawa T, Ochiai K, Kurosaki T, Igarashi K: **The transcription repressors Bach2 and Bach1 promote B cell development by repressing the myeloid program**. *Nat Immunol* 2014, **15**:1171–1180.

272. Watanabe-Matsui M, Muto A, Matsui T, Itoh-Nakadai A, Nakajima O, Murayama K, Yamamoto M, Ikeda-Saito M, Igarashi K: **Heme regulates B-cell differentiation, antibody class switch, and heme oxygenase-1 expression in B cells as a ligand of Bach2**. *Blood* 2011, **117**:5438–5448.

273. Lee C, Raz R, Gimeno R, Gertner R, Wistinghausen B, Takeshita K, DePinho RA, Levy DE: **STAT3 Is a Negative Regulator of Granulopoiesis but Is Not Required for G-CSF-Dependent Differentiation**. *Immunity* 2002, **17**:63–72.

274. Shimozaki K, Nakajima K, Hirano T, Nagata S: **Involvement of STAT3 in the Granulocyte Colony-stimulating Factor-induced Differentiation of Myeloid Cells**. *J Biol Chem* 1997, **272**:25184–25189.

275. Liu X, Cui Y, Li M, Xu H, Zuo J, Fang F, Chang Y: **Cobalt Protoporphyrin Induces HO-1 Expression Mediated Partially by FOXO1 and Reduces Mitochondria-Derived Reactive Oxygen Species Production**. *PLoS ONE* 2013, **8**:e80521.

276. Tothova Z, Kollipara R, Huntly BJ, Lee BH, Castrillon DH, Cullen DE, McDowell EP, Lazo-Kallanian S, Williams IR, Sears C, Armstrong SA, Passegué E, DePinho RA, Gilliland DG: **FoxOs Are Critical Mediators of Hematopoietic Stem Cell Resistance to Physiologic Oxidative Stress**. *Cell* 2007, **128**:325–339.

277. Molineux G, Foote M, Arvedson T: *Twenty Years of G-CSF: Clinical and Nonclinical Discoveries*. Springer Science & Business Media; 2012.

278. Drummond GS, Kappas A: **Prevention of neonatal hyperbilirubinemia by tin protoporphyrin IX, a potent competitive inhibitor of heme oxidation**. *Proc Natl Acad Sci U S A* 1981, **78**:6466–6470.

279. Schulz S, Wong RJ, Vreman HJ, Stevenson DK: **Metalloporphyrins - An Update**. *Front Pharmacol* 2012, **3**.

280. Vreman HJ, Hintz SR, Kim CB, Castillo RO, Stevenson DK: **Effects of oral administration of tin and zinc protoporphyrin on neonatal and adult rat tissue heme oxygenase activity**. *J Pediatr Gastroenterol Nutr* 1988, **7**:902–906.

281. Drummond GS, Rosenberg DW, Kappas A: **Intestinal heme oxygenase inhibition and increased biliary iron excretion by metalloporphyrins**. *Gastroenterology* 1992, **102**(4 Pt 1):1170–1175.

282. Morioka I, Wong RJ, Abate A, Vreman HJ, Contag CH, Stevenson DK: **Systemic Effects of Orally-Administered Zinc and Tin (IV) Metalloporphyrins on Heme Oxygenase Expression in Mice**. *Pediatr Res* 2006, **59**:667–672.

283. Fujioka K, Kalish F, Wong RJ, Stevenson DK: **Inhibition of heme oxygenase activity using a microparticle formulation of zinc protoporphyrin in an acute hemolytic newborn mouse model**. *Pediatr Res* 2015.